Microscale Approaches to the Design of Equilibrium Stage Separation Processes

This thesis was submitted to the University of London for the degree of

DOCTOR OF PHILOSOPHY

Karen E. Willson, B.Sc. M.Res.

The Advanced Centre for Biochemical Engineering
University College, London
Torrington Place
London, WC1 7JE

2008

ProQuest LLC
789 East Eisenhower Parkway
P.O. Box 1346
Ann Arbor, MI 48106-1346

This work was produced under exceptional circumstances and should not be used as a model for subsequent theses.

Acknowledgements

I would like to thank:

Dr. Gary Lye for his continued support, supervision, guidance and input to this work to help me realise my potential.

Prof. Mike Hoare for accepting me into the Biochemical Engineering Department at University College, London.

Biotechnology and Biological Sciences Research Council for their funding of this research.

The Centre for Scientific Enterprise for their financial support that gave me the opportunity to widen my perspective.

The members of the team from London Business school and UCL who played a valuable part in evaluating the technology: Martin Chirotarrab, Gerard Drenth, Paul Griffiths, Aeby Thomas, and Stephen Trainor.

Jason Wrigley for his expert training and continued support with the automated liquid handling workstation.

All members of the Biochemical Engineering department at University College, London, past and present for their help in and out the laboratory.

My friends within the department who helped me stay sane, provided me with opportunities for fun and laughter and support through the rewrites.

All my friends outside the department who helped me escape, have fun and gain a sense of reality within the rest of the world.

Those responsible for spectacles, computers, alcohol and drugs.

To my family for their love and support throughout my studies, especially my mother for being my eyes when the light grew dim.

God.

Table of Contents

Appendix

List of Figures

Chapter 1:

Chapter 2:

[1] Multiprobe II Ex® terminology defined in appendix 5

Chapter 4:

Chapter 5:

List of Tables

Chapter 1:

Chapter 2:

Chapter 3:

Chapter 4:

List of Abbreviations

\Abbreviation	Definition
3D	3 dimensional
6-APA	6-aminopenicilanic acid
AC	Activated carbon
ADME	Adsorption, distribution, metabolism & excretion
ave	average
BA	Butyl acetate
BMVO	*Baeyer-Villiger* Monooxygenase
C	Centigrade
C_{aq}	Concentration of the solute in the aqueous phase
CC	Combinatorial chemistry
CC-LLE	Counter current liquid-liquid extraction
CFA	Clinical failure assay
CH	Cyclohexane
C_{org}	Concentration of the solute in the organic phase
CSEL	Centre for Scientific Enterprise, London
CV	Coefficient of variance
d	Depth
D	Distribution ratio
DD	Drug discovery
d_B	Diameter of baffle
d_i	Internal diameter
d_{Resin}	Diameter of resin particles
d_{Tip}	Diameter of pipette tip
DMPK	Drug metabolism and pharmacokinetics
DNA	Deoxyribose nucleic acid
DoE	Design of experiments
DSP	Downstream processing
DNA	Deoxyribonucleic acid
E. coli	*Escherichia. coli*
ELISA	Enzyme linked immunosorbent assay

GC	Gas chromatography
gm	Genetically modified
GMP	Good manufacturing practice
GLP	Good laboratory practice
gm	Genetically modified
h	Height
H	Hexane
HEPES buffer	H
HLA	Human leucocyte antigen
HPLC	High performance liquid chromatography
HTS	High throughout screening
IL	Ionic liquid
IP	Intellectual property
IPTG	Isopropylthiogalactoside
IR	Infrared
K_D	Distribution constant
kDa	Kilo daltons
l	Length
LC	Liquid chromatography
LC/MS	Liquid chromatography gas chromatography
LHW	Liquid handling workstation
LLE	Liquid-liquid extraction
m	Million
M	Molar concentration
min	Minute(s)
mRNA	Messenger ribonucleic acid
n	Sample number
N	Population Number
Na	Not available
Nc	Number of mixing cycles
NCE	New chemical entities
Nd	Not detailed
NMR	Nuclear magnetic resonance spectroscopy
NPV	Net present value
OD	Optical density
OEM	Operational equipment manufacturers

PA	Penicillin acylase
PAA	Phenyl acetic acid
PC	Personal computer
PCR	Polymerisation chain reaction
Pen G	Penicillin G
PET	Polyethylene tetrachloride
PRF	Performance file
PTFE	Polytetrflurethelyene
PVC	Polyvinylchloride
RCV	Relative coefficient of variance
Re	Reynolds number
Re	Reynolds number
RNA	Ribonucleic acid
RO	Reverse osmosis
R&D	Research and development
rmm	Relative molecular mass
RP	Reverse phase
rpm	Revolutions per minute
RSE	Relative standard error
SD	Standard deviation
SE	Standard error
SMPE	Solid phase micro extraction
SOP	Standard operating procedure
SPE	Solid phase extraction
SS-PDO	Smart screening for process design optimisation
UHTS	Ultra high throughput screening
USP	Universal serial port
UV	Ultraviolet
V	Variance
Vis	Visible
vol	volume
V_{aq}	Volume of aqueous phase
V_{org}	Volume of organic phase
V_r	Volume ratio

List of Footnotes

Footnote Number	Footnote Definition	**Chapter**
1	Multiprobe Terminology defined in appendix 5	2,3,4,5
2	Standard deck[= configured with Flush/wash bowl with 2 reagent troughs, Tip chute, Box of small conductive disposable tips, 96-well glass plate and rak[1] containing 350uL HPLC vials.	2
3	Chromacol 350 µL HPLC vial from Chromacol, VWR, UK.	2
4	HPI Hydrophobic ionic liquid. Transfer to Rotary Evaporator to remove solvent and then redissolved in phosphate buffer).	2
5	Slurry of Activated carbon (granular), activated carbon (powder), XAD-7 or XAD-16 at a variety of concentrations)	2
6	Waste dispense mode aspirates a larger volume than it is programmed to dispense and then dispenses the required volume, wasting the excess volume.	2
7	Blowout dispensing mode that aspirates exactly the volume it is programmed to dispenses.	2
8	C18 = Octadecyl (non end-capped) manufactured using functionalized silica, , manufactured using trifunctional silanel C18 MF = Octadecyl (end-capped) functionalised; C8 = Octadecyl (non end-capped) functionalised silica, , manufactured using trifunctional silanel; C6 Hexyl (end-capped) functionalized silica, C4 = Butyl (end-capped); C2, = Ethyl (non end-capped) functionalized silica, manufactured using trifunctional silane; PH = Phenyl (non end-capped) functionalized silica, manufactured using trifunctional silane. and CN = Hydroxylated polystyrene-divinylbenzene	2
9	CV = Coefficient of Variance, defined in appendix 11	33
10	Definition of statistical terminology in appendix 11	3,4, 5
11	Definition of fluid dynamics terms in appendix 13: section A13.4	4
12	Energy per mole factor = Extraction time/ (PAA concentration x volume): microscale = 0.0004; laboratory scale = 0.08	4
13	SuperPro Designer is a tool for engineers and scientists used to aid process design for development and manufacturing.	6
14	30 man years to complete automation process fermentation of a process x (10 processes (purification + fermentation) + 20 man years for process integration, software development and data retrieval.6	

Chapter 1: Introduction

1.1 Introduction Outline

The introduction briefly outlines the current position of the pharmaceutical industry (section 1.2), documenting the history of the pharmaceutical industry that incorporated various scientific paradigms during its development. The research and development process for the generation of new pharmaceuticals (section 1.2.1) and the different experimental process scales that are used to achieve effective manufacturing of pharmaceuticals (section 1.2.2) were identified. The complexity of the pharmaceutical industry has resulted in a number of current problems (section 1.2.3), which are identified, together with their possible solutions (section 1.2.4). Many of these possible solutions have been generated as a result of the amalgamation of emerging technologies developed in other scientific fields. The research presented in this thesis will investigate the suitability of integrating automated platforms to accelerate the generation of bioprocess data for validating large scale equilibrium separation procedures.

The pharmaceutical industry has made wide use of the recent development of multiwell plates and their associated automated equipment (section 1.3). There are a variety of multiwell plates (section 1.3.1), which are compatible with many automated platforms and devices (section 1.3.2). The automated equipment is dominated by the liquid handling workstation (section 1.3.2.1.1), a robotic automated multi-channelled pipette that can rapidly deliver a range of liquid volumes to a variety of locations, facilitating a diverse range of experiments. The equipment has been used to generate a number of automated applications (section 1.4), including drug discovery, combinatorial chemistry, high throughput screening, biocatalyst screening, and bioanalysis. This has also been used to automate sample preparation, which uses a range of equilibrium based separation processes for compound purification. These equilibrium based separation processes (section 1.5) include liquid-liquid extraction and solid phase extraction, which are analogous to product purification techniques used in biochemical engineering.

The production of pharmaceuticals (section 1.6) uses various synthetic routes (section 1.6.1) containing chemical catalysts or biological catalysts (biocatalysts). These different synthesis routes are compared and are discussed in detail (section 1.6.1.1). Examples of commercial biocatalytic synthesis routes are identified (section 1.6.1.2), outlining the various methods of improving their performance (section 1.6.1.2.1), their bioconversion efficiency (section 1.6.1.2.2) and the proposed experimental model for this research (section 1.6.1.3). The biocatalyst (penicillin acylase) is discussed in detail (section 1.6.2) focussing on its structure, production, purification and bioconversion characteristics. Penicillin acylase hydrolyses penicillin to yield 6-aminopenicillanic acid (6-APA) and the purification of 6-APA is discussed (section 1.6.3).

Biochemical engineering experimentation is carried out at a range of different process scales to investigate the synthesis and purification routes. The investigations in this research are to be undertaken using commercially available automated platforms. The automated process and equipment requirements are considered (section 1.7), relating them to process automation (section 1.7.1), and the equipment used for individual microscale separation purification processes (section 1.7.2). The published literature (section 1.8) on the automated liquid-liquid extraction (LLE) and solid phase extraction (SPE) processes is reviewed chronologically to detail the background of this research. Finally, the specific aims and objectives of this thesis (section 1.9) are highlighted to indicate the future direction of this research.

1.2 Current State of the Pharmaceutical Industry

The pharmaceutical industry was developed by using knowledge and technology from a variety of scientific areas to understand the nature of pharmacologically active compounds (figure 1.2.1). The initial principles of pharmacology borrowed knowledge from chemistry to describe the pharmacological actions of the first pharmaceuticals, which were discovered in medicinal plants by the Egyptians using a trial and error approach. During the 19th Century, these pharmacologically active compounds were isolated and identified using analytical chemical techniques (Schmid and Smith, 2002). Examples of such biological compounds include the painkiller aspirin, isolated from willow tree bark and morphine, isolated from opium poppies in 1815. The chemical synthesis of aspirin instigated the diversification of the first company to commercially manufacture aspirin, was Bayer AG in 1889.

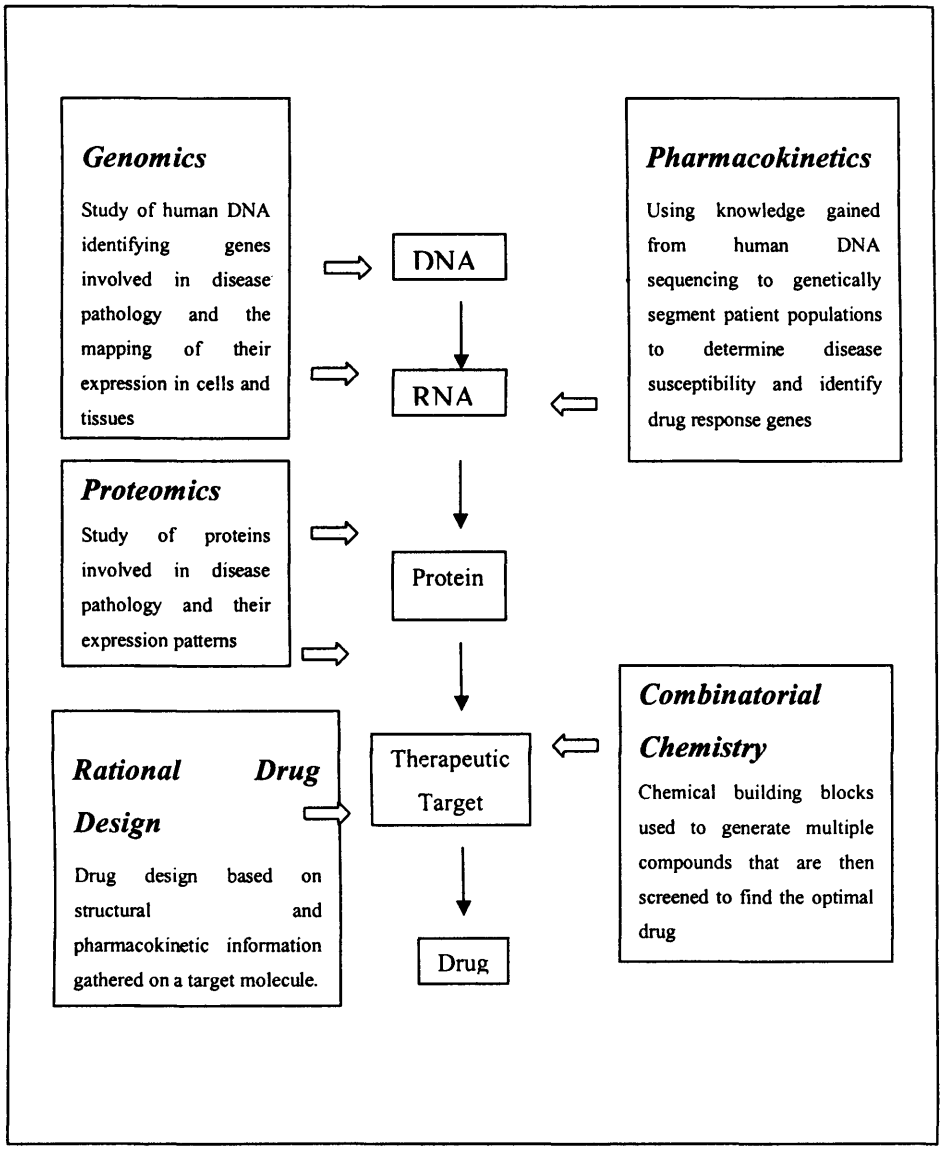

Figure 1.2.1. Diagram of the technologies driving pharmaceutical innovation, taken from Reuters (2001).

The pharmaceutical industry grew during the 20th century by the amalgamation of emerging technologies from other scientific areas to assist drug discovery (section 1.4.1). Collaboration between chemists and microbiologists led to the isolation of products from micro-organisms and in 1929 Fleming discovered penicillin from the *penicillium* mould. This instigated the development of a range of synthetic antibiotics used to treat bacterial infections. Innovative pharmaceuticals and agrochemicals were identified via the screening of secondary metabolites from micro-organisms, plants and animals (Thiericke, 2000).

More recent developments in the pharmaceutical industry have incorporated genomic and proteomic tools into the pharmaceutical industry to enhance drug discovery (Karri et al, 2001). The human genome project has characterized the genes, indicating that those related to specific diseases and proteomics have characterized their related proteins. These new tools are being exploited to generate the next generation of drug candidates, which can be synthesised using combinatorial chemistry (section 1.4.1) and selected by high throughput screening (section 1.4.1.2). These tools work with other research and development methods and process development approaches to facilitate the production of new pharmaceuticals.

1.2.1 Research & Development Processes

"The research and development process discovers new knowledge about products, processes, and services. The resulting knowledge is applied to create new and improved products, processes and services that fill market needs" (InvestorWords.com, 2003). Therefore, any activity that is classified as research and development (R&D) is characterized by its originality. *"Investigation is its primary objective and should have the potential to produce results that are sufficiently general for humanity's stock of theoretical and/or practical knowledge to be recognisably increased"*. (University of Western Sydney, 2003). These definitions describe R&D in general terms, though when describing specific pharmaceutical R&D, these definitions must be elaborated on.

Pharmaceutical R&D focuses on the identification of drug candidates and investigates their production and down stream processing (series of purification processes for new drug candidates). The effects of these drugs on known drug targets linked to specific diseases must be quantitatively and qualitatively tested before considering the optimal synthesis and

purification routes for their production. The synthesis route used to produce the drug and the nature of the drug itself both influence the selection of suitable purification processes. It can take many years to acquire the necessary information from this multifaceted R&D process before a new drug can be tested to generate pre-clinical and clinical information.

Pre-clinical experimentation , as well as phase I, II and III clinical trials produce toxicological information about the efficacy of a new drug, its pharmacokinetics and biological safety (Rang et al, 1999). The average duration of these pre-clinical studies is *circa* 10 to 15 years (figure 1.2.1.1). These clinical trials test the drug on animal and human subjects. The laboratory production and purification processes must then be scaled up in order to produce high quantities of the compound to undertake these studies (section 1.2.2). However, once a drug has cleared these stages there is another hurdle to overcome before it reaches the market. The process must be scaled up to achieve the commercial quantities required and this must pass manufacturing regulations (Jefferis, 1998, Sheridan, 2000). From discovery, a new drug candidate only has a 4% chance of reaching the market (Ivey School of Business., 2000).

1.2.2 Process Scales

The development of pharmaceutical production and purification processes is initially carried out at laboratory scale, <10 m^3 (Doran, 1998). Larger quantities of high quality pharmaceuticals are required for further R&D studies and clinical trials. Therefore, the process must eventually be scaled up to meet the commercial need. The unit operations of down stream processing (DSP) are considered as individual processes. Scaling up a process is not simple or linear. Therefore, intermediary stages are required, such as pilot scale. Scaling up DSP is affected by pH, temperature and shear affects, which may cause the product to degrade over time (van Brakel and Kleizen, 1990). The laboratory process is scaled up to pilot scale (10 to 149 m^3) to test the robustness of the process before reaching the manufacturing scale (150 to 250 m^3) for penicillin production (Doran, 1998).

Process development modifies the production and purification processes of a drug in order for it to be produced on a larger scale. This stage is time-critical as it is important to get the drug onto the market in order to extend its patent protected life (Mintzberg et al, 1996). The scale-up process must be efficient and reliable, which is the key objective of any

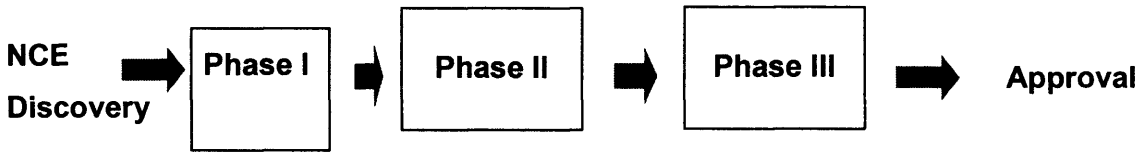

Description	Tests on 20 to 100 healthy volunteers	Efficacy testing on 100 – 300 patient volunteers	Efficacy testing on 1000 - 3000 patient volunteers
Cost	$58 million	$42 million	$117 million
% NCE Entering Phase	100%	70%	36%
Phase Duration	1 - 1.5 years	2 years	2.5 - 3 years

Figure 1.2.1.1. Diagram of the clinical trial stages involved in getting a pharmaceutical to market (NCE = New Chemical Entity), taken from source: Lehman brothers (1995).

pharmaceutical company. A good process can help make the most of the patent life, in some cases up to twenty years. If it is the first drug of its type to market it should initially achieve maximum market share. This allows development and production costs to be recouped and the company can enhance its profits (Roche Carolina, 2003). It is, therefore, important that process development is completed quickly and accurately (Conner, 1999). However, this aspect of product development has traditionally only been considered when needed, which has resulted in suboptimal processes being taken forward for regulatory approval by the Food and Drug Administration (US) or Medicines Control Agency (UK). These regulatory bodies determine the quality of the feed materials, process conditions, and the product itself by carrying out stringent testing. This testing involves the full training of personnel involved in manufacturing the product, and the writing of comprehensive documentation to support the entire process, all of which should ensure the commercial production quality of the compound.

1.2.3 Problems of the Pharmaceutical Industry

The pharmaceutical industry has been suffering from a series of problems including financial difficulties, lack of innovation, increasing R&D costs, and a development time-lag. These factors are severely affecting the profits and future direction of pharmaceutical companies (Foo et al, 2001).

The financial problems of the pharmaceutical industry are dominated by expiring patents and competition from generic compounds. These factors are compounded by price controls and restricted prescription drug sales. (Reuters, 2001). The limited numbers of patent protected products on the market have increased the vulnerability of the industry Schmid and Smith, (2002). This has resulted in a decrease in prescription pharmaceutical sales growth from 11% to 6% between 1980 and 1997 (PriceWaterhouseCoopers, 2000).

Concurrently, the pharmaceutical industry has brought insufficient innovative new drug candidates into the drug pipeline. The poor quality and low throughput of drug candidates reduced the productivity of drug discovery. This stimulated the pharmaceutical industry to invest in R&D, with costs rising from 1982 by *circa* 500% to £163.2 billion in 1995 (Key Notes, 1996). This money was spent on laboratory automation platforms, increasing the

number of compounds being synthesised by combinatorial chemistry (section 1.4.1.1) and screened by high throughput screening tools (section 1.4.1.2). The number of new drug candidates entering the pre-clinical trials in the drug pipeline increased from 2853 in 1996 to 3278 in 1998. However, many of these drug candidates failed to reach the market (96%) because of a number of problems (PriceWaterhouseCoopers, 2000).

Despite the increased R&D spending and use of automated laboratories, the number of new drug candidates reaching the market has been stagnant at 37 per year during the 1990s (Wess, 2002). This was because of innovation deficit, and problems with the early drug candidates which showed poor chemical and biological compatibility between the target and drug candidate compound libraries. This resulted in many lead compounds failing at clinical trials because of poor pharmacokinetic behaviour (Oprea, 2002).

The development time of many new drugs has increased because they are biopharmaceuticals, which are more complex drugs to produce. Another reason for this was the increased regulatory hurdles placed by the Food and Drug Administration (FDA) or Medicines and Healthcare products Regulatory Agency (MHRA) to control the release of safe new therapies. The approval process is fastidious, making the application process slow (Titchener-Hooker and Zhou, 2001. The backlog of FDA patent applications continues to delay the launch of new pharmaceuticals, despite the decrease in applications due to the additional time required for analysing the increased supporting documentation (NewsEdge Corporation, 2005).

This series of problems hindered the pharmaceutical companies in achieving their ambitious published goals of entering between 3 and 30 new drugs into their pipelines by 2003. These goals were considered by the financial industry as being unsustainable (PriceWaterhouseCoopers, 2000). The challenge of the pharmaceutical industry was to increase its innovation and productivity (Wess, 2002). The success rates for producing new drug candidates that will reach the market are low (*circa* 0.4%). More recently a number of strategic initiatives have been adopted by pharmaceutical companies to increase their research productivity. These include re-organising therapeutic areas, re-organising research areas, utilising spin out research by increasing collaboration with academia; forming consortiums with peer companies sharing key objectives; and improving in-licensing

capabilities to generate more new chemical entities. The focus is changing towards the use of large biological based drugs. These drugs are being tested in clinical trials on alternative patient populations including the Chinese (Hughes et al, 2005).

1.2.4 The Solution: Automation

The pharmaceutical industry has been driven by the emergence of technological advances. These have been used to tackle the current problems facing the industry. The current problems (section 1.2.3) include low prescription sales, limited discovery of innovative drugs, and dwindling patent protected portfolios of the pharmaceutical companies. It is hoped that these automated tools will reduce the high R&D costs and high development time. It is important that the prescription sales be increased by the development of new drugs. Therefore, innovative therapeutics need to target new markets, satisfying unmet medical needs. Initial automated drug discovery techniques have had limited success. Molecular biology, proteomics, and medicinal chemistry are being used to tackle this problem, increasing the success of drug discovery (Wess, 2002). The R&D costs will be negated as productivity increases, which will reduce the long R&D time-lag by the use of automated tools to rapidly synthesise and screen new drug candidates.

The innovation and quality of drug discovery is being improved by the use of molecular biology, which is seen as being the answer to the difficulties faced by the pharmaceutical industry (Schmid and Smith, 2002). Molecular biology has identified a plethora of potential therapeutic targets, identified from the 30,000 genes discovered through the human genome project, which are associated with many diseases and have facilitated the identification of potential interacting pharmaceuticals. The most suitable targets implicated in the disease process were identified with the use of proteomics, functional analyses and characterisation of the related proteins. These targets will facilitate the discovery of corresponding active therapeutic molecules and have been used to identify and optimise lead compounds (Lam and Renil, 2002).

Automation has accelerated drug discovery and could be used to rapidly optimise the synthesis or characterize the physiochemical properties of the drug, biological target efficacy, oral resorption, half-life and metabolism (Wess, 2002, Oprea, 2002). The automation of drug

metabolism, pharmacokinetics (DMPK) and absorption, distribution, metabolism, excretion (ADME) studies, rapidly provide information on pharmacokinetics, drug safety, side effect profiles, optimal dosing regimes and drug-drug interactions (Schmid and Smith, 2002). This information can now be discovered during product development, reducing development time (Watt et al, 2000) and increasing the success rate of the drugs (Oprea, 2002). These automated tools have shifted the R&D bottleneck from lead discovery and optimisation to scale-up issues for production to ensure good manufacturing practice is achieved.

1.3 Multiwell Plates & Automated Equipment

The pharmaceutical industry increased the numbers of samples investigated as a result of the development of multiwell plates. This format proved to be popular for a variety of scientific applications and the users' needs encouraged the manufacturers to develop a wide range of plate configurations (section 1.3.1). The 96-well plate also instigated the development of an entire support industry by providing reagents, devices and equipment designed specifically for use with the multiwell plates (section 1.3.2), which can be linked to build a fully automated laboratory.

1.3.1 Multiwell Plates

The term "multiwell plate" covers all plates containing a number of individual wells. The first plate was introduced by Dynex (formerly Dynatech Laboratories) as a 100-well plate (Johnson, 1999) and many companies have developed their own multiwell plates. Industry pressures influenced the development of these plates, favouring the 96-well plate. The National Institutes of Health designed the first commercially available plate in 1962 (Johnson, 1999). This plate had a 96-well format and was used to detect the presence of specific antibodies in biological samples using enzyme linked immunosorbent assay (ELISA) (Thompson, 2002). The 96-well plate facilitated the processing of high numbers of samples, and became the established format.

The standard 96-well plate had a footprint with outside plate dimensions of l = 127.76 mm x w = 85.48 mm (Society for Biomolecular Screening, 1996). The standard well diameter is 7

mm and the wells are arranged linearly in 8 rows and 12 columns, as shown in figure 1.3.1.1. This standard multiwell plate was manufactured from polystyrene (appendix 1). However, multiwell plates are now available in a diverse range of materials to meet the requirements of their users. Many other characteristics of the microplate were augmented including the number, shape, size, and material of the wells on the plate while maintaining the standard footprint dimensions (table 1.3.1.1). The range of multiwell plate configurations has increased their use in a variety of applications (section 1.4).

1.3.2 Automated Equipment & Devices

1.3.2.1 Automated Equipment

The mass production of 96-well plates stimulated the development of compatible automated equipment to facilitate the high number of sample pipetting and dilution stages required specifically for ELISA techniques (Keightley, 1986). The increased demand for their integration into a number of other scientific fields that need accelerated sample handling drove the development of these plates and equipment.

The automated equipment is designed to carry out one specific function that can be used for one of many purposes. Examples of equipment with a specific function and purpose include plate washers, plate centrifuges, evaporators, plate stackers and robotic arms, which are available from a number of manufacturers (appendix 1.4: table A1.4.1). The plate stacker was designed for a single function and purpose, to stack disposable labware (e.g. multiwell plates or disposable tips). However, the liquid handling workstations were designed for a single function, to automatically pipette liquid between locations, which serves multiple purposes. Not only can this be used to transfer liquid samples, but also for diluting or mixing purposes (section 1.3.2.1.1). This makes the workstation versatile enough to automate a variety of applications.

The range of available equipment is ever increasing as the multiwell plates are being used in more diverse research areas. The automated equipment can be used individually or integrated together to create an automated laboratory (Jandu, 2000) using the robotic arm to physically move the multiwell plate between them, linking them together to carry out a series of

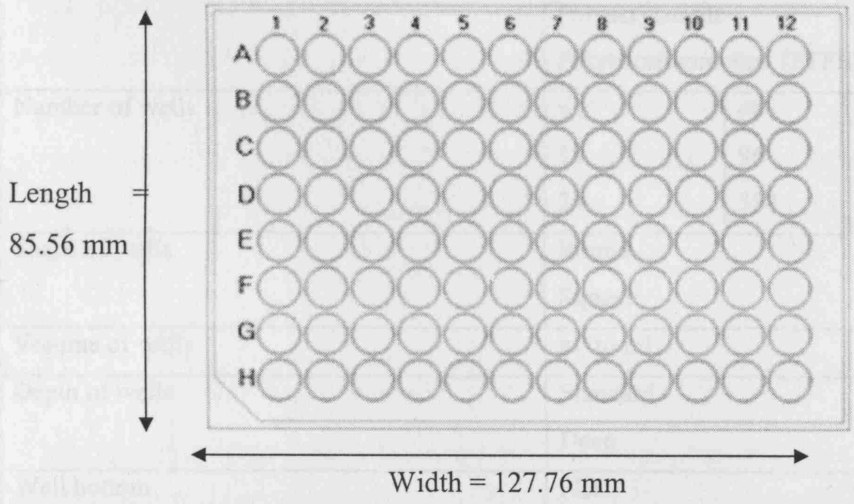

Figure 1.3.1.1. Schematic of a 96-well plate with standard footprint dimensions, provided by the Society for Biomolecular Screening (1996).

Characteristics of Multiwell Plates	Options		
Material of Construction	Polystyrene Polypropylene Polystyrene + cellulose acetate Polycarbonate Borosilicate Quartz Polyethylene tetrachloride (PET) Polycarbonate Polyvinyl chloride (PVC) Polyacrylamide Polytetrafluoroethyl (PTFE)		
Number of wells	6 12 24	48 96 384	1536
Shape of wells	Round Square		
Volume of wells	nL to mL		
Depth of wells	Standard Deep		
Well bottom	Flat Round Tapered		
Coatings (biological or chemical)	Antibody Cell culture		
Condition	Sterile Non-sterile		
Specialist Plates	Filter plates – Membrane 0.2 – 11 μm SPE resins –adsorbents 50 – 200 mg		

Table 1.3.1.1. Characteristics of multiwell plates with their various options (data from Johnson, 1999 and Thompson, 2002).

operations. It is vital for the equipment to have integrated control software that communicates by serial commands or relay control to co-ordinate operation.

1.3.2.1.1 Liquid Handling Workstations

The liquid handling workstation is an automated pipette with a number of pipette tips, which are fixed on a robotic arm (See section 2.2.1 for greater detail). The pipette tips can move around the deck (working area) of the workstation in the x, y and z directions, dispensing aliquots of liquids or reagent solutions. There are various workstations available with different numbers of pipette tips (1 to 96) and configurations (Schneider, 1997). The major manufacturers of this equipment are detailed in table 1.3.2.1.1.1. The workstation can transfer liquid between locations for a variety of purposes including aspirating reagents, dispensing reagents, mixing two reagents, diluting samples, timing pauses for reaction development and washing steps. These steps can be linked together to create an experimental test that will carry out specific methodologies. Additional devices (section 1.3.2.2) can be used with the workstation, increasing the number and type of applications, such as those outlined in section 1.4.

1.3.2.2 Automated Devices

A number of devices have been developed to complement the liquid handling workstation and increase its functionality in supporting a wider range of applications. These devices were designed to be compatible with the multiwell plates. They include filtration rigs, water baths, magnetic stirrers and balances (appendix 1.5: table A1.5.1). Most of these devices operate manually as they are relatively simple, but some can be automatically controlled by a personal computer (PC) linked via controller boxes to the equipment's universal serial port (USP). In order to automate these devices they require software that is compatible with the device, PC and monitoring software, ensuring the compatibility of software programming languages.

1.4 Applications of Automated Equipment

There are many applications using multiwell plates and various pieces of automated equipment, examples of which are shown in table 1.4.1. These include drug discovery (DD),

Trade names of Liquid Handling Workstation	Manufacturers
6700 automate nucleic acid workstation	Applied Biosystems
AQUAmas 1536	Molecular Devices
Biochip	Packard
Biomek 2000	Beckman Coulter
C-400	Cyberlab
CHOT-1 CHOT-2	Nichiryo America Inc
Constellation 1200	Gilson Inc
Gemini Genesis	Tecan
Hydra 96 Hydra 384	Robins Scientific
Multiprobe	Perkin Elmer
Microlab STAR Microlab 2200	Hamilton
pixSYS	Cartesian Engineering
Platemate	Matrix Technologies
Plate Trax	Carl Creative
Precision 2000 Plus	Bio-Tek
Quadra 96	Tomec
RapidPlate	Zymark
synQUAD	Cartesian Technologies
Universal Sample Preparation	Mettler Toledo
Wellpro 384	Therma Labsystems

Table 1.3.2.1.1.1. Liquid handling workstation trade names and their manufacturers (Information from company web pages).

Production	**Purification**	**Storage**	**Analysis**
Bioconversion	**Centrifugation**	**Biocatalysts**	**ADME**
CC synthesis	Crystallisation	CC libraries	Colorimetric Assays
Fermentation	DNA purification	Cell line stocks	DMPK
PCR	Filtration	Crystallisation	ELISA
Tissue & cell culture	LLE	Freeze dried samples	GC
	Protein precipitation	HTS hits	HPLC
LLE	RNA purification	UHTS hits	HTS
	SPE		Radiometric Assays
			Restriction enzyme digests
			UHTS

Table 1.4.1. Applications using multiwell plates and automated equipment to achieve sample production, preparation, storage and analysis experimentation.

combinatorial chemistry (CC), high throughput screening (HTS), biocatalyst screening, sample preparation, and bioanalysis. The automated research tools can deal with high numbers of samples and rapidly generate results, accelerating many parts of the R&D process.

1.4.1 Drug Discovery

Drug discovery is a key stage in the pharmaceutical R&D process, which identifies novel pharmaceutical compounds. The discovery of new pharmaceutical compounds has been enhanced by the use of genetics and proteomics that were integrated with computing technology and automated equipment. This has facilitated the rapid synthesis of compound libraries by combinatorial chemistry (section 1.4.1.1) and a high throughput screening of samples (section 1.4.1.2). The human genome project has aided drug discovery by identifying 1000 genes that are significantly indicated in the emergence and cause of specific diseases. Proteomics has identified the related proteins and their function in the disease process. This molecular understanding of disease has been used to identify new therapeutic drugs (Drews, 2000). Genes encoding for secreted proteins, such as interferons, and antibodies have also been identified as being useful therapeutic targets, which can be reproduced by recombinant DNA technology. There are currently 59 of these new biotechnological drugs on the market (Wess, 2002).

1.4.1.1 Combinatorial chemistry

Combinatorial chemistry rapidly generates vast numbers of compounds (Lam and Renil, 2002) using automated equipment to synthesise compounds on solid phase, on a chip or in the 96-well plate (Boyle and Janda, 2002). Discrete chemical elements (building blocks) are selected to produce a collection of compounds (libraries), representing permutations of a set of chemical or physical variables (Demuth et al, 2002). The libraries are designed using building blocks selected with the structural motifs identified from natural products or designed to interact with the target molecule to create new compounds (Nielsen, 2002).

At present, combinatorial chemistry is the major source of compound libraries for HTS programs. However, it is still important to screen natural compounds and substances derived from them because they currently account for 30% of the world's drug sales and 45% of the best selling 20 drugs (Thiericke, 2000). There is a great need to improve the success of combinatorial chemistry by producing new chemical entities (compounds), and these libraries are now designed using approaches from medicinal chemistry. This has increased the synergy between the biological target and the chemical structure of the therapeutic compounds to produce drugs that are theoretically target-specific drugs. Such drugs should minimise the problems caused by side effects. Dynamic combinatorial chemistry generates the compound libraries under equilibrium and thermodynamic conditions so that the building blocks are reversibly linked to enable their chemical response to exterior influences of molecular recognition events (Otto et al, 2002).

1.4.1.2 High Throughput Screening

High throughput screening uses automated assays to rapidly test compound libraries against biological targets and to identify therapeutically active compounds by using the multiwell format on automated equipment (Houston and Banks, 1997). The identified hits (compounds that elicit a positive response in a particular assay) are further screened to identify leads (compounds that continue to show a positive response in more complex analyses, such as cell or animal models). This technique uses efficient, low-cost and sensitive assays to analyse new chemical entities (Taylor et al, 2000). This rapid procedure has a screening rate of 100,000 samples per day, per workstation.

A diverse range of assays has been used to analyse compound libraries created using both combinatorial chemistry and natural sources. One of the bottlenecks in drug discovery has been assay optimisation, but this is now being developed using automated equipment (section 1.4.1.2.1) in order to increase drug sensitivity and robustness. In addition to screening new therapeutic compounds, HTS has been used to identify other useful compounds that catalyse reactions from chromium ethylene polymerisation (Jones et al, 2002). This automated technique has also been used to screen a range of individual compounds and combinations of compounds to enhance skin permeability for transdermal drug delivery (Karande and Mitragotri, 2002).

1.4.1.2.1 Assay Development

The automation of assays was one of the earliest applications designed for 96-well plates using liquid handling workstations, and there is now a great diversity of automated assays including:

- Lowry protein assay (Lane and Lynn, 1987).
- ^{3}H-acetylated collagen assays - used to screen collagenase inhibitors as a potential therapy linked to a range of pathological processes, such as embryonic development, bone turnover, and tumour metastases (Koshy et al, 1992).
- Cell based assays - used to investigate biomolecule-inhibitor interactions within living cells to give information about the receptor, binding protein or enzyme targets (Parandosh, 1997).
- Islet cell antigen, glutamic acid decarboxylase, protein tyrosine phosphatase assays and human leucocyte antigen (HLA) genotyping – used for testing serum auto-antibodies to identify type 1 diabetes (Woo et al, 2000).
- Human interferon γ immunoassay – used to screen interleukin-13 production inhibitors to discover anti-allergic drugs (Enomoto et al, 2002).

These assays fall into three distinct groups: homogeneous assays, in-plate assays, and assays requiring a filtration stage (Kolb, 1994). Each of these assays has been optimised for rapid analysis using automated equipment (section 1.3.2). Assays used in toxicology studies include the rational pre-screen, reporter screen, and clinical failure assays (CFA) that predict the drug's likely mechanism of action (Skehan, 2000).

1.4.2 Biocatalysis Screening

Automation technology has been used for screening biocatalysts (Doig et al. 2002) and chemical catalysts for the selection of suitable conditions and process routes (Lye et al, 2003). The technology has also been used to investigate cocatalysis conditions (reagent concentrations, reaction time) of meso-tetramesitylporphrin synthesis to optimise it for high yield (Wagner et al, 1999).

1.4.3 Sample Preparation Issues

1.4.3.1 Sample Handling

One of the most time consuming and labour intensive steps in DD is sample handling (Zhang et al, 2000a). The use of liquid handling workstations has automated and accelerated the transfer of samples between vessels. One of the difficulties with laboratory sample preparation has been the need for the manual uncapping and capping of sample tubes (Teitz et al, 2000). This problem has been overcome with the workstations by securing the tubes into a frame, and the use of pierceable caps. Automated sample handling has increased the efficiency of DD by reducing both the method's operational time and process scale.

1.4.3.2 Sample Preparation

The preparation of compounds from biological samples often requires numerous purification techniques and is "usually the rate limiting step in achieving high throughput bioanalysis" (Teitz et al, 2000). Sample preparation of active compounds from plants, animals, and micro-organisms must be undertaken to clean up these biological samples prior to their bioanalysis. Sample preparation isolates the pharmaceuticals and agrochemicals from these sources and patients' biological samples such as plasma, serum and urine (Zweigenbaum et al, 1999) taken at clinical trials. This preparation removes contaminating compounds, such as proteins, from the complex matrices as they interfere with bioanalysis.

The procedures used for biological sample preparation include; liquid-liquid extraction (LLE), solid phase extraction (SPE), protein precipitation, filtration, and centrifugation. These processes are time consuming and labour intensive, which makes them ideal for automation to efficiently deal with high sample numbers. Automated sample preparation is simple, fast, and reproducible, with a typical coefficient of variance (CV, appendix 11 .2.7) of 3% to 6% (Watt et al, 2000).

Automated sample preparation procedures have also been used for the analysis of pharmaceutical production and formulation quality. Tablet formulations were checked for

composition, content uniformity, weight variation, and degradation products using automated technology (Shamrock et al, 2000). This increased precision, reduced solvent waste and chemical exposure whilst providing an electronic audit trail.

1.4.3.2.1 Sample Preparation: Liquid-liquid extraction

Liquid-liquid extraction (LLE) has been used extensively to prepare biological samples, but the automation of this procedure was initially believed to be too difficult due to liquid handling problems and the lack of a compatible centrifuge for 96-well plates. These problems have been overcome by the use of diverse automated equipment that is now commercially available (section 1.3.2.1) for the LLE purification process (section 1.5.1). The technique is now used widely for plasma sample preparation despite its limited compatibility with polar molecules. Automated laboratory LLE equipment, such as ALLEX (extraction vessel = 26 mL) and ASPEC (extraction vessel = 20 mL) is being used to automate laboratory scale LLE systems.

1.4.3.2.2 Sample Preparation: Solid Phase Extraction

Sample preparation has been achieved using SPE techniques (section 1.5.2) to purify samples. The SPE process has traditionally used cartridges for laboratory scale experimentation, which has been time consuming for screening adsorbents and pH conditions. However, the automation of SPE has accelerated sample preparation (Rouan et al, 2001, Rouan et al, 2002). The procedure has since been simplified to a one step SPE procedure, developed to create high purity samples from fermentation broth using polystyrene resins (Thiericke, 2000). Its simplicity and wide application make SPE important for the generic extraction required in early drug discovery.

1.4.3.2.3 Sample Preparation: Protein Precipitation

Sample preparation using protein precipitation is labour intensive and hazardous. It mostly uses acids or organic solvents to remove the proteins by denaturation or precipitation. This technique is widely used in bioanalysis because of its compatibility with HPLC mobile phases (Blanchard and Fabrycky (1981) . The automated protein precipitation method (Bakhtiar et al, 2002) was used especially for the preparation of plasma samples

(Biddlecombe and Pleasance, 1999). The process was difficult to automate due to liquid handling and centrifugation problems. This was reflected in the low reproducibility of the method (CV 14%) compared to the traditional laboratory method using tubes (CV 3%), (Rouan et al, 2001).

1.4.3.2.4 Sample Preparation: Filtration

Filtration is often used with protein precipitation for sample preparation and there are a number of filter plates available (Rouan et al, 2002); the 3M, Empore, and Whatman protein precipitation microplates, all of which have double membranes with a coarse membrane and then a finer membrane. However, the low porosity membrane in the Whatman plate had a tendency to block (Rouan et al, 2002). The use of multiwell filter plates for sample purification was investigated to assess their performance. This showed the Porvair protein microplate to have the best precision and 80% recovery for sample purification, which was similar to SPE (80% to 90%, Biddlecombe and Pleasance, 1999).

1.4.4 Bioanalysis

Bioanalysis is another traditionally labour intensive and time consuming process that requires prior sample preparation, making it a bottleneck to lead optimisation in the discovery process. Therefore, robust automated quantitative methods have been developed. There are a number of analytical instruments that are available for the analysis of samples, as summarised in table 1.4.4.1. These instruments are becoming increasingly automated and compatible with multiwell plates to accelerate their sample throughput.

1.4.4.1 Analytical Methods

The accelerated drug discovery process requires faster bioanalytical and sample preparation techniques (Zhang et al, 2000a). This has moved the analytical methods from biochemical assays with detection by radiometric or spectrometric analysis to favour the use of liquid chromatography, mass spectroscopy or gas spectroscopy to increase selectivity and molecular identification (Zweigenbaum et al, 1999). There are also a number of immunochemical techniques that have been automated including ELISA, radioimmunoassay and fluorescent immunoassay techniques (Wilson and Walker, 1994).

Analytical instrument Manufacturers	Absorbance	Fluorescence	Luminescence	Scintillation Counters	Multilabel	HPLC	Gas Chromatograp	LCMS-MS	Laser Scanning	Infrared
Agilent Technologies							●	●		
Alcott Chromatography Inc.						●				
Applied Biosystems		●								
ARC Research Company				●						
Arganaut						●				
Bio-Rad	●	●								
Bio-Tek	●				●					
BMG Labtechnologies			●		●					
Colibri Robotics	●				●					
Dionex						●				
GBC Scientific Equipment						●				
Hudson Control Group								●		
Labsystems / Titertek	●	●	●		●					
Mirai Bio, Inc		●								
Molecular Devices	●	●			●					
Molecular Dynamics		●								
MTX Lab Systems										●
Perkin Elmer (Packard)	●	●	●	●		●	●		●	
Stratec Biomedical Systems AG			●							
Tecan	●	●			●				●	
Topix			●							
Varian Inc						●	●	●		
Wallac			●	●	●					
Zymark	●	●	●			●				

Table 1.4.4.1. Categories of automated analytical instrumentation compatible with multiwell plates provided by manufacturers (data from company web pages).

Mass spectrometry has become the most sensitive and selective analytical technique for the quantification of drugs and metabolites in biological fluids (Hsieh and Selinger, 2002, Rossi, 2002 and Zweigenbaum et al, 1999). This technique is also rapid, being capable of separating multiple compound mixtures in less than 30s (Zweigenbaum et al, 1999). Bioanalysis using Liquid Chromatography with tandem Mass Spectrometry (LC-MS/MS) achieved a throughput of 400 plasma samples per day per workstation using the Beckman Biomek (Watt et al, 2000).

1.5 Equilibrium Based Separation

1.5.1 Liquid-Liquid Extraction

Liquid-liquid extraction is a well established separation process, which became popular in the 1960s as an industrial process (Blanch and Clark, 1996). Later, the growing demands for high purity, temperature sensitive products, produced with greater efficiency, increased the use of LLE, along with the increased availability and selectivity of the solvents (Seader and Henley, 1998)

LLE has been used extensively in industry to separate a range of compounds including acetic acid and vitamin A (Seader and Henley, 1998). By the late 1960s more than 10,000 m^3 per day of liquid feed was processed using LLE. This has required the use of industrial equipment including mixer settlers and agitated towers that are operated batchwise or continuously (McCabe et al, 2001a).

LLE is a process that separates two or more components from the aqueous liquid feed by contact with a second liquid phase (solvent), which is usually an organic solvent (Thornton, 1992) . The simplest scenario described is a tertiary system, where the contaminating solute is transferred to the solvent, whilst the desired solute is insoluble or partially soluble in the solvent, allowing their separation. The pH conditions of the liquid feed influence the compound's net charge, which influences solubility in the phases. If a compound has a positive or negative charge at the liquid feed pH conditions, then it will be preferentially soluble in the aqueous phase. However, if the pH conditions neutralise the net charge on the molecule then the compound is preferentially soluble in the solvent phase. The preferential

solubilities of the compounds allow the separation of the desired compound from contaminants, which are reflected by their distribution constant (appendix 13.2).

LLE is the preferred separation process for the separation of dissolved or complex inorganic compounds in organic or aqueous phases, low concentration compounds, high melting point compounds, heat labile materials, and if separating mixtures according to their chemistries rather than their volatility or if the compounds have similar melting points. LLE is used to recover high value biopharmaceuticals, for example antibiotics (Blanch and Clark, 1996) due to their preferential insolubilities in organic solvents, which allows both product concentration and purification.

1.5.1.1 Scales of LE Process

1.5.1.1.1 Industrial LLE Equipment

The industrial LLE equipment is classified into gravity and centrifugally separated extractors (McCabe et al, 2001a). The factors that affect gravity separated extractors are long phase transfer times and impurities affecting the interfacial area. Partitioning must be achieved in a low number of contact stages, but if the distribution constant (K_D) value (appendix 13.2) is high (>100), then a single stage extraction produces a high yield. The centrifugally separated extractors are operated at a lower total throughput than the gravity separated extractors, but they can handle extreme phase ratios, operate continuously, enclose the reaction during their operation, concentrate the product, and require limited space and only a short residence time.

Centrifugally separated extractors and decanters, mixer-settler tanks, agitated mixers and agitated towers are used at a large scale (Asenjo, 2003). These all exploit the partitioning of the product between the feed stream and the solvent while minimising any detrimental effects of the process such as the emulsification or separating time of the phases (Seader and Henley, 1998). Many factors must also be considered when selecting the optimum solvent such as selectivity, regeneration, viscosity and density differences. These factors must all be considered in the overall running of the process (Cusack and Fremeaux, 1991).

This purification method is also used to recover enzymes and proteins from the aqueous broth to an immiscible solvent, such as ethyl acetate. The LLE process is used in the large scale purification of 6-APA using a mixer-settler device (Thornton, 1992). However, the large scale LLE process has a high Hazchem risk due to the large solvent volumes that are required. Therefore, the use of industrial scale LLE is limited to manufacturing, and process developments are carried out at laboratory and pilot scales. The scale-up of the LLE equipment has traditionally been carried out using results from pilot scale experimentation, together with engineering models.

1.5.1.1.2 Laboratory LLE

The laboratory scale LLE process equipment includes stirred tank or column extraction vessels that can be operated batchwise or continuously, which are mixed using an impeller or a horizontally rotating platform. This process scale can be carried out at 10 mL to 100 mL, but the Hazchem hazards and financial experimental costs become increasingly significant and limit the range of experiments.

There are a number of different types of automated laboratory equipment that can be used to carry out laboratory scale LLE processes, such as the Mettler Toledo's Myriad ALLEX LLE workstation (7 to 26 mL and ASPEC (20 mL) that provides two phase mixing, separation, dilution and reaction vessel washing functions. The equipment carries out simple and scalable liquid processing that uses flexible vial formats, similar to those used by chemists who need to work up multiple soluble products quickly and easily. This equipment can be operated within a flow cabinet, reducing the Hazchem risk and increasing the pipetting accuracy. The automated laboratory LLE equipment requires larger reagent volumes that increase the cost of experimentation, making them less suitable for initial optimisation experimentation when the new chemical entity is in short supply.

1.5.1.1.3 Automated Microscale LLE

LLE is one of many downstream processes that have been automated and its wide use as a primary purification technique to isolate compounds of interest makes it a valuable process for automation. The attributes of the automated LLE process are simple, rapid and convenient (Cusack and Fremeaux, 1991), which indicates its popularity as a separation process.

Automation has already been applied to the purification of biological samples and combinatorial chemistry libraries using existing liquid handling workstations or specific process equipment for small scale work (0.5 mL to 2 mL). The Tomec Quadra 96 liquid handling system (1.2 mL, Watt et al, 2000), the Packard Multiprobe II liquid handling workstation (1.2 mL, Zhang et al, 2000b), and the Beckman Biomek 1000 system (0.5 mL, Jemal et al, 1999) have been used for automated sample preparation. This research demonstrated the suitability of LLE in its translation to microscale experimentation, utilising the 96-well plate format and the liquid handling systems (section 1.8.2.1). However, these examples of small scale LLE processes required larger working volumes than those used in the microscale LLE, some of which were not fully automated. These automated laboratory LLE systems were not compatible with the 96-well format and were designed for a specific process operation.

1.5.2 Solid Phase Extraction

Solid phase extraction is an established purification process, which has been used to purify contaminants from a liquid feed (Sherwood 1952). Examples of SPE include the removal of trace organic compounds from drinking water using activated carbon particles, coloured compounds from vegetable oils, water from organic liquids and products from the reaction product stream (Seader and Henley, 1998). SPE is an important process for the purification of compounds that are not suited to distillation or crystallisation due to their chemical sensitivity, such as biopharmaceuticals.

SPE has been used extensively as an industrial process to concentrate and purify compounds from a liquid feed (adsorbate), which has been used for the large scale recovery of antibiotics (Jenkins, 1999). Large scale commercial SPE equipment includes fixed-bed adsorbers, which are stirred or sparged to keep the adsorbent in suspension in order to accelerate mass transfer (McCabe et al, 2001b). The SPE resin is added to the fermentation broth to remove the soluble products (*in-situ* product removal). The resin is agitated to facilitate mass transfer of the product onto the resin before the phases are separated and the product is eluted from the resin (Lye and Woodley, 1999). The adsorbate is recovered by the addition of an eluting solution which regenerates the adsorbent. This method of purification produces high

quantities of waste materials whose disposal generates environmental issues. The adsorbent can be regenerated to increase its use and cost effectiveness.

SPE involves the partitioning of a solute between the two phases: bulk solution and porous solids (Bailey and Ollis, 1984). This allows the separation of contaminants from gases or liquids onto small porous particles (500 $m^2.g^{-1}$ to 1000 $m^2.g^{-1}$) of adsorbent material. The SPE materials can be inorganic (silica, carbon, organic dextran, polystyrene) or composite (silica, dextran). Activated carbon is termed an organic adsorbent that is rigid, stable and polymorphous. It has low selectivity and its regeneration is difficult to perform (Jenkins, 1999). The contaminating material is adsorbed onto the particle surface or the walls of the pores within the particles by the hydroxy group that hydrogen bonds the solute to. The mass transfer of this material is accelerated by the SPE method, which enhances convective and diffusion mass transfer. Separation of the compounds occurs because of differences in their molecular weight, shape, and their polarities, which in turn influence the molecule to be preferentially retained on the adsorbent. The compound is held strongly at the surface or within the adsorbent's pores, however large compounds may have their access restricted due to their size.

Solid phase extraction is the preferred separation process for the separation of dilute, soluble compounds. SPE is used to directly recover high value biopharmaceuticals and proteins, as well as antibiotics (Chaubal et al, 1995) directly by *in-situ* product removal from the fermentation or bioconversion product streams, which allows both product concentration and purification.

1.5.2.1 Scale of Operation of SPE Process

There are a variety of scales of operation for the SPE process. The SPE process can be carried out at an industrial scale (section 1.5.2.1.1), laboratory scale (section 1.5.2.1.2) and microwell scale (section 1.5.2.1.3). These process scales are discussed and compared in detail below. The advantages and disadvantages of these SPE formats are highlighted in table 1.5.2.1.1. The scale up issues related to SPE are also considered (section 1.5.2.1.4).

SPE Formats	Advantages	Disadvantages
Cartridge	High purity devices with low extractable contents	Restricted flow rates Top frit plugging by suspended particles in sample – slowing process
Disk	Higher flow rates than cartridges without channelling and sorbent trapped in glass fibre matrix High cross sectional area Thin sorbent bed	Restricted flow rates Top frit plugging by suspended particles in sample – slowing process PTFE low flow rate due to low porosity
96-well plates	Small volume SPE (50 – 100 mg) Rapid sample preparation Low void volume Compatible for automation Low desorption volume (100 – 200 μL)	Difficulties in resin dispensing Fixed resin mass – unsuitable for characterisation studies
Pipette tip	Low void volume Compatible for automation Low sorbent bed masses Min desorption volumes	Not compatible with all pipettes or liquid handling workstations
Microfibre (Solid phase micro Extraction)	Direct desorption into GC for sample preparation	Unsuitable for resin characterisation studies

Table 1.5.2.1.1. Advantages and disadvantages of different solid phase extraction formats.

1.5.2.1.1 Industrial Scale SPE

Industrial scale SPE has been used for the large scale purification of many pharmaceuticals *e.g.* antibiotics. This process has been used with the adsorbent in a fixed bed separator that contacts the two phases whilst confining the solid phase. The fixed bed separator is a tank with perforated plates for the porous solids to sit on, allowing the liquids or gases to flow over them (McCabe et al, 2001b).

The concentration of the liquid phase decreases with time as the adsorbate is adsorbed onto the adsorbent particles. The rate of this is dependent on the position of the particles in the bed, with those most distant from the inlet having the longest delay in adsorbing onto the adsorbate. The concentration of the liquid phase decreases exponentially within the bed with the distance from the inlet and with the time taken to move the mass transfer zone down the bed. This phenomenon makes *in situ* analysis of the concentration profile difficult (McCabe et al, 2001b).

Fixed bed separators are designed by considering the adsorbent material, particle size and fluid velocity based on the bed length or breakthrough time (McCabe et al, 2001b). A shorter bed length requires less adsorbent material and a lower pressure drop, but requires more frequent regeneration. The solid-liquid adsorption process requires smaller particles and lower liquid velocities compared to the solid-gas adsorption process to facilitate mass transfer.

1.5.2.1.2 Laboratory Scale SPE

Laboratory scale SPE has traditionally been used to carry out preliminary investigations into the adsorbent and adsorbate in order to refine the SPE methodology prior to scale-up (Masel, 1996). This work has been carried out using stirred tank batch reactors or small packed columns to generate characteristic adsorbent capacity data and isotherms for the SPE process.

Laboratory scale SPE uses formats applicable to automation and has utilised a number of different formats in order to accelerate this research. Disposable cartridges were introduced in 1978, syringe-type in 1979 that were made from polypropylene or polyethylene, and in the early 1980s on-line pre-columns coupled with liquid chromatography, and more recently the

96-well plate format. The syringe format uses filter discs containing the SPE adsorbent particles entrapped on a membrane, which allows the elution of the compounds without any adsorbent fines contaminating the product, which is sensitive to blockages (Plumb et al, 1997). In addition, there was specific laboratory automated equipment designed for SPE using the 96-well format, such as ASPEC. This equipment could handle 8 mL samples (Dilkin et al, 2001) and helped to increase the throughput of the process. In addition, the extraction tubes are prepared using the semi-automated micropreparation system to contact the liquid phase with the pre-filled adsorbent tubes, which have previously been used for sample preparation (Kaye et al, 1996).

All of these laboratory scale formats were filled with an increasing range of adsorbent resins. These pre-filled SPE formats all contained a fixed mass of resin, which was in excess to ensure contaminant capture. This is useful for initial screening of the resins for sample preparation, adsorption and elution of a novel compound, but it is unsuitable for later stage process optimisation as these formats are not particularly versatile and cannot be used to generate adsorbent isotherms.

1.5.2.1.3 Automated Microscale SPE

Microwell scale SPE processes have been used to rapidly prepare samples from combinatorial chemistry libraries and high throughput screening experimentation (Welch et al, 2002). This has utilised various automated liquid handling workstations and a variety of adsorbents (table 1.5.2.1.3.1). The microscale SPE process used 96-well plates that were fitted with cartridges (Gauw et al, 2000) or microwell plates available pre-filled with a variety of adsorbent resins. These have been used for the simple sample capture stage of sample preparation and each well contained a fixed mass of adsorbent resin. The SPE process is suited to the 96-well format, making it one of the most popular sample preparation techniques (Biddlecombe and Pleasance, 1999).

A semi-automated SPE method was developed for purifying plasma samples (0.12 mL) for the extraction of fluprostenol (Gauw et al, 2000) and a cyclooxygenase inhibitor (Mathews et al, 2001). These semi-automated SPE methods used the automated workstation to prepare the

Authors	Workstations	Type of Adsorbents	Feed Streams	Adsorbate	Precision % CV
Parker et al, 1996	Zymate XP	C18. C8, PH, CH, C2, CN	Biological fluids – human plasma	Compound 1 & 11	2.5 – 2.9
Dilkin et al, 2001	ASPEC	C18 silica, SAX	Corn	Natural contaminants	3.7 – 4.4
Kristenson et al, 2001	ND	C18, C8 silica, silica gel	Fruit pulp	Pesticides	10 – 13
Steinborner and Henion, 1999	Quadra 96	ND	Plasma	Methotrexare, 7OH-MTX	<15
Chen et al, 2002	Quadra 96 Multiprobe	Verian Certify™	Plasma	hydromorphone	< 4.7
Janiszewski et al, 1997	Quadra 96	Empore particle loaded membrane Bonded silica in PTFE matrix	Serum	Ziprasidone	3.9 – 10.
Kaye et al, 1996	ND	C18 bondasil	Plasma	Darifenacin	3.6 – 18.8
Davis and Swayze, 2000	Parallel array synthesiser	Benzylamine, Phe-benzylamine, nosyl-Phe-benzylamine	ND	Combinatorial Chemistry Library	ND
Cheng et al, 1998	ND	Polypyrrole SPME	Urine, plasma, culture media	Verapamil, noraverapamil, gallopamil, D715	2.9 – 4.7
Papagiannopouloulos et al, 2002	ASPEC	Diatonamous earth	Malt residues	Malt proanthocyanidins	Reproducibility 5

Table 1.5.2.1.3.1. Automated solid phase extraction procedures with details of the authors, liquid handling workstations, type of adsorbents, feed stream compounds, adsorbates and precision values. (ND = Not detailed or stated in paper).

wells with liquid samples, but also required human intervention, which instigated the development of integrated vacuum devices to fully automate the SPE process. This automated SPE process used the 96-well format to rapidly prepare biological samples (Parker et al, 1996, Shou et al, 2002). The automated SPE methods used small sample volumes, such as 0.1 mL plasma samples for the extraction of protease inhibitors (Peng et al, 2000b). The samples can be processed in parallel, which increases the sample throughput, and this is now the technique of choice with LC-MS/MS analysis (Biddlecombe and Pleasance, 1998). The automated SPE method using 96-well plates has been developed for the clean up of samples (Shou and Pelzer et al. 2002, Peng et al, 2000b). The microscale SPE experimentation developed and investigated in this research will offer a fully automated, low volume approach to SPE process optimisation. It is hoped that this generic approach will be used in process design for new pharmaceuticals.

1.5.2.1.4 SPE Scale-up Issues

When considering the scale-up of the SPE process, the equipment, adsorbent and adsorbate must each be considered. There is great variation in the equipment used at each scale, so only limited direct extrapolation of the data can be carried out. However, the adsorption profiles for the adsorbents are characteristic of the resins themselves and this data is key to a SPE process. The microscale and laboratory scale SPE processes could be used to investigate the adsorbent and adsorbate equilibrium isotherms.

The study of industrial scale SPE equipment has produced a number of methods for designing similar new equipment. These methods can be used to predict the shape of the equilibrium isotherm, the width of the mass transfer zone, breakthrough volume and length of unused bed. There are a number of published calculations for the mass transfer zone and concentration profiles (Asenjo, 2003). Normally adsorbents are scaled up from laboratory experiments in small diameter beds to the larger scale maintaining the particle diameter, superficial velocity and bed length. However, this information could be elucidated using the microscale SPE process.

1.6 Synthesis of Pharmaceuticals

1.6.1 Synthesis Routes

The synthesis routes for pharmaceuticals describe how the pharmaceuticals are made using chemical or biochemical catalysts. A chemical catalyst is a chemical compound that changes the rate of reaction by lowering the energy required. Such compounds include transitional metal salts (zinc, cobalt and iron), which are cations. A biological catalyst lowers the reaction energy by using an enzyme from a biological organism. These catalysts are compared in section 1.6.1.1. The use of biocatalysts is discussed in section 1.6.1.2, detailing their improvements and their efficient use in bioconversions. The bioconversion model systems (section 1.6.1.3) are considered for the development of the microscale processes.

1.6.1.1 Comparison of Biochemical and Chemical Synthesis Routes

The synthesis route of a pharmaceutical can be achieved using a chemical or biochemical catalyst. The choice may depend upon the need for molecular stereoselectivity. This is important when synthesising pharmaceuticals and biological compounds. Different stereoisomers of a drug can produce considerable side effects, as seen with thalidomide. The biochemical and chemical synthesis routes are compared in table 1.6.1.1.1.

Traditional chemical catalysts have high efficiency, but can have limited stereospecificity, whereas biocatalysts have many benefits over conventional chemical catalysts including their stereospecificity, regiospecificity and mild reaction conditions. This makes them suitable to producing biological pharmaceuticals, such as antibiotics (Lilly, 1992). These benefits make biocatalysts more attractive than chemical catalysts for the synthesis of many pharmaceuticals, such as the asymmetric reduction of aldehydes to produce ketones (Tshaen et al, 1995). The new generation of biocatalysts is now able to work in a variety of conditions including organic liquids, high temperatures and extreme pH conditions (Lilly, 1992). There are now biocatalytic counterparts for almost all chemical catalysts (Taylor et al, 2000).

Key Factors of Synthesis Route	Biocatalyst	Chemical Catalyst
Reaction	Separate racemic chiral enantiomers Reduce activation energy of specific reactions, increasing conversion rate High reaction efficiency Self-regulate environment	No substrate inhibition No product inhibition
Biocatalyst	Substrate specificity Genetic engineering improvements to productivity	Not affected by pH Not destroyed by temperature extremes
Substrate	Regio & Stereo-specificity	No inhibition
Product	Stereo-specific conversion	No inhibition
Cofactors	Regeneration	None required
Operation	Mild conditions	Extreme conditions required Operational stability
Operational environment	Most, active in aqueous environments Some active in organic environments	Reagents soluble
Productivity	Improving with current research	Productivity high
Down stream processing	Few side reactions reduce DSP stages	Complex removal of contaminants
Environmental issues	Biodegradable catalyst Renewable source Less waste disposal Low energy demands	Harsh conditions of extreme pH and temperature conditions

Table 1.6.1.1.1. Comparisons of biochemical and chemical catalysts used in synthesis routes by assessing key factors affecting their operation.

1.6.1.2 Biocatalysts

Biocatalysts (biological catalysts) are used to catalyse bioconversions, synthesising biological pharmaceuticals. There are a variety of biocatalysts that are used for numerous bioconversions, as illustrated in table 1.6.1.2.1. The biocatalysts are obtained from a range of micro-organisms (appendix 2). They are used in a number of preparations including whole cells, membrane bound fragments, immobilised cells (appendix 3) and free or immobilised isolated enzymes (Lilly, 1992). There have been a number of alterations made to existing biocatalysts to improve their activity and performance. These include genetic improvements to the biocatalyst (section 1.6.1.2.1) and modifications to the bioconversion efficiency (section 1.6.1.2.2).

1.6.1.2.1 Biocatalyst Improvements

Improvements to biocatalysts and their producing micro-organisms increased their productivity, which has raised interest in the use of bioconversions for the synthesis of pharmaceuticals. This was due to improvements to the affinity and activity of the biocatalyst. This has been achieved by genetically engineering DNA of the micro-organisms by directed evolution or the addition of vector DNA. These techniques can alter the structure of the biocatalyst, improving its performance, binding affinities and catalytic activities. Additional benefits include the process being potentially cleaner by producing less waste and using kinder process conditions.

Genetic engineering has been used to improve the productivity of microbial strains by increasing the number of biocatalytic enzymes within the cell as a result of increasing the number of copies of the gene that encode for the biocatalyst. This increases the activity of the whole cell. This can also be achieved by replacing the promoter regulating the expression of the gene with a more active one, or by adding an inducer upstream of the gene that is regulated by the addition of a chemical inducer into the fermentation media to ***activate gene*** expression. One example, IPTG (isopropylthiogalactoside), is a lactose analogue that is a chemical inducer that artificially induces the lac operon. This regulates the production of the

Biocatalysts	Chemical Reactions	References
Agrobacterium radiobacter	D/L-isopropylhydantion -> D-valine	Battilotti et al, 1988
Alcohol dehydrogenase	NAD+ +H_2O ⇒ NADH + OH^-	Kawamoto et al, 1989
Alpha cymotrypsin	N-acetyl-L-phenylalanine ethyl ester ⇒ N-acetyl-L-phenyl- L-lysine	Asaro and Wilson, 1989
Aspergillus niger nitrilase	Progesterone ⇒ 1-alpha-hydroxyprogesterone	Taylor et al, 1999
Candida rugosa lipase	2,2,2-trifluoroethyl suprofen ester ⇒ (S)-suprofen ester	Tsai and Huang, 1999
Escherichia coli	2'Guo/2'Thd ⇒ 5'ethyluracil/(E)-5-(2-bromovinyl) uracil	Kalinichenko et al, 1990
Escherichia coli Transaminase	2-ketoacid L-aspartic acid ⇒ L-amino acid	Taylor et al, 2000
Geotrichum	2-substituted-3-carbonyl butanoate ⇒ 2-substituted-hydroxy butanoate	Pan Bingfeng et al, 1998
Gluconobacter oxydans	D-glucose ⇒ D-gluconic + keto-D-gluconic acids	Beschov et al, 1995
Glycosidase	Carbohydrate + vegetable oils ⇒ glycolipid	Lang et al, 1995
Humicola langinosa Lipase (Lipolase)	p-Nitroophenyl butyrate hydrolysis	Crooks et al, 1995
Lipase	Triacylglycerols -> acetylglycerols	ShoJung et al, 1995
Methylosinus trichosporium	*Methane ⇒ Methanol*	Sugimori et al, 1995
Micrococcus freudenreichii	Madelic acids ⇒ R-mandelic acid	Takashi et al, 1995
Nitrile hydratase	Acylonitrile ⇒ acylamide	Taylor et al, 2000
Penicillium roquetortii	Octanoic acid ⇒ 2-heptanone	Larroche et al, 1989
Pseudomonas dehalogernase	R-2-halopropionic acid +(R, S)-2-chloropropionic acid ⇒ (S)- 2-chloropropionic acid + (S)-lactic acid	Taylor et al, 2000
Rhizomucor miehei lipase (Lipozyme)	1-octanol + decanoic acid ⇒ octyl decanoate	Crooks et al, 1995
Thermolysin	Z-aspartate (alpha COOH) + phenylalanine methyl ester ⇒ Z-aspartame	Taylor et al, 2000

Table 1.6.1.2.1. Examples of chemical reactions catalysed using biocatalyst with relevant references.

protein, allowing the protein to be expressed once the fermentation broth has reached a suitable level of biomass.

1.6.1.2.2 Bioconversion Efficiency

The design of a bioconversion process must consider the properties of the biocatalyst, reactor and product recovery in order to create an efficient process. The characteristics (thermal and pH stability) of the substrate and products, as well as the biocatalyst itself, must be considered (Lilly, 1992). A compromise between the ideal conditions for each of these factors will be required to produce the optimum efficiency for the overall process.

1.6.1.3 Experimental Model

The experimental model used in this research for the basis of the feed material was the penicillin acylase (PA) bioconversion product stream. This is an important biocatalyst used in the bioconversion of penicillin to produce 6-APA. The product is the precursor of semi-synthetic antibiotics, including cephalosporin. The methods of production, isolation and immobilisation of this biocatalyst are identified in this section, together with the structure and properties of PA. The details of the hydrolysis reaction PA catalysed, its characteristics, and the kinetics of the bioconversion are explained in section 1.6.2.4.

1.6.2 Penicillin Acylase

1.6.2.1 Structure of Penicillin Acylase

Penicillin acylase is encoded by a specific nucleotide sequence (*pac* gene) that is translated into the amino acids sequence encoding for the enzyme (Chou et al, 1999). The expression of this *Escherichia. coli (E.coli)* gene is regulated *in vivo* by both temperature and phenylacetic acid concentration (Duggleby et al, 1995). The translation of the mRNA from this gene produces a periplasmic 80 kDa heterodimer containing the A and B chains of 209 and 566 amino acids separated by a 54 amino acid spacer, plus a 26 amino acid signal peptide. The signal peptide guides the heterodimer and is exported to the cytoplasm where the precursor is cleaved, producing the A and B chains (Mwangi and Garside, 1987), of 20.5 and 69 kDa (Oliver et al, 1985). The interaction of the amino acids forms the three-dimensional structure of the enzyme and the N terminal serine of the 69 kDa chain forms part of the catalytic site (Duggleby et al, 1995).

1.6.2.2 Production of Penicillin Acylase

Penicillin acylase is synthesised by a variety of organisms, including bacteria, fungi, yeast, asconomyces, plant cells and animal cells (Vandamme and Voets, 1974). The activity of PA was characterized into two distinct types (Warburton et al, 1973). Type 1 PA is isolated from fungi and *streptomyces*, which hydrolyse phenoxymethyl-penicillin (penicillin V) more readily than benzyl penicillin, (Pen G). Type 2 PA is isolated from bacteria that prefer benzyl penicillin (penicillin G) substrate, although there are some exceptions to this general rule (Cole et al, 1975).

PA is available in a number of different preparations (section 1.6.2.3), each with their own benefits and limitations for use in the bioconversion of penicillin. These include whole cells, free enzymes and immobilised enzymes. Both whole cell and immobilised enzyme preparations have restricted access for the substrate to diffuse to the active site of the enzyme compared to free enzymes. This is inhibited by the conditions within pockets of high product concentration, which reduce the efficiency of the process. However, the free enzyme is more sensitive to denaturing conditions. Immobilised enzymes have the greatest bioconversion efficiency, high mass transfer rates and increased stability, which make them suited to large scale bioconversions.

Penicillin G acylase was commonly commercially purified from genetically modified *E. coli* (Braun et al, 1989), or *Saccharomyces ceriviseae* (Abbot et al, 1976) because of the organism's high metabolism and rapid generation times. The PA isolated from these organisms had reduced substrate inhibition (Guisan et al, 1990), which produced high yields. The industrial PA fermentation process has been carried out in either a stirred tank or a fluid bed reactor.

1.6.2.3 Isolation of Penicillin Acylase

The typical isolation of penicillin acylase from *E. coli* requires a number of separate steps (Balsingham et al, 1972). The key stages of the isolation process are: cell separation, homogenisation, clarification, precipitation, and purification. The purification step is important to remove β lactamases, as they hydrolyse the amide bond of the β lactam ring,

denaturing penicillin to penicilloic acid. The purification step includes fractional precipitation, dialysis, and adsorption chromatography (Cole et al, 1975).

1.6.2.4 Bioconversion Characteristics of Penicillin G by Penicillin Acylase

Penicillin acylase hydrolyses penicillin G to produce 6-aminopenicillanic acid and phenylacetic acid (PAA) (Savidge, 2001). The enzyme binds the substrate and water nucleophiles attack the molecule, releasing the nucleus, 6-APA, and the side chain phenylacetic acid (PAA), as indicated in figure 1.6.2.4.1. These reagents have characteristic structures that effect their thermal and pH stability (appendix 4).

The PA reaction is carried out in a stirred tank or packed bed reactor with the enzyme, PA. The production of 6-APA generates 100 to 1000 Kg $_{6\text{-APA}}$ per Kg of immobilised enzyme for 7% to 10% Pen G depending on the degree of agitation and enzyme preparation. The enzyme produces more than 97% conversion within 90 to 180 minutes (Shewale and Shivaraman, 1989). The theoretical yield of this process is limited by the chemical equilibrium, which is dependent upon the rate of substrate association, formation of the acyl-enzyme complex, nucleophilic attack of water and dissociation of both the acyl-enzyme complex and the side chain, phenylacetic acid (Spiess et al, 1999, van der Wielen and Lankveld, 1996).

1.6.2.4.1 Penicillin Acylase Activity and Hydrolysis Conditions

The operational temperature and pH condition of the hydrolysis reaction must be carefully controlled to maximise its activity and stability of the PA. During the hydrolysis reaction, the conditions are maintained at p 7.5 and 37°C (Vandamme and Voets, 1974). The maximum activity of PA was seen at pH 7.8-8 and temperature 50-52°C, but these conditions would compromise the stability of the product, 6-APA. The hydrolysis of penicillin releases heat of 35.9 $\pm$ 5.7 kJ at 308 °K and pH 7.5 (Godoy et al, 1996), and heat is also generated by the neutralisation of the side product, PAA.

1.6.3 6-APA Purification

The purification process for 6-APA is outlined in figure 1.6.3.1. The isolation of 6-APA is carried out after the removal of PA from the hydrolysis reactor by filtering the fermentation broth and concentrating by reverse osmosis. This reduces the solvent costs in LLE and

increases the efficiency of the precipitation process. The removal of PAA and residual Pen G from the product stream is achieved by LLE at pH 2.5 with methylisobutyl ketone using a 0.5

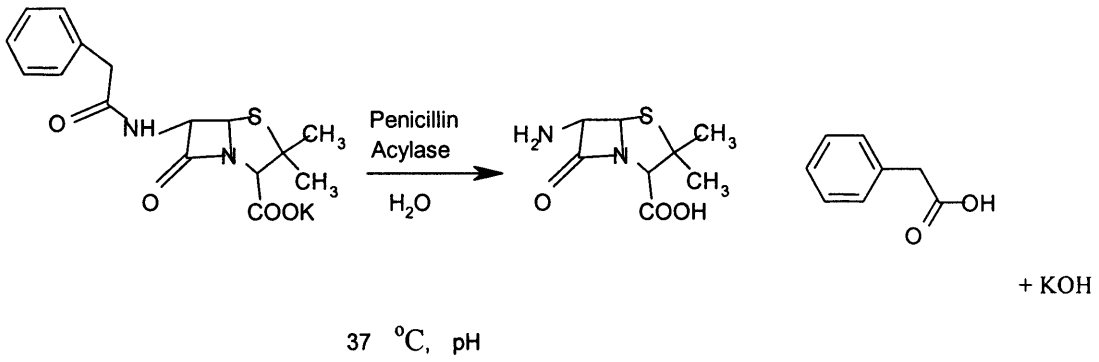

Pen G → 6-APA + PAA

37

(c) **(d)**

(pK = 4.5) (pK_1 = 2.5, pK_2 = 4.25) (pK = 4.9)

Figure 1.6.2.4.1. Structural formulae of the hydrolysis of benzyl penicillin (Pen G) by penicillin acylase (PA) to produce 6-amino penicillanic acid (6-APA) and phenylacetic acid (PAA) taken from Vandamme and Voets (1974) ,pK values taken from (van der Wielen and Lankveld (1996), Lee et al, (1998) and Rapson and Bird (1963).

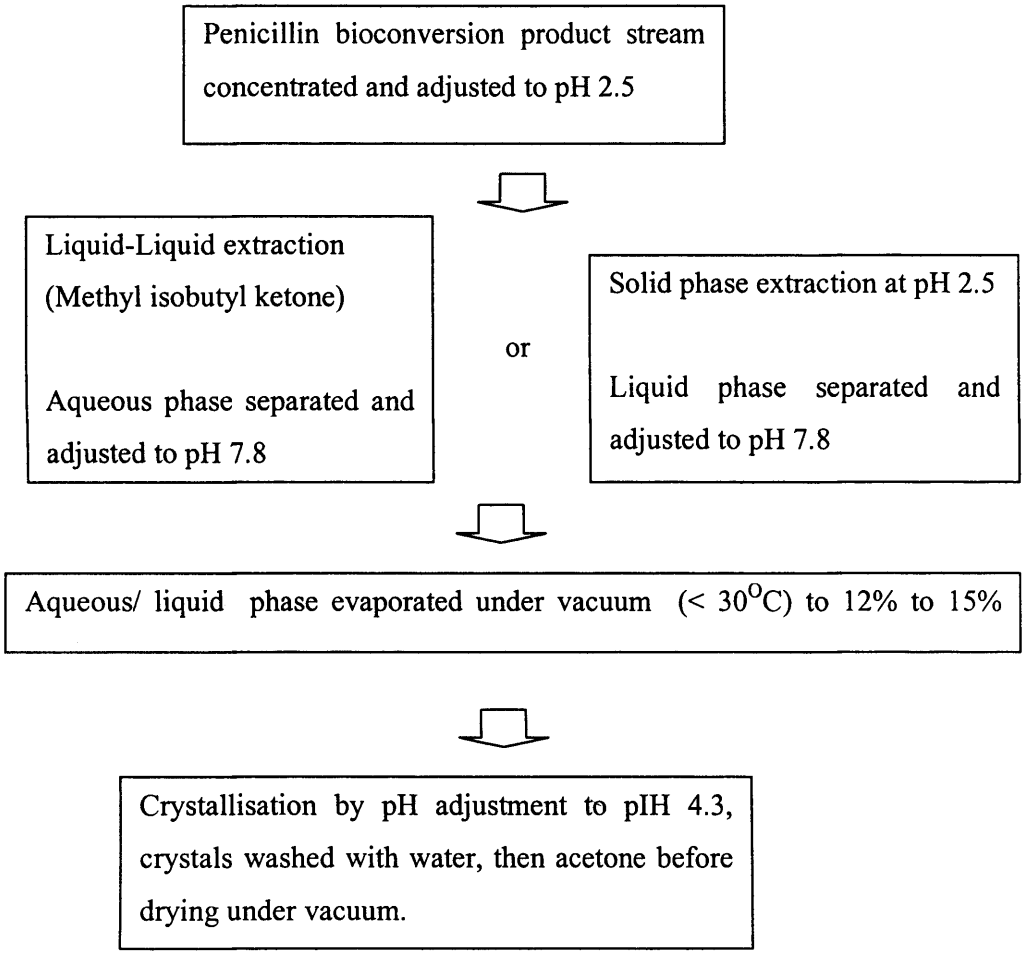

Figure 1.6.3.1. Flow diagram of the laboratory scale purification processes of 6-APA from the penicillin bioconversion product stream, information from Cole et al (1975) and Ghosh et al (1997 page 118).

volume fraction. After phase separation, the pH of the aqueous phase is adjusted to pH 7.8 in order to limit degradation of 6-APA (Vandamme and Voets, 1974). The 6-APA solution is concentrated by evaporation under vacuum (30 °C) to a concentration of 12-15%. The product is precipitated by adjusting the pH conditions to its equilibrium constant (pK), pH 4.3 and the crystals are washed with acetone prior to drying. The by-product, PAA, can be extracted and used in the fermentation process to adjust the pH conditions. Other solvents used for this extraction process include acetone, methylene chloride and butyl acetate (Shewale and Shivaraman, 1989). Alternatively, a spray drying method can be used for the isolation of 6-APA or PAA after extraction with amyl acetate or butanol. The reaction mixture can be spray dried directly and the acids extracted (Cole et al, 1975).

The final stage of the 6-APA purification process is crystallisation, which is achieved by pH precipitation. The overall yield of 6-APA is 90% and crystallisation efficiency is 94% (Tavare et al, 1999). In addition to this purification process, ion exchange chromatography (Van der Wielen and Lankveld, 1996) and SPE have been used to purify 6-APA.

1.7 Automated Process & Equipment Requirements

1.7.1 Process Automation

Automated equipment has been used extensively in high throughput screening and combinatorial chemistry to increase the speed of drug discovery. Many of the commercially available automated equipment and devices described in section 1.3.2 can be linked together to form an automated laboratory. These instruments will be used to automate the individual fermentation, bioconversion and various purification processes in order to automate another part of the R&D process. The use of this equipment will facilitate the rapid generation of experimental data and process optimisation.

The automated laboratory contains pieces of automated equipment and will be used to rapidly assess the entire microscale biochemical engineering process by screening process interactions, parameters, conditions and reagents (Hazard Evaluation Laboratories, 2000). The automated laboratory requirements are a combination of those for the individual processes and general logistical requirements, which are highlighted in table 1.7.1.1. These focus on the necessary compatibility of the equipment and validity of the data generated.

Microscale System Requirements	
Liquid handling	Accurate liquid withdrawal & dispensing into to a variety of locations
	Timed addition to specific wells
	No sample contamination
	Accurate transfer of samples between different microplate formats with sample identification
	Mixing
	Handle range of liquid viscosities
	Handle organic/ volatile liquids
Operation	Compatible with different size wells
	Capacity to transfer plates between equipment
	Spotting on solid surfaces
	Capacity to add solids
	Resistance to organic solvents
	Operate under CO_2 atmosphere
	Automation between different unit operations
	Ability to shear samples
	Capacity to centrifuge
Functionality	Capacity to filter
	Capacity to heat and cool
	Clean pipette tips & wells in place
	Agitation/ vibrating plate
	Continuous pH monitoring
Analysis	Spectrometric monitoring
	Rapid data retrieval and analysis
	Compatibility between equipment
Software	Windows operating system for ease of use/ programming
	Good data handling system
	Compatible with existing software packages
Robotic arm	Smooth transfer between pieces of equipment so no liquid displacement from the wells or cross contamination
	Software to communicate with other pieces of equipment and co-ordinate movements including opening lids

Table 1.7.1.1. Requirements of an automated system, focussing on key aspects of automated equipment.

1.7.2 Requirements of the Automated Equipment

The requirements of the individual automated equipment used for automating equilibrium separation processes will be discussed here. The key requirement for their reproducible operation is their accurate and precise liquid handling (section 1.7.2.1) and solid handling (section 1.7.2.2) capacity. The performance of the automated platform was assessed for its liquid handling (section 3.2.1) and solid handling (section 3.2.2).

1.7.2.1 Liquid Handling Requirements

Liquid handling capability is required by many pieces of automated equipment, such as automated samplers for analytical devices, liquid handling workstations and chemical synthesisers. The accuracy of liquid handling ensures that the results are quantifiable, allowing their use in mass balancing. The accuracy of the liquid handling must cover the required liquid volume and transfer the aliquot between locations, which is an important feature of the liquid handling workstation. This ensures the reproducibility of automated laboratory methods (appendix 10.4.2.2), such as those used in HTS and combinatorial chemistry.

Most automated equipment that can handle liquids has the facility to aspirate and dispense liquids. This is used to mix, dilute and transfer samples from a variety of receptacles and add reagents using a pause function to allow reaction progression. The liquid handling requirements of the workstation are stated in table 1.7.2.1.1. The accuracy of this operation must be achievable for a range of liquids with different viscosities and densities delivering them to correct locations. The liquid handling workstation has a number of parameters that can be modified within the performance files to ensure that this occurs (section 2.2.1.4.1).

The mixing of reagents is essential for homogeneity to ensure rapid mass transfer and reaction development. This is important for many processes including fermentation and equilibrium separation processes. Microscale mixing can be achieved using a variety of methods (section 1.8.2.1.3), including the liquid handing workstation, by repeatedly aspirating and dispensing a percentage of the total volume over a number of cycles (section 4.2.1.1). This transfers energy into the system and facilitates diffusion.

Liquid Handling Workstation Features	Microscale Considerations
Equipment	Liquid handling workstations (table 1.3.2.1.1.1)
1-200 μL (disposable tips)	Volume Accuracy Dispensing Precision Dripping after dispensing volume Cross contamination risk between wells
1-10,000 μL (fixed tips)	Volume Accuracy Dispensing Precision Dripping after dispensing volume, contamination risk Cross contamination risk between wells
Liquid sensing	Not for use with organic solvents
Reaction/ Extraction wells	Evaporate from sample in well: - affecting concentration - affected by well shape - prevented by PTFE lid/ adhesive seal
Sampling	No cross contamination between samples No contamination of another phase Use of compatible vials for analysis
Sample Separation in tip (air gap)	Evaporation in tip: - damages instrument, - contaminates samples - affects concentration
Mixing	Physical properties: Cycles of aspirating & dispensing Dielectric constant of reagents) Shear damage
Phase separation	See table 1.7.2.1.2
Clean in place	Possible during test between reagents to avoid contamination Internal and external tip surfaces Unknown effectiveness

Table 1.7.2.1.1. Microscale liquid handling considerations for the selection of liquid handling workstations.

The issues related to the separation of the two liquid phases are considered in table 1.7.2.1.2. This identifies the requirements for automated equipment to achieve liquid-liquid separation; equipment, operation, liquid handling, method of separation and sample analysis.

1.7.2.2 Solid Handling Requirements

Many biochemical engineering processes require initial preparation of reagents. This often involves dissolving or re-suspending reagents in crystalline, dry powder or resin forms. The dry reagents can be dispensed using a microbalance to a limited degree of accuracy, but the wet reagents such as immobilised enzymes, create a greater solid handling problem due to their cohesive nature. There are a number of instruments commercially available for solid handling (section 5.2.2.3) that have varying degrees of accuracy. The requirements of the solid handling automated equipment are detailed in table 1.7.2.2.1. These include accuracy, precision, reproducibility and reliability. The instruments must be compatible with multiwell plates and the existing automated equipment to facilitate the successful automated biochemical engineering laboratory.

1.7.2.3 Solid-Liquid Separation

The requirements of automated equipment and devices available for solid-liquid separation are highlighted in table 1.7.2.3.1. The liquid handling workstation is primarily used with a filtration rig fitted with specialist filter plates (section 1.3.1), which have been used in sample preparation (section 1.4.3.2.4).

Solid-liquid separation has a potential application in bioconversion for removing cells from a fermentation broth, beads with immobilised enzyme from a bioconversion reaction or removing crystallisation products. These applications share similar microscale issues with liquid handling and solid handling, which were previously discussed in sections 1.7.2.1 and 1.7.2.2, respectively.

1.7.3 Microscale Process Considerations

The processes within biochemical engineering will be discussed, investigating the suitability of existing automated equipment for the generation of an automated microscale process. This section will look at the considerations of automated equipment for fermentation,

Liquid-Liquid Separation Automated Equipment Parameters	Microscale Requirements
Equipment	Liquid handling workstation Centrifuge Filtration device
Operation	Compatible with multiwell plates, including deep well plates Compatible with other automated equipment Compatible software between equipment Minimal requirement for human intervention Speed of operation Rapid set up time required
Liquid Handling	Accuracy of liquid handling for preparation of extraction vessel Ease of dispensing liquid volumes required for microscale experimentation Total dispensing of liquid volume No cross contamination between samples Requirement for cleaning tips Sample contamination Poor liquid sensing boundary of organic and aqueous phases Difficult to recover 100% of one phase Requirement for cleaning in place
Method of Separation	Centrifugation: Equivalent rpm to larger scale equipment: Stability of plates Non adsorbent materials Total dewatering Removal of solids pellet Total well volume before/ after pellet No contamination of liquor with solids as may block pipette tips Filtration: Vary pressure Vary pore size of filter plates Non adsorbent materials Need for human intervention to secure seal on filter plate Danger of damage to membrane Requirement for isolating 1 well
Sample Analysis	Sampling from reaction well Accurate & precise liquid handling for sample removal No contamination between the phases during sampling Mass balancing Rapid quantification of mass in separated phases

Table 1.7.2.1.2. Requirements of automated equipment for reproducible liquid-liquid separation.

Solid Handling Station Features	Microscale Considerations
Commercially Available Equipment	DryPette™, Zinsser Analytic Flexchem rotating incubator system, Robbins Accelerator™ dosing station Resin loader, Radleys
Dispensing Solids	Precise quantification of mass dispenses (+/- 0.1 μg) Dispensing resins, crystals, powders cells and enzyme (sticky) Compatible with multiwell plates Rapid automated dispensing Compacting of solids affecting volume measurements
Transfer of Solids	Accurate transfer to specified location Accuracy and precision of dispensing Effect of static Losses of solids during transfer
Redissolving/ Resuspending Reagents	Compatibility with liquid handling workstation Compatibility with heater/ chiller Shear damage of fragile solids Requirement for mixing Speed of operation
Operation	Isolate 1 well No cross contamination between samples Rapid and effective cleaning in place Change solids during experimentation Time of set-up
Software	Compatible with other automated equipment Compatible with existing software

Figure 1.7.2.2.1. Microscale solid handling considerations for the selection of solid handling stations.

Solid-Liquid Separation Automated Equipment Parameters	Microscale Requirements
Equipment	Liquid handling workstation Centrifuge Filtration device
Operation	Compatible with multiwell plates, inc deep well plates Compatible with other automated equipment Compatible software between equipment Minimal requirement for human intervention to move plates between equipment Speed of operation Rapid set up time required Sampling of filtrate/ liquor for analysis
Liquid/ Slurry Handling	Accuracy of slurry handling Total dispensing of slurry mass No cross contamination between samples Requirement for cleaning automated equipment Sample contamination
Solid Handling	Accurate and precise solids handling Ease of dispensing Requirement for cleaning in place Sample contamination
Method of Separation	Centrifugation – Equivalent rpm to larger scale equipment Stability of plates Non adsorbent materials Total dewatering Removal of solids pellet Total well volume before/ after pellet Contamination of liquor with solids may block pipette tips Filtration – Vary pressure Pore size of filter plates Non adsorbent materials Need for human intervention to secure seal with filter plate Danger of damage to membrane Requirement for isolating 1 well
Sample Analysis	Sampling from reaction well Mass balancing Rapid quantification of mass in separated phases

Table 1.7.2.3.1. Requirements of automated equipment for reproducible solid-liquid separation .

bioconversion and various purification processes, focusing on the equilibrium separation processes that are also important in chemical engineering. Microscale equilibrium processes include LLE and SPE, which place specific requirements on the automated equipment. These will be discussed in sections 1.7.3.1 and 1.7.3.2 respectively.

1.7.3.1 Microscale Liquid-Liquid Extraction Considerations

The microscale LLE process requires an automated platform that reproducibly and reliably handles a variety of liquids with different viscosities or densities, accurately transfers the liquid to specified locations in multiwell plates, mixes the immiscible liquids efficiently, pauses for phase separation to occur, and removes uncontaminated samples. There are commercially available purpose built LLE instruments that operate at the mL scale (section 1.5.1.1) and evaporators (GenVac) that are designed to remove solvents from samples stored in tubes. The important issues arising from microscale LLE are addressed in table 1.7.3.1.1.

1.7.3.2 Microscale Solid Phase Extraction Considerations

The microscale SPE process requires automated equipment that reproducibly and reliably handles the resin solids and liquids, as well as separating them, as previously discussed in section 1.7.2. The required automated equipment includes a liquid handling workstation, solid handling equipment, filtration rig and specialist filtration plates. The use of many pieces of equipment requires software compatibility, as well as the individual accuracy and precision of the instruments (chapter 3). The microscale SPE issues are detailed in table 1.7.3.2.1.

1.8 Critical Review of Background Literature

The literature reviewed the evolution of laboratory equipment, focussing on developments in liquid handling systems and the generation of liquid handling workstations (section 1.8.1). The use of these workstations in the development of the LLE and SPE purification processes (section 1.8.2) assessed their developments by highlighting the limitations in their experimentation and the performance of the processes involved.

Liquid-Liquid Extraction Issues	Microscale Considerations
Equipment	Specific laboratory scale LLE equipment Mettler Toledo ALLEX with glass extraction vessels Chem Speed chemical synthesis station with glass extraction vessels
Liquid Handling	Accurate and precise liquid handling Accurate transferring of organic solvents Evaporation effects – use lid/ seal Cross contamination between samples Requirement for clean in place Minimal manual interaction Safe transfer of organic solvents Safe disposal of organic solvents Dispense required phase volumes
Phase Mixing	Method of mixing: Pipetting Vibrational plate Suitable for enhancing mass transfer Homogeneous reaction volume Turbulent flow Shear damage of fragile solutes Mixing time Mixing velocity Evaporation Degradation of solutes
Phase Separation	Phase settling time, sufficient for accurate sampling of each separated phase without contamination Effect of evaporation Pipette disturbs phase boundary during sampling lower phase, possibility to dispense air into well and delay before sampling Contamination of miscible solvents Method of separation – centrifugation, gravity

Table 1.7.3.1.1. Consideration of the liquid handling workstation for the development of microscale liquid-liquid extraction process.

Solid Phase Extraction Issues	Microscale Considerations
Equipment	Liquid handling workstation Solid handling station
Solid handling	Accurate and precise solid handling of adsorbent resins Cross contamination between samples Requirement for clean in place Minimal manual interaction Required phase masses for isotherm experimentation
Liquid handling	Accurate and precise solid handling of reaction feed Evaporation of conditioning or eluting buffer Safe transfer of conditioning of eluting solvents No cross contamination between wells
Phase mixing	Method of mixing: Pipetting Vibrational plate Suitable for enhancing mass transfer Homogeneous reaction volume Turbulent flow Shear damage of fragile solutes Mixing time Mixing velocity Evaporation Degradation of solutes
Phase separation	Phase settling time Solid- liquid separation sufficient for accurate sampling of each phase without contamination Effect of evaporation Method of separation – centrifugation, filtration

Table 1.7.3.2.1. Consideration of the solid handling station and liquid handling workstation for the development of microscale solid phase extraction process.

1.8.1 Evolution of Laboratory Equipment

The core pieces of laboratory liquid handling equipment were originally pipettes and pumps. "*Pipettes have evolved from little more than glass versions of drinking straws to diverse devices that may be electronic, multi-channel, automated or robotic*" (Lewis, 1997). The automated equipment evolved from developments in liquid handling capabilities and robotic technologies to initially create automated diluting devices. These devices contain a number of dilution programs and store reagents within them that are normally dispensed through either of two dispensing channels. Automated pipetting and diluting devices were developed to cope with the demand from immunoassays using many reagents including monoclonal antibodies in suspension within these multi-step procedures. These devices and the automated pipetting equipment had superior accuracy in relation to manual pipettes (Keightley, 1986). It was predicted that "*there would be a great need to handle a larger number of compounds dissolved in liquids and [a] diversity of assays to adequately measure them*" (Lewis, 1997). The 2-channelled static automated diluting devices were modified in order to create a more dynamic pipetting system. A number of different liquid handling systems were developed, including robotic sample processors, automated pipetting devices and bulk reagent delivery systems (Rogers, 1997) that were all later termed 'liquid handling workstations'. All of these liquid handling devices "*must be accurate and resist contamination, yet work quickly and comfortably in repetitive procedures*" (Lewis, 1997). Many recent applications, such as DNA analysis, require "*automated liquid handling systems to deliver precise volumes*" (Schneider, 1997).

There is a variety of automated liquid handling workstations, which were designed to rapidly deliver small volumes of liquid reagents to precise locations within a 96-well plate or other receptacles. The automated liquid handling equipment generated suitable "*liquid-liquid phase separation* [that] *was an important criterion in the process of drug discovery*" (Rollins and Pochert, 2000) for both analysis and purification. Phase separation was achieved by detecting the phase interface and liquid level by measuring a combination of pressure and capacitance (Rollins and Pochert, 2000). This was used to selectively separate organic and aqueous phases in high throughput screening.

One of these liquid handling workstations (section 1.3.2.1), the Multiprobe II Ex® workstation, can be configured with one to eight pipette tips and is capable of delivering 300

to 1700 samples per hour (Lewis, 1997). This has increased their productivity from preparing 200 multiwell plates per 3 months to 2000 in the same time (Lewis, 1997), which increased sample throughput in certain areas of pharmaceutical R&D. This equipment was routinely used in HTS and CC to accelerate drug discovery (section 1.4.1). The DD process was complemented by the miniaturisation of assays and this highlighted the need for a good maintenance regime to ensure the liquid handling workstation's reproducible operation (Driscoll et al, 1998).

A variety of liquid handling workstations have been developed to handle the delivery of precise volumes of exceedingly small liquid samples, including the second generation Multiprobe that offers *"easy integration and application versatility"* (Schneider. 1997). The automated workstations have used robotics to bring drug development up to speed (Jandu, 2000). The liquid handling workstation was the main piece of automated equipment in the automated platform that was used to carry out much of the experimentation in this research (chapters 3, 4 and 5).

1.8.2 Literature Review of Automated Purification Processes

The development of automated equipment instigated their use for a variety of applications in R&D as the result of their speed and accuracy. Early attempts to purify biological samples prior to their bioanalysis developed semi-automated LLE and SPE processes. These processes used large volumes and were poorly understood in terms of engineering principles or the way they related to other process scales. These methodologies were not generic nor were they fully assessed in comparison with other scales of operation.

The performance of automated liquid handling workstations was assessed in-house (appendix 7) and by a number of independent researchers to ensure accurate liquid handling was occurring. This quantitative analysis was vital for their use in reproducible research. The performance of each liquid handling device varies depending on the design of the equipment and between each piece of equipment. Consequently, it is important to analyse the performance of the workstation being used to carry out the envisaged experimentation. The performance of the C-400 and RapidPlate liquid handling workstations was assessed, quantifying their liquid handing accuracy and precision (Olsen, 2000) in dispensing 100 μL aliquots (n = 3) of fluorescin in HEPES buffer using the RapidPlate or Cyberlab C-400

workstations. The precision of these workstations was 3.5% to 7.3% CV and 3.1% to 5.8% CV (Olsen, 2000). The Tecan Genesis RSP 100 liquid handling workstation proved to be comparable in both precision and accuracy (Hanson and Cartwright, 2001). The performance of the automated equipment used within this research was calculated using statistical methods (chapter 3).

1.8.2.1 Literature Review of LLE Process

The limitations of the semi and fully automated LLE processes initially generated using a variety of liquid handling workstations are discussed (section 1.8.2.1.1), focussing on the variety of methodologies. The high extraction volumes (section 1.8.2.1.2) and labour intensive phase mixing methods (section 1.8.2.1.3) used in these LLE processes limited their full automation. The comparison of these LLE processes was made with manual processes at different scales of operation (section 1.8.2.1.4) and the statistical analyses of these processes (section 1.8.2.1.5) were also discussed.

1.8.2.1.1 Semi & Fully Automated LLE Processes

The LLE process required multi-step liquid handling of both samples and reagents and is repetitive, which makes it ideally suited to automation. This exploits the variety of liquid handling equipment, including semi-automated dilutors, dispensers or liquid handling workstations to prepare and carry out the sample purification (Keightley, 1986). The automated equipment facilitated the development of semi and fully automated methodologies.

The semi-automated LLE processes required manual intervention to transfer samples or generate phase mixing (section 1.8.2.1.3). Some semi-automated LLE processes were prepared by manual pipetting using a multi-channel pipette (Ramos et al, 2000), but many of these procedures used the automated equipment to prepare the extractions, transferring samples from other tubes or plates to the extraction vessel with a manual phase mixing procedure. The fully automated LLE processes were developed by using the automated liquid handling workstation to prepare and carry out experimentation by using automated phase mixing and transferring samples for analysis.

The first recorded semi-automated LLE experimentation was prepared using the Biomek workstation, which prepared and carried out counter-current distribution combining the separation of a dye from erythrocytes with bioanalysis in a 1 mL tube (Sutherland et al, 1989). Later, a 401 Gilson diluter was used to clean samples of pesticides in water prior to bioanalysis (van der Hoff and Baumann, 1993) as well as a Quadra 96 workstation for the preparation of analytes from plasma (Steinborner and Henion, 1999, Zhang et al, 2000b, Peng et al, 2000a). All of these methodologies encountered challenges regarding the reaction volume (section 1.8.2.1.2) and phase mixing techniques (section 1.8.2.1.3). The semi-automated LLE processes were designed mostly for the preparation of analytes from plasma samples prior to bioanalysis, and later LLE research also used other workstations.

In these early automated LLE processes, it was observed that there were difficulties in the liquid handling of the samples, which created cross contamination (Zhang et al, 2000a, Bolden et al, 2002). It was also observed that sample losses occurred due to evaporation, which were especially evident during back extraction (Hubert et al. 1992). Difficulties with evaporation and waste solvents were also encountered (van der Hoff and Baumann, 1993).

1.8.2.1.2 Automated Process Volume

Prior to the start of this research in 1999, the reaction volumes ranged from 450 µL to 8.2 mL and some researchers did not disclose this information in the scientific papers. The feed material was often plasma and the LLE process was used to purify the samples prior to analysis. Therefore, mass transfer during the extraction process was not considered. Phase mixing was achieved using a variety of methods, which often required manual intervention (section 1.8.2.1.3).

During 1999, there were a number of scientific papers published on the semi and fully automated LLE process. However, the volumes ranged from 1.1 mL to 131 mL. The phase mixing was achieved by a variety of techniques. By 2000 the volume range had decreased to 0.67 mL (Jing Ke et al, 2000) and 0.84 mL (Bolden et al, 2000), but these were not as low as the initial semi-automated LLE process that used only 0.45 mL (Sutherland et al, 1989).

1.8.2.1.3 Phase Mixing Methods

The early semi-automated LLE methods used a variety of mixing methods to generate phase mixing. These included manual shaking (Zhang et al, 2000a), vortexing (Hubert et al, 1992,

Jemal et al, 1999), bubbling (Turner et al, 2000), aspirating-dispensing cycles (Sutherland et al, 1989, van der Hoff and Baumann, 1993), rotor-rack vibrating plate (Steinborner and Henion, 1999) or even using magnetic stirring (Ruddick, 2000). The most popular techniques of these were the aspirating-dispensing pipetting method. However, a variety of different procedures testing the different pipetting techniques were used.

Phase mixing generated using the aspirating-dispensing repeated pipetting method used a variety of different numbers of mixing cycles from $n_c = 3$ (Sutherland et al, 1989) to $n_c = 6$ (van der Hoff and Baumann, 1993), without a consensus about aspirating, dispensing heights or even transferred volume. The liquid aliquot was aspirated with an air gap of 50 μL in the tip and dispensed 1 mm above the vial in an aspirating-dispensing mixing method (Zhang et al, 2000b). The air gap was also used later in a combined SPE/ LLE process using diatomaceous earth (Peng et al, 2001a) to prevent cross contamination of the samples. These experimental details relating to the automated LLE process were often not specified in the scientific papers, so no real conclusion about this methodology could be drawn. These scientific papers seemed to omit analysis of the effectiveness of mass transfer and it was assumed that all the contaminants were removed. For the effective use of this mixing technique further investigation was required regarding its kinetics, equilibrium position, and efficiency to generate a generic approach for the automated microscale LLE process.

1.8.2.1.4 Comparison with Manual Pipetting

Manual pipettes were gradually modified by creating multi-channelled pipettes and automated liquid handling workstations to carry out sample pipetting or diluting. Automation reduces the time required and human errors involved in the repetitive liquid handling experimentation. The manual LLE process (4.5 h) was shown to be considerably slower than the automated LLE process (1.5 h) in preparing 96 extraction wells for the LLE process (Zhang et al, 2000b). Improvements of LLE timings were seen with further comparison of the manual process (290 minutes) with the automated process (103 minutes) for processing 96 samples (Jemal et al, 1999) that had a *circa* three fold improvement. The manual LLE method was reported as *"less rapid, less sensitive and less precise than the fully automated method using solid-liquid extraction"* (Hubert et al, 1992), discussed in section 1.8.2.1.3.

1.8.2.1.5 Statistical Analysis of Automate LLE Processes

The analysis of the performance of the published automated LLE processes was assessed using statistical methods (appendix 11) by individual researchers, which showed good accuracy and precision (RSD = Relative Standard Deviation) results. The LLE of analytes from plasma showed a good accuracy (3.5% to 7.2%), which varied with the specific analyte, intra-run precision (2.9% to 3.6% RSD) and inter-run precision (3.5% to 3.7% RSD, Hubert et al, 1992). The LLE procedure with the Quadra 96 workstation produced varied accuracy (1.7% to 10.2%) for the analytes tested. However, similar precision for all of the analytes (3.8% to 7.5% RSD) was achieved, which demonstrated that the LLE process was reproducible (Steinerborner and Henion, 1999).

The accuracy of the automated LLE process (0.3% to 4.3%) demonstrated better performance than that of the manual LLE process (2.1% to 6.2%). The inter-run precision of these experiments showed a similar trend between the automated (2.6% to 8.4% RSD) and manual process (5% to 12% RSD). However, the intra-run data showed better precision for the manual process (2.4% to 7.6% RSD) than the automated process (5.1% to 7.6% RSD), despite there being more variability in the results from one experiment. This workstation produced similar accuracy results for the LLE process to those above (1.7% to 6.5%), although the precision depended on the specific analyte being purified and the quantification method used (Zhang et al, 2000a). These experimental methods used small numbers of replicate samples (n = 3 to 6) and the low sample sizes limited the significance of the data produced, but this was not investigated in relation to the volumes dispensed in previous experimentation.

1.8.2.2 Solid Phase Extraction Literature Review

The automated equipment (section 1.3.2.1) used to carry out SPE processes to purify a range of analytes from biological fluids, primarily plasma, was the liquid handling workstation. These instruments facilitated the rapid transfer of samples during the experimentation and were key in the development of automated SPE processes (section 1.8.2.2.1). The specifics of the automated SPE processes total extraction volumes (section 1.8.2.2.2) and the methodologies (section 1.8.2.2.3), such as the SPE formats were discussed. The performance of these automated SPE processes was compared with the manual SPE process and the

automated LLE process (section 1.8.2.2.4), which were analysed using statistical methods (section 1.8.2.2.5) to assess the significance of their conclusions.

1.8.2.2.1 Automated SPE Processes

The initial automation of the SPE process used the liquid handling workstations to transfer samples throughout the procedure and purify them prior to bioanalysis. These procedures still required a degree of manual intervention to move the multiwell plate between the equipment and scheduling their operation, as the pieces of automated equipment were not fully integrated together. The research into these initial automated SPE process used a variety of liquid handling workstations to transfer the samples into SPE formats, including Zymark XP (Parker et al, 1996), and the Multiprobe (Kaye et al, 1996 and Allanson et al, 1996). These processes used adsorbent resin contained in SPE cartridges, a micropreparation block, or Microelute SPE 96-well format cartridges containing a limited range of adsorbent resins of a fixed mass (Venn et al, 2005). The automated equipment transferred the samples from sample storage vials to the SPE format, which accelerated the preparation of these samples. However, the requirement for manual intervention hindered the process. The development of automated devices that could integrate with automated equipment, such as the vacuum manifold, facilitated the development of increasingly automated SPE processes.

The automated SPE process faced difficulties being accepted by analytical scientists in its use throughout the entire method life cycle of, development, characterisation, validation and application (Parker et al, 1996). However, the automated SPE process was considerably faster than the manual SPE process, as it has numerous liquid handling stages, making it ideal for automation. The automated SPE process using the microwell filter plate supported SPE process enhanced its capability to condition the adsorbent resins, load and wash 96 samples in 10 minutes (Janiszewski et al, 1997).

1.8.2.2.2 Solid Phase Extraction Volume

The initial development of the automated SPE process required a high total extraction volume of 24 mL (Parker et al, 1996), which included conditioning the reagents, loading samples, washing samples, and eluting reagents. Other automated SPE processes used lower total extraction volumes of 10.8 mL (Kaye et al, 1996), and 4.3 mL (Allanson et al, 1996), which reduced both the duration and cost of the experimentation. By 1998, the automated SPE process volume increased to 11 mL (Shimoyama et al, 1998) and 6 mL (Cheng et al, 1998),

but by 1999 the total volume for automated SPE processes had reduced to 0.9 mL (Davies et al, 1999). This sub mL SPE process used the Multiprobe liquid handling workstation to prepare the extraction wells, which were filled with C18 resin in a pre-filled microplate, used to purify the analyte, chlorambucil (an anti-cancer drug) and its metabolites from human plasma samples. The SPE microplate contained a fixed amount of resin (15 mg per well), which meant that it could not be used to screen and optimise certain process conditions, such as resin concentration to generate isotherms.

Later developments of the automated SPE processes did not reduce the total volume of the process and many researchers used comparatively high total extraction volumes (2.42 mL Zweigenbaum et al, 1999 to 15.2 mL Huang et al, 1999) with a number at *circa* 6 mL (Cheng et al, 1998, Gilar et al, 2001, Mathews et al, 2001). In addition, the automated laboratory scale extractor, ASPEC (Gilson, France), was used in conjunction with adsorbent resins to purify biological samples (4.77 mL, Peng et al, 2000b, 16 mL, Dilkin et al, 2001) although these processes required larger volumes than most automated SPE processes.

1.8.2.2.3 Automated SPE Methodologies

The automated SPE methodologies that were developed used a variety of different SPE formats, adsorbents, resins, and mixing conditions to purify specific analytes. These processes were not generic, neither did they investigate all the process parameters nor compare the efficiencies of the different scales.

The initial SPE formats used in the automated SPE process were SPE blocks and cartridges that were developed to fit a 96-well format and a pre-filled SPE 96-well plate. There was no research carried out for which to compare the efficiencies of these formats, but it was assumed that they were equivalent. The fixed resin cartridges were used for the complete capture of impurities with a selection of resins (Octadecyl (C18), Octyl (C8), Ethyl (C2), Cyclohexane (CH), Phenyl (PH), Hydroxylated polystyrene-divinylbenzene (CN) using a total volume of 24 mL of liquid reagents (Parker et al, 1996). Many of the SPE formats used in automated SPE processes were pre-filled with 100 mg (Huang et al, 1999) or 50 mg of C18 resin (Allanson et al, 1996). In addition, a multiwell filter plate was used to support the SPE adsorbent resins to accelerate the conditioning, loading and washing steps (Janiszewski et al, 1997). These approaches were suitable for the initial screening of suitable adsorbent resins to

extract an analyte, but did not facilitate the generation of adsorption isotherm data necessary for larger scale process design.

The solid and liquid reagents were mixed in the automated SPE processes using a variety of different methods, including pipetting (Parker et al, 1996), and vortexing (Kaye et al, 1996). However, the primary mixing method used was the automated liquid handling workstation to dispense the liquid onto the solid resin particles. The separation of the two phases was carried out using positive pressure, gravity or a vacuum (Harrison and Walker, 1998), with a variety of pressures and times.

It was predicted by researchers developing the early automated SPE process that there would be a requirement for a vacuum manifold with room for a collection plate to be linked to the workstation and an autosampler to fully automate the SPE process (Allanson et al, 1996). It was also observed by these researchers that they required a smaller mass of adsorbent resin (15 mg) rather than the standard pre-filled cartridges (50 mg), a greater selection of adsorbent resins and square column cartridges within a 96-well format to enhance the automated SPE process.

1.8.2.2.4 Comparison of the Automated SPE Methods

The automated SPE process was compared with the manual SPE process in relation to the duration of its operation. The automated SPE process (1 h) used the Quadra 96 workstation which was faster than the manual SPE process (5 h) to prepare samples using cartridges in a 96-well plate format (Allanson et al, 1996). The percentage recovery values also increased when comparing the manual and automated SPE processes. The automated SPE process had poor recovery. The manual SPE process produced 76% recovery using an 8 channelled manual pipette (Janiszewski et al, 1997).

Comparison was made between the automated and manual SPE processes for purifying analytes from breast milk and plasma using the Multiprobe liquid handling workstation or an 8-channelled manual pipette (Shimoyama et al, 1998). This increased to between 91% and 95% recovery of phenotytoin from plasma and 91% to 95% from breast milk using a C18 bonded cartridge (Shimoyama et al, 1998). The analysis of the data using each of these

processes showed that the automated SPE process had more accuracy and precision than the manual process (section 1.8.2.1.5).

The automated SPE process using the filter supported adsorbent "*resin compared favourably with those obtained using solvent and traditional SPE methods*" (Janiszewski et al, 1997), which have an intra-run precision of 1.1% to 8.0% RSD. These precision values did not correlate with the decrease in concentration and it was observed that the reproducibility (< 11%) was good across the entire plate.

The automated SPE process recovery was compared to that of the automated LLE process. The automated SPE process produced good analyte recovery (95% to 96% mean recovery) and precision (2.6% to 3.2%% RSD), which was shown to have higher efficiency and better reproducibility than the automated LLE process with 82% to 86% mean recovery and 4.4% to 5.2%% RSD (Jemal et al, 1999).

1.8.2.2.5 Statistical Analysis of Automated SPE Processes

The statistical analysis of the automated and manual SPE processes assessed their performance (appendix 11) by calculating the accuracy and precision of the data. These values depend on the number of replicate samples. The sample number of replicate process conditions tested using the automated SPE process in some research was low with n = 3 (Harrison and Walker, 1998, Peng, 2000b Mathews *et al*, 2001, Shou et al, 2002) and n = 6 (Peng et al, 2000b, Cheng et al, 1998). Some researchers did not specify this information, but others used significantly increased sample numbers in their research with n = 10 (Gauw et al, 2000), n = 12 (Cheng et al, 1998) and n = 24 (Davis and Swayze, (2000).

The statistical performance of the automated SPE experimentation had good accuracy. The best accuracy for an automated SPE process was achieved using the Tecan RSP workstation with a microprep SPE C18 block (0.65% to 5.4% accuracy, Kaye et al, 1996). This was seen in the early development of the automated SPE process scale, and there was no published data to supersede this data.

The precision of the data was assessed within an experimental run carried out on the same day (intra-run) and between experimental runs on different days (inter-run), where greater

variation was expected. The automated SPE process data generated inter-assay precision (3.8% to 6.7% CV serum, 2.5% to 6.7% CV plasma) and intra-assay precision (2.6% to 6.9% CV serum, 5.2% to 13.7% CV, plasma). However, these values for the coefficient of variance are specific to the experiment and cannot be used for comparative purposes with different volumes unless a relative value (RCV) is used.

The performance of the manual SPE process to purify the analyte (phenytoin) from both plasma and breast milk samples was assessed using the coefficient of variance (CV) of the data. The data had an inter-run precision of 1.1% to 4.8% CV and an intra-run precision 1.5% to 8.7% CV, with lower values from the milk samples in both cases (Shimoyama et al, 1998). These values gave information on the reproducibility and repeatability of the process, although the coefficient of variance measurements were not standardised values and therefore, could not be compared with other research data.

The repeatability and reproducibility of the data were assessed using RSD values, which were compared to different experimental data. The automated SPE process using membrane multiwell plates (Empore) on automated equipment operated in a semi-automated manner produced the best published inter-run precision data of 0.3% to 10.5% RSD (Janiszewski et al 1997) over the range of analyte concentration (1 $ng.mL^{-1}$ to 1000 $ng.mL^{-1}$). These values were variable and did not increase with the decrease in concentration, with the highest value being at 10 $ng.mL^{-1}$. Other inter-run precision values showed greater variation and gave both positive and negative values. This indicated that the processes had acceptable rigor in producing significant results.

The best intra-run precision was produced for the experimentation using the Quadra 96 workstation with the Walters Oasis HLB multiwell plate to purify verapamil (adrenaline) from plasma samples, which created 0.39% to 0.95% RSD (Cheng et al, 1998). These values indicated that the within-run variation was lower than the between-run values, indicating that, as expected, the process is more repeatable than reproducible. This indicated that there were fewer errors within an experiment than if it was repeated on different days, which indicated the occurrence of greater random errors. However, both the repeatability and reproducibility of these processes were acceptable.

It was observed that the automated SPE process raised some cross contamination issues due to *"sputtering of liquid from tips"* on the workstation (Allanson et al, 1996). It was estimated that cross contamination occurred < 0.01% (Gauw et al, 2000), which is an insignificant amount for large scale processes. This can be minimised by the development of good methodologies and regular maintenance of the automated equipment.

1.9 Aims and Objectives

The aim of this research is to investigate the development of automated platforms and assess their suitability for microscale equilibrium stage separation processes. This will enable automation of a part of the overall bioprocess research and development process in order to generate experimental data faster, facilitating the transfer of a new pharmaceutical entity from initial discovery to the market by increasing the speed of biochemical engineering data generation.

This will entail the establishment of microscale methods in order to obtain quantitative and reliable process design information for equilibrium stage processes such as LLE and SPE. In addition, the automation of microscale methods will be investigated to increase experimental throughput. The specific objectives to be addressed are as follows:

- Assessment of the liquid handling and solid handling capability of the automated platforms used within this research. Assessment of their performance and familiarisation with the use of the automated platform to achieve accurate and precise performance. This is dealt with in chapter 3.
- Development of the microscale liquid-liquid extraction process and its use to assess the effect of process parameters on mass transfer. Validation of the data from the microscale experimental methods by comparison with laboratory scale data and assessment of the performance of the processes. This will be dealt with in chapter 4.
- Development of the microscale solid phase extraction process and its use to assess the effect of process parameters on mass transfer. Validation of the data from the microscale experimental methods will be gained from comparison with laboratory scale data and assessment of the performance of these processes. This will be dealt with in chapter 5.

As a commercially relevant model system, this research will examine the purification of 6-APA from the PA bioconversion product stream using liquid-liquid extraction and solid phase extraction. These down stream processes will be carried out at laboratory scale (10 mL) to act as a positive control. They will be developed for automated microscale experimentation using the Multiprobe II Ex® liquid handling workstation and other automated equipment and devices.

The automated equipment will be used to develop the microscale processes, which will require the segmentation of the laboratory processes to enable the programming of the equipment to perform key stages. This microscale experimentation will be used to assess key parameters involved in these processes. The data generated from these microscale processes will be validated with the laboratory results and literature values.

It is hoped that pharmaceutical companies could predict the problems and parameter changes required at the larger scale using the microscale data. The microscale experimentation will be designed for commercially available equipment to facilitate its transfer into the pharmaceutical industry for use by many companies that already own automated equipment. This approach could be carried out in parallel with lead optimisation, analysis method development or phase I clinical trials, which could reduce the time for a new drug candidate to reach the market. The microscale methodologies will reduce the requirement for high quantities of materials, which will be advantageous for early stage development. It will also reduce the time for the development of larger process scales (pilot scale or manufacturing scale), which could be achieved by focussing on the key parameter ranges, limiting the need for vast experimentation.

The data generated from the microscale approach could be used to rapidly analyse the performance and economics of the production and purification processes, facilitating the decision making process. The Centre for Scientific Enterprise sponsored the evaluation of this research as a new technology venture (chapter 6). The automated process optimisation could increase the speed of the pharmaceutical to market. This information will be integrated into the automated synthesis and purification of therapeutic agents. HTS will screen their interaction with a range of therapeutic targets, which will contribute to the revolution of the research and development process of many industries including the pharmaceutical industry.

The results are drawn upon in the conclusion (chapter 7), identifying areas of future work related to the outcomes of this research.

Chapter 2: Materials and Methods

2.1 Materials

2.1.1 Materials for LLE Experimentation

2.1.1.1 LLE Aqueous Phases

Penicillin G potassium salt (Pen G, 4.0 $g.L^{-1}$, 12 mM), phenylacetic acid (PAA, 4.0 $g.L^{-1}$, 29.2 mM) or 6-amino penicillanic acid (6-APA, 4.0 $g.L^{-1}$, 18.5 mM) were dissolved in phosphate buffer (0.2 M, mono- and di-basic phosphate). Reverse osmosis (RO) water was used in the preparation of all buffers and the pH conditions of the solutions were adjusted using sodium hydroxide (0.1 M) or hydrochloric acid (1 M). The PAA and 6-APA solutions were heated at 37 °C for 30 minutes to aid dissolution. The simulated bioconversion product stream contained 10 mM Pen G, 190 mM PAA and 190 mM 6-APA, which were dissolved in phosphate buffer (0.2 M) at pH 4.5. All materials were obtained from Sigma Chemicals (Sigma-Aldrich Company Ltd., UK) and were of analytical grade (0.001% impurities).

2.1.1.2 LLE Organic Phases

Butyl acetate, cyclohexane, hexane and toluene were obtained from Sigma Chemicals and were of analytical grade. The hydrophobic ionic liquid, 1-butyl 3-methyl imidazolium 1-butyl-3-methylimidazolium chloride [Bmim][PF_6], was obtained from Covalent Associates (Covalent Associates Inc., USA).

2.1.2 Materials for SPE Experiments

2.1.2.1 SPE Liquid Phase

Amorphous crystalline 6-APA (4.0 $g.L^{-1}$) was dissolved in phosphate buffer (0.2 M, pH 4.5) and heated at 37 °C for 30 minutes. All phosphate buffers (0.2 M, mono- and di-basic phosphate) were prepared with RO water and were adjusted using sodium hydroxide (0.1 M) or hydrochloric acid (1 M) to produce the required pH.

2.1.2.2 SPE Solid Phases

The solid phases investigated were activated carbon (granular), activated carbon (powder), Amberlite XAD-7, and Amberlite XAD-16 resins, which were obtained from Sigma Chemicals (Sigma-Aldrich Company Ltd., UK). These resins were conditioned prior to use according to the guidelines recommended by the manufacturers, unless described in section 2.4.1. Penicillin acylase (PA), immobilised on Eupergit C beads, was obtained from Fluka (Sigma-Aldrich Company Ltd., UK) for the analysis of solid handling equipment.

2.1.3 Materials for HPLC Sample Analysis

HPLC grade methanol (0.001% impurities) and filtered (membrane pores = 0.2 μm) phosphate buffer (pH 7) were used in the preparation of the HPLC mobile phase (section 2.5.1). The HPLC system (Dionex, UK) was fitted with a C8 guard column (Jourguard, VWR, UK) and a C18-5 μm reverse phase (RP) column (150 mm x 4.6 mm) (Perkin Elmer, USA).

2.2 Automation Platforms

The automated platforms used in this research included the Multiprobe II Ex®, an automated liquid handling workstation (section 2.2.1) from Perkin Elmer, UK (now Packard Bioscience, UK) and the Accelerator™, a solid dosing station (section 2.2.2) from Chem Speed, Switzerland. These automated platforms are described in this section, featuring their mechanism of action, labware, software and programming.

2.2.1 Liquid Handling Workstation

2.2.1.1 Liquid Handling Workstation Description

The Multiprobe II Ex® liquid handling workstation (figure 2.2.1.1.1) is an automated multichannel pipette that is fixed to a robotic arm. The robotic arm moves from the aspirating location to the dispensing location positioned on the working area (deck[1]) of the workstation (h = 110 mm, d = 1099 mm, l = 387 mm) to dispense an aliquot of liquid from the pipette tip. It was used to carry out the majority of the automated microscale experimentation developed in this research. This automated pipetting platform delivers μL to mL volumes of a range of liquids to a variety of containers, including multiwell plates. The robotic arm can be configured with one to eight pipette tips, but the workstation used for this research contained four pipette tips. The mechanism of action of the workstation (section 2.2.1.2) considers its set up options and interaction with labware[1] (section 2.2.1.3) fitted to the deck[1], which is detailed with the experiential method of the tests[1]. The tests were designed using application software (section 2.2.1.4) to create bespoke programs (section 2.2.1.5).

2.2.1.2 Mechanism of Action of Workstation

The liquid handling workstation was operated using Windows-based application software (section 2.2.1.4) that identifies the required labware[1] (section 2.2.1.3), procedures and performance files. The deck[1] of the workstation must be set up with the correct labware[1]

[1] Multiprobe Terminology defined in appendix 5

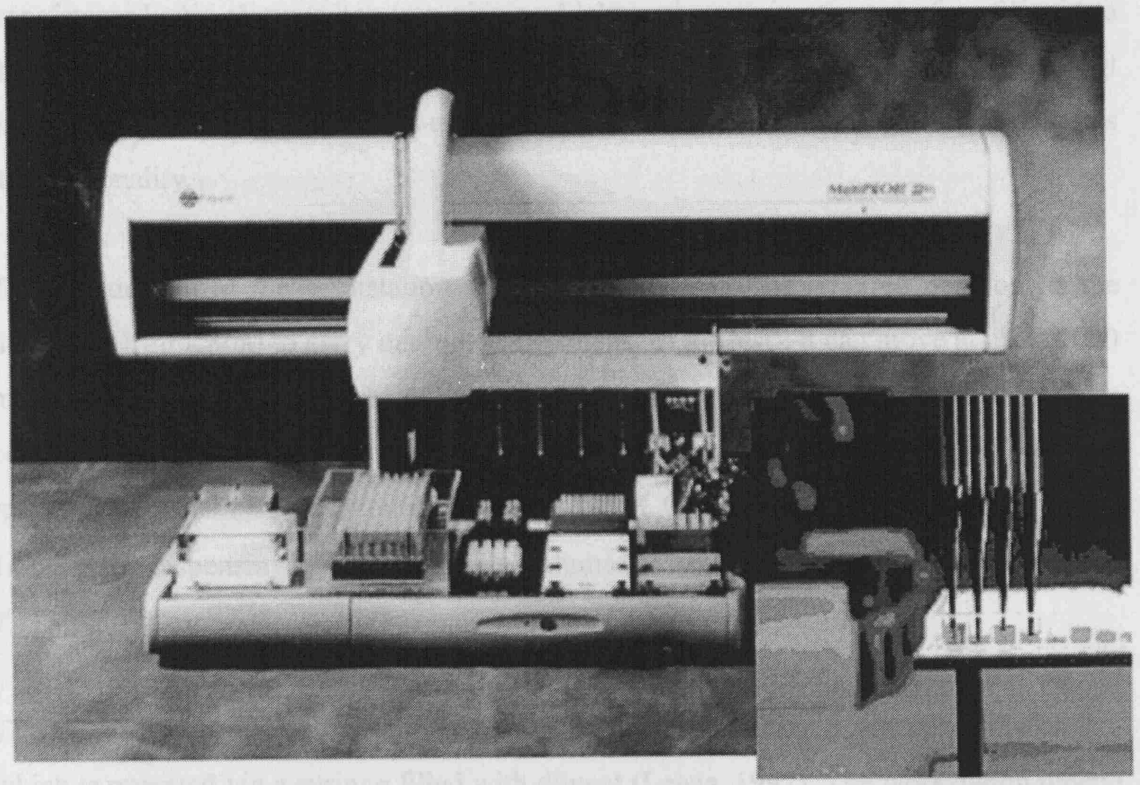

Figure 2.2.1.1.1. Picture of the Multiprobe II Ex® liquid handling workstation (Perkin Elmer) with an insert of the four Versa® pipette tips[1] attached to disposable tips. Workstation described in section 2.2.1. Pictures adapted from those on the Perkin Elmer website (perkinelmer, 2002).

[1] Multiprobe II Ex® terminology defined in appendix 5

for a specific program[1], which can be identified in the deck view window of the program (*i.e.* the series of procedures[1] making up an experimental method). The deck[1] can hold up to 32 pieces of labware, which are based on the footprint of a rak[1] designed to hold a standard multiwell plate (section 1.3.1). The labware includes multiwell plates, boxes of disposable tips, reagent troughs and their corresponding deck[1] locations. The robotic arm, containing the pipette tips, moves around the deck[1] collecting disposable tips and transferring liquid aliquots between pieces of labware[1], ensuring the transfer of liquid to the specified location on the deck[1]. In addition, the operating system can also control external equipment and devices, such as a spectrometer or filtration rig, which increases its functionality.

The robotic arm of the workstation moves the pipettes to the required position on the deck[1] (*X, Y* direction) to carry out the desired steps[1] of the test[1]. It can move at up to 1000 $mm.s^{-1}$, which allows a high throughput of samples. The operation of the workstation was considered to be consistent and reproducible by the manufacturer, creating high quality results with a claimed precision of 0.25% to 3.83% CV[9] and an inaccuracy of 0.72% to 14.64% for dispensing 1 µL to 100 µL volumes (Packard Bioscience, 2003, appendix 7.1).

The workstation pipettes the liquid aliquots by using positive pressure displacement, which is operated via a syringe filled with diluent (Lewis, 1997). The workstation pipette operates by mechanically moving a syringe plunger within its barrel controlled by a syringe pump with a series of micropumps and microvalves (Szita et al, 2001). The high precision syringe modules contain a syringe pump which controls each pipette tip and a stepper motor to move the plunger incrementally, that is controlled by a microprocessor. These modules comprise a syringe and valve assembly with a valve plug, which moves the liquid aliquot into the sample line by displacing the system liquid. There are a variety of syringe sizes available (0.5 mL to 2 mL) for the workstation, but the standard 1 mL syringe barrel was used in the set-up of the workstation used in this research. The workstation aspirates air prior and post liquid aspirations creating an air gap to prevent

[9] CV = Coefficient of Variance, defined in appendix 11)

liquid dripping from the pipette tips whilst in motion and to prevent mixing the samples in the sample line after repeated sampling.

The Multiprobe II Ex® workstation is operated with either fixed (re-usable) or disposable tips fitted to its robotic arm (figure 2.2.1.1.1 insert). The standard fixed tips are washable stainless steel tips with a Teflon® coating, which can be easily adapted for use with a variety of sterile or non-sterile disposable tips (20 μL or 200 μL), reducing the risk of cross contamination. The pipette tips can be cleaned in place using the system liquid (RO water) by operating the flush and wash procedures that clean both disposable and fixed tips internally and externally. This reduces the risk of contamination by reducing sample carryover to less than 1 x 10^6 (Packard Bioscience, 2003), and ensures accurate liquid handling.

The pipette tips move around the deck[1] in the *X*, *Y*, and *Z* directions to locate their fine positioning within the labware[1], adapting their position (*X*, *Y* direction), spacing (*X* direction) and height (Z direction) to reach the liquid within the wells arranged in a range of geometries. Each tip moves independently, their spacing varying from (9 mm to 20 mm) with use of the Varispan® feature, which allows sampling from a variety of multiwell plates and labware configurations. This movement is controlled by mechanical movement of the pipettes on the robotic arm using a ratchet mechanism.

Each of the four pipette tips can move independently to detect the liquid surface in each well by adjusting their height using the liquid level sensing technology, Accusense®. This facilitates the separation of two immiscible phases, which is suitable for a range of applications. The liquid level sensing detects the reagent by a combination of capacitance, pressure and conductivity measurements (Pochert, 2000). This information is used to control the motor driving the pipettes' height via a mechanical racket. This feature is potentially useful for liquid-liquid and solid-liquid separation. This feature has the potential to extend the functionality of the equipment to include the removal of a supernatant from the solids after centrifugation, avoiding solids entrainment or sampling

[1] Multiprobe Terminology defined in appendix 5

liquid from a settled slurry. This is useful for a variety of applications, such as HTS (section 1.4.1.2) and sample preparation (section 1.4.1.2 and 1.4.3, respectively).

2.2.1.3 Multiprobe Labware

The deck[1] of the Multiprobe II Ex ® was fitted with a variety of labware[1] for the LLE and SPE experimentation (figures 2.2.1.3.1 (a) and (b)). The common labware used in both the microscale LLE and SPE experimentation included the tip chute, flush/ wash bowl, small disposable tips and reagent troughs containing specific reagents required in the experimentation. The microscale experimentation used a variety of multiwell plates (appendix 1) with different characteristics (table 1.3.1.1) selected to suit the specific experimental requirements. The microscale LLE experimentation was carried out in a borosilicate 96-round well plate (Radleys, UK) with wells of 7.6 mm diameter and 13 mm height. The SPE experimentation used a 96-deep-square well plate with a conical base (Beckman Dickenson Bioscience, UK) with wells of 7.6 mm diameter, 36 mm height, a 24- deep-square well plate with round-bottomed base (3M, UK) with wells of 20 mm diameter, 36 mm height, 96-round well filter plates (Millipore, UK) with wells of 6.3 mm diameter, 12.2 mm height, 96-well collection plate (Costar) of 2 mL per well, 24-well filter plate (Perkin Elmer, UK) with wells of 6.8 mm diameter, 3.2 mm height and 24-well collection plates (Costar, UK) of 7 mL per well.

The 96-well filter plate (Millipore) contained a Durapore® membrane (polyvinylidene), which has broad chemical compatibility, hydrophobic nature, small pore size (0.45 μm), small well size (d = 3.2 mm) and small well volume (392 mm). The 24-well filter plate (3M, UK) contains a glass fibre membrane with a larger pore size (0.7 μm to 1.5 μm), larger well size (d = 6.8 mm) and larger well volume (625 mm^3). The commercially available filter plates were kindly donated by the following suppliers: 24-well (Packard Instruments, Packard Bioscience, UK) and 96-well (Millipore, UK). The Multiprobe II Ex® workstation was operated in compliance with the standard operating procedure for the workstation, which is detailed in appendix 9.

[1] Multiprobe Terminology defined in appendix 5

(a)

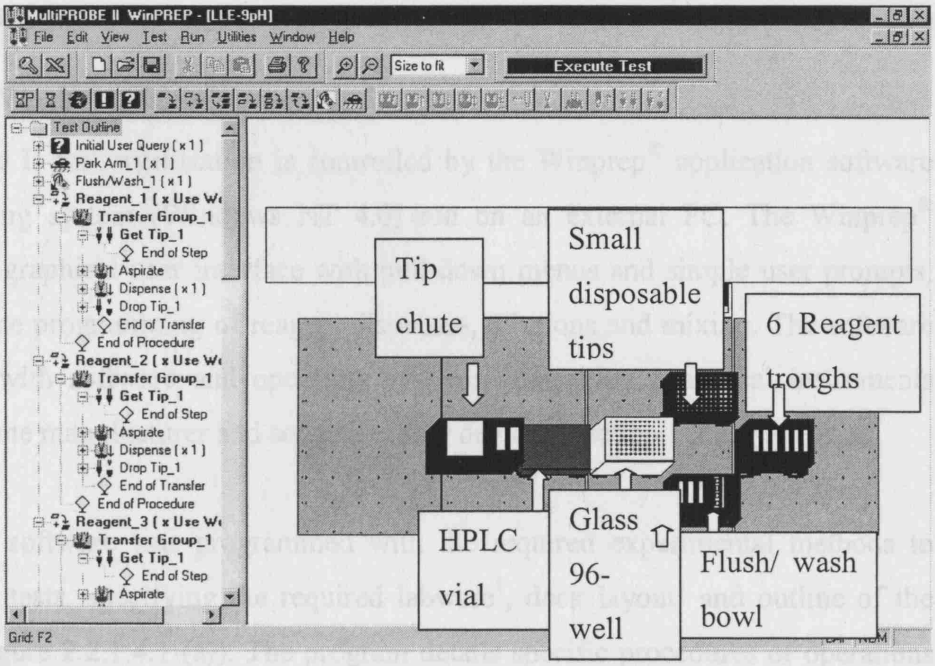

(b)

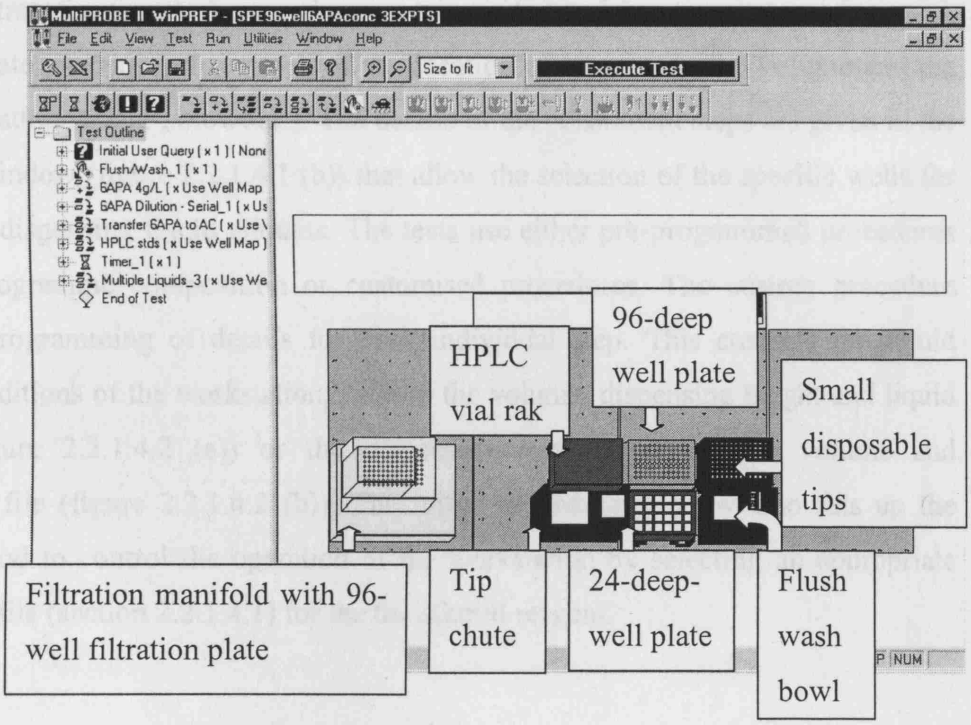

Figure 2.2.1.3.1. Multiprobe labware[1] for (a) automated microscale LLE experimentation
and (b) automated microscale SPE experimentation.

[1]Multiprobe Terminology defined in appendix 5

2.2.1.4 Workstation Software

The Multiprobe II Ex® workstation is controlled by the Winprep® application software and an operating system (Windows NT 4.0) run on an external PC. The Winprep® software has a graphical user interface with pull-down menus and simple user prompts, which allows the programming of reagent dispenses, dilutions and mixing. The software is compatible with software and operating systems controlling analytical instruments made by the same manufacturer and some ancillary devices (section 1.2.2.2).

The Winprep® software was programmed with the required experimental methods to create bespoke tests, specifying the required labware[1], deck layout[1] and outline of the procedures[1] (figure 2.2.1.4.1 (a)). The program details specific procedures or operations (*e.g.* reagent transfer, timer). A procedure contains individual functional steps[1] (*e.g.* pick up tips, aspirate, dispense) that specified the location of labware wells, volume and the mode of operation (waste[1], blowout[1]). The details of the constituent steps are given in the parameters window (figure 2.2.1.4.1 (b)) that allow the selection of the specific wells for aspirating or dispensing liquid aliquots. The tests use either pre-programmed procedures for quick programme composition or customised procedures. The custom procedure allows the programming of details for each individual step. This controls the liquid handling conditions of the workstation, such as the volume, dispensing height and liquid tracking (figure 2.2.1.4.2 (a)) or the dispensing step specifying the volume and performance file (figure 2.2.1.4.2 (b)). The initial procedure window also sets up the general method to control the operation of the workstation by selecting an appropriate performance file (section 2.2.1.4.1) for the transferred reagent.

(a)

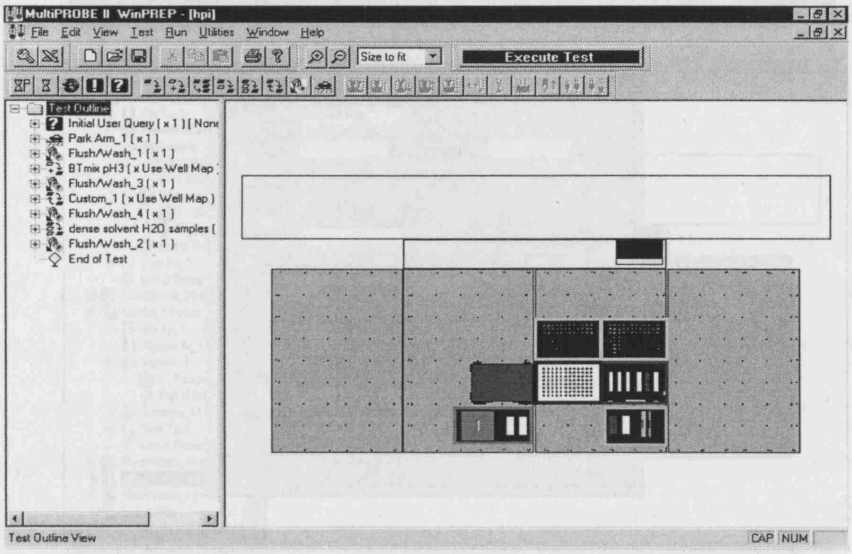

(b)

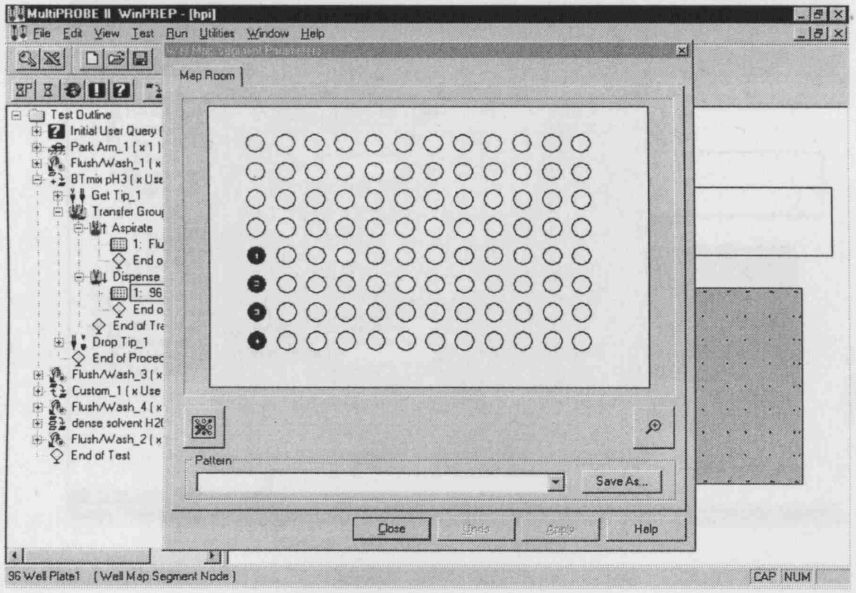

Figure 2.2.1.4.1. Illustration of the WinPrep® software used to control the Multiprobe II Ex® workstation: (a) Deck layout and test outline for the bespoke program 'hpi' test, showing the required labware and procedures of the test; (b) Labware used in the 'hpi' test with location of the reaction wells on the 96-well plate selected for dispensing liquid aliquots. Test detailed in table 2.2.1.5.1.

(a)

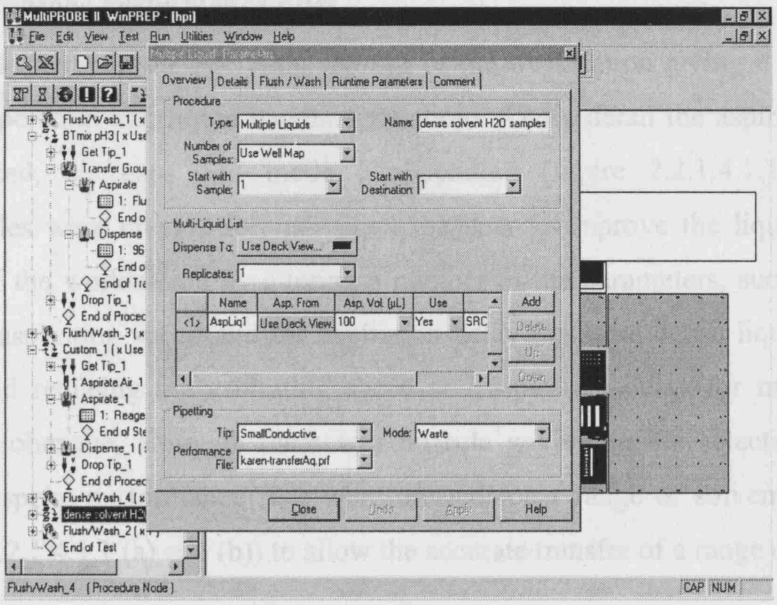

(b)

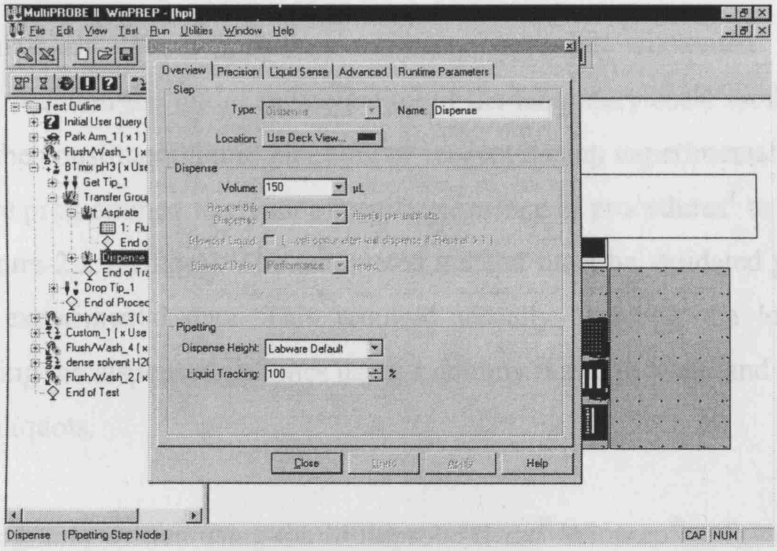

Figure 2.2.1.4.2. Illustration of a custom procedure within Winprep® software: (a) overview window showing programmable options to specify the operation of the liquid handling workstation, in this case volume, dispense height and liquid tracking; (b) Transfer Group Dispense Step Window showing programmable options to specify volume and performance files for the operation of the liquid handling workstation.

2.2.1.4.1 Multiprobe Performance Files

Performance files contain the operating settings of the workstation giving it instructions to control its operation and liquid handling functions. These detail the aspirating speed, dispensing speed, air gaps and mode of operation (figure 2.2.1.4.1.1). Bespoke performance files were created for individual reagents to improve the liquid handling performance of the workstation by altering a number of the parameters, such as greatly increasing the aspirating speed and the aspiration delay for more dense liquids like the ionic liquid and reducing the aspirating speed and aspiration delay for more viscous liquid like cyclohexane, although there was no rule governing the selection of these parameters. Bespoke performance files were created for a range of solvents and ionic liquids (table 2.2.1.4.1.1 (a) and (b)) to allow the accurate transfer of a range of liquids.

2.2.1.5 Programming the Workstation

The programming of the workstation to carry out the automated microscale experimentation required the initial segmentation of the laboratory scale methodologies. This identified the constituent liquid pipetting or reagent dosing experimental stages and these steps[1] were programmed to create a specific sequence of procedures[1] to operate the workstation (figure 2.2.1.4.1 (a)). The automated method must be validated prior to use for generating experimental data. This required visually checking the location and manually checking the dispensed volumes using a dummy run with water and gravimetric analysis of the aliquots.

The bespoke programs written using the Multiprobe II Ex® Winprep® software[1] (section 2.2.1.4) to investigate automated microscale LLE are documented in table 2.2.1.5.1. The automated microscale SPE tests are documented in table 2.2.1.5.2. The outlines of labware and deck[1] layout are detailed in all the program outlines of the tests used in this research (appendix 6).

[1] Multiprobe terminology defined in appendix 5

(a)

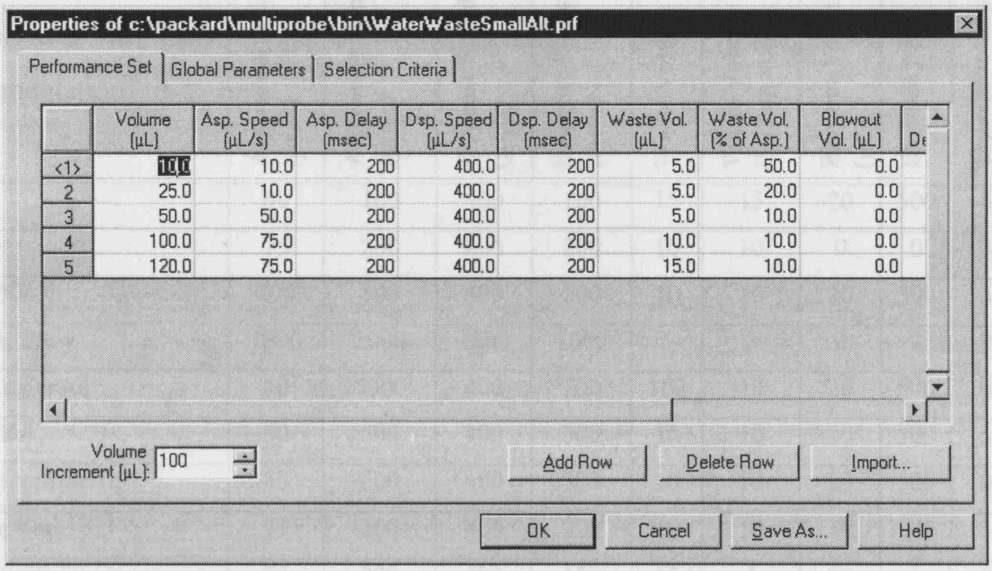

(b)

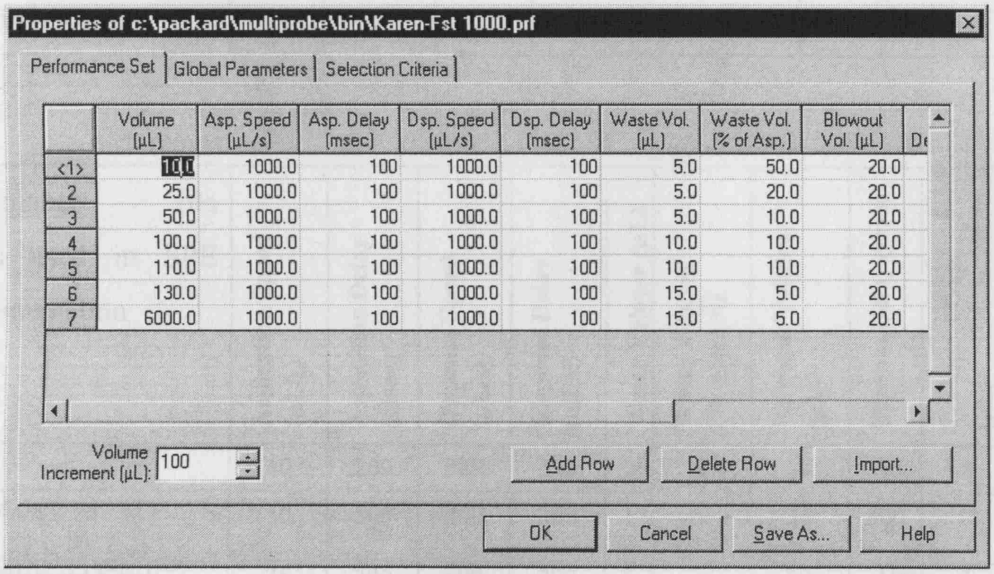

Figure 2.2.1.4.1.1. Illustration of the Winprep® software performance file (prf) showing the operational set-up: (a) Standard 'Waste Water.prf' and (b) Example prf for rapid dispension of 6-APA solution ('Karen Fst 1000.prf', renamed 'SPE Fst.prf' (detailed in Table 2.2.1.5.2)) used in the automated microscale solid phase extraction process, detailing changes to parameter settings for optimal pipetting performance.

(a)

Performance file names used in LLE experimentation	Aspiration Speed (µL/s)	Aspiration Delay (msec)	Dispense Speed (µL/s)	Dispense Delay (msec)	Waste Volume (µL)	Waste Volume (% Asp vol)	Blowout Volume (µL)	Blowout Delay (msec)	Transport Gap (µL)	Air Gap (µ L)	Submerge depth (mm)
CH	40	100	400	100	15	15	20	500	5	5	2
DMSO	75	200	400	200	10	10	0	0	3	5	2
HEXANE	200	800	400	500	10	10	20	500	5	0	2
HPIonic blow	1000	3000	1000	1000	5	5	0	0	0	5	2
HPItransferAq	50	5000	400	300	100	10	20	500	0	5	1
Karen BA	50	500	400	300	10	10	20	500	5	0	2
Karen transferAq	50	500	400	300	10	10	20	500	0	5	2
Syringe Test	75	200	400	200	10	10	10	10	3	5	2
TOLUENE	75	200	400	100	15	5	20	5	5	0	2
Water Blowout Small	75	200	400	200	0	0	20	100	3	5	2
Water Waste FT	75	200	400	200	10	10	0	0	3	5	2
Water Waste Small	75	200	400	200	10	10	0	0	3	5	2

(b)

Performance file names used in SPE experimentation	Aspiration Speed (µL/s)	Aspiration Delay (msec)	Dispense Speed (µL/s)	Dispense Delay (msec)	Waste Volume (µL)	Waste Volume (% Asp vol)	Blow)out Volume (µL)	Blowout Delay (msec)	Transport Gap (µL)	Air Gap (µ L)	Submerge depth (mm)
Slurry	10	200	1000	200	0	0	30	100	3	5	2
SPE Fst	50	500	400	300	10	10	20	500	0	0	2
Water Blowout Small	75	200	400	200	0	0	20	100	3	5	2
Water Waste FT	75	200	400	200	10	10	0	0	3	5	2

Table 2.2.1.4.1.1.Details of selected parameters in bespoke WinPrep® Software performance files used in: (a) LLE experiments and (b) SPE experiments.

File Names	Key Procedures	Additional Labware[2]	Performance Files	Dispense Mode
Hpi[4]	Reagent 150 µL PAA at nine pH conditions HPI[3]: 150 µL Mix 30 cycles Phase separation Sample Aq (100 µL)	None	Hpi	Blowout
LLE 9pH	Reagent: 150 µL PAA at nine pH conditions BA: 150 µL Mix 30 cycles Phase separation Sample Aq (100 µL)	6 Trough rak[1] Flush/Wash bowl fitted with three troughs	Waste Water Small Karen BA Karen Transfer Aq	Waste Waste Waste
LLE mass balance 1pH	Reagent: 150 µL PAA at pH 4.5 BA: 150 µL Mix 30 cycles Phase separation Sample Aq (100 µL) Sample Org (100 µL)[4]	350uL HPLC vial rak[1] must be refilled during test	Waste Water Small Karen BA Karen BA Karen Transfer Aq KarenBA transfer	Waste Waste Waste Waste Waste
LLE static v move	Reagent: 150 µL PAA at pH 4.5 BA: 150 µL Mix 0 or 30 cycle sat 2%. 1 mm below surface or default pipetting height with 0% or 100% tracking Phase separation Sample Aq (100 µL) Sample Org (100 µL)[4]	350uL HPLC vial rak[1] must be refilled during test	Waste Water Small Karen BA Karen BA Karen Transfer Aq Karen BA transfer	Waste Waste Waste Waste Waste
MIXhi150	Reagent: 150 µL PAA or 6-APA at nine pH conditions BA: 150 µL Mix at 30, 25, 23, 20, 18, 15, 12, 10, 5, 0 cycles Phase separation Sample Aq (Multiple Liquids): 100 µL	Small conductive tips (box 2)	Syringe Test Karen BA Water Blowout Small Water Blowout Small	Waste Waste Blowout Blowout

MIXhi150-PG	Reagent: 150 µL PEN Gat nine pH conditions BA: 150 µL Mix 30, 25, 23, 20, 18, 15, 12, 10, 5, 0 cycles Buffer: 100 µL Phase separation Sample Aq (Multiple Liquids): 100 µL	Fixed tips for Pen G and buffer transfer	Syringe Test Water Blowout Small Waste FT Water Blowout Small	Waste Blowout Waste Blowout
MixLO150-PG	Reagent: 150 µL PAA or 6-APA at nine pH conditions BA: 150 µL Mix 30, 25, 20, 15, 10, 7, 5, 2, 1, 0 cycles Buffer: 100 µL Phase separation Sample Aq (Multiple Liquids): 100 µL	Fixed tips for Pen G and buffer transfer	Water Waste Small Karen BA Karen BA Water blowout small Karen Transfer Aq	Waste Waste Waste Blowout Waste
PH HPLC BT mix	Reagent: 150 µL synthetic bioconversion product stream at nine pH conditions BA: 150 µL Mix 30 cycles Phase separation Sample Aq (100 µL)	6 Trough rak Flush/Wash bowl fitted with three Troughs	Waste Water Small Karen BA Karen BA Karen Transfer Aq	Waste Waste Waste Waste
PH-LLE-PG	Reagent: 150 µL PEN Gat nine pH conditions BA: 150 µL 30 mix cycles Buffer: 100 µL Phase separation Sample Aq Multiple Liquids): 100 µL	Fixed tips for Pen G and buffer transfer	Water Waste Small Karen BA Waste FT Karen Transfer Aq	Waste Waste Waste Waste
PH-LLE-PG2	Reagent: 150 µL Pen G at nine pH conditions BA: 150 µL Mix 2 cycles Buffer: 100 µL Phase separation Sample Aq Multiple Liquids) 100 µL	Fixed tips for Pen G and buffer transfer	Water Waste FT Karen BA Waste FT Karen Transfer Aq	Waste Waste Waste Waste
PH1-solvents Feb test	Reagent: 150 µL BT mix BA: 150 µL, 30 mixing cycles	Flush/Wash bowl with two Troughs	Water waste Karen-BA	Waste Waste

	CH: 150 µL, 30 mixing cycles		Karen-CH	Blowout
	H: 150 µL, 30 mixing cycles		Karen-HEXANE	Blowout
	T: 150 µL, 30 mixing cycles		Karen-TOLUENE	Blowout
	HPI: 150 µL, 30 mixing cycles		Karen-HPI	Blowout
	Buffer: 100 µL		Water waste	Blowout
	Multiple Liquids: 100 µL		Karen-SOLVTtransferAq	Waste
	Dense Aq Samples: 100 µL		Karen-HPItransferAq	Blowout

Table 2.2.1.5.1. Details of Multiprobe® programs for automated microscale LLE experimentation, indicating key experimental procedures, their associated labware and performance files and dispense modes[1]. Standard deck[2] configured with Flush/wash bowl with 2 reagent troughs, Tip chute, Box of small conductive disposable tips, 96-well glass plate and rak[1] containing 350uL HPLC vials[3]. HPI Hydrophobic ionic liquid[4]. Transfer of the organic phase to the Rotary Evaporator for removal of the solvent and then redissolve in phosphate buffer). The outline procedures and deck layout for each test are detailed in appendix 6.

[1] Multiprobe Terminology defined in appendix 5
[2] Standard deck[1] = configured with Flush/wash bowl with 2 reagent troughs, Tip chute, Box of small conductive disposable tips, 96-well glass plate and rak[1] containing 350uL HPLC vials.
[3]Chromacol 350 µL HPLC vial from Chromacol, VWR, UK.
[4] HPI Hydrophobic ionic liquid. Transfer to Rotary Evaporator to remove solvent and then redissolved in phosphate buffer).

File Names	Key Procedures	Additional Labware[2]	Performance Files	Dispense Mode
Slurry	Reagent (150 µL) slurry[5]	100 mL beaker	Karen Slurry	Waste & Blowout
SPE24W 6APAconc	Reagent (150 µL) PAA Sample	24-deep well plate 96-deep well plate	Karen Fst1000 Water Waste Small	Waste Waste
SPE 24well mixKinetics	Reagent (150 µL) PAA Sample	24-deep well plate[1] 24-deep well plate[2]	Karen Fst1000	
SPE 24 well ACconc	Dispense 6-APA to 24-well & 96-well plates Transfer Sample to HPLC vial	24 deep well plate 96- deep well plate HPLC vial rak 96-well plate	Water Waste Small Water Waste Small	Water Waste
SPE96well6APAConc 3EPTS	Reagent (150 µL) 6APA Dilute Transfer (150 µL) Timer Sample	24-deep well plate 96-deep well plate	Karen Fst1000 Waste Water Small	Waste Water
SPE 96-well ACconc	Dilute 6-APA Dispense 6-APA to 96-well plates Transfer Sample to HPLC vial	None	Karen Fst1000 Waste Water Small	Waste Waste

SPE testKEW	Condition filter Apply Vacuum Timer Reagent (300 µL) Timer Apply Vacuum Timer Sample (100 µL) Elution Solvent Timer Apply Vacuum Sample	SPE Manifold Filtration plate 2 Trough[1] Flush/wash bow[1] with 1 Trough	Waste Water Small Waste Water Small Waste Water Small Karen Fst1000 Waste Water Small	Waste Waste Waste Waste Waste
Slurry	Reagent (150 µL) slurry[5]	100 mL beaker	Karen Slurry	Waste & Blowout

Table 2.2.1.5.2: Details of Multiprobe programs indicating experimental parameters, key procedures, labware, performance files and operational modes. Standard deck configured with Flush/wash bowl with 1 Reagent trough, Tip chute and Small conductive disposable tips. ([5] = Slurry of Activated carbon (granular), Activated carbon (powder), XAD-7 or XAD-16 at a variety of concentrations). The outline procedures and deck layout for each test are detailed in appendix 6.

[5]Slurry of Activated carbon (granular), Activated carbon (powder), XAD-7 or XAD-16 at a variety of concentrations.

2.2.1.5.1Compatibility Issues of Automated Platforms

To create a fully automated process the automated platforms and ancillary devices must be compatible with the standard footprint of the multiwell plate (section 1.3.1) and possess a serial port in order to communicate with the PC controlling the workstation. Their software must also integrate with and be controlled by one main operating system that can control a number of different pieces of automated equipment in order to handle any scheduling or operating control issues. This additional equipment used to facilitate the automated experimentation is expected to increase the speed and accuracy of data generation. This will decrease the occurrence of human errors and their affect on the experimentation (section 3.2).

During the development of the automated microscale process, the automated platforms must be free from procedural errors occurring. The performance of the automated equipment and the microscale process itself should be evaluated by comparison with known standards (Dummer, 1974). This was achieved by comparing data from microscale experimental methods carried out at different scales (laboratory scale and manual microscale). The performance of the automated platforms was assessed by quantifying the inter-run and intra-run variation of the data (appendix 10). The accuracy and precision[10] of the data generated using the automated experimental techniques were validated against these data.

2.2.2 Solid-Dosing Equipment

The solid-dosing equipment used in this research was an automated solid dosing station (Accelerator™, Chem Speed, Switzerland) and the DryPette, a manual dry powder pipette (Zinsser Analytic, UK). These pieces of solid dosing equipment were investigated for their solid handling capability (section 5.2.2.3).

[10] Definition of statistical terminology in appendix 11

The Accelerator™ solid dosing station was used to investigate its automated microscale solid handling capability required by some of the solid phase extraction experimentation, which was developed in conjunction with the Multiprobe II Ex®. The Accelerator™ delivers mg to g masses of solids to a variety of containers. The robotic arm can be configured with a range of reagent containers (hoppers) that are suited to dispense a range of solids.

2.2.2.1 Solid Dosing Station Description

The solid dosing station is an automated solids and liquid dispenser (figure 2.2.2.1.1) that has a robotic arm to move around its working area. It was designed to accurately weigh out masses of solids (1 mg to 20 g) or liquids into a variety of containers located within its working area. The instrument contains a weighing balance that is housed within the solid dosing head (section 2.2.2.1). This automated equipment reduces the time required to repeatedly dispense solids into many containers.

The manufacturer quoted that the dosing station is capable of dispensing up to 95% of solid and liquid chemicals, making it suitable for a variety of biotechnological and chemical applications. The dosing station was specifically used in this research for its solid handling capability for the preparation of adsorbent resins and other solid reagents. Its liquid dispensing capability was not used and, therefore, will not be considered further.

2.2.2.2 Mechanism of Action of Dosing Station

The dosing station contains a robotic arm that attaches to a non-resident solid dosing unit (figure 2.2.2.1.1 insert), which can move to transfer solids between receptacles. The solid dosing unit is able to rotate 360° and move in the *X*, *Y*, and *Z* directions over the working area of the dosing station. The dosing station was housed within an exhaust hood (h = 1950 mm, d = 950 mm, l = 1400 mm) to facilitate its use with hazardous chemicals, such as organic solvents, and protect the operator.

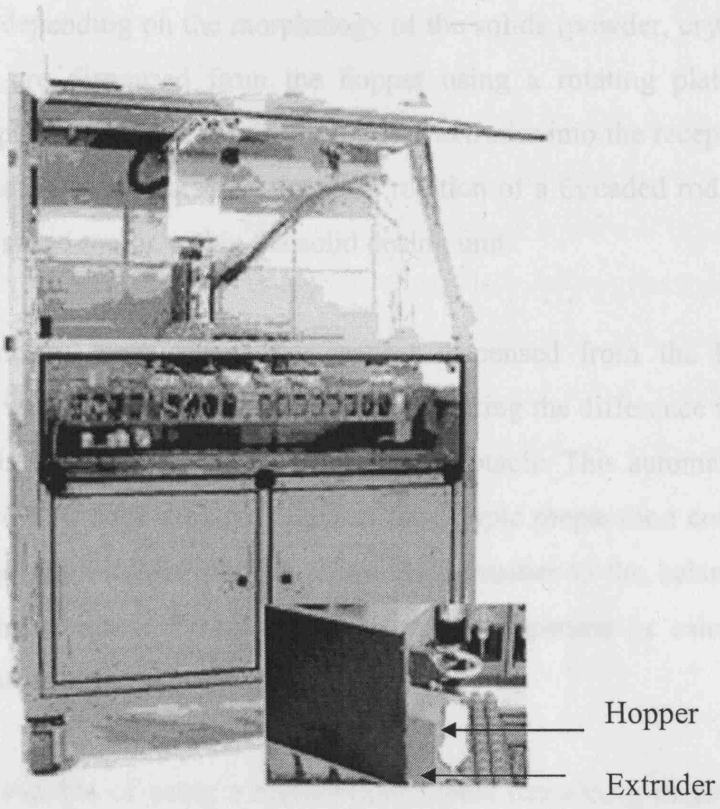

Figure 2.2.2.1.1. Picture of the Accelerator™ solid dosing station (Chem Speed) with an insert of the solid dosing head (detailed in section 2.2.2). Pictures adapted from those on the Chem Speed website (chemspeed, 2002).

The solid dosing station connects to the solid dosing unit containing an accurate and sensitive balance, which attaches to a hopper and extruder (figure 2.2.2.1.1 insert). The solids are contained within a chamber (hopper), which is fitted with a variety of extruders to allow the free flow of the solids and channel their passage into the containers. The extruders are selected depending on the morphology of the solids (powder, crystalline or granular). The solids are dispensed from the hopper using a rotating plate moving downwards in the hopper, forcing the solids through the extruder into the receptacle. The linear movement of the plate is created by the axial rotation of a threaded rod, which is powered by a variable speed motor within the solid dosing unit.

The balance in the dosing unit detects the reagent dispensed from the hopper in increments of 0.1 mg, weighing the solids in-line by calculating the difference in mass of the hopper as the solids are dispensed directly into the receptacle. This automatic weight recording was designed to reduce the time required for sample preparation compared to the manual method by removing the need to move the container to the balance before manually recording the weights. The mass of the solids dispensed is calculated by deductive measurements taken on the balance.

The dosing station is capable of using a number of hoppers containing different solids during a program and these can be changed during use. Therefore, the dosing station can be used to prepare many different samples within one run. However, the hopper can not be cleaned in place, as the equipment must first be dismantled and the hopper and extruder washed separately. This is necessary at the end of the run and occasionally during the run if the dosing mechanism becomes clogged with fine solids. This is an important consideration for dispensing very fine particles or powders as they can easily clog the rotating mechanism of the plate within the hopper, preventing the dispensing of the solids.

The dosing station is operated by specific application software (section 2.2.2.3), which determines the operating parameters. The operational parameters include the fine dosing amount, fine dosing speed, mass flow and filter coefficient. The application software of

the dosing station has a teaching tool that selects the operation parameters of the equipment required for a specific reagent to facilitate the rapid and accurate dosing of the solid.

2.2.2.3 Dosing Station Software

The Accelerator™ dosing station (Chem Speed) was connected to, and controlled by, a PC running an external operating system (Windows 2000) and its application software. The application software detailed the operating performance parameters of the equipment via a versatile electronic interface that can also control ancillary devices, such as filtration rigs. The application software detailed the labware, their location, and reagent to be dispensed. The dosing station software selected these operational parameters by activating a series of tests to dispense a specific solid reagent and optimise the handling of these particles to ensure its effective operation.

The manufacturer achieved good performance of the automated platform for dispensing specific solids (appendix 7.2) and this indicated its suitability for dosing reagents used in this research. However, further investigation was carried out to assess the accurate dispensing of these solids and assess its performance (section 3.2.2) to analyse the types of error (appendix 10) associated with the use of this equipment.

2.2.3 Assessing the Performance of the Automated Platforms

The performance of each of the automated platforms was assessed using gravimetric measurements of the dispensed liquid volumes or reagent masses recorded using an analytical DHALAS balance (Heraeus Instruments, UK). The reagents were dispensed into pre-weighed vials (Chromacol, VWR, UK) under a variety of different scenarios detailed below, sealed with their specific lids and re-weighed. The gravimetric data was analysed using statistical methods (appendix 11) to quantify the performance (accuracy and precision) of the automated platforms (section 3.2) by calculating 2SE and %CV[9].

[9] CV = Coefficient of Variance, defined in appendix 11

The performance of the analytical balance (section 2.7.3) quantified its associated errors by evaluating the repeated measurements of a polypropylene weighing boat (2.2 g, n = 39), paper (1.7 mg, n = 16) and activated carbon (0.9 mg, n = 17) (Sigma Chemicals, UK). These gravimetric data were analysed using statistical methods to quantify the performance of the analytical balance (appendix 12).

2.2.3.1 Assessing the Liquid Handling Performance

The performance of the liquid handling workstation was assessed gravimetrically for dispensing liquid aliquots (section 3.2.1). The workstation ran the bespoke 'dispense' program written using the Winprep® software, and contained a single reagent step[1] to transfer liquid (RO water, unless specified) from a reagent trough[1] to a HPLC vial over a range of operating conditions (Table 2.2.3.1.1).

The workstation was fitted with small conductive disposable tips to dispense replicate (n = 12) liquid aliquots of 1 µL, 5 µL, 10 µL, 100 µL and 150 µL RO water (pH 7 to pH 12) or fixed tips to dispense liquid aliquots of 1 µL, 5 µL, 10 µL and 100 µL RO water (n = 4) or micro conductive disposable tips to dispense liquid aliquots of 1 µL, 5 µL and 10 µL RO water (n = 4 - 8) and the workstation was operated with waste water performance files. The workstation was fitted with small disposable conductive tips to dispense liquid aliquots of 175 µL RO water using either waste[6] or blowout[7] modes (n = 20). The workstation was fitted with small conductive disposable tips to dispense 150 µL RO water aliquots (n = 15 to 18) at different dispensing speeds (10 $\mu L.s^{-1}$, 400 10 $\mu L.s^{-1}$ or 1866 $\mu L.s^{-1}$). The workstation was fitted with small conductive disposable tips to dispense 150 µL RO water or butyl acetate aliquots (n = 8) and operated using the specific performance file created for these liquids.

[6] Waste dispense mode aspirates a larger volume than it is programmed to dispense and then dispenses the required volume, wasting the excess volume.

[7] Blowout dispensing mode aspirates exactly the volume it is programmed to dispense.

Parameter	**Operating Conditions**			
Volume	1 µL - 175 µL			
Reagent	RO water		Butyl Acetate	
Nature of tip	Small conductive		Fixed	
	Micro	Standard		
Operating conditions	Waste[6]		Blowout[7]	
Dispensing speeds	10 µL.s^{-1}	400 µL.s^{-1}	1866 µL.s^{-1}	
Performance files	Standard	Reagent	BA	Transfer

Table 2.2.3.1.1: Conditions evaluated to assess the performance of the Multiprobe®.

[6] Waste dispense mode aspirates a larger volume than it is programmed to dispense and then dispenses the required volume, wasting the excess volume.

[7] Blowout dispensing mode aspirates exactly the volume it is programmed to dispense.

The liquid aliquots were dispensed into pre-weighed HPLC vials (VWR, UK) and re-weighed on an analytical DHALAS balance (Heraeus Instruments, UK). These gravimetric measurements of the vials containing the dispensed liquid aliquots were used to calculate the weight and volume of the dispensed liquid. These measurements were then assessed using analytical and statistical methods (appendix 11) to quantify the accuracy and precision of the automated liquid handling equipment. In addition, the workstation was assessed for its slurry handling capability (section 2.4.2.2.2) over a variety of conditions: investigating the effects of pipette tips: slurry handling procedure: resin particle size: slurry concentration and performance file settings.

2.2.3.2 Assessing Solid-Dosing Equipment

2.2.3.2.1 Evaluating the Dosing Station's Performance

The Accelerator™ dosing station (Chem Speed, Switzerland) was kindly loaned by GlaxoSmithKline (Tonbridge, UK) and was used to assess its ability to dispense dry granular activated carbon, conditioned granular activated carbon (Sigma Chemicals) and Eupergit beads prepared with immobilized penicillin acylase (Fluka). The Accelerator™ prepared adsorbent resin samples of dry granular activated carbon (1 mg to 80 mg) to assess its performance in handling solids and was compared to other solid dosing equipment. (section 5.2.2.3). The dosing station software (section 2.2.2.3) selected the operational parameters required for dispensing dry granular activated carbon prior to experimentation to ensure its effective operation. Solids were dispensed into pre-dried, pre-weighed HPLC vials and stored with screw-top lids (Wheaton, Supleco, UK) until used in microscale SPE experiments (section 2.4.4 and 2.4.6) or for particle size analysis (section 2.4.3).

The solids were repeatedly dispensed into vials and then re-weighed on an analytical DHALAS balance (Heraeus Instruments, UK). The gravimetric measurements of these dispensed solids were assessed using analytical and statistical methods (appendix 11) to quantify the accuracy and precision of the equipment. This procedure was repeated (n =

10) to generate a number of data points to allow statistically significant analysis of the solid-handling performance (section 3.2.2).

2.2.3.2.2 Evaluating the Dry Powder Pipette

DryPette™ (Zinsser Analytic, UK) is a semi-automated hand held dry powder pipette, which was investigated for dispensing a series of reagents (unconditioned granular activated carbon (Sigma Chemicals) and Eupergit beads prepared with immobilized penicillin acylase (Fluka)). The dry pipette was set at its smallest cavity and used to transfer each reagent into a pre-weighed receptacle (section 5.2.2.3).

2.3 Methods for LLE Experimentation

The methods for the LLE experimentation investigated the principles of the extraction technique (section 2.3.1), the method development of the automated microscale LLE (section 2.3.2), microscale LLE methods (section 2.3.3), laboratory LLE methods (section 2.3.4) and visualisation of LLE fluid dynamics (section 2.3.5). All LLE experimentation samples were transferred into HPLC vials with a 100 µL insert, sealed with screw-top lids (Chromacol, VWR, UK) and analysed by HPLC (section 2.5.1).

2.3.1 Principle of the Extraction Technique

The basic principles of the LLE process and the key mass transfer theories are detailed in appendix 13. The laboratory and microscale LLE experiments were carried out at a phase volume ratio ($V_r = V_{org} / V_{aq}$, where V_{org} is the volume of the organic phase and V_{aq} is the volume of the aqueous phase of 1. The aqueous phase contained either the individual compounds, Pen G, 6-APA or PAA at 4.0 $g.L^{-1}$ (12 mM, 18.3 mM and 29.2 mM, respectively) or the simulated bioconversion product stream (10 mM Pen G, 190 mM PAA and 190 mM 6-APA) dissolved in phosphate buffer (0.2 M). The organic phase used was butyl acetate (BA), unless otherwise specified. All experimentation was carried out at ambient temperatures (20 °C) unless specified. The extraction of Pen G and the

simulated bioconversion product stream were carried out on ice (5 °C) to limit compound degradation (section 4.2.1.4.1). The separated aqueous phase samples containing Pen G were diluted 1:1 with phosphate buffer (pH 7) prior to HPLC analysis (section 2.5.1) to limit compound degradation.

The equilibrium distribution constant (K_D) for each solute was calculated using equation 2.1:

$$K_D = \frac{C_{org}}{C_{aq}} \qquad [2.1]$$

where K_D is the distribution constant, C_{org} is the concentration of the solute in the organic phase at equilibrium and C_{aq} is the concentration of the solute in the aqueous phase at equilibrium. These experiments were repeated (n > 12) and the mean values of the data points were plotted with 2SE error bars.

The distribution ratio (D) for each solute was calculated using equation 2.2:

$$D = \frac{C_{org}(t)}{C_{aq}(t)} \qquad [2.2]$$

where D is the distribution ratio, C_{org} (t) is the concentration of the solute in the organic phase at time (t) and C_{aq}(t) is the concentration of the solute in the aqueous phase at time (t). These experiments were repeated (n > 12) and the mean values of the data points were plotted with 2SE error bars.

The distribution constant was used when the liquid-liquid extraction system reached equilibrium after a fixed time point of phase mixing, for example in the mass balance experimentation. The distribution ratio was used for analyzing a dynamic liquid-liquid extraction system when the samples were removed at specific time points within LLE, for example, to assess the mixing kinetics of the automated microscale LLE process during

method development and the experimentation showing the effect of pH conditions on LLE.

2.3.2 Development of Automated Microscale LLE

The microscale LLE process was designed and developed on the automated liquid handling workstation (Multiprobe II Ex®) using a glass 96-well plate (Radleys, UK). The method development experimentation investigated the effect of the operating parameters on the microscale LLE process, including various mixing parameters, mass balance, complex reagents from the bioconversion product stream, compound degradation and reagent evaporation.

2.3.2.1 Microscale Liquid-Liquid Mixing Conditions

The method of liquid-liquid mixing used in the microscale LLE process (section 4.2.1.1) was achieved by repeated aspirating and dispensing of a liquid aliquot (150μL). The mixing experiments were performed using PAA (4.0 $g.L^{-1}$) with an organic phase of butyl acetate, each phase being 150 μL. The bespoke workstation program 'LLE static v move' (Detailed in table 2.2.1.5.1 and appendix 6) investigated three parameters: phase mixing; height of pipette tip and tracking. The phase mixing investigated the use of 0 or 30 aspirating and dispensing mixing cycles. The height of the pipette tip when dispensing was investigated at 2% above the well bottom or 1 mm below the liquid surface. The pipette tracking[1] experimentation (*i.e.* movement of the pipette tip to follow the liquid level as it is aspirated or dispensed), investigated the use of 0% or 100 % tracking. The automated microscale LLE process was carried out and the PAA concentration of each of the aqueous phase samples was analysed on the HPLC (section 2.5.1). The extraction wells were replicated ($n = 4$) in each experiment and the experiment repeated ($n > 3$) to generate sufficient data ($n > 12$).

2.3.2.2 Analysis of the Mass Balance for the LLE process

The mass balance of the automated microscale LLE process (section 2.2.7.1) was achieved by quantifying the mass transfer in the LLE process. The solute, PAA (4.0 $g.L^{-1}$, pH 4.5), was prepared (section 2.1.1.1) and the pH conditions measured on a MP225 pH meter (Mettler Toledo, UK). PAA was extracted with butyl acetate and samples (100 µL) of the feed material (4.0 $g.L^{-1}$), separated post extraction, equilibrium aqueous and organic phases were collected. The samples were transferred to HPLC vials with a 100 µL insert (Chromacol, VWR, UK) and analysed on the HPLC (section 2.5.1).

The samples of the separated organic phase that were stored in HPLC vials with a 100 µL insert (Chromacol, VWR, UK) were evaporated in a rotary evaporator (Speed Vac, Thermo Sa, USA) that was operated at the low temperature setting until dry. The dried PAA samples were re-dissolved in 100 µL phosphate buffer (pH 7, 0.2 M) and mixed by inversion before being analysed on the HPLC (section 2.5.1).

The sample's PAA concentrations were quantified and the mean solute concentrations were used to calculate the distribution constants to follow the mass balance for the LLE process (section 4.2.1.3: table 4.2.1.3.1 (a)).

2.3.2.2.1 Comparison of Mass Balance Data at Different Scales

The mass balance for the LLE of PAA (4.0 $g.L^{-1}$, pH 4.5) with BA was carried out at different scales of operation: laboratory (section 2.3.4); automated (section 2.3.3.1) and manual microscale (section 2.3.3.2). The automated microscale LLE process used the workstation program LLE mass balance 1pH, as detailed in table 2.2.1.5.1 and outlined in appendix 6. The phases were mixed with 30 mixing cycles[1] with the pipette tip at 2% above the well bottom and with 0% tracking. The manual microscale LLE process used a manual 1 mL pipette to create these mixing conditions during the LLE process. The laboratory LLE process used magnetic stirrers to create phase mixing at 1000 rpm. The phases were left to separate under gravity into two distinct phases for 10 minutes.

Samples of the feed material, equilibrium aqueous and organic phases from each scale were collected and analysed (section 2.3.2.2). The mean PAA concentrations of the samples were used to quantify the mean solute concentrations, which were used to calculate the distribution constants to assess the mass balance for each of the LLE process scales (section 4.2.1.3: table 4.2.1.3.1 (b)).

2.3.2.3 LLE of the Simulated Bioconversion Product Stream

The LLE of the simulated bioconversion product stream (10 mM Pen G, 190 mM PAA and 190 mM 6-APA) was carried out using the automated microscale method (section 2.3.3.1) and the laboratory LLE method (section 2.3.4). The feed material was dissolved in phosphate buffer (0.2 M) at pH 2.5 and the extractions were carried out using BA, which were repeated at each scale (laboratory n = 3, microscale n = 12). Samples (100 µL) of the feed material were taken pre- and post-extraction for both of the process scales and transferred into HPLC vials and analysed on the HPLC (section 2.5.1).

2.3.2.4 Compound Degradation

The degradation of Pen G dissolved in phosphate buffer (0.2M) was investigated over time (5 hours) at different pH conditions and temperatures. Samples of Pen G (4.0 $g.L^{-1}$) were prepared at pH 7 and stored at different temperatures with samples kept on ice (5 °C) and in the laboratory (20 °C). The samples were analysed using HPLC analysis (section 2.5.1) and the mean concentration data was plotted against time for Pen G and the degradation products, 6-APA and PAA (figure 4.2.1.4.1.1).

Pen G samples (4.0 $g.L^{-1}$) were prepared at different pH conditions (pH 2.5, pH 4.2 and pH 7) to investigate the effects on its degradation over time (10 hours). They were prepared initially at pH 7 and then divided for adjustment to different pH conditions. All the initial samples were kept on ice (5 °C) prior to experimentation and analysis. The

[1] Multiprobe terminology defined in appendix 5

samples were transferred to laboratory temperature for the duration of the experiment and aliquots (10 μL) of each sample were analysed on the HPLC (section 2.5.1). The Pen G concentration values were plotted against time for each of the pH conditions (figure 4.2.1.4.1.2).

2.3.2.5 Microscale Evaporation Studies

The evaporation of the LLE phases from the microscale extraction well was studied at 20 °C over time to investigate the effect on the microscale LLE process (section 4.2.1.5). Aliquots of the reagents: 150 μL aqueous phase (PAA 4.0 $g.L^{-1}$); 150μL butyl acetate or both phases (total volume 300 μL), that were dispensed in each order, were dispensed into HPLC vials with a 100 μL insert (Chromacol, VWR, UK). The HPLC vials were fitted with screw-top lids then weighed, unsealed for use in the experiment to store the liquid aliquots, sealed and re-weighed on an analytical balance (Heraeus Instruments, UK). The vials were periodically re-weighed over 24 hours to generate a series of gravimetric measurements that were analysed to generate evaporation rates for each sample, and the data presented as a plot of volume lost by evaporation against time in figure 4.2.1.5.1.

2.3.3 Microscale Liquid-Liquid Extraction Method

The microscale LLE method was modified from the laboratory method (section2.3.4) and developed for the automated liquid handling workstation (section 2.3.3.1), as well as the manual pipette (section 2.3.3.2). The LLE aqueous/ organic phase system maintained the phase volume ratio of 1 and the microscale extractions were carried out at a total volume of 300 μL in a glass 96-well plate (Radleys, UK). The glass 96-well plate contained wells (diameter 7.6 mm, height 13 mm) with a total volume of 540 μL and was resistant to organic solvents. The extraction conditions were repeated in 4 replicate wells, the experiment was repeated ($n > 3$) and the mean values were calculated to produce statistically significant data. The mean aqueous phase solute concentration was used to calculate the distribution constant (equation 2.1).

The phases were mixed using repeated aspirating and dispensing mixing cycles[1] of the automated or manual pipette, transferring a 150 μL aliquot containing both phases from a static position at 2% above the bottom of the well. The phases were left to separate under gravity (10 min) to allow the extraction volume to separate into two distinct phases. Each sample of the separated aqueous phase (100 μL) was transferred from the extraction well into a HPLC vial and analysed on the HPLC (section 2.5.1). The aqueous phase compound concentration values were used to calculate the mean concentration value and the distribution ratio. This microscale LLE method was used as the basis of subsequent investigations into LLE kinetics (section 2.3.3.3), aqueous phase pH conditions (section 2.3.3.4), solvents (section 2.3.3.5) and dispensing speed (section 2.3.3.6) that were carried out using the automated liquid handling workstation (section 2.3.3.1).

2.3.3.1 Automated Microscale Liquid-Liquid Extraction

The automated microscale LLE method was designed for the liquid handling workstation (Multiprobe II Ex®) using its Winprep® software to generate a bespoke program containing the detailed experimental method and selected operational parameters (table 2.2.1.5.1). This automated microscale LLE process program (LLE 150 HPLC v350) was developed using results from automated microscale LLE method development experimentation (section 4.2.1) to generate the microscale LLE method (section 2.3.3.1). This program contained steps[1] to transfer each sample of the aqueous phase into a HPLC vial (Chromacol, VWR, UK), which was then sealed with a screw-top lid (Chromacol, VWR, UK) prior to HPLC analysis (section 2.5.1). The bespoke Winprep® software 'LLE 150 HPLCv350' program is outlined in appendix 6 and details are highlighted in table 2.2.1.5.1.

This process used aqueous (PAA, 4.0 $g.L^{-1}$) and organic phases (BA) of 150 μL each, which were mixed by repeatedly pipetting , transferring a 150 μL aliquot of the combined LLE phases into and out of the liquid within the extraction well for 30 mixing cycles

from 2% above the well bottom with 0% tracking[1]. The samples of the separated aqueous phase (100 µL) were aspirated from 2% above the well bottom and were transferred to the HPLC vials with inbuilt 350 µL inserts (Phenomenex, UK) or HPLC vials with separate 100 µL inserts (Chromacol, VWR, UK). The samples were analysed on the HPLC (section 2.5.1) to quantify the solute concentrations and calculate the distribution ratios (section 2.3.1). These data were compared with the manual microscale LLE process data (section 4.2.3.2) and the laboratory LLE process data (section 4.2.3.1).

2.3.3.2 Manual Microscale LLE Process

The manual microscale LLE process used the microscale method (section 2.3.3) to carry out the LLE experimentation using a manually operated P200 pipette (Gibson, UK) fitted with P200 disposable pipette tips (internal diameter = 0.625 mm). This manual microscale LLE process was used to validate the automated microscale LLE process (section 4.2.3.2). The aqueous phase (150 µL) contained PAA (4.0 $g.L^{-1}$) and was prepared under a range of pH conditions (pH 2 to pH 8), which were measured on a MP225 pH meter (Mettler Toledo, UK). The organic phase (150 µL) was butyl acetate. The phases were mixed by repeated (aspirating and dispensing) mixing cycles[1] (n_c = 30) with the pipette in a fixed position near the bottom of the well, removing an aliquot (150 µL) containing both phases. The mixture was left for 10 minutes to separate into two distinct phases before the aqueous phase samples (100 µL) were removed and analysed on the HPLC (section 2.5.1). The manually prepared microscale experimentation was carried out in replicate wells (n = 4) that had identical conditions and the experiment was repeated (n > 3) to generate representative mean values of the distribution constants. The automated microscale distribution constants from section 2.3.3.1 were plotted against the manual LLE distribution constant data with 2SE error bars (figure 4.2.3.2.1).

[1] Multiprobe terminology defined in appendix 5

2.3.3.3 Kinetics Studies of Automated LLE Process

The liquid handling workstation was operated using a bespoke program, which was written by modifying the automated microscale LLE method (section 2.3.3.1). This program was used to study the kinetics of the LLE process for each of the individual compounds (Pen G, PAA and 6-APA, 4.0 $g.L^{-1}$) or the synthetic bioconversion product stream (BTmix) over a range of mixing conditions (0 to 30 mixing cycles (aspirating and dispensing)) to achieve phase mixing. The corresponding times for the duration of the mixing cycles were measured using a stop-watch (Radleys, UK).

The compounds were dissolved in phosphate buffer (0.2 M). The pH conditions used for Pen G, PAA and 6-APA were pH 4.5, 2.5 and 2.5, respectively. The liquid handling workstation was operated using bespoke programs written for each of the compound's requirements and different kinetics investigations, which included 'MIXhi150', 'MIXhi150-PG' and 'MixLO150-PG' characterized in table 2.2.1.5.1 and outlined in appendix 6. The microscale LLE process used either 'hi' mixing kinetics with higher mixing conditions (0, 5, 10, 12, 15, 18, 20, 23, 25, 30 mixing cycles) or 'low' mixing conditions (0, 1, 2, 5, 7, 10, 15, 20, 25 or 30 mixing cycles) to investigate the LLE kinetics of PAA and Pen G. The phases were separated under gravity (10 min) and samples of the aqueous phases were transferred into vials for analysis by HPLC (section 2.5.1). The mean concentration values were used to calculate the distribution constants. These values were plotted against the mixing cycles and associated mixing times with 2SE error bars (figure 4.2.2.1).

2.3.3.4 Effect of pH on Equilibrium Solute Distribution

The effect of aqueous phase pH conditions on solute partitioning in the microscale LLE process was investigated on the workstation operating the 'LLE 9pH', 'PH-LLE-HPLCv350-010201', 'PH-LLE-PG', 'PH-LLE-PG2' and 'PH HPLC BT mix' programs, as detailed in table 2.2.1.5.1 and outlined in appendix 6.

The liquid handling workstation operated the 'LLE 9pH' and 'pH-HPLC-BTmix' programs to generate the experimentation for PAA (4.0 $g.L^{-1}$) and the synthetic bioconversion product stream (BTmix). The microscale LLE experimentation used aqueous phases that contained the individual compounds (Pen G, 6-APA or PAA, 4.0 $g.L^{-1}$) dissolved in phosphate buffer (0.2 M) prepared over a pH range of pH 1.5 to pH 8.0. The pH conditions were measured on a MP225 pH meter (Mettler Toledo, UK). These compounds were extracted into butyl acetate using the automated and manual microscale LLE methods (section 2.3.3.1 and 2.3.3.2, respectively). Samples of the separated aqueous phases were analysed on the HPLC (section 2.5.1). The concentration of the samples was used to calculate the distribution constants, which were plotted against the equilibrium pH with 2SE error bars (figure 4.2.3.1).

2.3.3.5 Screening of Automated LLE Process Solvents

A range of solvents with different physical and chemical properties (table 4.2.4.1.1) was screened using the automated workstation. The solvents screened were butyl acetate, cyclohexane, hexane, toluene and a hydrophobic ionic liquid, [Bmin][PF_6]. These analytical grade solvents were used for the extraction of PAA from the simulated product stream (section 2.1.1.1) at pH 3.0. The microscale LLE process (section 2.3.3.1) was modified to screen these solvents by generating the 'PH1-solvents Feb test' program (section 2.2.1.5), which operated the workstation using their specific performance files (section 2.2.1.4.1) to efficiently transfer them.

The 'hpi' program was generated for the LLE with hydrophobic ionic liquid, as the heavy phase contained the solvent rather than the light phase used in the case of the other solvents. Samples of the aqueous phase (100 µL) were analysed on the HPLC (section 2.5.1). The distribution constants were calculated from the mean aqueous phase PAA concentration values and plotted against the corresponding values achieved at the laboratory scale (section 2.3.4).

2.3.3.5.1 Kinetics of LLE with Different Solvents

The kinetics of the LLE of PAA (4.0 $g.L^{-1}$, pH 3) were carried out using different solvents: butyl acetate, cyclohexane and the ionic liquid [Bmim][PF_6]. The kinetics of LLE using each solvent were assessed over 0 to 30 mixing cycles (0, 5, 10, 15, 18, 20, 23, 25, 30 mixing cycles). This used the automated microscale LLE process for the workstation, which was modified from the 'MixHI150' program (section 2.3.3.3) using the specific performance files for each of the solvents. The microscale LLE process data was collected from replicate experiments (n = 3) that had identical conditions in 4 extraction wells. The mean concentration values were used to calculate the corresponding distribution constants data and then plotted against the number of mixing cycles, as well as the associated mixing times with 2SEerror bars (figure 4.2.4.1.1).

2.3.3.5.2 Solvent Screening for Automated LLE

The solvents were screened for their efficiency in extracting PAA from the synthetic bioconversion product stream (section 2.1.1.1) using the automated workstation operating the 'PH1-solvents Feb test' program, detailed in table 2.2.1.5.1 and outlined in appendix 6. The program was modified from the automated microscale LLE method (section 2.3.3.1) with the specific performance files (section 2.2.1.4.1) for each solvent to achieve their efficient transfer. The aqueous phase (pH 2.5) was extracted with butyl acetate, cyclohexane, hexane, toluene and ionic liquid (1-butyl 3-methyl imidazolium 1-butyl-3-methylimidazolium chloride). The analysis of the aqueous phase PAA concentrations were used to calculate the distribution constants for each of the solvents, which were plotted with statistical analysis of the results (figure 4.2.4.2.1).

2.3.3.6 Automated Microscale LLE Process Dispensing Speeds

The liquid handling workstation was operated over a range of dispensing speeds (10 $\mu L.s^{-1}$ to 1866 $\mu L.s^{-1}$) for the extraction of PAA (4.0 $g.L^{-1}$, pH 3) with butyl acetate. The experimentation was carried out by the workstation operating the 'MIXhi150' program at these different dispensing speeds, which was modified from the automated

microscale LLE method (section 2.3.3.1) to assess the kinetics of these extraction processes over a range of mixing cycles (n_c = 0 to 30) with the workstation operated at each dispensing speed. The microscale data was collected from replicate experiments that had identical conditions and the samples analysed on the HPLC (section 2.5.1). The mean concentration values were measured to calculate the distribution constant data, which was plotted against the mixing cycles and the associated dispensing times with 2SE error bars (figure 4.2.5.1). These data plots were used to calculate the k_La values associated with each of these dispensing speeds (figure 4.2.2.1).

2.3.4 Laboratory Scale Liquid-Liquid Extraction (10 mL scale)

The laboratory scale (10 mL) LLE experiments were carried out in flat-bottomed glass universal tubes (20 mL) using Pen G, PAA, 6-APA (4.0 $g.L^{-1}$) or the simulated product stream with BA, at a phase volume ratio of 1. The tubes each contained a magnetic flea (8 mm x 0.5 mm) and were placed on a 9-position magnetic stirrer (Radleys, UK). This mixed the phases at 1000 rpm for $\geq$ 1 hour at 20 °C to achieve mass transfer equilibrium between the phases. The phases were left for 30 minutes to allow the mixture to separate into two distinct phases. The separated phases were transferred by manual pipetting into tubes and stored at 5°C. Analysis was made of the aqueous phase pH conditions at the end of the experimentation using a MP225 pH meter (Mettler Toledo, UK). A sample of the separated aqueous phase (0.5 mL) was taken from each extraction vessel and analysed using the HPLC (section 2.5.1).

The laboratory scale LLE method was used to show the sample of the aqueous phase pH conditions on solute partitioning (pH 2 to pH 8) on the extraction of PAA (4.0 $g.L^{-1}$). The laboratory scale LLE method was also used with different solvents (butyl acetate, cyclohexane, hexane, toluene and a hydrophobic ionic liquid, [Bmin][PF_6] in the extraction of PAA (4.0 $g.L^{-1}$, pH 2.5), mimicking the conditions used in the microscale LLE experimentation. The results were compared to those from the microscale LLE experimentation (section 4.2.3.1 and section 4.2.4, respectively).

2.3.4.1 Mass Balance of Laboratory Scale LLE

The mass balance of the laboratory LLE process of PAA (4.0 $g.L^{-1}$, pH 4.5) with BA, which was mixed and separated as detailed in section 2.3.2.2, was made by HPLC analysis of the separated organic and aqueous phases. The aqueous phase samples were analysed directly on the HPLC (section 2.5.1). Samples of the organic phase of the laboratory LLE were collected and the solvent evaporated using the Speed Vac evaporator (Thermo Sa, USA). The Speed Vac was run for 4 hours at the lowest temperature setting (30 °C) to limit the degradation of the compounds, whilst removing the solvent. The dried compounds were redissolved in phosphate buffer pH 7.65 and mixed by inversion. A 0.5 mL sample was taken from each redissolved organic phase sample and analysed using the HPLC (section 2.5.1). The results were compared to the other LLE scales (section 4.2.1.3) as previously described in section 2.3.2.2.

2.3.5 Visualisation of Liquid-Liquid Fluid Dynamics

The microscale and laboratory scale LLE processes were visualized using a NAC HSV500 digital high-speed camera borrowed from the European Physical Sciences Research Council equipment loan pool. This captured the phase mixing within the LLE vessels by adding a blue food dye (Sainsbury's, UK) to the aqueous phase to enhance the visualisation of the phase boundary.

The fluid dynamics of a variety of mixing methods (manual pipetting, horizontal shaker and magnetic bars) were investigated for their suitability in the laboratory scale LLE process. The manual pipetting method used 30 mixing cycles, transferring 50% of the total extraction volume in and out of the extraction vials. The samples in the extraction vials secured to the horizontal shaker (UKA Laboratechnik) were mixed at 1000 rpm for 30 minutes. The magnetic bars were placed within the extraction vials, which were located on top of a magnetic plate (5 arbitrary units) and the samples were mixed for 1 hour.

The visualization of the microscale LLE process investigated mixing created by repeated pipetted mixing cycles using manual or automated pipetting (section 2.3.5.1) as described in the microscale methods (section 2.3.3.1 and 2.3.3.2), or mixed using oscillating platforms. The manual microscale LLE process (section 2.3.3.2) was prepared using a manual pipette to transfer the reagents to the multiwell plate and the samples were mixed using the horizontal oscillating platform (Thermomixer, Eppendorf, UK) at 250 rpm or on a bench shaker (UKA Laboratechnik) at 1000 rpm. All fluid dynamic analysis experimentation was carried out at ambient temperature and pressure. The results were presented as selected frames from the video sequence (section 4.2.1.2). Images of all stages of the manual microscale LLE process were taken investigating the reagent transfer and phase mixing using each of the mixing methods.

2.3.5.1 Visualisation of Automated Microscale LLE

The fluid dynamic analysis of the automated microscale LLE process investigated a number of parameters involved in the use of the liquid handling workstation. These parameters included the aqueous phase reagents, organic phases and various parameters affecting the inter-phase mixing characteristics, including dispensing speeds, performance files and the use of the pipette tracking function, which were all investigated to ensure that good phase mixing was occurring using the workstation.

Images were taken of the automated microscale LLE process experimentation, screening the process conditions investigating solutes (section 2.3.3.4), solvents (section 2.3.3.5) and dispensing speeds (section 2.3.3.6). The aspirating and dispensing characteristics of the aqueous phase (150 μL) were investigated using RO water, Pen G, PAA and 6-APA (4.0 $g.L^{-1}$) dissolved in phosphate buffer (pH 7), together with the butyl acetate organic phase (150 μL) using the high-speed camera to visualise the microscale LLE process (section 2.3.3).

2.4 Methods for SPE Experimentation

2.4.1 Conditioning of Adsorbents

2.4.1.1 Activated Carbon

The granular and powdered activated carbon was conditioned by wetting the dry adsorbent with RO water contained in a 500 mL beaker and mixed with a magnetic flea (40 mm x 10 mm). The slurry was gently agitated for 30 minutes and then left to settle for 30 minutes. The waste water was decanted from the solids before the procedure was repeated. The conditioned granular activated carbon was stored with enough water to cover the particles in a sealed container at ambient temperature until required.

2.4.1.2 Amberlite XAD Resins

The Amberlite XAD resins (XAD-7 and XAD-16) were conditioned according to the manufacturer's guidelines, which were similar to the conditions used to condition activated carbon (section 2.4.1.1).

2.4.2 SPE Process Characteristics

The SPE process characteristics investigated a range of adsorbent resins (section 2.4.2.1) to select the most suitable for the adsorption of 6-APA. The preparation of the microscale SPE formats with the adsorbent resin was considered by investigating the slurry handling options (section 2.4.2.2) using the manual and automated slurry handling equipment (section 2.2.1).

2.4.2.1 Adsorbent Selection

The adsorbent resins were initially screened for their absorption of 6-APA (4.0 $g.L^{-1}$) from an aqueous solution (phosphate buffer 0.2 M, pH 4). The adsorbent resins investigated were granular activated carbon (4.0 $g.L^{-1}$), Amberlite XAD –7 (4.0 $g.L^{-1}$) and Amberlite XAD-16 (4.0 $g.L^{-1}$). The adsorbent resins were conditioned (section 2.4.1) and

manually weighed into 50 mL vials. The resins were contacted with 50 mL 6-APA solution (4.0 $g.L^{-1}$) dissolved in phosphate buffer (0.2 M, pH 4.5) and mixed on a bench shaker (UKA Laborortechnik) at 1000 rpm at 20 °C for 24 hours. Samples of the liquid phase were regularly removed within the 24 hour period and the aliquots were prepared for analysis using the Megafuge centrifuge (Heraeus Instruments, UK) for 5 minutes to separate any resin particles. The supernatant was transferred to a clean HPLC vial (Chromacol, VWR, UK) and the samples analysed on the HPLC (section 2.5.1).

The liquid phase 6-APA concentration data were plotted against time (figure 5.2.1.1.3.2) to follow the SPE kinetics at laboratory scale for the adsorbent resins (figure 5.2.1.1.3.1). The equilibrium liquid phase concentration data generated after 24 hours contact between the phases was used to calculate the absorbed 6-APA mass, which was used in the calculation of the maximum adsorption ($g_{6\text{-}APA}.g_{resin}^{-1}$) values.

2.4.2.1.1 96-well Format 1 mL Cartridge Resin Screening

The commercially available non-polar application development kit (Isolute, Jones Chromatography, UK) contained 1 mL square cartridges pre-filled with one of an array of adsorbents (25 mg) arranged in a 96-well format. The adsorbents (C18, C18 MF, C8, C6, C4, C2, PH and CN[8]) were conditioned with 1 mL of RO water and the solvent was removed from the conditioned cartridges under negative pressure (0.5 mmHg, 40 s) before an aliquot (1 mL) of the aqueous 6-APA (4.0 $g.L^{-1}$, pH 4.5) was contacted with the adsorbent for 15 minutes. The liquid phase samples were removed from the cartridges under pressure (0.5 Hg, 40 s) and transferred to HPLC vials and sealed with screw-top lids (Chromacol, VWR, UK). The adsorbed 6-APA was eluted from the resins in the

[8] C18 = Octadecyl (non end-capped) functionalized silica, manufactured using trifunctional silanel, C18 MF = Octadecyl (end-capped) functionalized silica, manufactured using trifunctional silanel, C8 = Octyl (non end-capped) functionalised silica, manufactured using trifunctional silanel, C6 Hexyl (end-capped) functionalized silica, manufactured using trifunctional silanel, C4 = Butyl (end-capped) functionalized silica, manufactured using trifunctional silanel, C2 = Ethyl (non end-capped) functionalized silica, manufactured using trifunctional silanel, PH = Phenyl (non end-capped) functionalised silica, and CN = Hydroxylated polystyrene-divinylbenzene.

cartridges by elution with ethanol (1 mL), before the addition of an aliquot of phosphate buffer (1 mL). Each of these samples were removed under pressure and transferred to HPLC vials and sealed with screw-top lids prior to HPLC analysis (section 2.5.1). The 6-APA concentration in the liquid phase was quantified from the HPLC data and the 6-APA adsorbed onto the adsorbents was calculated, which was used to calculate the percentage adsorbed 6-APA values.

2.4.2.2 Slurry Handling

The activated carbon slurries were prepared by manually weighing conditioned granular activated carbon adsorbent into a 100 mL beaker and suspending them in 50 mL of phosphate buffer (0.2 M). The slurry (25 $g.L^{-1}$ or 100 $g.L^{-1}$, as specified) was stirred with a six bladed Rushton turbine (diameter = 20 mm) on an overhead motor (Stuart Scientific SS10) and operated at 1000 rpm to maintain the suspension's homogeneity. The impeller was maintained at a fixed height (10 mm) above the base of the beaker. Samples were taken from the same height and location inside the beaker (2 cm height, central location, unless specified) and dispensed into pre-weighed Eppendorf tubes. These tubes were weighed and stored open in a rack and dried overnight at 100 °C in an oven (Heraeus Instruments, UK) to dry the resin samples, before the tubes containing the solids were re-weighed. The dispensed slurry data was used to calculate the dispensed volume and solids, which were calculated as percentages of the target values to quantify the slurry handling performance (section 5.2.2.1) by statistical analysis of the data (appendix 11).

2.4.2.2.1 Manual Slurry Handling

The slurries were transferred using the manual slurry handling equipment to assess its performance when fitted with different pipette tips and operated under different scenarios (detailed below). The SPE resins were conditioned (section 2.4.1) and the slurries (25 $g.L^{-1}$ or 100 $g.L^{-1}$) were prepared in a 100 mL beaker mixed using a Rushton turbine fixed to an overhead motor (UKA Laborortechnik) (1000 rpm) to create homogeneous slurry (Re = 1115).

The manual handling equipment contained the P200 and P1000 manual pipettes (Gilson, UK) fitted with disposable tips. The P200 pipette was fitted with the P200 disposable tips (d_i = 0.625 mm). The P1000 pipette was fitted with a range of disposable pipette tips: standard (d_i = 0.85 mm) or wide bore (d_i = 1.2 mm) (Molecular Bioproducts, UK). Aliquots of the slurry (25 $g.L^{-1}$ or 100 $g.L^{-1}$ for 1.22 mm tip data) were dispensed into tubes and prepared as described in section 2.4.1. Slurry aliquots (150 µL) were transferred from a stirred vessel to pre-weighed tubes (section 2.4.2.2) to quantify the dispensed volume and resin mass of the transferred slurries. Mean values of the dispensed liquid volumes and resin masses were plotted alongside the target values for each reagent.

This method was used to investigate the performance of manual slurry handling of different pipette tips by comparison with a negative control (RO water) over a range of aliquot volumes for powdered resin slurries. The slurry concentration was increased from previous experimentation (25 $g.L^{-1}$) to 100 $g.L^{-1}$ to assist the manual slurry handling resin mass transfer performance by theoretically increasing the probability of transferring the solids. The slurry aliquots were transferred from the stirred vessel into pre-weighed tubes, which were weighed, dried in an oven and re-weighed (section 2.4.2.2) in order to quantify the volume and mass of the transferred slurries.

The manual slurry handling equipment detailed above was fitted with modified disposable pipette tips (standard = 0.85 mm, cut #1 = 1.1 mm and cut #2 = 1.22 mm prepared in-house and 1.2 mm from Molecular Bioproducts (UK). Aliquots of 0.15 mL of the conditioned granular activated carbon slurry (25 $g.L^{-1}$) were dispensed into tubes and prepared as described in section 2.4.2.2.

The manual slurry handling equipment was assessed for dispensing pure RO water and conditioned granular activated carbon (100 $g.L^{-1}$). The 1 mL pipette tip was fitted with the wide bore pipette tips (1.2 mm) and transferred aliquots (0.15 µL) of the reagents from the stirred vessel to pre-weighed tubes as described in section 2.4.2.2. The mean

actual volume and resin mass values were calculated, together with statistical analysis of the data, and plotted with 2SE error bars (figure 5.2.2.1.2.1).

The manual slurry handling method used the 1 mL pipette fitted with the wide bore pipette tips (1.2 mm) to assess its performance in transferring different volumes (200 µL to 1000 µL) of conditioned granular activated carbon slurries (25 $g.L^{-1}$) for each of the slurry volumes (0.2 mL, 0.4 mL, 0.8 mL and 1 mL). The aliquots were dispensed into tubes and prepared as described in section 2.4.2.2. The mean actual volume and resin mass values were calculated and plotted with the target values, together with 2SE error bars (figure 5.2.2.1.3.1).

The manual slurry handling equipment was used to assess the slurry handling of powdered activated carbon (0.15 $g.L^{-1}$) suspended in phosphate buffer (0.2 M, pH 7) from a 100 mL stirred vessel containing the slurry. The samples were removed from the vessel at different heights (0 mm, 15 mm and 20 mm). For each of the slurry sampling heights, the aliquots were transferred from the stirred vessel into tubes as described in section 2.4.2.2. The dispensed slurry volume and resin mass were calculated, together with statistical analysis of the data (table 5.2.2.1.4.1).

2.4.2.2.2 Automated Slurry Handling

The automated slurry handling capability of the liquid handling workstation (Multiprobe II Ex®) was assessed over a variety of operating conditions. The workstation ran the 'Slurry' program, as detailed in table 2.2.1.5.2 and outlined in appendix 6. The conditioned activated carbon slurry was held in a 100 mL beaker (d = 48 mm, h = 75 mm) that contained glass baffles (d_b = 2 mm), mixed using a magnetic flea (35 mm x 8 mm) on a magnetic plate (Radleys, UK). The slurry aliquots were dispensed and weighed, as described in section 2.4.2.2. These gravimetric measurements were used to calculate the dispensed liquid volume and resin mass. These measurements of the dispensed liquids were assessed using analytical and statistical methods (appendix 11) to quantify the accuracy and precision of the automated liquid handling equipment. This

procedure was repeated for a sufficient number of data points to generate statistically significant analysis of the liquid handling performance (section 3.2.1).

The workstation was operated under a variety of conditions to assess its slurry handling capacity. The workstation was assessed by repeatedly dispensing samples (n = 12) of 165 µL of activated carbon slurry (91 $mg.L^{-1}$). The workstation was fitted with disposable 200 µL pipette tips that had different internal diameters; standard small conductive tips (d_i = 0.85 mm) and wide bore non-conductive tips (d_i = 1.4 mm) (Molecular Bioproducts, UK). The automated slurry handling procedure investigated the configuration of the beaker containing the slurry. The workstation was fitted with wide bore disposable pipette tips to transfer 150 µL aliquots of the powder activated carbon slurry (100 $g.L^{-1}$) from the bulk slurry. This slurry was mixed in the 100 mL beaker with a magnetic flea (length 8 mm, diameter 35 mm) rotating at *circa* 12 rpm (3 arbitrary units on the magnetic plate (Radleys, UK) to pre-weighed HPLC vials (VWR, UK)). These samples were then prepared as described in section 2.4.2.2. The samples (n = 12) were pipetted from different pipetting heights (0%, 15% or 20% above the vessel bottom) and with the bulk slurry mixed over a range of mixing speeds (1 to 6 arbitrary units).

The workstation transferred 150 µL aliquots of a variety of different slurry preparations: granular (147 $g.L^{-1}$ or 300 $g.L^{-1}$) or powdered (147 $g.L^{-1}$ or 300 $g.L^{-1}$) activated carbon.The workstation fitted with wide bore disposable tips dispensed repeated samples (n = 12) of 150 µL aliquots of 300 $g.L^{-1}$ powdered, 147 $g.L^{-1}$ powdered, 147 $g.L^{-1}$ ground and 300 $g.L^{-1}$ granular activated carbon slurry. The workstation was fitted with disposable wide bore pipette tips to dispense a variety of granular activated carbon slurry concentrations and volumes. Repeated samples (n = 12) were prepared of granular activated carbon slurry of 150 µL at 13.3 $g.L^{-1}$, 100 µL at 26.6 $g.L^{-1}$, and 50 µL at 66.7 $g.L^{-1}$ and 25 µL at 156.7 $g.L^{-1}$. The samples were prepared (section 2.4.2.2) to generate the gravimetric measurements. This data was used to assess the effect of pipette tips (section 5.2.2.2.1), slurry handling procedures (section 5.2.2.2.2), resin particle size (section 5.2.2.2.3), slurry concentration (section 5.2.2.2.4) and performance files (section 5.2.2.2.5) on the workstation's solid-handling performance.

2.4.3 Particle Size Analysis

The particle size distribution of the commercially available powdered and granular activated carbon was analysed using a Malvern particle sizer (Malvern Instruments Ltd., UK). The ground granular and GSK Chem Speed Accelerator™ dispensed granular activated carbon samples, which were prepared, as detailed below, and were analysed to determine their particle sizes (figure 5.2.2.2.2.1).

The ground granular activated carbon sample was prepared using a pestle and mortar to break up the larger particles within the granular activated carbon (Sigma-Aldrich, #3014). The GSK Chem Speed Accelerator™ granular activated carbon sample was prepared by dispensing granular activated carbon from the Chem Speed Accelerator™ dosing station. All the activated carbon preparations, except the GSK granular activated carbon, were conditioned as described in Section 2.4.1, prior to analysis of their particle size. The reagents were powdered activated carbon (0.5762 g), granular activated carbon (1.3654 g), ground granular activated carbon (0.41 g), GSK Chem Speed Accelerator™ granular activated carbon (0.1581 g) and ground activated carbon (0.4101 g). Each in turn was added to the aqueous dispersant (300 mL) before the particle size distribution was analysed.

2.4.4 Microscale SPE Methods

The microscale SPE experiments were carried out at two different volumes using 24-deep well and 96-deep well plates. The liquid phase (section 2.1.2.1) was contacted with unconditioned granular activated carbon. The microscale SPE experiments investigated the microscale phase mixing (section 2.4.4.1), the kinetics of the SPE process (section 2.4.4.2), the effect of liquid phase pH conditions on kinetics (section 2.4.4.3), the adsorption isotherms (section 2.4.4.4) by investigating the adsorbent and adsorbate concentrations and the effect of pH conditions of the liquid phase. The microscale SPE experiment end point liquid phase samples were transferred to HPLC vials with a 100 μL

(Chromacol, VWR, UK) and sealed with screw-top lids (Chromacol, VWR, UK) for HPLC analysis on the HPLC (section 2.5.1).

2.4.4.1 Microscale Solid-Liquid Mixing

The solid-liquid mixing was achieved using the horizontal rotating platform (UKA Laborortechnik) rotating at 1000 rpm for 24 hours. The extraction wells of the 24-well plate were sealed with an adhesive film (Radleys, UK) and the mixed multiwell plate was secured to a horizontal shaker. The liquid phase was contacted with the solid phase using manual pipetting, and disposable tips (d_i = 0.625 mm) were used throughout the experiment to minimise the risk of cross cross-contamination between the wells. The microscale SPE (6000 μL^{-1}) of 6-APA (4.0 $g.L^{-1}$, pH 4.5 at 20 °C) with conditioned granular activated carbon (13.3 $g.L^{-1}$) was manually prepared in two 24-well multiwell plates. The activated carbon samples were prepared at the microscale and contacted with the liquid phase (4.0 $g.L^{-1}$ 6-APA, pH 4.5) using the liquid handling workstation and the vials were sealed. The static multiwell plate was left on the laboratory bench at 20 °C throughout the experiment.

Samples (100 μL) of the liquid phase were periodically removed from the extraction well and transferred to a HPLC vial (Chromacol, VWR, UK) to be analysed on the HPLC (section 2.5.1). The samples were left for an additional 5 days and samples of the liquid phase were transferred and analysed. The mean 6-APA concentrations of the liquid phase samples were plotted against time to show the adsorption kinetics (figure 5.2.2.4.1), which fitted exponential decay curves. The data was statistically analysed to generate 2SE values.

2.4.4.2 Microscale SPE Adsorption Kinetics

The granular activated carbon was automatically dispensed (Accelerator™, Chem Speed, Switzerland) or manually weighed into glass vials (section 2.2.3.2), which were emptied into the wells of a 24-deep well plate. Replicated wells were prepared (n = 3). The adsorbent was contacted with 6000 μL of feed material, containing 6-APA (4.0 $g.L^{-1}$),

dissolved in phosphate buffer (0.1 M, pH 4.5), using the automated workstation running the 'SPE 24well mix Kinetics' program. The plates were covered with an adhesive film (Radleys, UK), secured to a horizontal shaker (UKA Laborortechnik) and mixed at 1000 rpm for 24 hours at ambient temperature (*circa* 25 °C). Samples of the liquid phase (100 µL) were periodically pipetted from the wells after the adsorbent had settled under gravity and were dispensed into HPLC vials (Chromacol, VWR, UK) for HPLC analysis (section 2.5.1). The mean 6-APA concentration of the liquid phase samples was plotted against time to show the adsorption kinetics (figure 5.2.2.3).

2.4.4.3 Effect of pH Conditions on Microscale SPE Kinetics

The 24-well microscale SPE adsorption kinetics method (section 2.4.4.2) was used to analyse the effect of liquid phase pH conditions on the extraction of 6-APA (4.0 $g.L^{-1}$) dissolved in phosphate buffer (0.1 M) prepared at different pH conditions (pH 4.5. pH 6.5 and pH 7.5) with conditioned activated carbon (0.01 $g.L^{-1}$). The pH conditions were measured using the MP225 pH meter (Mettler Toledo, UK) and adjusted with the drop-wise addition of hydrochloric acid (1M) or sodium hydroxide (1M). The microscale SPE process was carried out using 24-well plates (6000 µL), which were prepared using manual solids dispensing and liquid pipetting (Gilson, UK). The kinetics of the extraction of 6-APA in the wells were assessed over 24 hours with sequential sampling of the liquid phase (20 µL) that was transferred to HPLC vials fitted with 100 µL inserts (Chromacol, VWR, UK) and analysed on the HPLC (section 2.5.1). The 6-APA concentration in the liquid phase was plotted against time for each of the pH conditions (figure 5.2.3.4).

2.4.4.4 Microscale SPE Adsorption Isotherms

The microscale SPE adsorption isotherm experiments used the microscale SPE method (section 2.4) to prepare the extraction wells of a 96-deep well or 24-deep well plate. The unconditioned granular activated carbon masses were prepared using automated solid-dosing equipment and the conditioned granular activated carbon masses were prepared

using manual equipment. The solids were dispensed into the wells of a 96-deep well or 24-deep well plate.

The automated workstation ran a range of programs, as detailed in table 2.2.1.5.2 and outlined in appendix 6, to prepare the wells by contacting the resin with the liquid phase (6-APA, pH 4.5), which was prepared by dissolving the 6-APA in phosphate buffer (0.1 mM). The multiwell plates were sealed with an adhesive film (Radleys, UK) and were agitated at 1000 rpm on a horizontal shaker (UKA Laborortechnik) at ambient temperature (20 °C) for 24 hours. Samples of the liquid phase (100 μL) were manually pipetted from the wells, after the adsorbent had settled under gravity, to vials and analysed on the HPLC (section 2.5.1). The liquid phase 6-APA concentrations were used to calculate the values of the adsorbed 6-APA per gram of activated carbon, which were plotted against the liquid phase 6-APA concentration. The isotherm experimentation investigated the sample of the liquid phase adsorbent concentration, 6-APA concentration and liquid phase pH conditions on the adsorption of 6-APA with granular activated carbon.

The activated carbon concentration isotherm experimentation was prepared by using the automated dosing station to dispense a range of adsorbent concentrations into the wells of a 96-deep well plate (1.0 mg to 40.0 mg) and 24-deep well plate (1.0 mg to 80.0 mg). The absorbent was contacted with 1500 μL or 3000 μL of liquid phase containing 6-APA (4.0 $g.L^{-1}$, pH4.5) and mixed over 24 hours. The liquid phase samples were analysed on the HPLC (section 2.5.1) and the adsorbed 6-APA per gram of activated carbon values were calculated and plotted against the liquid phase 6-APA concentration. The isotherm data was displayed over the adsorbent range at the 96-well and 24-well scales (figure 5.2.4.1.1 and figure 5.2.4.2.1, respectively)

The 6-APA concentration isotherm experiments were prepared using either automated or manual solid dosing or pipetting methods. The 6-APA samples were prepared from a stock solution (4.0 $g.L^{-1}$), which was prepared with phosphate buffer (0.1 M, pH 4.5). This was serially diluted 1:1 with phosphate buffer (0.1 M, pH 4.5) in the wells of a 24-

deep well plate (initial well volume = 2 mL) by manual pipetting or using the automated liquid handling workstation running the SPE 96-well 6-APAconc' or 'SPE 24-well 6-APAconc' programs (table 2.2.1.5.2) to prepare a range of 6-APA concentrations (0.005 $g.L^{-1}$ to 4.0 $g.L^{-1}$). The 6-APA samples (1500 µL) were transferred to a 96-deep well plate with pre-dispensed unconditioned granular activated carbon (20 mg). The plates were sealed with an adhesive film (Radleys, UK). The plates were shaken on a bench shaker (UKA Laborortechnik) at 1000 rpm at ambient temperature for 24 hours. The phases were left to stand for 30 minutes to allow the activated carbon to settle under gravity. Samples of the liquid phase (100 µL) were analysed on the HPLC (section 2.5.1).

The microscale SPE process was carried out at 96-well and 24-well scales using different liquid phase pH conditions for the extraction of 6-APA (4.0 $g.L^{-1}$) with conditioned granular activated carbon (13.3 $g.L^{-1}$). The liquid phase was prepared at pH 4.5, pH 6.5 and pH 7.5 using phosphate buffers (0.1 M). The adsorbent was manually dispensed into plates that were sealed with an adhesive film (Radleys, UK) and contacted with the liquid phase before being secured to the horizontal shaker (UKA Laborortechnik) and mixed at 1000 rpm for 24 hours. The phases were left to stand for 30 minutes to allow the activated carbon to settle under gravity. Samples were prepared as previously described and analysed directly on the HPLC (section 2.5.1). The liquid phase 6-APA concentrations were used to calculate the maximum adsorption values for each of the pH conditions, which are presented in table 5.2.5.1. The equilibrium isotherm was calculated Q_{max} ($g_{6\text{-}APA} \cdot g_{adsorbent}^{-1}$) using the aqueous liquid phase 6-APA concentration.

2.4.4.4.1 SPE Isotherm Calculations

The isotherm experiments over a range of activated carbon concentrations, aqueous phase concentrations or liquid phase pH conditions were generated from the HPLC analysis of the end stage liquid phase 6-APA concentrations. These values were used to calculate the maximum mass of 6-APA adsorbed per gram of resin (Q_{max}) using equation 2.3:

$$Q_{max} = \frac{G_{6\text{-APA}}^{resin}}{G_{Resin}} \quad [2.3]$$

where Q_{max} is the maximum amount of solute bound to the adsorbent resin ($g_{6\text{-APA}}^{resin}.g_{resin}^{-1}$), $G_{6\text{-APA}}^{resin}$ is the mass in grams of 6-APA adsorbed onto the resin and G_{Resin} is the mass in grams of the resin.

2.4.5 Laboratory Scale SPE Methods

The laboratory scale SPE experiments (10 mL or 50 mL) were carried out in: extraction vessels, universal tubes (20 mL) or large tubes (50 mL). The conditioned granular activated carbon (Sigma-Aldrich, UK) was dispensed manually into the extraction vessels and weighed using an electronic balance (Radleys, UK). The liquid phase contained 6-APA (4.0 $g.L^{-1}$, pH 4.5), which was dissolved in phosphate buffer (section 2.1.2.1). The adsorbent resin was contacted with the liquid phase by manual pipetting (P1000 & P5000 pipettes, Gilson, UK) in the extraction vessels, which were sealed with screw-top lids. The vessels were secured to the horizontal shaker (UKA Laborortechnik) and mixed at 1000 rpm at ambient temperatures (20 °C) for 24 hours to ensure that equilibrium was reached. The samples were left to stand for 30 minutes for the resin to settle under gravity before samples of the liquid phase (1 mL) were removed for analysis on the HPLC (section 2.5.1).

The laboratory SPE process was adapted to investigate adsorption kinetics, adsorbent selection (section 2.4.2.1), degradation of 6-APA (section 2.4.5.1), laboratory adsorption kinetics (section 2.4.5.2), and laboratory adsorption isotherms (section 2.4.5.3). The laboratory scale SPE experiment liquid phase samples (1 mL) were manually transferred using a P1000 manual pipette (Gilson, UK) to HPLC vials (Chromacol, VWR, UK) and analysed on the HPLC (section 2.5.1).

2.4.5.1 Degradation of 6-APA

The SPE liquid phase contained the adsorbate, 6-APA, and samples were stored at different temperatures to investigate the effects of temperature on its degradation. Samples of 6-APA (0.27 $g.L^{-1}$) dissolved in phosphate buffer (0.1 M, pH 4.5) were prepared and stored in the fridge (5 °C) or at room temperature (20 °C). These samples were replicated three times in order to generate statistically significant data. Aliquots (0.5 mL) were taken from each of these samples periodically over 24 hours and analysed on the UV/ Vis spectrometer (Unicam UV/ Vis spectrometer, UK) at 257 nm. The samples (1 mL) were analysed on the HPLC (section 2.5.1). The concentrations of the aliquots were calculated from the absorbance readings and the mean values plotted against time with error bars of 2 2SE errors (figure 5.2.1.1).

2.4.5.2 Laboratory Adsorption Kinetics of SPE Resins

The initial laboratory scale SPE process investigated the conditioned granular activated carbon (section 2.4.1.1) kinetics of 6-APA adsorption. The conditioned granular activated carbon adsorbent (13.3 $g.L^{-1}$) was dispensed into a 100 mL beaker fitted with an overhead motor (Stuart Scientific SS10) with a 6-bladed Rushton turbine (diameter = 20 mm) positioned 10 mm above the bottom of the vessel and operated at 1000 rpm to maintain the suspension's concentration throughout the bulk liquid. The adsorbent was contacted with 100 mL of the liquid phase (6-APA 4.0 $g.L^{-1}$, pH 4.5) and mixed at 20 °C for 24 hours. Samples of the liquid phase were removed periodically over 24 hours and pipetted into Eppendorf tubes. The Eppendorf tubes were centrifuged (Megafuge centrifuge, Heraeus Instruments, UK) at 13,000 rpm for 2 minutes. The samples (1 mL) were taken from each vessel and were manually transferred using a P1000 manual pipette (Gilson, UK) to vials (Chromacol, VWR, UK) for analysis on the HPLC (section 2.5.1). The mean 6-APA concentrations were calculated and plotted against time (figure 5.2.1.1.3.1).

The adsorption kinetics of 6-APA (4.0 $g.L^{-1}$) onto conditioned granular activated carbon were investigated at laboratory scale (50 mL). The SPE resin was conditioned (section 2.4.2) and the adsorbent was weighed into replicate 50 mL tubes (n = 3) over different

adsorbent concentrations (1.0 $g.L^{-1}$, 2.0 $g.L^{-1}$ and 4.0 $g.L^{-1}$). The adsorbents were contacted with 50 mL of the liquid phase, containing 6-APA (4.0 $g.L^{-1}$, pH 4.5). The SPE phases in the extraction vessels were mixed using a horizontal shaker (UKA Laborortechnik) at 1000 rpm at ambient temperature (20 °C) for 24 hours. The SPE tubes were periodically left to stand during the experiment for the large resin particles to settle under gravity before liquid phase samples (1 mL) were taken from the extraction tube and pipetted into labeled Eppendorf tubes (VWR, UK). The Eppendorf tubes were centrifuged (Megafuge centrifuge, Heraeus Instruments, UK) at 13,000 rpm for 2 minutes. Samples of the liquid phase (0.5 mL) were analysed on the HPLC (section 2.5.1). The mean liquid phase 6-APA concentrations were plotted against time to show the activated carbon SPE kinetics at laboratory scale (figure 5.2.3.3).

2.4.5.3 Laboratory Adsorption Isotherms

The laboratory scale activated carbon concentration isotherm was prepared using conditioned granular activated carbon (section 2.4.1.1) that was manually weighed into a series of 20 mL tubes (0.001 g to 2.5 g). The adsorbent was contacted with 10 mL of the liquid phase, containing 6-APA (4.0 $g.L^{-1}$) prepared in phosphate buffer (0.1 mM, pH 4.5). The sealed tubes were agitated on a horizontal shaker (UKA Laborortechnik) at 1000 rpm, at 20 °C for 24 hours. The extraction vessels were left to settle under gravity for 10 minutes, allowing phase separation. Samples of the liquid phase (1 mL) were transferred to vials and analysed directly on the HPLC (section 2.5.1). The 6-APA concentration values were used to calculate the SPE isotherm (section 2.4.4.4.1). The values for the laboratory scale adsorbed 6-APA per gram of activated carbon were plotted against the liquid phase 6-APA concentration over the adsorbent mass range (figure 5.2.4.3.1).

The laboratory SPE process (10 mL) was modified to prepare the adsorbate (6-APA) concentration equilibrium isotherm experimentation to extract a range of 6-APA concentrations (0.005 $g.L^{-1}$ to 4.0 $g.L^{-1}$) from an aqueous solution using conditioned granular activated carbon (4.0 $g.L^{-1}$). The 6-APA samples were prepared from the bulk

liquid phase (4.0 $g.L^{-1}$) dissolved in phosphate buffer (0.1 M, pH 4.5), which was diluted 1:1 with phosphate buffer (0.1 M, pH 4.5). The resin was contacted with the liquid phase in the extraction vessels, which were mixed on the horizontal shaker (UKA Laborortechnik) for 24 hours to ensure that equilibrium was reached. The samples were left standing for 10 minutes to settle under gravity and samples (1 mL) of the liquid phase were transferred to vials for analysis on the HPLC (section 2.5.1). The adsorbent concentration was altered for subsequent experimentation from 4.0 $g.L^{-1}$ down to 0.125 $g.L^{-1}$ to attempt to gain reproducibility of the results.

The laboratory scale SPE process was carried out at different liquid phase pH conditions for the extraction of 6-APA (4.0 $g.L^{-1}$) with conditioned granular activated carbon (13.3 $g.L^{-1}$). The liquid phase was prepared at pH 4.5, pH 6.5 and pH 7.5 using mono and di-sodium phosphate buffers (0.1 M). The adsorbent was manually dispensed into 50 mL tubes and contacted with the liquid phase before being secured to the horizontal shaker (UKA Laborortechnik) and mixed at 1000 rpm for 24 hours. The phases were left to stand for 30 minutes to allow the activated carbon to settle under gravity. Samples of the liquid phase (1 mL) were transferred into vials for analysis directly on the HPLC (section 2.5.1). The liquid phase 6-APA concentrations were used to calculate the maximum adsorption values (section 2.4.4.4.1) for each of the pH conditions, which are detailed in table 5.2.5.1).

2.4.6 Supported SPE Experimentation

The supported SPE methodology was developed by investigating the use of commercially available filter plates (Millipore, 3M) as a support matrix for the adsorbent resin (granular activated carbon) used in the automated SPE experimentation. The membrane pore size, water retention and solute (6-APA, 4.0 $g.L^{-1}$) retention of the filter were investigated. The supported SPE method used a 96-well filter plate (Millipore) and 24-well plate (3M, UK), which were kindly supplied by the respective manufacturers. The supported SPE methodology was used to assess the capacity and percentage recovery of 6-APA with the supported granular activated carbon.

2.4.6.1 Membrane Pore Size

The membrane pore size was investigated for retaining granular activated carbon particles from the dispersant (RO water) in the activated carbon slurry (13.3 $g.L^{-1}$). The disc filters investigated had pore sizes of 0.2 μm, 0.45 μm, 1 mm and 11 mm (glass fibre). An aliquot of the granular activated carbon slurry (1 mL) was dispensed through the filter using a disposable 1 mL syringe (Beckton Dickenson, UK). Samples of the feed stream and the filtrates were collected and analysed using an UV spectrometer at 220 nm (Unicam UV/ Vis spectrometer, UK). The optical density measurements of the filtrate samples were used to calculate the percentage clarity (OD_{Sample}/ $OD_{Activated\ carbon\ slurry}$ x 100) and were plotted for each of the membrane pore sizes (figure 5.2.2.1.1).

2.4.6.2 Membrane Retention

The commercially available filter plates investigated were the 96-well filter plate (Millipore, UK) and the 24-well filter plate (3M, UK). The 96-well filter plate contained a Durapore® membrane (polyvinylidene), which has broad chemical compatibility, hydrophobic nature, small pore size (0.45 μm), small well size (3.2 mm) and a small well volume (392 mL). The 24-well filter plate contains a glass fibre membrane with a larger pore size (0.7 μm to 1.5 μm), larger well size (d = 6.8 mm) and a larger well volume (625 mL). The commercially available filter plates were kindly donated by the suppliers: 24-well (Packard Instruments, Packard Bioscience, UK) and 96-well (Millipore, UK). These filter plates were investigated for their retention of water and aqueous 6-APA (4.0 $g.L^{-1}$) on the membrane.

The liquid phase was manually pipetted onto replicate wells (n = 3) on the filter plates (200 μL 96-well, 600 μL 24-well) and left for 10 minutes before applying a vacuum to the SPE filtration manifold (Millipore, UK) for 20 seconds. The filtrate samples were collected in a 96-well collection plate (Costar, USA) or 24-well collection plate (Beckton Dickenson, UK). The filtrate samples were transferred to HPLC vials and sealed with

screw-top lids (Chromacol, VWR, UK) for analysis of the filtrate and feed samples by HPLC (section 2.5.1). The mean filtrate 6-APA concentration was plotted with 2SE error bars for each of the samples (figure 5.2.2.1.1.1).

2.4.6.3 Supported Microscale SPE

The supported microscale SPE experimentation was carried out using an automated liquid handling workstation (Multiprobe II Ex®, Perkin Elmer, UK) with the Winprep® software running the bespoke 'SPE test KEW' program, as detailed in table 2.2.1.5.2 and appendix 6 (method adapted from Zweigenbaum et al, 1998). The granular activated carbon particles were dispensed by the automated liquid handling workstation (dried automated slurry handling samples), the unconditioned adsorbent was weighed using the Chem Speed Accelerator™ dosing station (section 2.4.4) or dispensed using manual weighing methods and stored until use in vials sealed with screw-top lids (Chromacol, VWR, UK). The activated carbon particles (4.0 mg) were dispensed into the wells of the 96-well filter plate (Millipore, UK) or 24-well filter plate (3M, UK).

The filter plates containing the adsorbent were conditioned with 200 μL of conditioning solvent (RO water), which was removed by vacuum filtration at 1 mmHg for 20s. The liquid phase (200 μL) containing 6-APA (4.0 $g.L^{-1}$, pH 4.5) was contacted with the SPE resin by the liquid handling workstation and the filter plates were sealed with adhesive film (Radleys, UK). The filter plates were left *in situ* for 24 hours. The SPE manifold (Millipore, UK) applied a vacuum for 20 seconds to remove the filtrate samples, which were collected in the 96-well collection plate (Costar, UK). The samples (100 μL) were transferred into HPLC vials (Phenomenex, UK) for HPLC analysis (section 2.5.1).

The adsorbed 6-APA was washed from the adsorbent in the filter plate with 200 μL RO water, which was removed under vacuum (1 mmHg, 2- s). An aliquot (200 μL) elution solvent (Methanol) was contacted with the adsorbent in the filter plate for 30 minutes to elute the adsorbate from the activated carbon adsorbent. The elution solvent was removed from the adsorbent under vacuum (1 mmHg), which was applied using the filtration rig

and manifold for 20 seconds, into a 96-well collection plate (Costar, UK). Samples of each of the eluates were analysed on the HPLC (section 2.5.1).

2.4.6.4 Supported Microscale SPE Capacity

The capacity of the activated carbon adsorbent was investigated using the supported microscale SPE process (section 2.4.6.3). The 96-well filter plate was filled with 19.5 mg per well^{-1} of unconditioned activated carbon (Sigma-Aldrich, UK). The experimentation was carried out using the automated workstation (Multiprobe II Ex®) running the 'SPE test KEW' program, which conditioned the adsorbent with the conditioning solvent (300 μL RO water) for 15 minutes. The conditioning solvent was separated from the adsorbent in the 96-well plate under vacuum (1 mmHg, 20 s) using the filtration manifold fitted to a filtration rig (Millipore, UK). The liquid phase 6-APA (4.0 g.L^{-1}, .2 M, pH 4.5) was sequentially added to the adsorbent in aliquots of 300 μL, which was left in contact with the solid phase for 15 minutes at 20°C. The phases were separated under vacuum (1 mmHg, 20 s) using the vacuum manifold fitted to a filtration rig (Millipore, UK), transferring the filtrate to a 96-well collection plate (Costar). The filtrate samples were analysed on the HPLC (section 2.5.1). Another aliquot of 6-APA was then added to the SPE adsorbent in the wells in aliquots of 300 μL to each well. The 6-APA concentrations of the filtrates were used to calculate the liquid phase and adsorbed 6-APA concentrations. These data were plotted against the total liquid phase volume added and the total 6-APA added to the adsorbent in the extraction well (figure 5.2.2.3.1).

2.4.6.5 Supported Microscale SPE Recovery

The supported microscale SPE recovery experimentation used the supported microscale SPE method (section 2.4.6.3) to condition the granular activated carbon (13.3 g.L^{-1}) with RO water (300 μL), which was prepared using the automated workstation (Multiprobe II Ex®) running the 'SPE test KEW' program. The conditioning solvent was removed using the filtration manifold (Millipore, UK) under vacuum (1 MmHg, 20 s). The conditioned

granular activated carbon adsorbent was contacted with an aliquot (200 μL) of the liquid feed containing 6-APA (4.0 $g.L^{-1}$, pH 4.5) in replicate (n = 6) wells of the deep 96-well plate (Beckman Dickenson Bioscience, UK) for 15 minutes. The phases were separated under vacuum (1 MmHg, 20s) and the filtrate was collected in the 96-well collection plate (Costar, UK). Aliquots of the filtrates (100 μL) were transferred to vials for HPLC analysis (section 2.5.1). The 6-APA concentrations of the filtrate and the feed samples were used to calculate the percentage adsorbed 6-APA values ($C_{6\text{-APA}}$ sample / $C_{6\text{-APA}}$ feed x 100). The percentage adsorbed 6-APA values were plotted for each sample (figure 5.2.2.4.1).

2.5 Quantitative Analytical Techniques

2.5.1 HPLC Analysis

HPLC analysis of Pen G, PAA and 6-APA was performed on a Dionex HPLC system with a GP40 pump, an AS 3500 autosampler and an AD20 spectrometer (257 nm). A C18 pecosphere 5μm RP column (150 mm x 4.6 mm (Perkin Elmer, USA) fitted with a C8 guard column (Jourguard, VWR, UK)) was used on the HPLC to analyse these compounds, as recommended by the Perkin Elmer handbook. Isocratic chromatography was employed using a mobile phase consisting of 64% v/v phosphate buffer (0.1 M, pH 7) and 36% v/v methanol (HPLC grade with 0.001% impurities). The analytical column was maintained at 20 °C at a flow rate of 1 $mL.min^{-1}$. The injection volume was 10 μL for all samples. The total run time was 6 minutes for individual samples of 6-APA and PAA, whilst it was 12 minutes for the simulated bioconversion product stream and Pen G samples. The retention times for the individual compounds were at 1.5 minutes (6-APA), 2 minutes (PAA) and 7 minutes (Pen G) (appendix 15).

2.5.1.1 HPLC Calibration Curves

Samples of the individual compounds in the PA bioconversion product stream (Pen G, PAA and 6-APA) were prepared in phosphate buffer (section 2.1) at pH 7.8 and pH 2.

The samples were serially diluted over the concentration ranges 0.02 $mg.mL^{-1}$ to 50 $mg.mL^{-1}$ (Pen G), 0 $mg.mL^{-1}$ to 10 $mg.mL^{-1}$ (PAA) and 0 $mg.mL^{-1}$ to 25 $mg.mL^{-1}$ (6-APA), which were selected due to their respective solubility limitations. Samples of 1 mL were analysed on the HPLC (section 2.5.1). This experiment was carried out in triplicate and the mean peak height values were plotted with error bars of 2 standard deviations to generate a calibration curve of absorbance against concentration (appendix 15).

2.5.2 UV/Vis Spectrometric Analysis

The 6-APA concentrations in the samples were spectrometrically analysed in a 2 mL cuvette read using the UV/ Vis spectrometer (Unicam UV/ Vis spectrometer, UK) at 220 nm for slurry samples and 257 nm for 6-APA samples. The absorbance readings were compared to a negative control (RO water) or a positive control (6-APA 4.0 $g.L^{-1}$) respectively and were used to calculate the percentage clarity or 6-APA concentrations of the samples.

2.5.2.1 UV/Vis Calibration Curves

Samples of 6-APA were prepared in phosphate buffer (section 2.1) at pH 7.0. The samples were serially diluted over the concentration range (0 $g.mL^{-1}$ to 4.0 $g.mL^{-1}$). Samples of 1 mL were dispensed into plastic cuvettes (VWR, UK) and analysed on the UV/Vis spectrometer at 257 nm (section 2.5.2). This experiment was carried out in triplicate and the mean absorbance values were plotted with 2SE error bars to generate a calibration curve of absorbance against concentration (appendix 16).

2.6 Quantifying Error

The quantification of errors associated with the automated platforms was achieved by evaluating gravimetric measurements of dispensed liquid volumes and solid masses. These reagents were dispensed into vials and weighed on an analytical balance (section

2.2.3). The analytical balance is considered to be precise as it has four decimal places and can measure minute amounts (80g to 0.0001g). The balance incurs such small errors that they are considered insignificant (Inforplease, 2004). The analytical balance was kept in a glass case to limit the effects of dust particles and moisture. The balance was regularly calibrated to ensure its accuracy. The repeatability of an analytical balance is quoted as ± 0.1 mg (Acculab ALC, Analytical Balance (Precision Weighing Balances, 2004)).

The performance of the analytical balance is important for analysing the automated equipment, as the dispensed reagents were gravimetrically measured. Evaluating the performance of the analytical balance itself was quantified by repeatedly weighing a polypropylene weighing boat, 2.2324 ± 0.0058 g (appendix 12: Figure A12.1). Analysis of the data indicated that the performance of the balance was excellent, with precision of 0.2% CV. This reflected the low occurrence of systematic errors. The mean value has a 95% confidence[10] in being the true value, which was generated from 39 replicate measurements (appendix A12.1). This illustrated the accuracy of the analytical balance. The accuracy of the balance matched the published data (0.1 mg (Precision Weighing Balances, 2004)) and so was not considered further in the evaluation of the automated equipment (section 3.2).

The analytical balance was used to evaluate gravimetric data for a small mass of paper (appendix 12) to assess the effect of using two measurements to calculate mass. The mass of paper was 1.7 ± 0.1 mg with a precision of 6.1% CV (appendix 12: Figure A12.2). The mean mass was within the 95% confidence interval and was therefore close to the true mean. Variation in these measurements was caused by random errors occurring due to dust particles or moisture in the air encountered whilst transferring the sample, which slightly altered the measurements. These results had good precision and validated the use of the gravimetric technique for evaluating the automated equipment (section 3.2).

[10] Definition of statistical terminology in appendix 11

Chapter 3: Statistical Analysis of Automation Platforms

3.1 Introduction

The automated platforms used in this research to generate data included the Multiprobe II Ex® liquid handling workstation (section 2.2.1) used to prepare the liquid reagents and the Accelerator™ dosing station (section 2.2.2) used to prepare the solid reagents for use in the microscale experimentation. The workstation is a standard piece of equipment used in many pharmaceutical and research laboratories. The dosing station was an emerging piece of equipment for use in automated laboratories. Both of these automated platforms were designed to rapidly handle large sample numbers to generate rapid and accurate experiment data.

The statistical analysis of these automated platforms was used to investigate various characteristics of the workstation and the dosing station. The workstation characteristics of operation were investigated to assess their affects on performance. The workstation was used to assess its performance when operated using a variety of operational scenarios: the affect of the type of pipette tips; operational mode; dispensing speed; and performance files on dispensing liquid aliquots. This statistical data was compared to the manufacturer's data (appendix 7.1). The performance of the dosing station in dispensing activated carbon was assessed and compared to the manufacturer's performance data (appendix 7.2).

The sources of error associated with both the laboratory and automated microscale equipment used in this research are identified in section 3.1.1. These addressed the three types of error that were encountered within the experimental procedures. The inherent errors (defined in appendix 10) associated with the automated platforms are discussed in relation to their reliability (appendix A10.4.3). These sources of error were quantified (Appendix 11) and the performances of the automated platforms were evaluated using statistical analysis (appendix 11) to quantify their accuracy and precision. The performance of the automated platforms indicated their suitability for microscale process research and the impact of these results is concluded in section 3.3.

3.1.1 Identifying Sources of Experimental Errors

The experimental errors encountered within this research, using both laboratory equipment and microscale automated platforms, were considered in relation to the main categories of error: gross errors; systematic errors and random errors (appendix 10) that are encountered within experimental procedures. This allowed the minimisation of these errors and the generation of accurate and precise results (table 3.1.1.1).

Gross errors associated with the automated and laboratory equipment would be related to any errors in calibrating, programming, setting up of reagents or operating the equipment, assuming the reliability of the equipment. These errors could be a result of human error or equipment malfunction. Any equipment failures or other gross experimental errors required the abortion of the experimentation.

Systematic errors associated with both the laboratory or automated equipment would be related to errors resulting in poor calibration or operation of the equipment. The performance of the automated platforms was assessed by their manufacturers using in-house accuracy studies of their performance (appendix 7). The systematic errors associated with the automated experimentation were assumed to be primarily related to the performance of the automated and analytical equipment.

Random errors associated with the microscale experimentation were related to the operation of the automated equipment and preparation of the reagents. Inadequate alignment of the labware or deck could cause positioning errors of the pipette tips of the workstation or dosing unit of the solid dosing station, which could lead to the liquid aliquot or solids missing the container and the subsequent wasting of the reagents. In addition, operational errors of the automated equipment or errors with the laboratory equipment could generate random errors, such as the concentration of the stock solutions during its preparation, which was sensitive to weighing errors, transfer losses and minute volume errors.

The microscale experimentation was sensitive to errors in the set-up, cleaning and operation of the equipment. The analytical techniques were sensitive to errors created from the operation of the analytical instruments (section 2.2). It was, therefore, important to reduce these errors and to take great care during the experimentation at all times to ensure the

accuracy and precision of the results generated. These errors (table 3.1.1.1) were minimised by the use of standard operating procedures (appendix 9), regular equipment maintenance, calibration and good laboratory practice.

The automated platforms have a rapid speed of operation and greatly increase the speed of experimentation by allowing more experimental runs compared to laboratory experimentation. The automated equipment reduced the occurrence of gross and random human errors, as observed in manual experimentation, because automated platforms remove operational errors, which reduces variability in experiments.

Experimentation using automated equipment increased sample numbers (appendix 11.2.1) and precision (appendix 11.4.2), which minimised intra-observer variability and inter-observer variability. However, all human errors are not eradicated and random errors still occur due to the minute experimental differences in the calibration and operation of the automated equipment. The microscale experimentation produces a large number of samples that generate a large set of data, which make the results more significant. Each of the microscale experiments produce four replicate wells with the same conditions and the experiments were repeated at least three times on different days to produce a representative sample size (n = 12).

3.2 Evaluation of Automated Equipment Performance

The performance of the automated equipment used in this research for dispensing liquids or solids was assessed to quantify their accuracy[10] and precision[10] using gravimetric measurements. This ensured that these data generated by these automated equipment were reproducible and repeatable. Statistical analysis of the data generated from the automated equipment was undertaken and compared with literature data to validate their performance.

3.2.1 Evaluation of the Multiprobe II Ex® Performance

The manufacturer of the Multiprobe II Ex® assessed its performance in-house (section 3.2.1.1), which demonstrated good accuracy and precision. This data indicated different

[10] Definition of statistical terminology in appendix 11

Experimentation Stages	Experimentation Actions	Sources of Error	Gross	Random	Systematic
Preparation of reagents	Weighing solids	Balance inaccuracy	•	•	•
		Effect of temperature differences		•	
	Transferring solids	Loss of solids		•	
	Dispensing solvent	Inaccurate volume		•	
	Dissolving solids	Heating denatures compound		•	
		Heating destroys compound	•	•	
		Incomplete solubility		•	
Experimental procedures	Liquid handling	Pipetting: Workstation & Manual		•	•
		Poor cleaning		•	
		Poor orientation	•	•	
		Evaporation		•	
		Programming	•		
	Solid handling	Dosing: Accelerator, Drypette &		•	•
		Manual		•	•
		Balance		•	
		Transfer orientation	•		
		Logistics	•		
		Programming	•		
	Mixing	Liquid handling	•	•	•
		Orientation	•	•	
		Programming	•		
Analytical technique	Sampling	Liquid handling	•	•	•
		Transfer orientation	•	•	
		Programming	•		
	Instrument	Operation	•	•	•
		Calibration		•	•
		Programming	•		

Table 3.1.1.1. Sources of error associated with the automated equipment used in the microscale LLE and SPE experimentation, focussing on various experimentation stages and actions to determine the type of errors (gross, random or systematic).

targets for factory and customer specifications (appendix 7.1), so the performance of the workstation used in this research was investigated prior to its use in the development of microscale experimentation.

Evaluation of the performance of the liquid handling workstation was analysed for a range of operating parameters to quantify its liquid handling capability. This investigated the key feature of the workstation, its ability to accurately and reproducibly deliver aliquots of liquid to a variety of receptacles located anywhere on the deck[1] of the workstation.

The performance of the workstation was tested under a variety of operational scenarios. The workstation was operated with different types of pipette tips, operating modes, dispensing speeds and performance file settings used to dispense a range of liquids. For each experimental scenario the target volume was programmed into the workstation that dispensed the liquid volume, which was gravimetrically analysed. Analysis of its accuracy[10] and precision[10] under each of these scenarios produced quantifiable data (CV = Coefficient of variance, 2SE = 2 standard error[10]), which could be compared to identify the scenario with the best performance for the workstation.

3.2.1.1 Manufacturer's Evaluation of Workstation Performance

The manufacturer's analysis of the workstation's performance (appendix 7.1) was generated from dispensed volume data that included a range of pipette tips and volumes. This data showed that the actual data achieved during their testing had higher inaccuracy and imprecision than the target values over the dispensed volume range investigated (1 µL to 100 µL). The accuracy of the manufacturer's data showed that the actual results for dispensing 100 µL aliquots (0.72% inaccuracy) was less accurate than the target value (0.5% inaccuracy), indicating that this may be an ambitious target. The manufacturer's precision for dispensing 100 µL aliquots showed that the actual data (0.25% CV) was more precise than the target data (0.50% CV), indicating that the manufacturer's actual operation of the workstation was more precise than expected. This disparity in the performance and its range indicated the need for independent analysis of the performance of the workstation used in this

[1] Multiprobe Terminology Definitions appendix 5

[10] Definition of statistical terminology in appendix 11

research over a range of volumes and operational modes to fully assess the actual performance that was achievable within the laboratory.

3.2.1.2 Effect of Pipette Tip Type

The performance of the workstation in dispensing a range of volumes (1 μL to 100 μL) of RO water was assessed for the fixed, small conductive disposable and micro conductive disposable pipette tips. The correlation between the target data, the actual dispensed volume generated experimentally and the data provided by the manufacturer (appendix 7.1) is illustrated in figure 3.2.1.2.1 (a). All of these data series showed a good linear correlation with the target volumes (R^2 = 0.999 to 0.100 accuracy) for both the experimental and manufacturer's data, which fitted closely with the target volumes on the line of parity. The percentage accuracy values calculated here did not increase linearly with the dispensed volumes, regardless of pipette tip type, but varied throughout the range.

Data for the workstation dispensing 100 μL aliquots with each pipette tip showed that the percentage accuracy of the small conductive tip data (1.1% inaccuracy) was more accurate than the fixed tip actual data (2.6% inaccuracy), despite both pipette tips having orifices of the same internal diameter. This indicated that the nature of the composition material of the different tips affected the accuracy by effecting frictional stress caused by the interaction with the reagent. The friction factor is related to the surface bumps and the pipe's diameter, as well as being a function of Reynolds number. This phenomenon was believed to be a curiosity of the equipment and could have been related to the mechanism of action (section 2.2.1.2) or limitations of the tips as this volume approaches the lower volume limit. These challenges to the accuracy of the workstation were expected to generate a graduated increase in inaccuracy (i.e. a 1 μL error would generate 1% inaccuracy in dispensing 100 μL, 10% inaccuracy in dispensing 10 μL and 20% inaccuracy in dispensing 5 μL and 100% inaccuracy in dispensing 1 μL). Therefore, the error may be generated by random events, such as droplet's tear formation at the pipette tip or loss of liquid due to low surface tension as later seen in developing performance files for more viscous solvents (section 2.2.1.4.1).

Inaccuracy was observed for dispensing the lowest aliquot volumes (≤ 10 μL) in both the experimental and manufacturer's data. This was due to the volume limitations of small disposable tips (20 μL to 200 μL) and the workstation's mechanism of action affecting the

(a)

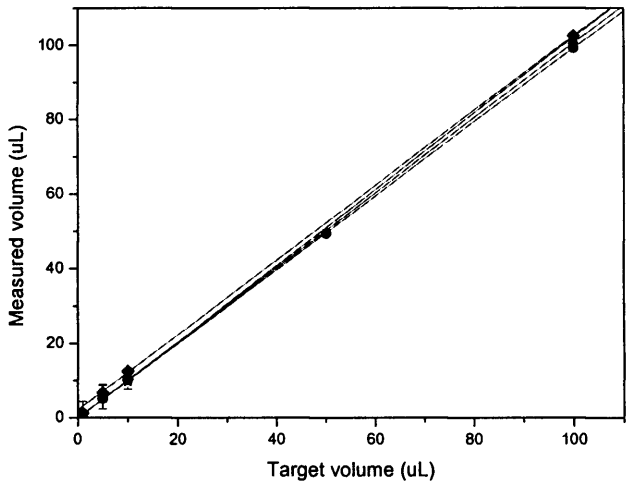

(b)

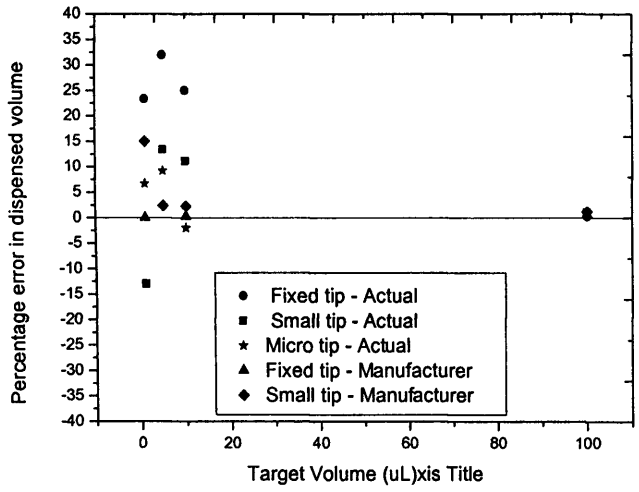

Figure 3.2.1.2.1. Analysis of the accuracy of dispensing RO water aliquots using the Multiprobe II Ex® workstation to assess the affect of pipette tip size presented as: (a) parity plot of actual volumes dispensed against target volumes (1 µL to 100 µL) and (b) plot of percentage error in dispensed volumes against target volumes (1 µL to 100 µL). Data: manufacturer's published values (n = 8) for the workstation fitted with (■) 1 mL fixed tips; (●) 200 µL disposable tips and actual data measured for the workstation used in this research fitted with (♦) 1 mL fixed tips, (▲) 200 µL disposable tips or (★) 20 µL disposable tips. Mean gravimetric data (n = 4 to 8) plotted with 2SE error bars (plot a < 1%) and solid line represents the linear regression of the data. Method detailed in section 2.2.3.1.

accurate movement of the syringe plunger, making incremental changes in the volume aspirated or dispensed.

The errors associated with these volumes dispensed with the range of pipette tips were more closely analysed by assessing the percentage error related to these data (figure 3.2.1.2.1 (b)). These percentage error values for the experimental and manufacturer's data are intermingled and distributed either side of the axis with a predominance of over dispensing, especially at the lower volumes. This indicated that neither workstation used here nor the one investigated by the manufacturer have total superior performance as both incurred random errors and these results were inconclusive about the pipette tips. Further analysis of this data was made by statistical analysis to give more detailed insight into the associated degree of error.

The statistical analysis of the mean[10] gravimetric data for this evaluation of the workstation was displayed in table 3.2.1.2.1, which assessed the accuracy[10] and precision[10] of the dispensed volumes for each type of pipette tip. The 2SE values for the volume range dispensed by the workstation fitted with the micro conductive disposable tips improved with increasing volume, but the percentage CV values varied throughout the range. The performance values (2SE, % CV) for the small and fixed pipette tips did not increase linearly with the increased volumes, which indicated that there was a small degree of error associated with the operation of the workstation. The small error bars (2SE = 0.01 to 3.5) indicated that the data had good accuracy for all the pipette tips investigated, and the experimentation had low occurrence of systematic errors.

The incomparability of the accuracy data with the dispensed volumes has been seen in other statistical analysis of data for automated dispensing 10 μL aliquots to replicate plates, which reported values between 92% to 113% accuracy. This scatter of data reduced as the dispensed volume increased to 35 μL (Olsen, 2000). This scatter was also seen with increases in concentration of an analyte, Ziprasidone (Janiszewski et al, 1997). The precision of the data was analysed to quantify the random error associated with the workstation and the intra-run data were collected for sequential experimentation. The mean dispensed volume values were higher than the inter-run data due to the larger sample size and removal of outliers. The reproducibility is a measurement of the between-run precision of actual dispensed volume

[10] Definition of statistical terminology in appendix 11

(a)

Micro Conductive Disposable Tips			
Volume (μL)	**1**	**5**	**10**
Mean Volume (μL)	1.1	5.5	9.8
% Inaccuracy	6.7	9.2	-2.0
2SE	3.25	3.10	2.17
% CV	3737	75.1	27.1

(b)

Small Conductive Disposable Tips				
Volume (μL)	**1**	**5**	**10**	**100**
Mean Volume (μL)	0.87	5.67	11.13	101.07
% Inaccuracy	-13.3	13.4	11.3	1.1
2SE	0.87	0.95	0.65	2.18
% CV	10.9	14.6	7.1	2.9

(c)

Fixed Tips				
Volume (μL)	**1**	**5**	**10**	**100**
Mean Volume (μL)	1.2	6.6	12.5	100.2
% Inaccuracy	23.3	32.0	25.0	2.6
2SE	0.36	2.37	0.14	0.07
% CV	25.1	31.1	0.8	0.1

Table 3.2.1.2.1. Statistical analysis[10] of the accuracy and precision of the experimental data generated dispensing 1 μL to 100 μL RO water using the Multiprobe II Ex® fitted with: (a) Micro conductive disposable tips (n = 16); (b) Small disposable tips (n = 32); (c) Fixed tips (n = 16) and operated with waste water performance files. Method detailed in section 2.2.3.1.

data which, like the percentage inaccuracy data, varied throughout the range of dispensed volumes.

The precision of the fixed tip data (2.6% to 32.0% CV) was better than the small conductive tip data (2.9to 39.1% CV) over this dispensed volume range. The micro conductive tip data was imprecise over the dispensed volume range (3.7% to 75.1% CV). The micro tip data for 1 μL to 10 μL data was expected to have improved precision as it was designed to handle these lower volumes. As this research did not use micro conductive disposable pipette tips, these low volumes were not further investigated. The best precision was seen with dispensing 100 μL with the fixed tips, which was probably due to lack of errors incurred with the use of disposable tips, the sub-optimal performance of the workstation with the micro tips or the low sample number. The initial volume dispensed was reported as being larger than the target volume in a series of replicate samples (Szita et al, 2001), which may be a cause for the variation.

The experimental data was compared to the manufacturer's data (appendix 7.1), which was statistically analysed. The manufacturer's performance data (section 3.2.1.1) over this volume range generated data for small conductive tips (0.72% to 14.6% inaccuracy) with factory specifications (1.5% to 24% recommended inaccuracy) and customer specifications showing acceptable limits for experimental data (2% to 28% recommended inaccuracy). These performance limits were more generous than the target % accuracy values (0.5% inaccuracy to 6.0% inaccuracy) (appendix 7.1.1).

The experimental data was compared with the manufacturer's data (section 3.2.1.1) using a Chi^2 and student's t tests (appendix 11.3). The Chi^2 test investigated the hypothesis that the manufacturer's precision data is true and the hypothesis that the accuracy of the experimental data fell within that of the manufacturer's data. The precision of the automated pipetting was assessed by gravimetric analysis of the dispensed liquid aliquots (section 2.2.3.1) and statistical analysis of the data (standard deviation (SD[10]) values) for both the disposable and fixed pipette tips. The mass of these aliquots was measured on an analytical balance and the precision of the analytical balance (Appendix 11) was used to calculate the precision associated with the workstation (equation A11.5). The precision related to the pipetting

[10] Definition of statistical terminology in appendix 11

measurements generated with the disposable tips of SD = 3.1 x 10^{-3} (calculated from 2SE = 2.18 x 10^{-3}) or fixed tips of SD = 7.0 x 10^{-5} (calculated from 2SE = 7.0 x 10^{-5}) (section 3.2.1.1) and the analytical balance had a precision of SD = 1.8 x 10^{-4} (calculated from 2SE = 5.8 x 10^{-5}), (appendix 12). Therefore, the precision associated with the workstation for the small disposable tips was SD = 3.07 x 10^{-6} and for the fixed tips 2.7 x 10^{-8}, which indicated that the precision of the fixed tip data was better than that of the manufacturer's data.

The precision measurements of the workstation with the small disposable tips were used in the Chi^2 analysis (equation A11.6) to compare the gravimetric data for the workstation with the precision of the manufacturer's data (appendix 7). The results of the Chi^2 test showed that the disposable tips (16) were outside the 95% confidence interval of the Chi^2 distribution ($z \geq$ 14.06) and this indicated that there was evidence to suggest that the precision of the workstation used in this research was smaller than the manufacturer's data as the null hypothesis was false.

Further analysis of the data with a student's t test used the manufacturer's precision to compare with its accuracy (equation A11.7) to assess the accuracy of the workstation determined in the experimentation (section 3.2.1.2). The results of the student's t test (0.54) showed that the disposable tips were within the 93% confidence interval for the t-distribution (2.365). This indicated that the null hypothesis was true and there was no reason to distrust the accuracy of the workstation.

Both the Chi^2 and student's t tests showed that the experimental performance data was within the acceptable limits of the manufacturer's performance data. This validated its use in the development of the microscale processes and the operational scenarios were screened to identify the most appropriate scenario for the experimentation.

The small conductive disposable pipette tips were recommended for use with the workstation based on their performance over the dispensed volumes and the statistical analysis of the workstations performance. Pipetting with small disposable tips generated better accuracy than fixed tips relating to fewer systematic errors. The use of disposable tips greatly reduced the risk of cross contamination of the samples (Zhang et al, 1999, Bolden et al, 2002). Experimentation with 96-well plates has a high risk of cross contamination due to the close proximity of the sample wells, especially during mixing. This was reduced by using a sealed

mat cap during mixing and by selecting suitable dispensing depths for the pipette tips (1 mm to 2 mm from the bottom of the well) to reduce the risk of spillage (Bolden et al, 2002).

Cross contamination between the wells of a multiwell plate prepared using an automated liquid handling workstation was not investigated in this research as the use of disposable tips and washing procedures greatly reduced this risk. The risk of cross sample contamination using the Tecan Genesis liquid handling workstation was previously evaluated for dispensing 100 μL. The observed tip carryover from pipetting 50 μL radio labelled BSA to 96 wells detected 85,000 counts per well and 20 counts per well after tip washing, This indicated that washing would reduce the risk of contamination (Astle TW & Akowitz, 1996). The liquid handling workstation had good accuracy and precision in dispensing liquid volumes with fixed and disposable tops operated in waste mode and using 400 $\mu L.s^{-1}$ dispensing speed, making it suitable for the development of automated microscale process development.

The range of volumes dispensed by the workstation fitted with the small conductive disposable tips were extended to 150 μL RO water, as this volume was selected for the phases in the microscale LLE experimentation (section 2.3.2). The workstation was operated in the waste mode (section 3.2.1.3) and fitted with small disposable tips to assess its performance. The linear correlation between the programmed volume and the dispensed volume was assessed at this higher volume (figure 3.2.1.2.2 (a)), which fitted the linear regression $Y = 1.001X - 0.565$ with a R^2 value of 1.000 with an error bar of 2SE (0.33). Analysis of the percentage error value for dispensing 150 μL (figure 3.2.1.2.2 (b)) decreased exponentially with volumes over 10 μL. The accuracy and precision of the 150 μL data was analysed statistically and had a percentage inaccuracy of 0.3% with a percentage CV of 0.4% and 2SE value of 0.327. These results supported the improvement in performance with the increase in volume as the error becomes less significant.

The statistical analysis of performance with the previous evidence of sterility (Brush, 2002) and the effect of volume indicated that the performance of the workstation fitted with small conductive disposable tips for dispensing 150 volumes produced data that was acceptable. Therefore, these pipette tips and volumes were selected for use in subsequent experimental work using the automated workstation.

(a)

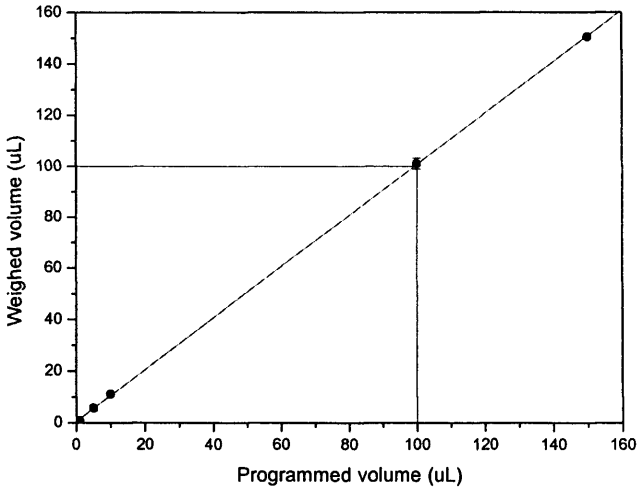

(b)

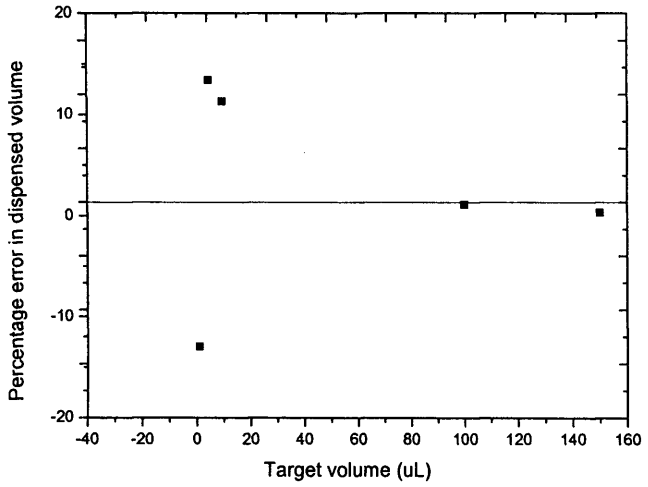

Figure 3.2.1.2.2. Analysis of the accuracy of dispensing RO water aliquots using the Multiprobe II Ex® workstation fitted with disposable tips and operated in the waste mode to investigate a wider volume range (1 μL to 150 μL), exceeding that investigated in figure 3.2.1.2.1. Data presented as (a) parity plot of actual volumes of RO water aliquots dispensed against target volumes and (b) plot of percentage error in dispensed volumes against target volumes. Mean gravimetric data (n = 12) plotted with 2SE error bars (all <1%) and solid line represents the linear regression of the data. Method detailed in section 2.2.3.1.

3.2.1.3 Effect of Operational Modes

The workstation has two operational modes; blowout and waste. These were assessed for their affects on liquid handling performance of the workstation. The equipment was fitted with disposable tips and was assessed for its ability to dispense 175 µL of RO water (table 3.2.1.3.1). There was little difference in the accuracy or percentage target volume value for the blowout and waste modes (99.9% compared to 101.1% accuracy) with a low volume difference (1.15%). The dispensing in the waste mode was more reproducible than the blowout mode (1.2% CV compared to 2.2% CV), but both were acceptable. The performance files (section 2.2.1.4.1) associated with the blowout and waste modes aspirate and dispense the liquid at the same speeds (75 $\mu L.s^{-1}$ and 400 $\mu L.s^{-1}$, respectively). The performance of the workstation operated in the waste mode had greater precision than the blowout mode. Precision is more important than accuracy for generation of results from automated experimentation, as this analyses random errors and ensures the robustness of the procedure. Therefore, the waste mode was selected for the development of the microscale experimentation.

3.2.1.4 Effect of Dispensing Speeds

The liquid handling workstation can be operated at a variety of dispensing speeds, which can be selected in individual performance files and these were used in automated experiments to examine their affects on the microscale LLE (section 4.2.5). The workstation was fitted with disposable tips using the waste mode and was operated at the extreme dispensing speeds (10, 400 and 1866 $\mu L.s^{-1}$) to assess its performance to dispense 150 µL RO water.

The statistical analysis of the gravimetric data (table 3.2.1.4.1) illustrated how the accuracy decreased with the increase in dispensing speed from 10 $\mu L.s^{-1}$ (98.8% accuracy) to 1866 $\mu L.s^{-1}$ (98.0% accuracy), although these effects alone were minimal. This was expected as the incremental changes to the mechanical syringe motor increased with the speed, making the workstation less accurate.

The precision of the data generated at each dispensing speed followed a similar trend to that of the percentage inaccuracy values, increasing with the speed selected (0.3% CV, 3.2% CV and 23.7% CV for 10 $\mu L.s^{-1}$, 400 $\mu L.s^{-1}$ and 1866 $\mu L.s^{-1}$, respectively). This indicated that the

Operational Mode	Waste	Blowout
Target Volume (µL)	175	175
Mean Volume (µL)	176.8	174.8
% Target Volume	101.1	99.9
% Inaccuracy	1.052	0.112
2SE	0.60	1.08
% CV	1.2	2.2

Table 3.2.1.3.1. Experimental analysis of the accuracy and precision of dispensing 175 µL RO water aliquots using the Multiprobe II Ex® workstation fitted with disposable tips and operated in waste or blowout mode (Sample size =20). Method detailed in section 2.2.3.1.

Speed ($\mu L.s^{-1}$)	10	400	1866
Mean Volume (µL)	151.8	152.4	153.0
% Target Volume	101.2	101.6	102.0
% Inaccuracy	1.2	1.6	2.0
2SE	10.4	2.3	1.1
% CV	14.1	3.2	1.5

Table 3.2.1.4.1 Analysis of the accuracy and precision of experimental data generated dispensing 150 µL RO water aliquots using the Multiprobe II Ex® workstation fitted with disposable tips (n = 15 to 18) and operated at different dispensing speeds (10 $\mu L.s^{-1}$ to 1866 $\mu L.s^{-1}$). Method detailed in section 2.2.3. 1.

data was less precise, as the dispensing speeds increased and the larger sample size (n = 11 to 18) made the data more significant, with the mean being closer to the true mean value[10]. The intermediary dispensing speed data indicated that a mid point in the dispensing speed range produced an acceptable performance for the operation of the workstation. This data was similar to the previous data for different dispensed volumes, which were dispensed at 400 $\mu L.s^{-1}$ (0.3% inaccuracy, 0.4% CV). These results were better than the manufacturer's recommended specification for accuracy (+/- 2% inaccuracy), although they did not achieve their target precision (0.5% CV). Therefore, these dispensing speeds were considered acceptable for use in the automated LLE experimentation (chapter 4).

3.2.1.5 Effect of Performance Files

A number of performance files (section 2.2.1.4.1) were written to control the operation of the liquid handling workstation in order for it to handle a range of liquids, including organic solvents and an ionic liquid, which were used within the microscale experimentation (section 4.2.4). It has previously been demonstrated that different liquids affect the performance of workstations in dispensing volumes of 85 µL of DMSO (101.1% accuracy) and water (84.2% accuracy) (Olsen, 2000). The accuracy of the workstation operated under each performance file was gravimetrically measured and the data statistically analysed for its accuracy.

The performance of the workstations operated under these performance files was assessed to ensure that the optimum performance was achieved. This used similar gravimetric measurements of the workstation dispensing 100 µL or 150 µL aliquots of RO water or BA, depending on the experimental step, to assess the reagent, BA and transfer steps within the microscale LLE experimentation (table 3.2.1.5.1). The data was analysed, generating percentage inaccuracy values of the performance of the workstation and generated a high degree of accuracy with 0.33%, 0.54% and 0.51% inaccuracy for the respective performance files. The precision of this data was analysed and generated good percentage CV values of 0.4%, 0.5% and 0.74%, respectively. This indicated that the data for all performance files investigated was of high precision and suitable for use in the development of the microscale LLE process.

[10] Definition of statistical terminology in appendix 11

Reagent	BA	Water	Water
Target Volume (μL)	150	150	100
Mean	150.5	149.2	100.5
% Inaccuracy	0.3	0.6	0.5
2SE	0.3	0.5	0.4
% CV	0.4	0.5	0.7

Table 3.2.1.5.1. Analysis of the accuracy and precision of experimental data generated dispensing 150 μL RO water or butyl acetate or 100 μL RO water aliquots using the Multiprobe II Ex® workstation fitted with disposable tips for water samples or fixed tips for BA samples (n = 8) and operated using specific performance files for the liquids. Method detailed in section 2.2.3.1.

3.2.1.6 Comparison to Published Data on Workstation Performance

There are numerous liquid handling workstations currently commercially available. The selection of one depends upon the user's requirements, budget, performance, safety expectations, availability of consumables and service (Zimmermann, 2000). Since the initial development of the liquid handling systems there have been new developments to improve their accuracy and precision for dispensing micro and sub-microlitre volumes (Szita et al, 2001). The performance of the liquid handling workstation used in this experimentation was compared with the performance of a number of other liquid handling systems (Rapid Plate 96 (Zymark), Hydra 384 (Robbins Scientific), PixSys (Cartesian Engineering), BioChip (Packard), Quadra 96 (Tomtec), C-400 (Cyberlab) and Genesis (Tecan) workstations.

The liquid handling accuracy and precision of different workstations used to dispense liquid aliquots have been assessed to quantify their performance. This data was used to compare their operational performances by quantifying their precision, as the accuracy was optimised by the set-up and calibration of the equipment. The Rapid Plate 8-channel and Cyberlab C-400 96-channel pipettors were compared for dispensing 100 μL aliquots (n = 3) of fluorescin in HEPES buffer, which had 3.5% to 7.3% CV and 3.1% to 5.8% CV, respectively, calculated from gravimetric measurements of the dispensed aliquots (Olsen, 2000). These pipettors could only dispense liquid aliquots (section 1.8.1). It was observed that the pipetting of DMSO was more accurate than water, which was due to its lower volatility and higher density. This equipment showed better performance than the precision of both the Tecan Genesis SP100 liquid handling workstation (9.7% CV) which compared favourably with Eppendorf 4850 manual multichannel pipettor fitted with 1000 μL disposable pipette tips (10.8% CV) to dispense 100 μL water aliquots (Hanson and Cartwright, 2001). The comparison of the workstation with the automated pipettors indicated the improved precision that was achievable.

The precision of these workstations was assessed by various researchers for their ability to dispense aliquots of RO water. Several types of liquid handling workstation were compared for low volume pipetting (0.5 μL to 100μL) for water and DMSO (Stevens et al, 1998). The Quadra 96 (Tomec), Rapid Plate 96 (Zymark), Plate Trax (Carl Creative) and Plate Mate (Matrix) workstations were evaluated by Stevens for accuracy in dispensing sub micron

aliquot range approach (58% to 138% for H_20 and 99% to 159% for DMSO). The dispensing performance improved for larger volumes of 10 µL to 100 µL (98.5% to 101.5% for RO water and DMSO samples (calculated from published data)). The precision at 100 µL ranged from 1.26% to 2.3% CV for water and 1.1% to 3.5% CV for DMSO with the best performance from the Plate Trax workstation for dispensing water and rapid Plate 96 for dispensing DMSO. The programming of the assay took 10 to 45 minutes with Plate Trax being the easiest to program, which also had the fastest speed of operation. This indicated that the performance of the workstations was affected by the nature of the liquid dispensed, as was shown in this research.

The research carried out here on the Multiprobe II Ex® workstation showed better performance than the Rapid Plate 8-channel, Cyberlab C-400 96-channel pipettors, Genesis SP 100 workstation and Eppendorf 4850 manual multichannel pipettors for dispensing 100 µL aliquots for both the disposable tips (1.7% inaccuracy, 2.1% CV) and fixed tips (2.6% inaccuracy 0.1% CV from (table 3.2.1.2.1)). This improved performance was achieved despite the use of an alternative reagent (RO water) that had higher volatility and lower density than DMSO and HEPES buffer. The Multiprobe workstation used a higher number of replicate samples ($n \leq 12$) in the experimentation, which increased the significance of the findings. This data validated its use in the development of automated microscale experimentation. The Multiprobe II Ex® compared favourably with these workstations, which were assessed for dispensing µL and nL volumes (Bateman *et al*, 1999, Hanson and Cartwright, 2001).

The performance of the Rapid Plate 96 (1 µL 9.5% CV, 10 µL 6.4% CV) and Hydra 384 (1 µL 2.8% CV, 10 µL 1.4% CV) systems had better precision than the PixSys and BioChip systems (Bateman et al, 1999). The accuracy of these systems was not investigated as they were assumed to be accurate as each system could be modified to increase the volume accuracy if required. The performance of the C-400 workstation improved with the increase in dispensed volume from 10 µL to 100 µL (4.3% CV, 4.1% CV), which was better than the performance of the Rapid Plate 96 workstation (4.1% CV, 4.9% CV) at the higher volumes within this range (Olsen, 2000). The precision of the Quadra 96 workstation also improved as the dispensed volume increased from 10 µL to 100 µL (2.26% CV and 1.25% CV) but this

precision had greater variation than that observed using the C-400 (Lab STAR) workstation (Astle and Akowitz, 1996).

The Multiprobe II Ex® workstation's accuracy and precision data for different performance files compared well with that for dispensing DMSO using the C-400 workstation (117% inaccuracy, 3.04% CV), which was worse than pure water (0.3% inaccuracy, 0.8% CV) (Olsen, 2000). The high performance of the automated workstations supported their use for generating accurate and reproducible liquid dispenses for the development of microscale process screening experimentation, assuming that these or similar operating conditions are used.

The Microlab STAR system has liquid level detection to produce accurate and reliable liquid transfers. Liquid level detection uses a combination of capacitance and conductivity as the pipette is moving towards the liquid to detect the liquid level by measuring pressure and capacitance, which set the liquid level within 10 msec. Capacitance restricts the use of polar liquids. The use of both methods of liquid level detection allows the detection of inhomogeneous liquid that may contain bubbles at the surface (Pochert, 2000). The performance of the Lab STAR workstation was within the performance range set by the other workstations compared by Pochert, 2000). The microlitre liquid handling capability over 1 μL to 1000 μL was assessed, which produced 1% to 7.5% accuracy and 0.75 = 6% CV precision (DiLorenzo et al, 2001). The accuracy and precision increased with the volume except for the 10 μL. The pipette tips positioning had a 1 mm accuracy in the *X*, *Y* and *Z* directions, whilst a good reproducibility of 0.01 mm to 0.05 mm. Although, this statistical information is for the performance of other workstations than that used in this research, the results are expected to be similar as they were designed for a similar function.

The use of automated equipment can accelerate the experimentation and generate rapid results. The automated liquid handling equipment varies in its speed of operation to transfer between locations the liquid from one 384 well plate to another plate taking from 4 minutes to 288 minutes (Bateman et al, 1999). The automated assay prepared using the Genesis workstation was compared to the manual assay, which took 13,185 minutes compared to 14,807 minutes to complete 30 experiments where the samples each took 2.6 to 3.68 minutes to process.

Automated liquid handling systems are suited to a range of high throughput operations, which require sterility that is achieved by the use of disposable tips (Brush, 2002). Therefore, the automated methods become more complex and require more liquid handling stages. However, the advantages are that it can rapidly generate high sample numbers and investigate many experimental scenarios, but this raises data handling issues.

3.2.1.7 Summary of Workstation's Performance

The manufacturer's analysis of the workstation's performance (section 3.2.1.1) showed grater error associated with the actual data than the target values for both accuracy and precision over the dispensed aliquot volumes investigated (1 μL to 100 μL), except for the highest volumes. The accuracy of the manufacturer's data showed that the actual results for dispensing 100 μL aliquots (0.72% inaccuracy) has more error associated with it than the target value (0.5% inaccuracy), indicating that this may be an ambitious target. However, the precision for dispensing 100 μL aliquots showed that the actual data (0.25% CV) was lower than the target data (0.50% CV), indicating that the actual operation of the workstation was more precise than expected.

The workstation used in this research was set up with 1.0 mL syringe barrels rather than0.5 mL syringe barrels which were used on the manufacturer's workstation to test its performance. This increased the functionality of the workstation, but was not ideal for optimising its performance, so the workstation used in this research was expected to have lower performance in accurately dispensing low volumes.

The performance of the workstation used in this research was analysed over a range of dispensed volumes (1 μL to 150 μL) using a variety of pipette tips (micro conductive disposable, small conductive disposable and fixed). The statistical analysis of the gravimetric data for these dispensed aliquots $\leq$150 μL using the workstation fitted with disposable tips was more accurate than with the fixed tips (section 3.2.1.2). The accuracy data for the disposable tips compared favourably with the manufacturer's recommended customer specification data for dispensing 100 μL, although the fixed tip data fell just outside this data (2.5% inaccuracy) the accuracy data for both pipette tips fell within an acceptable limit of experimental error (10%).

The precision of the workstation used in this research to dispense 100 μL fitted with disposable tips (2.1% CV) was also associated with more error than the manufacturer's precision data (actual 0.25% CV, target 0.5% CV), but fell within the target values for the precision of the fixed tip data. Dispensing with the fixed tips (0.1% CV) was more precise than disposable tips (1.15% CV). Therefore, both of these options were used in the automated microscale experimentation, as using the fixed tips accelerated the process and allowed the transfer of reactive solvents, whilst the disposable tips minimised contamination. The data from dispensing under different operational modes showed that the waste mode was the most accurate and precise so this was used in the automated experimentation. The workstation showed good performance at all dispensing speeds and using all performance files. Therefore, the workstation used in this research was fitted with disposable tips for dispensing aliquots of ≥100 μL of liquids. It was operated in the waste mode using all dispensing speeds and use of performance files in experimentation, which generated good performance data.

3.2.2 Evaluation of the Accelerator™ Performance

The Accelerator™ dosing station is an automated solid and liquid dispenser that was used in this research to dispense specific masses of solids. This dosing station has the capability to dispense 1 mg to 20 g of solids of various morphologies (powder, crystalline, granular) at fast operation speeds (Chemspeed, 2003). The performance analysis of the manufacturer's data (section 3.2.2.1) showed good accuracy and precision. However, further analysis was made for dispensing the reagents required in this experimentation (section 3.2.2.2). The operation of the dosing station was optimised using the application software tool (section 2.2.2.3) to screen the required parameters for dispensing specific solids, including granular activated carbon. Comparison of the performance data was made with the manufacturer's data (section 3.2.2.1) in section 3.2.2.3.

The performance of the automated dosing station was assessed on its ability to dispense a range of activated carbon masses (1 mg to 80 mg) into HPLC vials. Gravimetric methods (section 2.2.3.2.1) allowed the measurement of the predicted mass dispensed by the dosing station and the actual mass dispensed within the vial. This data was used to quantify the performance of the dosing station for this operation. Analysis of the prepared samples produced data for assessing the accuracy and precision of the equipment, which was compared to the claims made by the manufacturer about its performance.

3.2.2.1 Manufacturer's Evaluation of Dosing Station's Performance

The manufacturer of the Accelerator™ dosing station assessed its performance in-house, which demonstrated good accuracy and precision (appendix 7.2). The effect of dosing speed was investigated and the data analysed (section 3.2.2.1.1) to demonstrate its affect on sample throughput. This data was later compared to the performance of the dosing station used in this research (section 3.2.2.3).

The manufacturer published marketing literature on the precision of the Accelerator™ dosing station as ±0.1 mg. However, experimental data provided by Chem Speed evaluated the precision of an Accelerator™ dosing station dispensing 200 mg silica gel and 10 mg starch (appendix 7.2). The data generated mean values of 203.1 ± 0.45 mg (data range 200 mg to 212.2 mg) and 9.9 ± 0.059 mg (data range 9.8 mg to 10 mg) respectively. The analysis of the manufacturer's solid handling performance showed that the actual data achieved by the manufacturer during testing had good accuracy and precision for both the silica (0.4% inaccuracy, 0.45% CV[9]) and starch (0.9% inaccuracy, 0.5% CV) samples. However, the precision of this data indicated that the 10 mg data was more precise than the 200 mg data, but this could have been due to the different morphologies and operation parameters of the equipment. These data indicated that the dosing station was accurate and reliable, but further investigation was carried out on the performance of the dosing station used in this research (section 3.2.2.2).

3.2.2.1.1 Effect of Dosing Speed

The dosing speed of the dosing station was assessed for dispensing the silica gel data (appendix 7.2), provided by Chem Speed. These data showed that the average dosing time for the dosing station to dispense 200 mg silica gel was 20 s, although this ranged from 16 s to 32 s per dose across 96 samples due to the different operation parameters selected in the software (section 2.2.2.3). This automated dosing station can, therefore, prepare a 96-well plate with 200 mg of one solid reagent in 32 minutes. This indicated that the operation of the automated dosing station was suitable for the preparation of large numbers of containers with

[9] CV = Coefficient of Variance, defined in appendix 11

reagents, making it ideal for microscale applications including the preparation of microscale SPE reaction wells.

3.2.2.2 Dosing Station's Performance

3.2.2.2.1 *Dosing Station Accuracy*

The gravimetric results over the range of activated carbon masses were measured by the dosing station, calculating the dispensed mass measured by the dosing station (predicted mass), and using an external balance to measure the actual mass dispensed into vials (actual mass). The mean of these results were plotted against the target mass with 2SE error bars (figure 3.2.2.2.1.1 (a)). This illustrated the linear correlation of both the predicted masses and actual masses with the target mass. The predicted mass data fitted the $Y = 1.00X - 0.00015$ correlation with a R^2 value of 0.999 and the actual mass data fitted the $Y= 1.06X–0.0021$ correlation with a R^2 value of 1.000. The accuracy of both sets of data did not increase linearly with the increase in mass dispensed, which indicated random error associated with the dosing station. The accuracy data (table 3.2.2.2.2.1) for the predicted measurements (85% to 100.4%) was better than the accuracy of the actual measurements (52% to 104.6%).

The values larger than the target mass indicated that more mass was dispensed into the vials, which indicated the difficulties associated with dispensing larger masses from the platform due to the reagents morphology. Values lower than the target indicated difficulties in dispensing the mass due to misalignment of the solid dosing unit with the container, which restricted the solids transfer into the vials. This problem continued after changing the vials for ones with wider orifices and indicated a design restriction of the automated equipment, which could not be reliably and safely modified in the laboratory.

The manufacture states that the dosing station has an inaccuracy of 1%, illustrated by their data for dispensing 10 mg starch (0.9% inaccuracy) and 200 mg silica gel (0.4% inaccuracy) (appendix 7.2). These values are similar to those stated in the Chem Speed literature, with any difference being very small. Modification of the operational parameters of the equipment for dispensing the silica gel produced variation in the results from 0.4% to 18.5% inaccuracy and to achieve the best accuracy required increased dosing time. The manufacturer's inaccuracy data was a lot better than that achieved for the activated carbon samples, but this

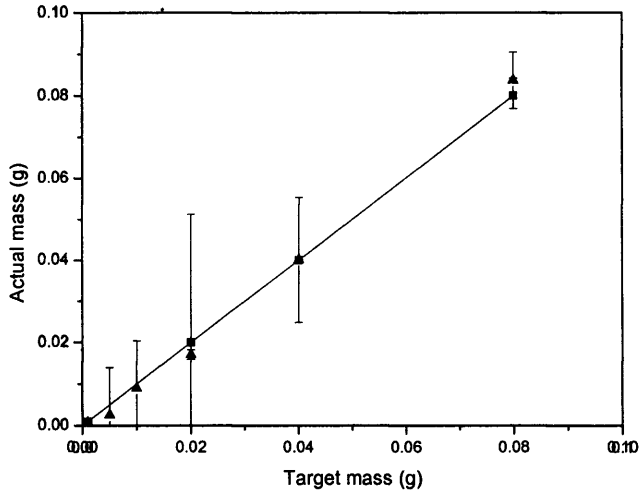

(b)

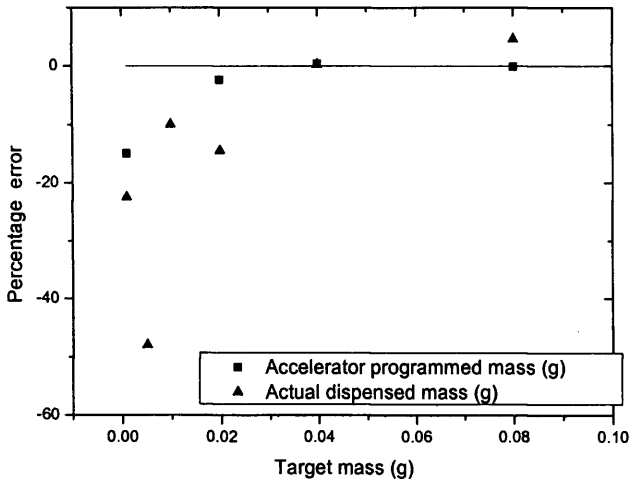

Figure 3.2.2.2.1.1. Analysis of dry granular activated carbon (1 mg to 80 mg) dispensed using the Accelerator™ solid dosing station (Chem Speed): (a) parity plot of (■) predicted mass and (▲) actual mass against target mass and (b) plot of percentage error in dispensing solids against target mass for (●) Chem speed calculated mass and (★)actual weighed mass. Mean data (n = 10) plotted with 2SE error bars and solid line represents the linear regression of the data. Method detailed in section 2.2.3.2.1.

Target Mass Activated Carbon (mg)	% Accuracy	
	% Predicted Mass	% Actual Mass
1	85.0	77.5
5	-	52.0
10	-	90.5
20	97.7	85.5
40	100.4	100.3
80	99.9	104.6

Table 3.2.2.2.1.1. Analysis of the accuracy of experimental data generated from dispensing 1 mg to 80 mg unconditioned activated carbon (n = 2 to 20) using the Accelerator™ solid dosing station (Chem Speed, Switzerland). Method detailed in section 2.2.3.2.1.

Target Mass Activated Carbon (mg)	Predicted Mass (mg)	2SE Predicted Mass	Predicted % CV	Actual Mass (mg)	2SE Actual Mass	Actual % CV
1	0.85	0. 29	38.0	0.775	0.055	71.5
5	-	-	-	2.6	1.14	309.6
10	-	-	-	9	1.14	100.0
20	19.53	0.12	10.6	17.1	3.42	100.0
40	40.15	0.015	0.5	40.1	0.15	19.0
80	79.90	0. 0545	1.9	83.69	0.68	13.0

Table 3.2.2.2.2.1 Analysis of standard error for experimental data generated from dispensing 1 mg to 80 mg unconditioned activated carbon (n = 2 to 20) using the Accelerator™ solid dosing station (Chem Speed, Switzerland). Method detailed in section 2.2.3.2.1.

could have been due to the morphologies of the different reagents or sub optimal set up of the equipment.

The percentage error associated with dispensing the solid masses was plotted against the target mass (figure 3.2.2.2.1.1 (b)) for the actual and predicted data (table 3.2.2.2.1.1). This plot clearly illustrates the variation of both the Chem Speed predicted masses and the actual dispensed masses from the target values, which demonstrated that there were errors associated with both data sets. The data below 40 mg showed a lower mass, whilst the data for 80 mg showed a slightly higher value that reflected difficulties encountered in dispensing the amorphous crystalline reagent. The percentage error values did not reduce linearly with the increase of mass, but the predicted data had lower percentage error values than the actual data. The variation of the actual data indicated that random errors related to the automated dosing station were occurring.

3.2.2.2.2 Dosing Station Precision

The precision of the predicted mass and actual mass data generated from the dosing station dispensing a range of activated carbon masses (1 mg to 80 mg) was assessed using statistical methods (appendix 11). These individual gravimetric measurements (n = 6 to 30) were assessed to quantify the statistical value of percentage CV and the 2SE values (table 3.2.2.2.2.1), which indicated the degree of variation associated with the data and the operation of this automated platform. The dosing station showed more acceptable SE values for the larger masses, indicating that less significant errors occurred. The predicted data has a smaller degree of spread than the actual data, as reflected in the percentage CV values (0.5% to 38% CV and 13.0% to 309.6% CV, respectively). This was expected as it reflected the difference between the precision of the measurements. The precision of the solid dosing at the lower end of the range of masses indicated a higher degree of scatter than the larger masses, which was expected due to the variation in the morphology and size of the granular amorphous compound.

3.2.2.3 Comparison with Manufacturer's Performance Data

Comparison of the performance of the Accelerator dosing station dispensing activated carbon was worse than the manufacturer's data for either silica or starch (section 3.2.2.1.1). This was

due to the amorphous nature of the SPE resin and difficulties in the accuracy and precision of its operation. The dispensed samples were re-weighed manually on an analytical balance before their use in microwell SPE experiments (section 2.4.4). The Accelerator was deemed not suited to the dispensing of adhesive solids, such as immobilised enzymes or pre-wetted, conditioned resins, which limit its potential utilisation (section 5.2.2.3).

3.3 Conclusion

The automated platforms used in this research contained the Multiprobe II Ex® liquid handling workstation and the Accelerator™ solid dosing station. These individual pieces of automated equipment were assessed, identifying any errors associated with them. The performance of the equipment was assessed by analysing their accuracy and precision using gravimetric measurements of dispensed reagents. This quantified any related errors. The assessment of the performances of the liquid handling workstation (section 3.3.1) and solid dosing station (section 3.3.2) indicated their suitability for automated microscale experimentation in this research (section 3.3.3). The occurrence and prevention of any inherent errors related to each piece of equipment was considered, together with the impact of these errors on microscale experimental methodologies.

3.3.1 Liquid Handling Workstations

There are over 25 liquid handling workstations that are currently commercially available including the Genesis®, Rapid Plate® and the Multiprobe II Ex® workstations. Each of these workstations has their own features, limitations and performance for dispensing a range of volumes, which are all used to compare the different workstations. The liquid handling workstation used in this research was the Multiprobe II Ex®, that was assessed for its performance and in the design of microscale equilibrium separation processes.

The Multiprobe II Ex® liquid handling workstation demonstrated acceptable performance over the higher range of dispensed volumes. The small disposable pipette tips had better accuracy than the fixed pipette tips and had the advantage of reducing the risk of cross-contamination. Statistical performance of the data compared favourably with the manufacturers data for both pipette tips, which showed acceptable accuracy compared to the customer specifications. Divergence of the measurements from the target values may have

been due to differences in the set up of the instrument. The precision of this liquid handling workstation showed good repeatability and reproducibility. The minimum volume used in the development of microscale methods in this research was 100 μL. Variation in the pipetting precision could be attributable to the difference between the various pipette tips of the multichannel system, which created a 5.9% CV for dispensing 100 μL (Bateman et al, 1999).

The performance of the workstation fitted with the small conductive disposable tips operated within the waste mode, using bespoke performance files for the dispensed liquid generated good results and the performance of the workstation increased by decreasing the dispensing speed. The accuracy values were within the expected customer specifications of the manufacturer and the precision of these experimental data was outside the limits of the manufacturer's target data for 100 μL. The precision of the volumes dispensed, using decreasing dispensing speeds, increased. At the lower dispensing speeds the precision was expected to be high, but the motor that controls the syringe plunger moves in set increments, which loses the fine control of the volume due to gravity and surface tension.

3.3.2 Solid Dosing Stations

The solid dosing station was analysed for its performance at dispensing adsorbent resins. It demonstrated the solid dosing of dry granular activated carbon, but was less successful with dispensing the wet conditioned resin as only the moisture was squeezed from the resin. This indicated the limitations of this automated equipment for its use in automated microlitre processes (investigated further in chapter 5). The gravimetric measurements of predicted mass of activated carbon showed good correlation with the target mass over the range of dispensed mass. However, the actual mass of solids dispensed into the container was below the mass predicted by the solid dosing station over the range of dispensed mass (52% to 104.6% accuracy). The scatter of the data for these samples was due to limitations of the equipment caused by the unbalanced dosing head moving freely, resulting in misalignment of the dosing head with the vial, which caused the reagent to be wasted by spillage. This was an inherent problem of the equipment and had been observed by its regular users. The performance results were worse than those quoted in the Chem Speed literature (1% inaccuracy) and the data from their in-house experimentation carried out with silica gel (0.9% inaccuracy) and starch (1.6% inaccuracy). The best performance was for dispensing 40 mg dry activated carbon, achieving high accuracy for both the predicted mass (100.4%) and the

actual mass (100.3%). However, the variation in the other masses dispensed had inadequate accuracy, which made the dosing station unsuitable for dispensing the solids required in the microscale processes. Therefore, there was a need for an additional manual weighing method in conjunction with the automated dosing station to gravimetrically measure the masses prior to their use in process experimentation.

The solid dosing station is one of many approaches being used in the automated laboratory to automate the preparation of solid reagents. It is also now possible to carry out gravimetric measurements using an ancillary device that can be integrated with a number of liquid handling systems (Bruner et al, 2001). The Mettler Tolledo balance can be controlled by both the Tecan Gemini and Multiprobe II Ex® workstation application software via their operating systems. This allows the automatic weighing of containers and data collection. The integration of a gripper arm would be required to move the containers between locations on the workstation to allow additional experimentation to occur. However, further research would be necessary to ensure the accuracy and precision of these instruments to deliver the required small masses before their use in automated microscale process development.

3.3.3 Summary of the Analysis of Automated Platform

The automated platforms (Multiprobe II EX® and Accelerator™) were quantitatively assessed to evaluate their performance. This research evaluated their liquid and solid handling capabilities to deliver quantitative measurable experimental approaches. The liquid handling workstation showed good performance at delivering larger microlitre liquid volumes and was recommended for the development of automated microscale processes. The dosing station showed inadequate accuracy in dispensing the solids and it was recommend for restricted use in the microscale experimentation working in conjunction with additional gravimetric measurement of the masses prior to their use in process experimentation. These automated platforms were considered for their use in the development of microscale liquid-liquid extraction (chapter 4) and solid phase extraction (chapter 5) experimentation.

Chapter 4: Microscale Liquid-Liquid Extraction

4.1 Introduction

Having considered the basic performance of the automation platforms in chapter 3, this chapter examines one of the equilibrium stage separation processes to be implemented on them: liquid-liquid extraction (LLE). Liquid-liquid extraction has been extensively applied as a primary purification technique for the isolation of compounds of interest from varied contaminants (Blanch and Clark, 1996). The use of LLE increased as the range of available solvents increased during the 1950's (Seader and Henley, 1998). LLE is a highly selective process that can preserve biological activity of the compounds and has been easily scaled up to isolate manufactured pharmaceuticals, biomolecules and chemical compounds (Asenjo, 2003).

The LLE process is well characterized for the equipment used at larger scales (section 1.5.1.1), generating fundamental mass transfer principles of the processes (appendix 13). The basic principle of separation in LLE is that one or more compounds are separated from contaminants in the aqueous liquid feed by their selective partitioning after contact with an immiscible liquid phase, based on their different solubilities in each phase. The rate of mass transfer and equilibrium partitioning (appendix 13.2) between the two immiscible phases is affected by a number of factors, such as aqueous phase pH conditions, molecular size and hydrophobicity of the compounds.

The automated liquid handling workstation was investigated to develop a fully automated microscale LLE process method (section 4.2.1) within a 96-well plate by assessing the effect of various parameters of both the equipment and process on mass transfer for the purification of 6-APA from the simulated penicillin acylase bioconversion product stream. The microscale LLE process was used to investigate the key parameters of the process in order to optimise the purification of the compound from its contaminants. The results of these investigations were

discussed (section 4.2) and the wider application of the automated experimentation was presented (section 4.3).

4.2 Results & Discussion

The automated microscale LLE method was developed and used to investigate key factors influencing the microscale LLE process for the rapid generation of accurate and reproducible process data (section 1.8.2.1.5). In contrast to the previous studies (section 1.8.2.1), the automated microscale process used a smaller extraction volume of 300 µL and *in-situ* phase mixing. This reduced the reagents' cost, experiment duration and degree of manual intervention, whilst increasing the throughput, making it ideal for the initial assessment of the automated platforms for their suitability to the automation of this purification process.

The experimentation utilised the PA product stream reagents to investigate the automated microscale LLE process and its key process parameters (section 4.2.1). The factors affecting the microscale LLE process that were investigated included automated extraction kinetics at the microlitre scale (section 4.2.2) and the variation of the distribution ratio (D) with the aqueous phase pH conditions (section 4.2.3), the influence of the organic solvents' characteristics (section 4.2.4) and the effects of the pipetting dispensing speed on LLE kinetics (section 4.2.5). Comparison of the automated microscale data was made with the manual microscale and laboratory scale LLE experimental data was used to assess the validity of the microscale experimentation. The effect of the workstation pipetting speed on the LLE process kinetics was investigated and the data was fitted to a model to illustrate mass transfer kinetics (section 4.2.6). The accuracy and precision of the microscale LLE process data was quantified to assess the reproducibility and reliability of the microscale LLE process (section 4.2.7). Sources of error associated with the use of the workstation were observed and identified during the development and use of the automated microscale LLE experimentation (section 4.2.8).

4.2.1 Microscale LLE Method Development

The microscale LLE method was developed by considering the commercially available equipment and their operation to assess their suitability in achieving efficient mass transfer.

Phase mixing was required for efficient mass transfer between the phases. Phase mixing can be achieved using a number of external mixing systems, such as tiny magnetic bars designed for 96-well plates with electrical motors to create vortexes, horizontal rotating platforms or repeated pipetting mixing cycles using an automated liquid handling workstation (Sutherland et al, 1989). The microscale LLE process assessed the use of a 96-well plate horizontal orbital shaker (Thermomixer) and a liquid handling workstation to achieve suitable phase mixing. Care was taken with these methods to ensure that volume losses were avoided, preventing solute spillages, hazardous chemical issues and cross-contamination between the wells.

Liquid handling equipment (section 2.2.1) has been previously used to carry out LLE for the separating of compounds from biological materials prior to analysis (section 1.8.2.1). These LLE processes used a range of extraction methods, volumes and mixing methods, which were compared to manual processes by analysis of their statistical performance. This identified the most popular method of mixing as being automated pipette mixing cycles (Sutherland et al, 1989; Peng et al, 2000b), which repeatedly aspirated and dispensed an aliquot of liquid from the extraction well using a range of mixing cycles (n_c = 3 to 6) for large alliquot volumes (450 µL to 0.8 mL). These automated processes reduced the time required to complete the equivalent manual method and showed improved statistical performance (0.3% to 4.3% inaccuracy) than for the manual process (2.1% to 6.2% inaccuracy) (Jemal et al, 1999).

The automated microscale LLE process was designed using a liquid handling workstation (Multiprobe II Ex®). The microscale LLE experimental method was developed as a batch process that was carried out in a 96-well plate at a total reaction volume of 300 µL. The automated microscale LLE process was adapted from the laboratory LLE method whilst maintaining a phase volume ratio of 1. Phase mixing was achieved using the aspirating and dispensing mixing cycle feature of the workstation to repeatedly mix the contents of the well by transferring half of the total reaction volume. Disposable tips (d_{id} = 0.625 mm) were used throughout the experimentation to minimise the risk of cross-contamination between the wells. The automated microscale LLE process is illustrated schematically (figure 4.2.1.1), which showed the four main stages of the microscale process: aqueous phase addition; organic phase addition; phase mixing

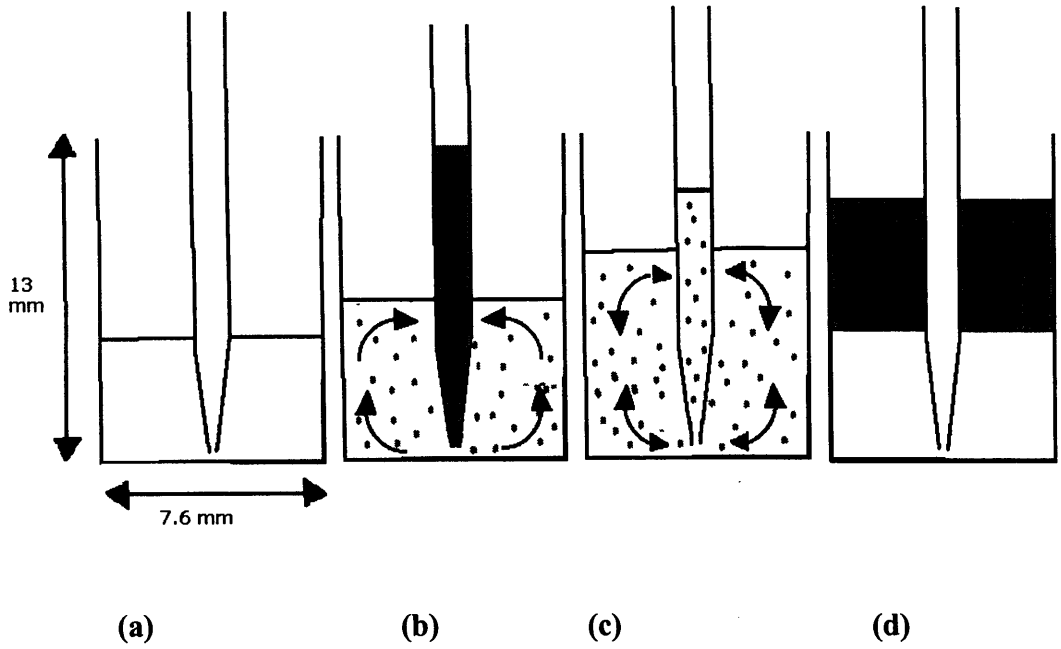

Figure 4.2.1.1. Schematic representation of the microscale liquid-liquid extraction process (total liquid volume = 300 μL) indicating the four main stages of the process: (a) dispensing heavy phase, (b) dispensing and dispersion of light phase: (c) repeated apiration and dispension of biphasic liquid aliquot and (d) phase separation. Method detailed in section 2.3.3.

by repeated aspirating; and dispensing mixing cycles and phase sampling after phase separation under gravity.

The liquid handling workstation was investigated for its capability to generate efficient phase mixing by modifying its parameters to achieve mass transfer (section 4.2.1.1). The fluid dynamics of the LLE process were investigated to demonstrate microscale mixing (section 4.2.1.2). The mass balance of the LLE process was carried out at both scales (section 4.2.1.3). The LLE of the bioconversion product stream is discussed in section 4.2.1.4. The compounds used in this experiment were fairly stable, but there was a minor degree of degradation that occurred under certain conditions (section 4.2.1.4.1). The evaporation of the compounds at the microscale was studied for its effects on the microscale LLE process (section 4.2.1.5).

4.2.1.1 Automated Microscale Phase Mixing

The automated microscale process used the liquid handling workstation to prepare the LLE reaction wells by transferring an aliquot of the phases and creating phase mixing using its repetitive mixing cycle feature. The aliquot was transferred in and out of the same well to promote adequate mass transfer. Various mixing parameters of the workstation were investigated to assess the most suitable scenario for the automated microscale LLE process to increase the interfacial area between the two immiscible liquids, which minimised the contact time required to achieve equilibrium. The method development experimentation (section 2.3.2.1) investigated these mixing parameters to assess the need for mixing (0 or 30 mixing cycles), the pipetting height in the well (2% or 100% of well height) and movement (tracking[1]) of the pipette tips during the dispensing stage of the mixing cycles (0% or 100% tracking). In each experiment the phases were left to settle under gravity and form two distinct phases following phase mixing.

The position of the pipette tip within the well also affected the phase mixing, as the height the liquid fell created a pseudo jet stream from the pipette tip, which created turbulence and dispersed on contact with the bulk liquid in the well or the well bottom itself. The liquid

[1] Multiprobe Terminology defined in appendix 5

dispensed at 2% well height had a higher yield than if dispensed at 100% well height. This was more prominent with 0 mixing cycles, increasing the yield from 79.7% to 87.6% PAA recovery. However, this trend was still seen when the samples were mixed with 30 mixing cycles and 0% tracking (90.6% PAA recovery at 2% above the well bottom compared to 88.3% at 100% well height). Dispensing at 2% well height with 0% tracking and 30 mixing cycles created conditions for the best mass transfer in the automated microscale LLE process.

The statistical analysis of the between-run variation in aqueous phase PAA concentration data for each of the scenarios investigated (table 4.2.1.1.1) showed that the experiments had a high degree of variation (0.2% to 69% CV[9]), which indicated that errors occurred during the experimentation. This may have been a result of poor calibration of the laboratory equipment used to prepare the bulk PAA solution, inaccurate measurements of buffer volumes that the compound was dissolved in or variation in the pH conditions, which would all affect the consistency of the bulk aqueous phase. In addition, there was variation in the performances for each of the mixing scenarios that was related to the performance of the workstation (section 3.2.1) and indicated the occurrence of errors associated with the automated LLE process (section 4.2.8). The automated process had high numbers of liquid transfer stages, which may have been a source of error if the operation of the workstation caused minute variations in the final extraction volume due to losses of aliquot volumes, positioning errors of the pipette tip (random errors) or calibration discrepancies. These problems could be minimised by taking greater care in performing the experimental method, more effectively calibrating the laboratory equipment and automated workstation prior to their use as well as the use of suitable performance files (Section 3.2.1.4).

The phase mixing scenarios affected the performance of the automated LLE process differently as the samples prepared without a mixing stage were more accurate and precise than the mixed samples. This was due to the additional use of the automated workstation to generate mixing. The bulk reagent was prepared using laboratory equipment prior to the experimentation, which

[9] CV = Coefficient of Variance, defined in appendix 11

Mixing Conditions	**Mixing Cycles (n_c)**	0	0	0	0	30	30	30	30
	Pipette Tracking (%)	100	100	0	0	100	100	0	0
	Pipette Height (% well height)	100	2	100	2	100	2	100	2
Equilibrium Aqueous Phase PAA Concentration ($mg.mL^{-1}$)		0.814	0.496	0.635	0.429	0.546	0.464	0.467	0.376
Distribution Ratio ($C_{org}.C_{aq}^{-1}$)		3.9	7.1	5.3	5.3	6.3	7.6	7.6	9.6
PAA Recovery into Organic Phase (%)		79.7	87.6	84.1	89.3	86.4	88.4	88.3	90.6
2 SE		0.57	0.001	0.002	0.006	0.151	0.035	0.201	0.044
% CV		69.0	0.2	1.3	0.2	33.7	9.5	48.0	15.4

Table 4.2.1.1.1. Effect of phase mixing conditions on the automated microscale liquid-liquid extraction of PAA (4.0 $mg.mL^{-1}$ at pH 2.5) with butyl acetate investigating the requirement for automated pipette mixing cycles (n_c = 0 or n = 30), pipette tracking (movement of pipette tip during dispensing liquid) and pipette dispensing height (2% or 100% well height) using the method detailed in section 2.3.2.1. The aqueous phase PAA concentrations were quantified by HPLC and the statistical analysis of the mean data (n = 12 to 28).

equally effected these data. The variation in the performance of the mixed LLE process scenarios indicated that the workstation's parameters affected its performance with the best precision (0.2% CV and lowest 2SE value of 0.001%) achieved at 2% pipette height with 100% tracking. However, the highest percentage recovery value (90.6%) was achieved for samples prepared with 0% tracking, which had a degree of scatter in the data (15.4% CV) that reflected the occurrence of random errors associated with the phases mixing and higher 2SE value of 0.04.

Based upon these observations it was recommended that all further automated microscale experimentation was carried out using 30 mixing cycles with the aliquot dispensed from a static pipette tip (0% tracking) positioned 2% above the well bottom with the pipette located in the centre of the well as a default setting. Further investigation into phase mixing during the automated microscale LLE process was required to assess the extraction kinetics for each of the compounds in the experimental model feed stream (section 4.2.2). The kinetics of phase separation were not investigated because contamination with butyl acetate (BA) interfered with the HPLC analysis of the aqueous phase. Later experimentation investigated the workstation's use of suitable performance files (section 2.2.1.4.1) to enhance its performance.

4.2.1.2 Fluid Dynamics of Microscale LLE Process

Visualisation of the LLE processes was performed using a high-speed video camera, as described in section 2.3.5. This demonstrated the phase mixing and separation at various LLE process scales using a variety of equipment. Visualisation of the fluid dynamics of the laboratory LLE process was used to investigate an automated phase mixing method using magnetic fleas, manual pipetting and a horizontal shaker. The pipetting and shaking methods appeared to be insufficient to bring about phase mixing. The manual pipetting method dispensed the liquid too slowly to generate turbulence due to the mechanism of the equipment and risked volume wastage due to spillage. The horizontal shaker was not shown to disturb the interface between the two phases. The high-speed video camera recorded the fluid dynamics of the magnetically stirred laboratory extraction vessel, the manual microscale process mixed using a normal pipette or on a horizontal shaker, and the microscale process mixed using automated workstation mixing cycles. It recorded the phase mixing and separation stages of the LLE process.

Visualisation of the laboratory scale process mixed with magnetic bars (figure 4.2.1.2.1) indicated that this method of mixing suitably disturbed the phase boundary, which suggested that this method of mixing would achieve suitable mass transfer. Further investigation into the kinetics of the laboratory LLLE process was carried out (figure 4.2.1.2.1). Mixing with magnetic stirrers was suitable for the laboratory LLE method, which was considered the positive control for the mass balance analysis of different LLE process scales (section 4.2.1.3).

The manual microscale method investigated the use of a horizontal shaker to create phase mixing. The visualisation of the fluid dynamics illustrated the behaviour of the liquid within the wells (figure 4.2.1.2.2). The fluid dynamics of mixing with the horizontal shaker illustrated its unsuitability, as the liquid displaced from side to side within the well without disturbing the phase boundary, plus there was evidence of liquid loss and cross-contamination between the wells. This indicated that phase mixing and mass transfer using this method of mixing was inadequate for the microscale LLE process. Instead, the phases were mixed using repeated mixing cycles carried out by manual pipetting as this generated good dispersion of the two phases.

The phase mixing of the automated microscale process used the automated liquid handling workstation's pipetting cycles. The fluid dynamics during this mixing method were again visualised (section 2.3.5.1), which showed the stages of the microscale LLE method (figure 4.2.1.2.3) and phase mixing was seen by the distribution of aqueous dye between the phases (figure 4.2.1.2.3 (c)). Phase separation occurred under gravity and the kinetics of this stage were visualised (figure 4.2.1.2.4). This indicated that these mixing cycles provided suitable phase mixing by creating phase dispersion, which increased the interfacial area available for mass transfer. Visualisation of the phase separation kinetics also validated the settling time of 10 minutes used in the experimental methods as ample.

Visualisation of the fluid dynamics of the automated microscale LLE process analysed the stages of the phase mixing cycle. The microscale LLE process consisted of four distinct stages (figure 4.2.1.2.3), which identified the schematic stages (figure 4.2.1.1) and demonstrated that the static

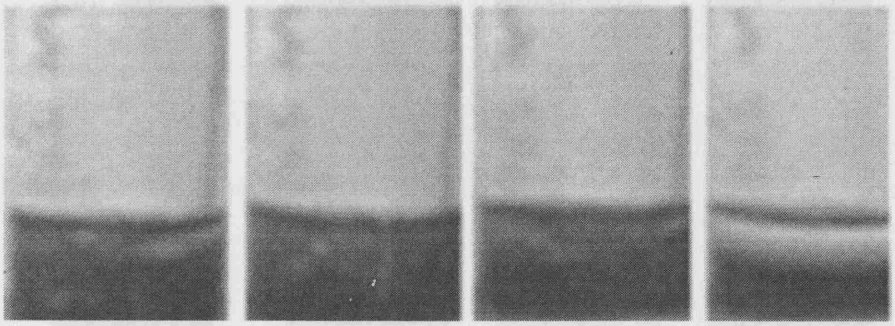

(a) (b) (c) (d)

Figure 4.2.1.2.1. Still images from a high-speed video camera of the fluid dynamics of the laboratory LLE process (total volume = 10 mL) mixed using a magnetic bar (80 mm x 1.5 mm) on a magnetic plate. Method described in section 2.3.4 detailing the mixing of the heavy phase (water) and light phase (BA). Images taken at: (a) 0.008 ms, start of mixing, (b) 0. 194 ms, mixing, (c) 0. 578 ms, end of mixing, and (d) 30 ms after separation indicting the phase boundary. Visualisation method detailed in section 2.3.5.

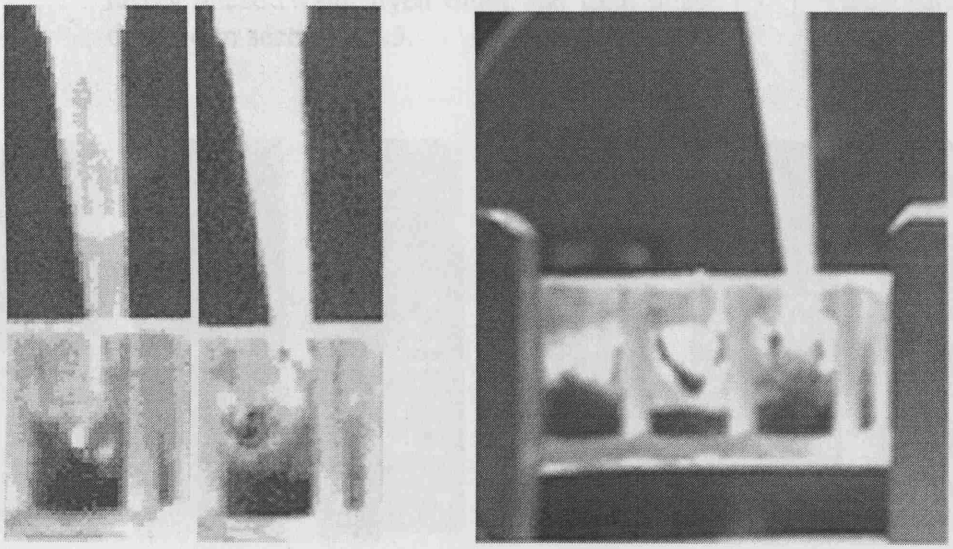

(a) **(b)**

Figure 4.2.1.2.2. Still images from a high-speed video camera of the fluid dynamics of the manual microscale LLE process (total volume = 300 μL) carried out using (a) manual pipette fitted with disposable pipette tip (d = 0.625 mm) and (b) a horizontal rotating platform (Thermomixer) to mix the phases in a well of the 96-wellplate (250 rpm). LLE method and visualisation method detiled in section 2.3.5 with a heavy phase (water) and light phase (BA).

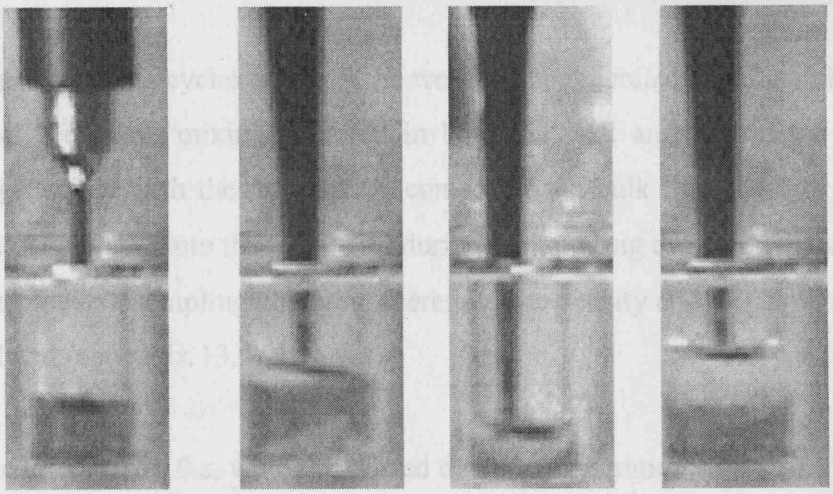

(a) (b) (c) (d)

Figure 4.2.1.2.3. Still images from a high-speed video camera of the fluid dynamics of the automated microscale LLE process (total volume = 300 μL) carried out at a dispensing speed of 400 $\mu L.s^{-1}$. Stages of LLE process: (a) dispensing of heavy phase with fixed tip, (b) dispensing and dispersion of light phase with disposable tip: (c) repeated aspirating and dispersing of liquid dispersion and (d) final phase separation. LLE method detailed in section 2.3.2.1 with a heavy phase (water dyed blue) and light phase (BA). Visualisation method detailed in section 2.3.5.

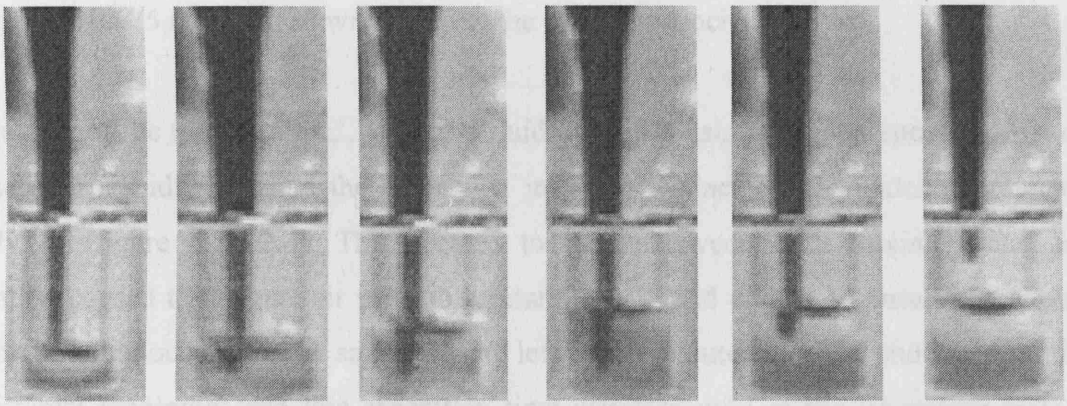

(a) (b) (c) (d) (e) (f)

Figure 4.2.1.2.4. Still images from a high-speed video camera of the fluid dynamics of phase separation stage of the microscale LLE process using a heavy phase (water dyed blue) and light phase (BA). Record of phase separation as a function of time for a dispensing speed of 400 $\mu L.s^{-1}$: (a) t = 0 s taken at beginning of dispensing the organic phase or at the first mixing cycle, (b) t = 0.7 s, (c) t = 1.1 s, (d) t = 1.6 s, (e) t = 2.3 s and (f) t = 2.5 s. Method for LLE described in section 2.3.2.1 and visualisation method detailed in section 2.3.5.

(0% tracking) pipette mixing cycles at 2% of the well height generated adequate phase mixing. It was believed that the phase mixing occurred in both the well and within the pipette tip as turbulence was generated with the jet stream[11] contacting the bulk liquid, tip or well surfaces. The 150 μL aliquot aspirated into the pipette tip during each mixing cycle consisted of both phases due to the pipette's sampling position. Therefore, the density and viscosity of the biphasic liquid was calculated (appendix 13.4.2).

The mixing cycle took *circa* 10 s, which consisted of a slow aspiration of a 150 μL aliquot at 75 $\mu L.s^{-1}$ and then its dispension at 400 $\mu L.s^{-1}$, including time for movement of the pipettes and delays to aspirate air within the programme. The dispensing speed was expected to create a jet from the pipette tip (d = 0.625 mm), dispensing the liquid aliquot into the remaining fluid in the reaction well and generating turbulence that promoted phase mixing and droplet breakage[11]. As the jet contacted the bulk liquid in the well it would break, increasing the interfacial area, which facilitated mass transfer. The jet was estimated at having a diameter of 0.63 mm, using the values for the system length, which are the height of the liquid in the well (0.266 mm) and velocity of the jet (23.6 $m.s^{-1}$) (appendix 13.4.3). Both the fixed and disposable tips have the same internal diameter (d_i = 0.625 mm) and so will generate the same jet velocity.

Visualisation of the microscale LLE process fluid dynamics using the high-speed video camera was shown to rapidly separate the dispersion into two distinct phases under gravity, within typically 1s (figure 4.2.1.2.4). This seemed to occur between each mixing cycle, as the workstation paused to aspirate air prior to aspirating the liquid aliquot to ensure that complete solute partitioning occurred. The samples were left for 10 minutes to settle under gravity due to their different rheologies and this separation time was also used at the laboratory scale. The microscale phase separation time was similar to that used to separate two soluble dyes with different distribution coefficients from each other and partition human and rabbit erythrocytes using an automated counter-current aqueous two-phase system (Sutherland et al, 1989). These samples were made up in the upper polyethylene glutamate-rich phase, which gave the solution a higher viscosity than the aqueous solutes used in this research. This settling time was considered

[11] Definition of fluid dynamics terms in appendix 13: section A13.4

to be adequate, if not a little excessive, for the microscale LLE process and the variety of reagents extracted. This settling time provided enough time for the phases to reach equilibrium and total phase separation before the phases were sampled. The focus of this research was proving the principle of microscale LLE, the process accuracy and reliability rather than its speed of operation, which could be accelerated once this process was established.

4.2.1.2.1 Reynolds Number of Automated Microscale LLE Process

The Reynolds number[11] (Re) of the microscale LLE process was calculated (appendix 13.4.1: equation A13.8) to further assess fluid dynamics. The Re was calculated for the flow of the liquid as it was dispensed from the pipette tip into the well, identified by analysis using the high-speed video camera (section 4.2.1.2). The Reynolds numbers for dispensing water at 400 $\mu L.s^{-1}$ were the same for fixed and disposable tips (Re = 815) as the tips have the same internal diameter (0.625 mm). As the aliquot was aspirated from 2% of the well height the Re should be calculated for a biphasic liquid (section A13.4.2) for each of the dispensing speeds, assuming that 92% of the removed aliquot contained the aqueous phase, based on the calculated well and pipette tip geometries. The biphasic nature of the transferred aliquot would alter the liquid's density (appendix 13: equation A13.9) and viscosity (appendix 13: equation A13.10). The rheology of the biphasic mixture of water and butyl acetate in the transferred aliquot was calculated to have a viscosity (0.00125 $kg.m^{-1}.s^{-1}$) and density (988.6 $kg.m^{3}$).

The workstation was capable of generating a range of dispensing speeds that effected the velocity of the fluid dispensed from the pipette tip (1 $\mu L.s^{-1}$ to 1866 $\mu L.s^{-1}$), which altered the Re (20 to 3803), calculated using the rheology of water. However, the dispensed liquid contained fractions from both phases as previously discussed. The transferred aliquot was aspirated from the same well height (2%), had the same volume ratio and rheology of the biphasic liquid (appendix 13.4.2). The biphasic rheology of the biphasic mixture in the transferred aliquot is the same as neither the volume ratios nor the physical properties of the transferred aliquot changes significantly as the phases separate within the time taken for the workstation to aspirate air between dispensing and aspirating the aliquot. The Reynolds numbers for each of the dispensing

speeds were calculated using the biphasic rheology and these were higher than those previously stated, generating a range from 23 to 4323 over the same range of dispensing speeds. The dispensing speed was investigated for its effect on the automated microscale LLE process (section 4.2.5).

4.2.1.3 Experimental Mass Balance Data

The mass balance experiments (section 2.3.2.2) assessed the extraction of aqueous PAA (4.0 $g.L^{-1}$ at pH 4.5) with BA at different LLE process scales using the automated microscale method (section 2.3.3.1), manual microscale LLE method (section 2.3.3.2) and the laboratory scale LLE method (section 2.3.4.1), which was used as a positive control. The PAA concentrations of both phases for each of the LLE scales were quantified using HPLC analysis (section 2.5.1) and the data was assessed to compare these LLE processes. The mass balance of the LLE process was determined experimentally for the automated microscale LLE process by quantifying the PAA concentration in both liquid phases and the organic phase PAA concentration was also calculated (table 4.2.1.3.1 (a) and (b)).

The experimental data for the automated microscale LLE process quantified the PAA concentration of the aqueous feed, post extraction aqueous phase and the evaporated organic phase re-dissolved in phosphate buffer. The PAA concentrations were used to investigate mass transfer within the LLE system (table 4.2.1.3.1 (a)). The organic phase was not compatible with the HPLC mobile phase (section 2.5.1) and any contamination of the aqueous phase with the organic phase would make the data unusable. Therefore, a 67% fraction of the aqueous phase was sampled, which was removed from 1 mm below the phase surface. The organic phase samples were not analysed directly on the HPLC, but were dried by evaporation of the solvents and PAA was re-dissolved in pH 7 phosphate buffer to allow minimum degradation of the compound during HPLC analysis. The organic phase concentration values were calculated from the aqueous phase concentration pre and post experimentation. The total PAA mass in the reaction well was calculated using the re-dissolved dried PAA from the organic phase, which was within 1% of the calculated organic phase data (0.6 g).

(a)

LLE Process Streams	IN	OUT		
		Aq	Org Dry	Org Calculated
PAA mass (g)	0.60	0.23	0.37	0.37
Concentration PAA ($g.L^{-1}$)	4.0	1.55	2.44	2.45
Total PAA Mass (g)	0.600	-	0.599	0.600
Distribution Constant ($K_D = C_{org}.C_{aq}^{-1}$)		-	1.6	1.6
PAA Recovery (% w/w)		-	61.0	61.1
Intra-run 2SE		0.05	0.39	-
Intra-run RCV		2.1	5.7	-

(b)

LLE Process Streams at Different Scales	IN	OUT					
		Automated Microscale		Manual Microscale		Laboratory Scale	
		Aq	Org	Aq	Org	Aq	Org
Concentration PAA ($g.L^{-1}$)	4.00	1.07	2.93	1.13	2.88	0.99	3.02
Distribution Constant ($K_D = C_{org}.C_{aq}^{-1}$)		2.7		2.6		3.1	
PAA Recovery into Organic Phase (% w/w)		73		72		75	
Inter-run 2 SE		0.1		0.4		14.4	
Inter-run % RCV		0.1		0.4		9.3	

Table 4.2.1.3.1. Mass balance analysis of extraction of aqueous PAA at pH 4.5 with butyl acetate: (a) automated microscale liquid-liquid extraction process and (b) the calculated mass balance for automated microscale, manual microscale and laboratory scale liquid-liquid extraction (Aq = aqueous phase, org = organic phase). Method detailed in sections 2.3.2.1, 2.3.2.2 and 2.3.4.1 and mean data displayed (n = 12).

The distribution constants for the automated microscale extraction were lower than for latter experiments (k_D^{PAA} = 1.6 compared to 2.6 to 3.1), which were believed to be due to slightly increased pH conditions (pH 4.55), variations in the pH conditions due to degradation products and concentration variation of the feed material. The degradation of the reagents may have been affected by the laboratory's temperature and this effect was investigated (section 4.2.1.4.1). The percentage recovery value for the automated microscale LLE (61%) was therefore lower than the values for the automated microscale LLE process data from the mass balance experiment (73% recovery), which compared favourably with the other process scales investigated (72% to 75% recovery from table 4.2.1.3.1. (b)), which were all carried out at pH 4.5. The statistical analysis of the data indicated that the aqueous phase data was more accurate (0.05 2SE) than the re-dissolved organic phase (0.39 2SE), and more precise (2.1% RCV) than the re-dissolved dried organic phase PAA data (5.7%RCV). This was expected due to the increased number of experimental stages required to prepare the re-dissolved dried organic phase PAA samples that may each incur a degree of error due to degradation during evaporation.

The different experimental process scales were analysed to assess their relative performance and validity (table 4.2.1.3.1. (b)). The concentration, distribution constant and percentage recovery values for the mass transfer of PAA from the aqueous phase to the organic phase generated similar results (72% to 75% recovery). The highest recovery was achieved using the laboratory LLE process (75%). The laboratory process was carried out for a longer mixing time (60 minutes) using a horizontal shaker and the microscale process reagents were mixed for 3 minutes. The laboratory process, therefore, had increased energy added to the system per mole of extractant as it was shaken for longer[12], which increased the mass transfer and fluid dynamics of the system, indicating the significance of the mixing conditions. This experimental data agreed with the laboratory process recovery being higher than the microscale process. The manual microscale LLE process percentage recovery was less than that for the automated microscale process, as the pipetting speed was slower and so less mixing and less mass transfer occurred. The experimental pH conditions varied slightly between the process scales from pH 4.35 to pH

[12] Energy per mole factor = Extraction time/ (PAA concentration x volume): microscale = 0.0004; laboratory scale = 0.08

4.4 for the laboratory scale process. The slight variation in the pH conditions of the aqueous phase had only a little impact on the equilibrium distribution constant measured and was investigated (section 4.2.3).

The statistical analysis of the inter-run data revealed that the reproducibility of the data varied with the specific LLE process scale in both accuracy (0.1% to 14.4% $2SE^{10}$) and precision (0.1% to 9.3% RCV^{10}). The best performance was seen in the automated microscale process data with 0.1% accuracy and precision, which was a result of the greater performance of the automated workstation (section 3.2.1). The performance decreased for the manual microscale process as there were more variations and random errors associated with this method. The laboratory scale LLE had the highest values of 2SE and RCV, which indicated the poorest accuracy and precision. This was surprising because the larger volumes were more expected to have reduced relative errors compared to the microscale process.

The automated microscale LLE process mean aqueous phase PAA concentration values (1.07 $g.L^{-1}$) were higher than those seen in the results of automated microscale method development experiments (section 4.2.1), despite both being carried out at pH 4.5. These data were different due to variations in the actual pH conditions. The aqueous phase concentration was 0.376 $g.L^{-1}$ for the LLE of PAA using 30 mixing cycles with BA at pH 2.5. The effect of the aqueous phase pH conditions on LLE was further investigated (section 4.2.3). The automated microscale LLE method development data used a higher sample number (n = 4, repeated x 5) than the mass balance data (n = 16) and were considered more statistically significant. The percentage recovery value (73%) was higher than those from the mass balance experimentation (61%), but lower than those from the automated microscale method development experiments (90.6%) that were generated at pH 2.5. The differences in the percentage recovery values with those from the mass balance data were probably due to slight deviations in the aqueous phase pH conditions or PAA concentration, which affected the partitioning. The yields achieved were higher than those with ethyl acetate, generating 40% to 50% purity, which is not the same as yield as it is dependent on the selectivity of the process (Ghosh et al, 1997).

4.2.1.4 LLE of PA Bioconversion Product Stream

The LLE of the simulated product stream with butyl acetate was carried out at the microscale and laboratory process scales in order to analyse the purification of 6-APA from a complex solution (section 2.3.2.3). The LLE was a one stage equilibrium process. The HPLC traces of the aqueous phase pre and post extraction at the microscale and laboratory scales showed the purification of 6-APA from the contaminants (figure 4.2.1.4.1). The HPLC traces for the laboratory and microscale extraction showed similar results with 95.7% and 91.3% removal of Pen G at microscale and laboratory scale, plus significant reduction in the PAA of 85.9% and 88.9% and its removal at the relevant process scales. The microscale LLE samples appeared to have a reduced 6-APA concentration, but this may have been due to the non-homogeneity of the feed material or the degradation of the reagents (section 4.2.1.4.1) during the delay before analysis. Further experimentation showed that these two process scales were consistent in their performance (section 4.2.7).

4.2.1.4.1 Compound Degradation

All chemical compounds degrade when stressed by extremes of temperature, pressure or pH conditions, especially if their chemical structure makes them sensitive, as is the case with Pen G. The spontaneous degradation of Pen G produced 6-APA and PAA, which is accelerated by their conditions. This degradation was observed in Pen G samples analysed on the HPLC over time. The degree of degradation was investigated for the effect of time, temperature and the pH conditions of the samples (section 2.3.2.4).

The effect of temperature on the degree of spontaneous degradation was shown for samples stored on ice (5 °C) and samples stored at the laboratory's temperature (20 °C) to illustrate the temperature sensitivity of Pen G (figure 4.2.1.4.1.1 (a)). This graph illustrated that the rate of degradation increased at higher temperatures, although total degree of degradation was similar for both temperatures. The data from the samples stored at 5 °C fitted a polynomial regression curve of $Y = 3960 + 7.2X - 0.007X^2$ with a R^2 value of 0.98. The data from samples stored at laboratory temperatures fitted an sigmoidal curve of $Y = 3941\ e^{(-x/35.8)}$ with a R^2 value of 0.983.

a)

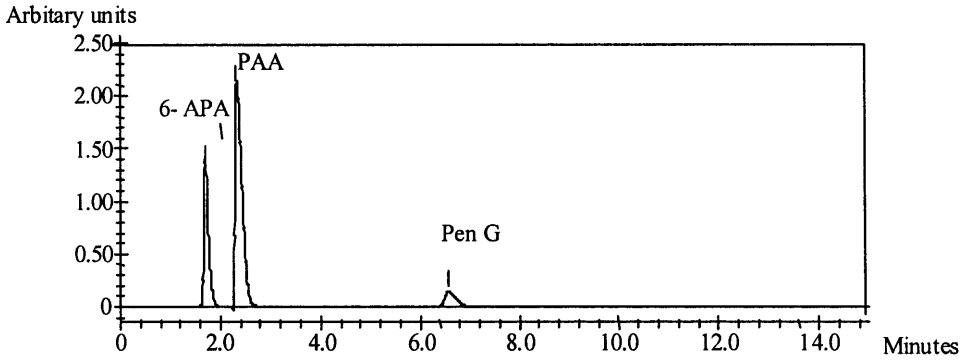

(b)

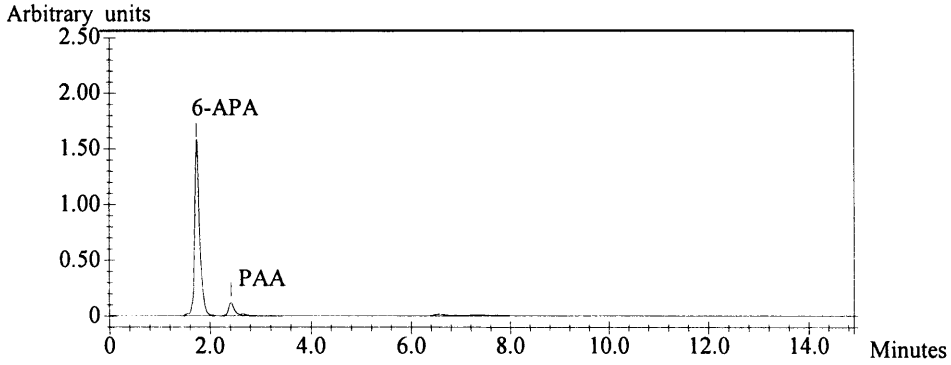

(c)

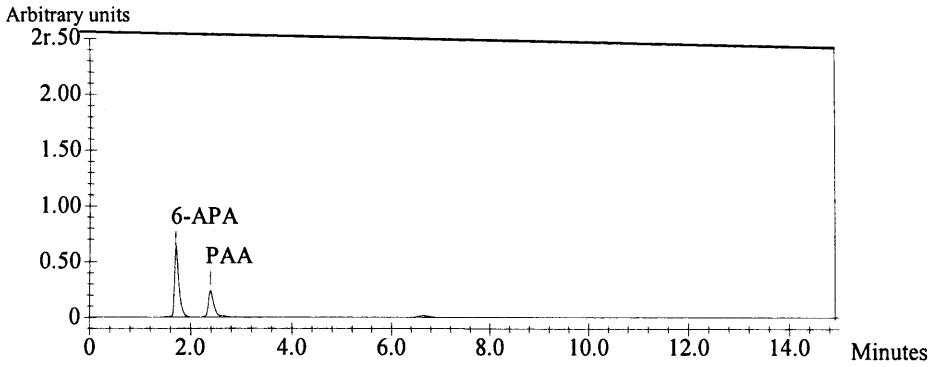

Figure 4.2.1.4.1. HPLC traces of the aqueous phase containing the simulated penicillin acylase bioconversion product stream (10 mM Pen G, 190 mM PAA, 190 mM 6-APA): (a) prior to extraction with butyl acetate; (b) after laboratory scale liquid-liquid extraction and (c) after automated microscale liquid-liquid extraction (retention times: Pen G = 7 minutes, PAA = 2.5 minutes and 6-APA = 1.8 minutes at pH 7).

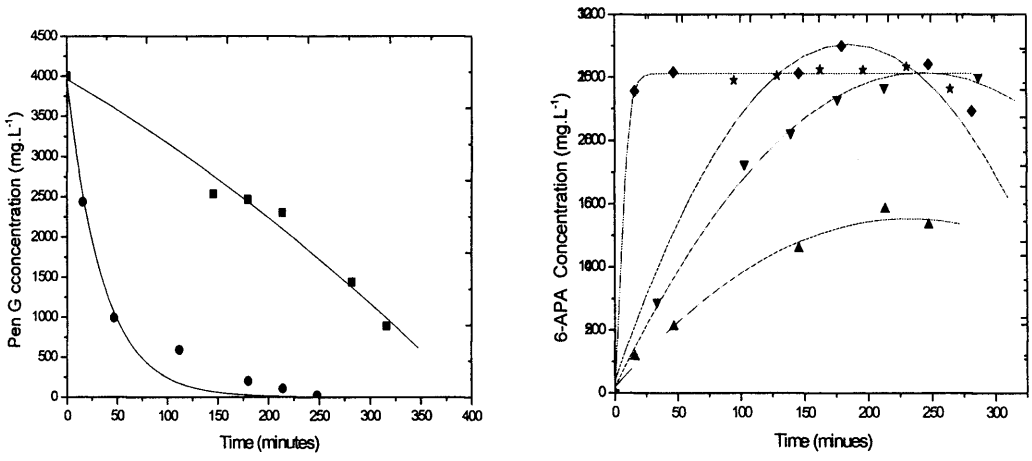

(a) (b)

Figure 4.2.1.4.1.1. Degradation of Penicillin G (4.0 $g.L^{-1}$) in phosphate buffer at pH 2.8 over time analysing: (a) the feed material and (b) the spontaneous degradation products with samples stored at different temperatures (on ice and at room temperature). Samples: (■) Pen G at 5 °C, (●) Pen G at 20 °C, (▲) 6-APA at 5 °C , (▼) 6-APA at 20 °C, (◆) PAA at °C and (★) PAA at 20 °C. Method detailed in section 2.3.2.4.

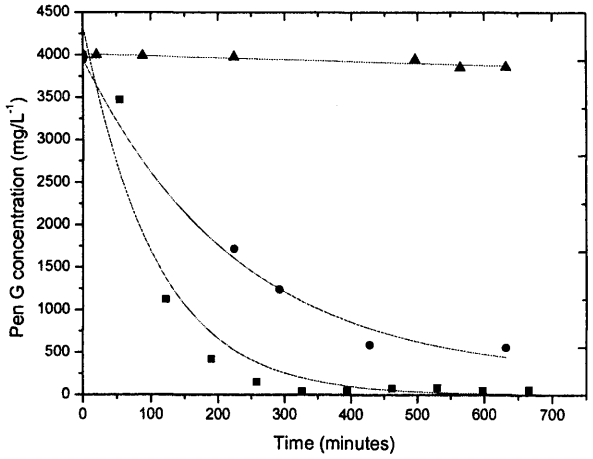

Figure 4.2.1.4.1.2. Degradation of Penicillin G (4.0 $g.L^{-1}$) in phosphate buffer at different pH conditions (■ pH 2.5, (● pH 4.15 and (▲) pH 7) over time with the samples stored at room temperature of 20°. Method detailed in section 2.3.2.4 and concentration of Pen G monitored using HPLC analysis (section 2.5.1).

The spontaneous decomposition of Pen G over time was completed within 5 hours at pH 2.8, which produced 6-APA and PAA.

The formation of the degradation products of Pen G at pH 2.8 was monitored over time (5 hours) with samples stored at different temperatures. The samples were kept on ice (5 °C) or in the laboratory (20 °C). The samples' concentration values (figure 4.2.1.4.1.1 (b)) illustrated the formation of the degradation products of Pen G, 6-APA and PAA, over time at each of these temperatures. The production of 6-APA and PAA occurred at the same molar rate, but their concentration profiles were different due to their different molecular masses. Therefore, the concentration of 6-APA (216 relative molecular mass (rmm) increased over time slower than PAA (156 rmm) at each of the temperatures. The data for 6-APA samples stored on ice fitted the polynomial regression curve of $Y = 18.6 + 4.6\ X - 0.01\ X^2$ with a R^2 value of 0.990. The data for 6-APA samples stored at laboratory temperatures fitted the polynomial regression curve of $Y = 43.7 + 18.4\ X - 0.04\ X^2$ with a R^2 value of 0.996, which indicated that the 6-APA was formed faster at higher temperatures.

The spontaneous formation of PAA is rapid, within 30 minutes, but further degeneration of PAA resulted in a reduction of PAA concentration. The extreme pH conditions used within LLE (pH <3.5) caused Pen G to spontaneously hydrolyse, which produced a range of side products (Ghosh et al, 1997): penillic acid is formed in acidic conditions and penicilloic acid in alkaline conditions before its degradation to penilloic acid (Vandamme and Voets, 1974). The data for PAA samples stored on ice (figure 4.2.1.4.1.1(b) fitted the sigmoidal curve $\left(Y = \frac{o - 16.7 + 1.2}{1 + e^{(-0.001X/0.0005)}} + 1.2\right)$ between –837 and 2530 X and between -1.056 and 9.4 with a R^2 value of 0.975. The data for PAA samples stored at laboratory temperatures fitted the polynomial regression curve of $Y = 94.2 + 26.3\ X - 0.07\ X^2$ with a R^2 value of 0.969, which indicated that the data fitted the trend line with some variation and was subject to a degree of error.

The formation of the side product PAA is enhanced by extreme temperature and pH conditions in the presence of organic solvents. The carboxylic acid group of PAA forms dimers with neighboring molecules and monomers in non-polar solvents, such as hexane (Maryott et al,

1949). The degradation of 6-APA can occur spontaneously forming penicic acid, which is coupled to the dimer forming poly 6-APA (Shengshui and Zaofan, 1991). The stability of 6-APA in acidic conditions is greater than that of Pen G. However this effect is reversed in the presence of CO_2, which is present in the bioconversion of Pen G. The conditions of the aqueous phases containing 6-APA or PAA (pH 2.5) were prepared to mimic the industrial conditions.

The effect of pH conditions of the aqueous samples (pH 2.5. pH 4.15 and pH 7) on the degradation of Pen G at room temperature was assessed over time (figure 4.2.1.4.1.2). This illustrated that the rate and degree of degradation was affected by the pH conditions with greater effects at extreme acidic conditions. The pH 7 data showed the least degradation and fitted the exponential decay curve of $Y = -7671 + 80781\ e^{(-x/36183)}$ with a R^2 value of 0.85 indicating a 3.6% degradation of the solute. The pH 4.15 data fitted the exponential decay curve of $Y = 1351\ e^{(-x/106.2)}$ with a R^2 value of 0.98 indicating a 37.5% degradation of the solute. The pH 2.5 data demonstrated the rapid degradation of Pen G, fitting to the exponential decay curve of $Y = 2347 + 1660\ e^{(-x/226)}$ with a R^2 value of 0.992, reducing the concentration by 98.5%.

The kinetics of Pen G degradation were measured over *circa* 10 hours, which equated with the time required for the analysis of 40 samples from the automated microscale LLE experimentation. These results indicated that the Pen G samples would be minimally degraded at pH 7 with the samples maintained at room temperature as they maintained a fairly constant concentration, losing 3.6% over 10 hours. Therefore, the Pen G and simulated product stream samples were stored on ice and diluted with phosphate buffer pH 7 to neutralise the post LLE samples prior to HPLC analysis.

4.2.1.5 Effect of Evaporation on Automated Microscale LLE

The evaporation of the phases from the microscale extraction well was investigated under laboratory conditions using gravimetric measurements (section 2.3.2.5). The evaporation of the individual phases was investigated, together with the combined phases used in the LLE of 6-APA. The combined phases were added in different orders, adding either the aqueous phase or the organic phase first to investigate their interaction affect on evaporation. The reaction conditions were also repeated in 4 replicate wells on different days to produce statistically

significant results. The evaporation data was plotted on a scatter graph and a linear regression line added (figure 4.2.1.5.1).

The evaporation rates of the compounds at 20 °C, calculated from the gravimetric data, were 0.103 $\mu g.h^{-1}$ for aqueous 6-APA, 0.127 $\mu g.h^{-1}$ for butyl acetate (BA), 0.234 $\mu g.h^{-1}$ for BA plus aqueous 6-APA and 0.225 $\mu g.h^{-1}$ for aqueous PAA plus BA. The molar evaporation rates would indicate that the rate of BA evaporation was higher than that for the aqueous 6-APA solution due to its relative molecular mass and increased volatility. The evaporation rates from the combined phases were both slightly greater than the sum of the evaporation rates for the individual reagents, regardless of the reagents' order of addition. However, the lower combined reagent evaporation rate was found with the aqueous phase being added first and this order of phase addition was used in the LLE experimentation.

To limit the evaporation losses during the automated microscale LLE process a PTFE lid was used to cover the 96-well plate after mixing, although this could risk cross-contamination if not washed thoroughly. The samples were positioned in the centre of the plate (rows C-F, columns 2 to 10) to limit the losses due to evaporation.

4.2.2 Kinetics of the Automated Microscale LLE Process

The kinetics of the automated microscale LLE process were studied using the individual compounds contained within the bioconversion product stream (Pen G, 6-APA and PAA, 4.0 $g.L^{-1}$) with butyl acetate at pH 2.5. pH 4.5 and pH 4.5, respectively (section 2.3.3.3). The aqueous samples contained PAA at pH 2.5, 6-APA at pH 2.5 and Pen G at pH 4.5.

The microscale LLE of Pen G and PAA was initially carried out using a range of mixing cycles (n_c = 0 to 30) transferring aliquots from the extraction well to create phase mixing (section 4.2.1.1). The aqueous phase compound concentrations were plotted against the corresponding time (0 to 154 s) and the number of mixing cycles (0 to 30) (figure 4.2.2.1 (a)). The dispensing time is linearly related to the mixing cycles (Dispensing time = ((Mixing cycles + 1) x 5) + 4).

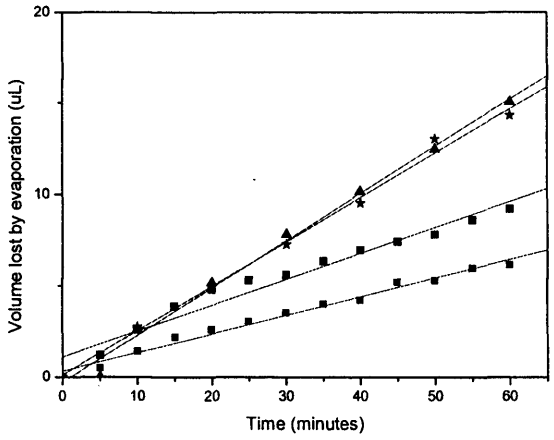

Figure 4.2.1.5.1. Evaporation from a 96-well model of a range of reagents carried out at 20 °C and atmospheric pressure. Samples: (■) aqueous 6-APA, (●) butyl acetate, (★) aqueous 6-APA plus BA and (▲) BA plus aqueous 6-APA from a multiwell plate (150 µL per phase). Method described in section 2.3.2.5 and mean gravimetric measurements displayed with 2SE error bars (n = 3). Solid line represents a linear regression fitted to the volume evaporation data.

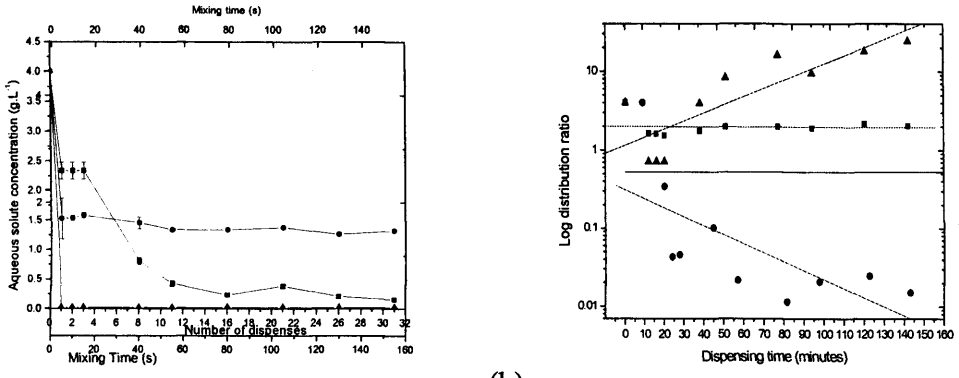

(a) (b)

Figure 4.2.2.1. Kinetics of automated microscale liquid-liquid extraction of (■) 4.0 $g.L^{-1}$ PAA at pH 2.5, (●) Pen G at pH 4.5 and (▲) 6-APA at pH 2.5 with butyl acetate (K_D^{PAA} = 24, $K_D^{Pen\ G}$ = 2, $K_D^{6\text{-}APA}$ = 399). Data presented as (a) concentration against dispensing time and (b) log distribution ratio against log dispensing time. Mean concentration values ($n \geq 12$) plotted with 2SE error bars. Method detailed in section 2.3.3.3.

The distribution ratio values at each of these time points against the corresponding dispensing time were plotted on a log graph (figure 4.2.2.1 (b)) that showed how the LLE process reached equilibrium. The PAA data fitted a linear trend line Y =0.123 X + 0.058 with a R^2 value of 0.915, Pen G data fitting Y = 0.9052 X + 0.073 with R^2 of 0.776, and 6-APA data fitting Y = 1.576 - 1.965 with R^2 of 0.970. This indicated that mass transfer equilibrium was reached after 30 mixing cycles or 142 seconds for PAA and only 2 N_c or 20 seconds for Pen G with the aliquots dispensed 31 and 3 times, respectively (figure 4.2.2.1). The kinetics of the different compounds were expected to be different due to their specific chemistries, which affected their molecular charge and phase distribution in the aqueous phase pH conditions (Ghosh et al, 1997).

The distribution constants, calculated from the data, were K_{PAA} = 24 and $K_{Pen\ G}$ = 2. The distribution constant produced in previous experimentation for PAA was K_{PAA} = 9.6 (table 4.2.1.1.1) at pH 2.5. The phase mixing experiments were carried out in late autumn when the laboratory temperature was reduced as it was ventilated with external air, which reduced the distribution constant. The mass balance experimentation produced distribution constants of microscale K_{PAA} = 1.6 and laboratory K_{PAA} = 2.6 at pH 4.5 (table 4.2.1.3.1), which were expected to be lower due to the increased pH conditions. The purification efficiency achieved by automated microscale LLE was 96% for PAA calculated from data in figure 4.2.2.1. The reduced efficiency for the microscale LLE of PAA may be due to the effect of the pH conditions or temperature during the experimentation, which would influence the mass transfer. The workstation was originally housed in a temperature-controlled laboratory, but was later moved to the solvent suite in order to fit an extraction hood to meet health and safety guidelines.

The Pen G distribution constant was considerably lower than 48 for its extraction at pH 4.0 at 0°C reported by Reschke and Schugere (1984). The reduced temperature limited the degradation (section 4.2.1.4.1) and the lower pH conditions enhanced the extraction efficiency (98%). Similar purification efficiency was achieved by LLE (87%) for Pen G at pH 2.5, which was quantified from data in figure 4.2.2.1.

The distribution constants for LLE of the bioconversion product stream data at pH 7 (K_{PAA} = 6, $K_{Pen\ G}$ = 8) calculated from figure 4.2.1.4.1 showed that the higher pH conditions limited the

extraction of PAA. The extraction of Pen G was enhanced by these conditions as less degradation occurred. Therefore, the effects of pH conditions were subsequently investigated (section 4.2.3).

The kinetics of microscale LLE of 6-APA were also investigated, but the concentration values were low due to its minimal mass transfer at pH 2.5. This was due to the compound existing as zwitterions because of its chemical structure that contains both carboxylic and amino acid groups. The literature ionisation points (pI) for 6-APA were pH 2.5 and pH 4.91 when the molecule is neutrally charged, favouring its solubility in the organic phase. At all other pH values the 6-APA molecules have an overall charge favouring its partitioning into the aqueous phase (Rapson and Bird, 1963). The reactive extraction of 6-APA was carried out at conditions above pH 6 and the distribution constants ranged between pH 8 and pH 23 over pH 6.2 to pH 8 (Bora et al, 2000).

This research demonstrated that the mixing conditions of the microscale LLE must be investigated for each compound to ensure that the mass transfer equilibrium is reached. This was achieved for the extraction of the penicillin acylase bioconversion product stream within 30 mixing cycles. A high number of mixing cycles were used to facilitate the development of a generic automated microscale LLE method.

4.2.3 Effect of Extraction pH Conditions

The automated microscale LLE process (section 2.3.3.4) investigated the effect of the aqueous phase pH conditions over the range pH 2 to pH 8 on the equilibrium distribution ratio for the extraction of PAA and Pen G with butyl acetate (figure 4.2.3.1). The extraction of each of the compounds within the bioconversion product stream confirmed the pK value for each compound. The distribution ratios were a function of pH, the slope increasing sharply after reaching pH 4.9 for PAA, which matched the literature pK value (Lee and Su, 1998). The same trend was seen for Pen G, whose pK value was at pH 4.5, which was also recorded by Lye (1993). All the data showed good statistical analysis, which was reflected in the small error bars, except for an initial PAA data point that had a large error, possibly due to variation in the feed material or instrument

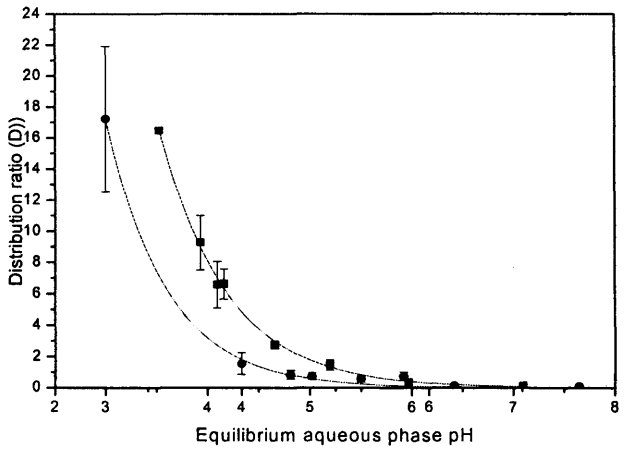

Figure 4.2.3.1. Effect of aqueous phase pH conditions on the equilibrium distribution ratio of (■) PAA and (●) Pen G with butyl acetate over the pH range (pH 3 to pH 8). Extractions carried out using 4.0 $g.L^{-1}$ PAA or Pen G at 20 °C at a phase volume ratio of 1 (total volume = 300 µL) and average data (n = 12) plotted with 2SE error bars. Method detailed in section 2.3.3.4.

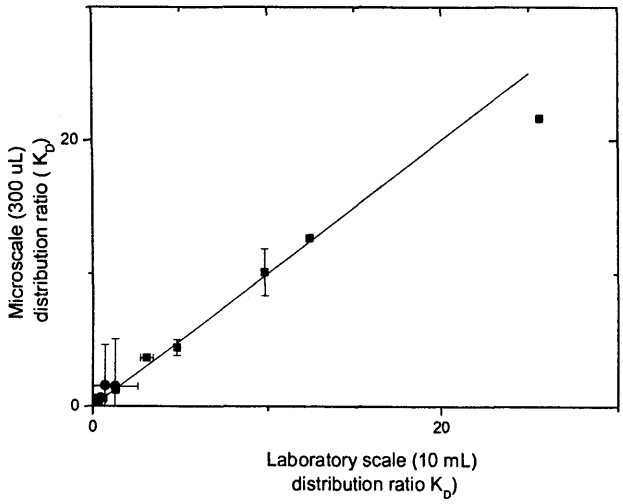

Figure 4.2.3.1.1. Parity plot of the equilibrium distribution ratios of PAA (■) and Pen G (●) as a function of pH (pH range pH 2 to pH 8) from liquid-liquid extraction with butyl acetate at microscale (300 µL) and laboratory scale (10 mL) using 4.0 $g.L^{-1}$ PAA or Pen G at 20 °C and a phase volume ratio of 1. Method detailed in section 2.3.3.1 and 2.3.4. Solid line shows line of parity and the mean data (n = 12) plotted 2SE error bars.

performance.

The correlation of the aqueous phase pH with the equilibrium distribution ratios was expected (Bora et al, 2000) as the pH conditions effect the molecular charge of the compounds, which affected their mass transfer and distribution ratios. The pH conditions of the LLE process are selected to minimise damage to the product being purified, whilst removing virtually all the contaminants in a single stage or contact step. If this were not possible, a multistage method or counter current extraction method (Sutherland et al, 1989) would be required to carry out the process.

The automated microscale LLE of PAA and Pen G were used to rapidly produce accurate and reproducible screening of the aqueous phase pH conditions in order to optimise the LLE process. This method would be ideally suited to the initial screening of the LLE process for the purification of a new pharmaceutical, prior to other process optimisation experimentation. The pH conditions for other automated microscale LLE experimentation with the compounds were selected to enhance the mass transfer and replicate the conditions used in the industrial and laboratory LLE processes. The data showed good accuracy and precision for LLE of PAA and Pen G experimentation.

4.2.3.1 Comparison with Laboratory Scale LLE

The comparison of the automated microscale LLE process with the laboratory scale LLE process was carried out for the extraction of PAA and Pen G over a range of aqueous phase pH conditions (pH 2 to pH 8). The parity plot of the distribution ratios at the different scales showed good linear correlation (figure 4.2.3.1.1), which was reflected in the regression coefficient' (R^2) values calculated for the data sets. These data for both compounds fitted close to the Y = X line with slightly higher values for the microscale data for PAA and Pen G. The linear analysis of the PAA data fitted the line with 0.996 R^2 value and the Pen G data fitted the line with a 0.100 R^2 value. The mixing times of the laboratory LLE process (60 minutes) were in excess of the microscale process (3 minutes), but the use of different mixing methods generated different energy inputs into each system.

The laboratory data distribution ratios were higher than those obtained from the microscale data. However, the laboratory data showed a similar pH trend to the microscale process, with the distribution ratios decreasing from pH 2.8 to pH 4.5. This corresponds with the literature value for the ionisation ratio of 2.73 (Rapson and Bird, 1963). The use of the microscale data for predicting the larger scale process may overestimate the efficiency of the process by around 10%. This is an acceptable degree of error for process design and could be factored into any calculation.

There was greater deviation from the linear line at the higher distribution ratio extremes created at the lower extreme of the aqueous phase pH conditions. The statistical analysis of the data indicated that the laboratory data had 0.016% to 1.8% CV, which was less precise than the automated microscale data with 0.01% to 0.5% CV. This could be due to manual pipetting errors involved in sampling the laboratory aqueous phase. The increased sample numbers of the automated microscale process ensured that the mean value was close to the true mean. The error bars for the microscale LLE were larger than those for the laboratory LLE, which was expected due to the larger number of repeated samples at this scale. These errors could be accounted for by inaccuracies in liquid handling, evaporational losses, poor sampling, sample degradation or inaccuracies in the HPLC analysis.

4.2.3.2 Comparison with Manual Microscale LLE

The automated microscale LLE process was compared to the manual microscale LLE process to assess the benefits of the equipment. The effects of the aqueous phase pH conditions on the distribution ratio for PAA extracted into butyl acetate were carried out using the automated and manual microscale LLE process. The methods were compared using the data plotted on a parity plot (figure 4.2.3.2.1).

The different methods of microscale LLE mixing (manual and automated) produced similar distribution ratios over the pH range (pH 2 to pH 7). However, the data fitted slightly above the parity plot of Y = X (figure 4.2.3.2.1). The automated microscale data was previously demonstrated to compare favourably with the laboratory data (section 4.2.3.1).

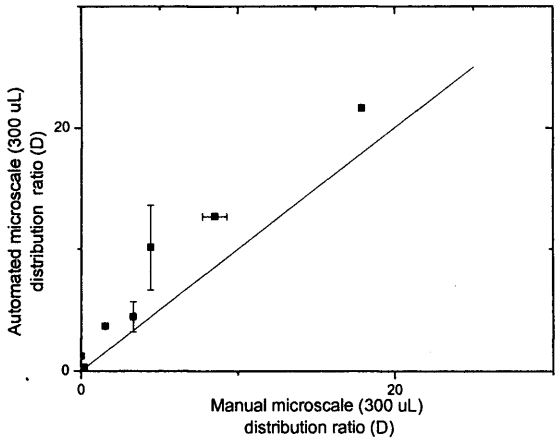

Figure 4.2.3.2.1. Parity plot of the distribution ratios for LLE of (■) PAA as a function of pH (pH 2 to pH 7) carried out using the automated and manual microscale liquid-liquid extraction processes (total volume 300 µL) extraction into butyl acetate were carried out using 4.0 $g.L^{-1}$ PAA at 20 °C and a phase volume ratio of 1. Method detailed in section 2.3.1 and 2.3.3.2. Solid line represents the line of parity and the mean data (n=12) was plotted with 2SE error bars.

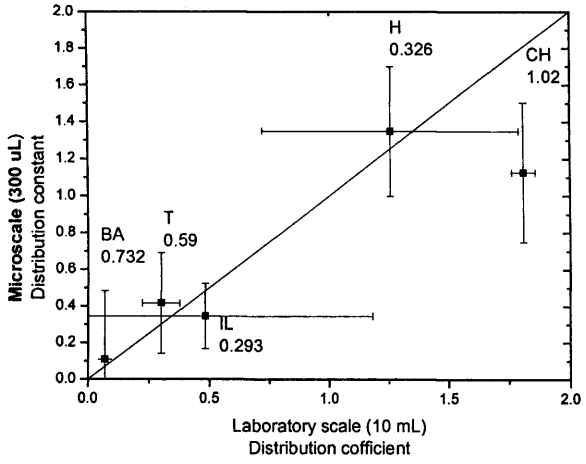

Figure 4.2.4.1.1. Parity plot of equilibrium distribution ratios for PAA (4.0 $g.L^{-1}$, pH 2.5) extraction from the bioconversion product stream (10 mM Pen G, 190 mM PAA and 190 mM 6-APA) with a range of solvents using automated microscale (300 µL) and laboratory scale (10 mL) liquid-liquid extraction methods. (BA = butyl acetate, CH = cyclohexane, H = hexane, T = toluene, IL = ionic liquid), displayed with viscosity data (cp). Method detailed in section 2.3.3.1 and 2.3.4. Solid line represents the line of parity for the mean data (n = 12) plotted with 2SE error bars.

The disparity with the manual microscale LLE data was, therefore, due to it's lower mass transfer generated by the slower dispensing speed and fluid velocity of the manual equipment (section 4.2.1.2). The PAA distribution ratios for the automated process fitted more closely to the parity line than the microscale data. The disparity with the manual data was, therefore, due to the lower mass transfer generated by the manual mixing method. However, extraction at the lower pH conditions showed less disparity between the mixing methods as there was greater movement of PAA between the phases. The distribution ratio was highest at pH 3.12 using either mixing methods and supported the data from figure 4.2.3.1.

The distribution ratios were affected by small changes in pH conditions during the experimentation (section 4.2.3). The variation was quantified by statistical analysis, which showed that the manual data was more accurate than the automated data, as illustrated by the error bars, but the automated data (0.01% to 0.5% CV) was more precise than the manual process (0.6% to 1.1% CV). The errors may have been caused by impurities in the extraction wells, inaccuracies in the preparation of pH conditions or concentration or the reagent due to random errors in the calibration of pH equipment. These statistics for the automated process were similar to those for experiments previously carried out on the Multiprobe (4% RSD, Jemal et al, 1999). This strengthened the robustness of the microscale process, although it is essential that increased repetition of the samples is required to provide good statistical analysis.

4.2.4 LLE Solvent Screening

A number of organic phases were screened for the LLE of PAA to select the best solvent for the purification of PAA, a contaminant of the PA bioconversion product stream. The microscale solvent screening method (section 2.3.3.5) was developed from the automated microscale method (section 2.3.3.1) and the microscale solvent kinetics method (section 2.3.3.5.1) was adapted from the automated microscale kinetics method (section 2.3.3.3). The method was modified by the development of specific performance files (section 2.2.1.4.1) for each of the solvents used in the automated microscale LLE experimentation in order to ensure its accurate and precise performance (section 3.2.1). The performance of the workstation in dispensing

individual liquids was monitored using gravimetric measurements of the dispensed aliquots, which demonstrated an accuracy of $\geq$ 99.7% and a precision of $\geq$ 0.4% CV for butyl acetate (table 3.4.1).

4.2.4.1 Automated LLE Solvent Screening

The automated microscale LLE process (section 2.3.3.5) investigated the effect of different organic phases on the extraction efficiency for the purification of PAA. This, together with the other experimentation, aimed to rapidly optimise the LLE process conditions, which could facilitate the development of purification processes for new pharmaceuticals.

A range of organic phases with different rheologies was screened for the extraction of PAA from the simulated bioconversion product stream (section 2.1.1). The organic solvents had different chemical and physical characteristics (table 4.2.4.1.1) and these were chosen to investigate their purification of PAA, as well as investigate the versatility of the workstation. The organic solvents, therefore, have different dipole moments that affect their polarity and the distribution constant of the extracted compound. PAA was extracted from the aqueous phase (pH 4.0) with butyl acetate, cyclohexane, hexane, toluene and ionic liquid (1-butyl 3-methyl imidazolium 1-butyl-3-methylimidazolium chloride). Hexane has a lower viscosity and surface tension than water and cyclohexane making it more difficult to pipette. The ionic liquid has greater density than water, which affected the biphasic system within the pipette tip, causing it to be dominated by the aqueous phase, and the dispensing delay increased the mass transfer, as well as the droplet lifetime[11] once the aliquot was dispensed into the bulk liquid. The performance of the automated workstation was optimised for each solvent by the careful selection of suitable performance files with specific aspirating and dispensing speeds, delays and air gaps, in order to generate reproducible data.

The automated microscale LLE experimentation was compared to the laboratory scale to validate the results. The equilibrium distribution constant data from the process scales for each of the

[11] Definition of fluid dynamics terms in appendix 13: section A13.4

solvents were plotted on a parity plot (figure 4.2.4.1.1). The data lay either side of the parity line (Y = X) and the data points fitted closely with the linear plot, indicating that there was correlation between the experimental scales. However some solvent data showed variation, especially the cyclohexane data. The cyclohexane data deviated from the parity line and had large error bars for the automated data, which suggested that the discrepancy was related to errors associated with the workstation (section 4.2.8). Extraction with butyl acetate and toluene showed the best correlation between the process scales, as these data points were closest to the parity line. The cyclohexane data were the furthest from the parity line and this indicated that there were differences between pipetting this solvent at both scales, which was due to its rheology (table 4.2.4.1.1).

The highest distribution constants were produced using hexane and cyclohexane, suggesting that they were better at extracting the contaminant, PAA, from the product stream than the other solvents. However, as there were higher errors associated with the cyclohexane data, the preferred solvent was hexane. The extraction with the ionic liquid produced a lower D value that was similar to toluene, which was expected (Cull, 2000). The extraction with butyl acetate produced a lower distribution constant (K_D^{PAA} = 0.1) than those generated from previous experiments (K_D^{PAA} = 24, section 4.2.2) and literature values (K_D^{PAA} = 48) due to variation in the aqueous pH, inefficient phase mixing, degradation and other random errors. The data was also contrary to the pH trend (section 4.2.3). The low equilibrium BA distribution constant generated in the solvent screening experimentation suggested that the BA data incurred operational systematic errors, which questioned the validity of this data.

These errors may have been incurred by inaccurate preparation of the feed material, low dispensed aliquot volumes, inaccurate analysis of the pH conditions or inaccurate HPLC analysis of the feed stream and post extraction aqueous phase samples. The errors associated with the data were illustrated in the error bars, which were large for both process scales compared to previous experimentation.

The development of solvent specific performance files did not eradicate the occurrence of errors in the LLE process due to pipetting difficulties related to the properties of the solvents. The

largest error for the automated data was associated with the cyclohexane value. Difficulties pipetting cyclohexane were due to its relatively high viscosity and lower surface tension compared to water, which increased the likelihood of dripping. The hexane and ionic liquid data lay close to the parity line, indicating their accuracy, but the large error bars indicated poor precision. The size of the error bars was due to many of the distribution constants being below 1.0, which amplified their size. The relative standard error values were much smaller and did not give cause for concern. The numbers of samples were larger for the automated data than the laboratory data (sample size = 16 TO 24 compared to 8 TO 24), which generated larger error bars. The automated hexane and ionic liquid data also had large error bars.

The automated data showed greater precision than the laboratory data, reflected in the relative sizes of the error bars for the ionic liquid and hexane data. However, this trend was not seen using the other solvents. The performance of the manual laboratory pipetting of ionic liquid was particularly inaccurate because of its relatively high density, requiring a long delay after pipetting to ensure that an accurate volume was transferred. This problem was limited for the automated process by altering the performance file's aspirating and dispensing delay times. The manual pipetting of hexane also had large errors associated with the laboratory data, which was due to the low density and low surface tension that encouraged dripping from the pipette tips. The other laboratory data points had smaller errors associated with the experimentation, as the outlying points were removed and the smaller sample sizes were used (n = 8 TO 24). The slow pipetting speed of the manual liquid handling made these results more random than the automated process.

The unexpected extraction results of the solvent screening experimentation generated low distribution constants and large error bars, instigating an investigation into the extraction kinetics of the individual solvents (section 4.2.4.2). The solvent specific performance files were used in workstation programmes for experimentation to investigate the kinetics of the automated microscale LLE process for a range of solvents.

4.2.4.2 Kinetics of LLE with a Range of Solvents

The kinetics of the automated microscale LLE of PAA were assessed using cyclohexane, ionic liquid and butyl acetate (figure 4.2.4.1.1). The method (section 2.3.3.5.1) was adapted from that used in section 4.2.2 by the selection of appropriate performance files for each solvent. Investigation into the LLE kinetics of PAA with BA showed that equilibrium was reached using 30 mixing cycles of the automated phase mixing (section 4.2.1.1) in the microscale LLE method and these other solvents were investigated over this range of mixing cycles.

The kinetic data for these solvents were plotted with the log distribution ratios against the log dispensing time (figure 4.2.4.2.1). The CH data fitted a linear trend line Y = 0.008 X - 0.579 with a R^2 value of 0.508, IL data fitted a Y = 0.008 X - 0.685 with aR^2 value of 0.398, and BA data fitted a linear trend line Y= 0.014 X - 0.134 with a R^2 value of 0.648. The regression analysis of these data are low due to the initial variation of the data from the trend, however this was the best fit of the curves to the data. The data for cyclohexane and ionic liquid was approaching equilibrium but had not seemed to reach complete equilibrium after 30 mixing cycles. The distribution ratios were still increasing and it was postulated that equilibrium would have been reached within 40 mixing cycles. This investigation could have been extended to widen the range of mixing cycles, but this experimentation was not carried out due to time restrictions.

The butyl acetate distribution ratio (K_D^{PAA} = 60) was higher than that previously achieved in the initial screening of the extraction kinetics of PAA at pH 2.5 (section 4.2.2) that generated a distribution ratio of 24, suggesting that the actual pH conditions were lower than pH 2.5, which could be caused by the degradation of the compound during experimentation, releasing more hydrogen ions (section 4.2.1.4.1). The previous analysis of the range of pH conditions for the extraction of PAA (section 4.2.3) did not cover this pH extreme, generating a k_D^{PAA} value of 18 at pH 3, and so this postulation was not confirmed. To confirm these findings an investigation of a wider pH range could have been required, but this was not carried out due to difficulties of degradation caused by the lower pH conditions and time restrictions.

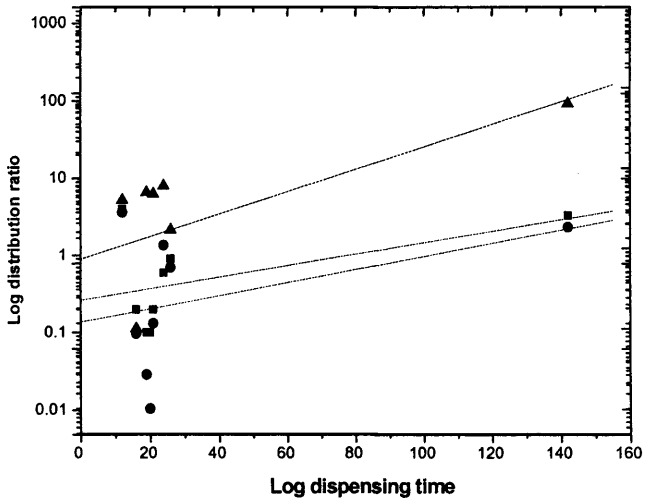

Figure 4.2.4.2.1. Log graph of kinetics of automated microscale liquid-liquid extraction of PAA (4.0 $g.L^{-1}$, pH 2.5) by a range of solvents over a range of dispensing times (0 to 142) carried out using the automated microscale liquid-liquid extraction method with (■) cyclohexane, (●) ionic liquid and (▲) butyl acetate. Method detailed in section 2.3.3.5.1 and mean data (n = 12) plotted with 2SE error bars.

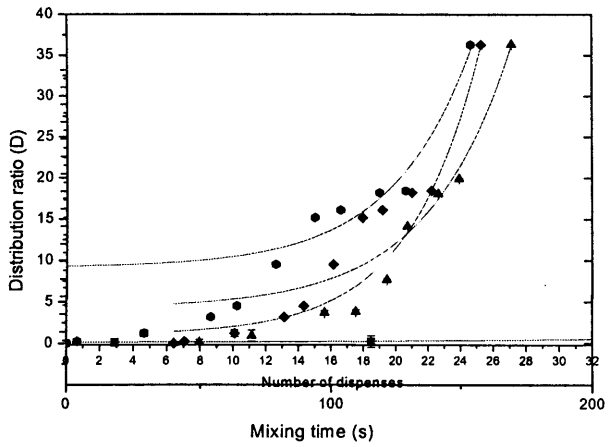

Figure 4.2.5.1. Effect of aspirating and dispensing speed on the automated microscale liquid-liquid extraction kinetics of PAA (4.0 $g.L^{-1}$, pH 4) with butyl acetate carried out at (■) 10 $\mu L.s^{-1}$, (▲) 200 $\mu L.s^{-1}$, (●) 400 $\mu L.s^{-1}$ and (◆) 1000 $\mu L.s^{-1}$. Method detailed in section 2.3.3.6, carried out at 20 °C and atmospheric pressure. Mean data (n = 12) plotted with 2SE error bars and fitted to solid lines represent exponential decay curves.

4.2.5 Effect of Dispensing Speed on Microscale LLE Process

The dispensing speed of the liquid handling workstation during the mixing cycle was investigated for its effect on extraction kinetics during the automated microscale LLE process (section 2.3.3.6). Repeated mixing cycles were used to generate efficient phase mixing in the automated microscale LLE process, as described previously (section 4.2.1.1). The dispensing stage of the mixing cycle was investigated by visualisation of the fluid dynamics (section 4.2.1.2) and analysis of the Reynolds number (section 4.2.1.2.1). This demonstrated that the most liquid movement was created during the dispensing stage of the mixing cycle at the dispensing speed (400 $\mu L.s^{-1}$) that was higher than the aspirating stage of 75 $\mu L.s^{-1}$. The dispensing speeds (10 $\mu L.s^{-1}$ to 1000 $\mu L.s^{-1}$) correlated with the mixing times (15 s to 0.08 s) to transfer 150µL, which affected the mass transfer and kinetics of the LLE process.

The kinetics of the LLE of PAA (4.0 $g.L^{-1}$, $_{pH\ 4}$) with butyl acetate using the automated microscale LLE process generated for each of the dispensing speeds (10 $\mu L.s^{-1}$ to 1000 $\mu L.s^{-1}$) were plotted with 2SE error bars (figure 4.2.5.1). This plot of the aqueous phase PAA concentration against the dispensing times and dispensing cycles fitted the expected exponential curves for all dispensing speeds except for 10 $\mu L.s^{-1}$ data that fitted a linear correlation. The final PAA concentrations were the same for each dispensing speed, validating that equilibrium had been reached in each scenario. The dispensing times were proportional to the dispensing speeds that were proportional to the equilibrium times (table 4.2.5.1). The equilibrium distribution ratio for this data was 37, which was a little higher than that in earlier data and closer to the literature values. This was expected to correlate directly with the improved mass transfer and may have been due to the actual lower pH conditions of the aqueous phase. The data from the slowest dispensing speed showed higher variability and a more gradual gradient, which was expected as the phase mixing would have been minimal.

The dispensing stage of the mixing cycle created a jet stream from the pipette tip (section 4.2.1.2), generating phase mixing, which was quantified by calculating the associated Reynolds number (appendix A13.4.1: equation A13.8). This was calculated for each of the dispensing

Dispensing Speed ($\mu L.s^{-1}$)	**100**	**200**	**400**	**1000**	**1866**
Dispensing Times for 30 Mixing Cycles (s)	600	162	154	147.5	146
Reynolds number	16	322	645	1612	3009

Table 4.2.5.1. Pipe flow Reynolds numbers of liquid dispensed during the automated microscale liquid-liquid extraction process as a function of dispensing speed, calculated according to equation A13.8 (appendix 13.4.1), and the corresponding dispensing times for 30 mixing cycles at each dispensing speed.

speeds used in the experimentation. As expected, the Re value increased as the dispensing speed increased, which generated more phase mixing and mass transfer (table 4.2.5.1). The workstation's maximum dispensing speed (1866 $\mu L.s^{-1}$) was investigated and it generated a high Re value, but the LLE data was not displayed as it closely followed the trend of the 1000 $\mu L.s^{-1}$ dispensing speed, but greater scatter in the data was observed.

4.2.6 Quantification of Mass Transfer Kinetics

The automated microscale LLE process dispensing speed kinetic data fitted the mass transfer model proposed by Lye (1993) for the extraction of proteins using reverse micelles. The mass transfer model was dependent on dispensing speed and was used to investigate the microscale extraction data for extracting PAA with BA. The automated microscale LLE process (section 2.3.3.1) was modified for the preparation of samples over a range of mixing times (equivalent to 0 to 30 mixing cycles) as detailed in the automated microscale kinetics method (section 2.3.3.3). The aliquot containing both phases was transferred to enhance mass transfer, as quantified by equation 4.1. This equation allowed the data to be plotted as $\ln\left(\frac{C_1(t)}{C_1(0)} - \frac{mV_r}{(1+mV_r)}\right)$ against time (figure 4.2.6.1) to determine a certain value of k_La for each dispensing speed.

$$\ln\left(\frac{C_1(t)}{C_1(0)} - \frac{mV_r}{(1+mV_r)}\right) = -\frac{K_La}{V_1}.(1+mV_r)t \qquad [4.1]$$

where $C_1(0)$ is the initial concentration of PAA in the aqueous phase, $C_1(t)$ is the concentration of PAA in the aqueous phase at time t, V_r is the volume ratio, V_1 is the volume of the aqueous phase, k_La is the overall liquid phase mass transfer coefficient, and m is the distribution ratio. The data fitted a linear correlation for each of the speeds, with R^2 values of 0.997 for 10 $\mu L.s^{-1}$, 0.995 for 200 $\mu L.s^{-1}$, 0.989 for 400 $\mu L.s^{-1}$ and 0.989 for 1000 $\mu L.s^{-1}$. It was observed that the data normally fitted more closely to the trend line at the higher dispensing speeds, as the accuracy and precision of this data was greater because of the use of a higher number of mixing cycles. These data were used to calculate the k_La values for each dispensing speed, which were plotted against the dispensing speeds (figure 4.2.6.2). This formed a first order exponential curve of equation Y

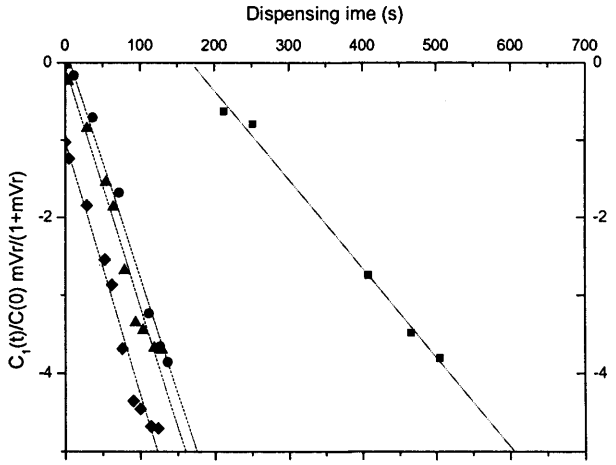

Figure 4.2.6.1. Plot of $\left(\frac{C_1(t)}{C_1(0)} - \frac{mV_r}{(1+mV_r)}\right)$ against time for microscale liquid-liquid extraction of PAA with butyl acetate over a range of dispensing speeds: 10 $\mu L.s^{-1}$ (■), 200 $\mu L.s^{-1}$ (●), 400 $\mu L.s^{-1}$, (▲) and 1000 $\mu L.s^{-1}$ (◆). Data taken from figure 4.2.5.2. Solid lines fitted according to equation 4.1.

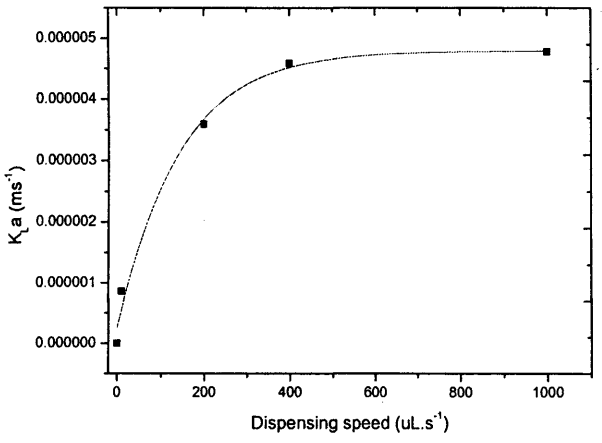

Figure 4.2.6.2. Combined overall solute mass transfer coefficient (k_La) as a function of dispensing speed for the microscale liquid-liquid extraction of PAA with butyl acetate. k_La values determined from figure 4.2.6.1 according to equation 4.1.

$= 4.8 \times 10^{-6} - 4.2 \times 10^{-6} e^{(-x/157)}$, which fitted the data with a R^2 value of 0.999. This plot illustrated that the highest dispensing speed (1000 $\mu L.s^{-1}$) created the maximum mass transfer, although there was little increase in efficiency as the dispensing speed increased above 400 $\mu L.s^{-1}$. These results were in the same order of magnitude as those reported for erythromycin (Lye. 1993).

4.2.7. Performance of the LLE Processes

The performance of the LLE process data was analysed using statistical methods (chapter 3) to calculate the accuracy and precision of the experimental data (table 4.2.7.1). The performance of the microscale LLE process was compared to the laboratory LLE process using the data from the experimentation investigating the effect of the aqueous phase pH conditions (section 4.2.3). It was observed that the process performance varied with the process scale and often varied between the experiments due to the occurrence of experimental variation.

The accuracy of the microscale pH LLE process data showed good comparison with the laboratory scale data, which validated the data as being the true values. The error bars for both of these process scales were small, although the automated data were slightly larger than the laboratory data for one point, but were considered acceptable relative errors. The distribution ratios for the manual microscale data were lower than those for the automated microscale data and both of these data sets showed slightly larger error bars, indicating random errors and variations in this experimentation. This may have been due to the effect of the different mixing techniques on mass transfer and the experimental variation in the actual aqueous pH conditions, which may have also affected the precision of the results.

The automated microscale LLE data fitted better with the laboratory data than the manual microscale data. This was due to the laboratory method having increased fluid flow from the horizontal shaker and the higher pipetting dispensing speed of the workstation compared to manual pipetting. The concentration values were calculated compared to a standard control in order to remove any systematic errors and allow comparison between data sets. Therefore, the accuracy values were not calculated for each experiment. The precision of the experimental data

Process Scale	Manual Microscale	Automated Microscale	Laboratory Scale
Distribution Ratio	2.6	2.7	3.1
2 SE	0.72	0.25	0.75
% CV	1.30	0.73	0.45

Table 4.2.7.1. Performance data for LLE of PAA (4.0 $g.L^{-1}$) with butyl acetate over a range of aqueous phase pH conditions (pH 2.5 to pH 8) using the manual microscale (300 µL), automated microscale (300 µL) and laboratory scale (10 mL) processes at 20 °C and a phase volume ratio of 1. Method detailed in section 2.3.3, 2.3.3.1 and 2.3.4 and mean data (n = 12) displayed.

was calculated for each experiment (repeatability) and for the repeated experiments (reproducibility). The repeatability of the data between the wells and different pipettes ranged from 0.01% to 5% CV for the microscale data and 1% to 10% CV for the laboratory data, which showed the benefits of automated pipetting. The automated data compared favourably with the published precision data of 15% (Steinborner and Henion, 1999) or 4 % RSD or CV (Jemal et al, 1999). The reproducibility statistics indicated a smaller error than the repeatability statistics as the occurrence of gross errors were detected, which were removed from the data. The reproducibility of the data was presented on the individual experimental graphs as 2SE error bars. All efforts were made to reduce the occurrence of experimental errors as discussed in chapter 3.

Experimental methods and equipment involved in the microscale LLE process development were robust, so they were not easily affected by external factors that could cause variability. To ensure that the microscale LE process was robust, the calibration of the equipment was carried out regularly to limit its effect on the performance of the process. These factors were analysed to identify which of these are controllable and the data for this was illustrated in chapter 3. The microscale process was found to be adequately robust and matched other automated experimental processes.

4.2.8 Sources of Error Related to the Automated LLE Process

It was observed during the implementation of the LLE experimentation some of the results showed significant random errors. The potential sources of error related to the automated and laboratory equipment themselves and their use in the LLE experimentation. The specific errors related to the instrumentation were considered and described in chapter 3. The errors related to the use of the automated equipment to undertake the LLE experimental processes are discussed further below.

4.2.8.1 Liquid Handling Workstation Calibration Issues

The workstation was routinely calibrated prior to its use in the automated LLE experimentation. It was noted that errors became more significant the longer the interval between the calibration of the equipment and the conclusion of the last experiment, especially when at one point two experiments were conducted back to back (though this was never repeated). It is probable that these errors were due to the workstation varying its relative physical location after its initial calibration, although this could also be the result of the increased delay required before HPLC analysis of the samples when degradation of the compound might have occurred (section 4.2.1.4.1), which is more likely. An example of these physical errors is the *XY* position of the centre of the pipette tip not being exactly coincident with the centre of the well, which may have influenced the fluid dynamics of the extraction system. Also, if air bubbles were caught up in the internal system liquid of the workstation or if the disposable pipette tips were not fully secured onto the pipette due to positing variations, there could be nanolitre variations in the microlitre volume of the liquid aspirated.

The workstation errors (identified above) could be reduced by calibrating prior to each experiment. This would add half an hour to each experiment (the time required for each calibration) and would potentially introduce further opportunities for human error as the *X, Y* and Z coordinates are aligned by eye. The root cause of these errors and machine instabilities was the variation in equipment maintenance procedures.

4.2.8.1.1 Labware Cleaning Issues

Normally, in automated experimentation using the liquid handling workstation disposable labware was used, removing the need for careful cleaning. It was not possible to use disposable plates during the LLE experiments because of the solvents incompatibility with the plastics from which disposable multiwell plates are constructed. Therefore, glass plates and fixed or resistant tips had to be used instead, as noted earlier (section 2.2.1.3).

This requirement for cleaning the glass 96-well plate before and after each experiment was a difficult and laborious task. However, if the cleaning was not carried out meticulously this could

introduce contamination between experiments, as the compounds often adhered onto the glass surfaces of the wells. Since most solvents react with the plastics used in manufacturing disposable plates, the only way to avoid this problem would be consistent and thorough cleaning of the non-disposable plates as using new plates for each experiment would prove expensive. The use of an automated plate washer was considered to achieve thorough cleaning of the plate, but the logistics of the equipment and solvent contamination of the waste water presented an environmental hazard. Therefore, the principles of the plate washer were manually applied, rinsing each well with plenty of water.

4.2.8.2 Liquid Phase Preparation

The liquid phase was prepared using standard reagents and laboratory equipment prior to each set of LLE experiments to ensure consistency and facilitate comparison between scales or conditions. Some errors in the LLE experimentation were attributed to the preparation of the liquid phase due to the difficulty in manually dispensing accurate amounts of the compounds. The compounds were supplied as powders or granular amorphous solids, which contained particles of specific sizes that limited the accuracy of the dispensed mass often not exactly matching the required amount. The significance of this type of error is low as in most general laboratory experiments, but at the microscale it can become highly significant. However, this is a physical limitation that would be difficult to overcome. The absolute particle sizes and the precision of the analytical balance affected the accuracy of the dispensed mass. Inaccuracies in the bulk phase's composition were reduced by comparing each sample to a standard (the feed material), which also removed the significance of errors incurred during the delay before HPLC analysis.

4.2.8.2.1 Aqueous Phase pH Issues

The pH conditions of the aqueous phase were quantified using laboratory equipment (pH stat), which was subject to variation. This variation in the measurements of the aqueous phase pH conditions affected the LLE process results, which was seen in the inconsistency between some experiments.

The possible sources of error associated with the pH stat were related to its calibration, the instrument sensitivity, precision of pH adjustments and compound degradation. The pH stat was calibrated using two buffers with known standard pH conditions, but these degraded over time and could have affected the accuracy of all pH measurements. The sensitivity of the machine was within only 0.01 pH units and may have been less frequently calibrated. The set pH conditions of the bulk aqueous phase were achieved using drops of acid or alkali to change the conditions. These aliquots were dispensed manually into the bulk feed material in imprecise amounts using a disposable Pasteur pipette, which resulted in imprecise changes to the pH, and the delay in the pH stat taking readings may have resulted in variation in the actual pH conditions of the solution. The extreme pH conditions may have caused certain compounds to degrade, releasing acids and changing the actual pH conditions. This was important to the efficiency of the LLE process, as the pH conditions would have influenced the mass transfer of the compounds (section 4.2.3).

4.3 Conclusion

The experimental results discussed in this chapter have developed the microscale LLE process beyond the previously published data by reducing the extraction volume and fully automating the extraction process to increase the automated mixing method. The automated microscale LLE process had a smaller working volume (300 μL) than that previously used (≥450 μL). Many researchers previously used manual mixing methods before the LLE process became fully automated with repeated pipetting mixing cycles. This microscale LLE process was used to investigate a number of key parameters to understand the challenges of using the automated equipment and optimise the extraction of 6-APA from the PA bioconversion product stream contaminants.

The automated microscale LLE process was developed for a 96-well plate using the Multiprobe liquid handling workstation by investigating the phase mixing conditions, fluid dynamics, mass balance data, LLE of the PA bioconversion product stream contaminants, effect of evaporation and compound degradation. The automated microscale LLE process was demonstrated to have efficient phase mixing at 2% well height and 0% tracking that achieved good mass balance data,

which agreed with the laboratory and minimal processes. These processes demonstrated efficient phase mixing and good mass balance data with minimal evaporation or degradation losses using a single compound or a complex feed solution. The tested automated microscale LLE process was used to investigate the effect of kinetics, pH conditions and solvents on the equilibrium process. The highest K_D values were achieved by extracting PAA with butyl acetate using the automated microscale LLE method with phase mixing of 30 mixing cycles dispensed from 2 mm above the well bottom and aspirated without moving the pipette tip.

The microscale LLE data matched the laboratory data, but the use of the microscale LLE process used faster sample handling and lower chemical volumes, reducing the cost of the experiment and man hours. This resulted in experimentation to rapidly optimise the extraction of a given compound from feed material. This method of rapidly screening the LLE of a compound could be used to purify a new chemical entity prior to the scale-up of its purification process for manufacturing. The automated microscale LLE process was comparable with the laboratory LLE process and this validated the experimental method, showing equivalent yields. The automated microscale LLE process was superior to the manual microscale LLE process, as the automated microscale LLE process generated higher yields than the manual microscale LLE process. The microscale process produced low mass transfer and was time consuming to prepare. The increased speed of operation of the automated process and its ability to generate many replicate samples increased the dataset used to optimise the process.

The validated automated microscale LLE process was further investigated to demonstrate the effect of the workstation's dispensing speed on mass transfer and the distribution ratio and k_La values were calculated to further understand the possibilities of the automated workstation. The mass transfer increased with the dispensing speed up to 1000 $\mu L.s^{-1}$ and increases beyond this value were insignificant as the mixing times were similar. The liquid handling workstation can operate under a range of dispensing speeds and the effect of these dispensing speeds on the phase mixing and mass transfer were analysed to enhance the automated microscale extraction of PAA. The results were used to fit to a mass transfer model of the process and generate a k_La curve to show the maximum dispensing speed (1000 $\mu L.s^{-1}$) that generated the highest k_La value. The

dispensing speed of > 400 $\mu L.s^{-1}$ generated similar distribution ratios, as they had similar mixing times (147.5 s to 154 s).

The statistical performance of these methods were also assessed and showed that the automated method had improved performance compared to the manual and laboratory methods. The highest overall K_D values were achieved using the automated microscale LLE process to extract PAA with phase mixing of 30 mixing cycles, aqueous phase of pH 2.5 with butyl acetate. Each of the experimental scales were statistically analysed, which demonstrated the effect of errors. Taking care in the preparation of materials is important for reducing the occurrence of errors, especially at microscale.

The benefits of the automated microscale LLE process were clearly indicated. The automated microscale LLE process was used to rapidly generate large sample numbers, generating statistically significant data with a high degree of accuracy and precision. This automated microscale LLE process could be used in the development of multi-step downstream processing sequences for product recovery and purification, which are currently both time consuming and expensive (Conner, 1999). Microscale approaches to experimentation in downstream processes have the potential to reduce the requirement for high quantities of starting materials, experimental costs, laboratory space and personnel costs. Coupled with the use of existing HTS equipment, such an approach could facilitate the rapid selection of efficient process routes and operational conditions. Liquid handling technologies have already been used for some downstream processes, such as liquid–liquid extraction, solid phase extraction and filtration for the preparation and initial clean-up of biological samples (Hubert et al, 1992), (Peng et al, 2000a) prior to their analysis. However, if such approaches are to be used for process development purposes, it will be necessary to relate the results obtained at the microscale to those determined at conventional laboratory and pilot scales.

Further validation of the microscale LLE process would be required prior to its utilisation as a generic technique for LLE optimisation and its integration into a multi-step purification process. This would require data from the extraction of other bioconversion product streams to investigate the extremes of the key parameters investigated within this research. In addition the development

of microscale counter current LLE techniques would be useful for optimisation, especially as this technique is used extensively in industry (section 7.3.1).

This chapter investigated the use of automated platforms for the development of the initial microscale equilibrium stage separation process, LLE. These automated platforms will be further used to investigate their suitability for developing another equilibrium stage separation process: solid phase extraction (chapter 5).

Chapter 5: Microscale Solid Phase Extraction

5.1 Introduction

Solid phase extraction (SPE) is an equilibrium stage separation process, which has similar characteristics to liquid-liquid extraction (chapter 4), but operates by a process of solid-liquid adsorption or sorption. The SPE process is more selective than LLE, although both of the processes separate compounds according to their different hydrophobicities. SPE has been used especially for the isolation of pharmaceutical compounds from samples of complex biological matrices, including plasma, serum and urine. This makes SPE an important separation technique for the removal of contaminating components prior to quantitative analysis and it is frequently used in sample preparation (Parker et al, 1996), as previously discussed (section 1.5.2).

The solid phase extraction process exploits chemical and physical properties to selectively and reversibly adsorb solutes onto the solid particles (Gregg and Sing, 1967). The term 'adsorption' was originally introduced in 1881 by Kayser to denote the condensation of a gas onto a free surface. Later, in 1909, the term 'sorption' was used by McBain to describe the phenomena of adsorption and absorption (Thornton, 1992). Sorption occurs when solutes are selectively transferred to the surface or bulk of insoluble rigid particles suspended in a vessel or packed bed. There are a variety of types of adsorption: solid-gas; solid-liquid and liquid-gas. The adsorbent types have different properties according to their categories (section 5.2.1.1).

SPE is a primary purification process that separates the compound of interest from a solution containing contaminants with either the solute or contaminants being adsorbed onto the solid phase due to their differences in surface charges and hydrophobicities. The development of the microscale SPE process considered the SPE characteristics (section 5.2.1): adsorbent resin; adsorbent material; bed weight or diameter and device (tubes, cartridges). The adsorbent materials used in the SPE process must bind the

adsorbate reversibly and details of the principles of SPE are summarised in appendix 14, considering the structure of the adsorbent solid's surface, the binding of molecules to the surface, equilibrium adsorption isotherms and adsorption kinetics.

SPE has been used since the 1960's for the industrial separation of a range of compounds, such as antibiotics from fermentation broths and impurities from contaminated aqueous samples (Asenjo, 2003). The SPE process is a constituent unit operation in the industrial down stream processing of the penicillin acylase bioconversion product stream (van Brakel and Kleizen, 1990). The compound of interest (6-APA) is selectively adsorbed, washed and eluted from the resin particles in a reduced solvent volume, which concentrates and purifies the solute to facilitate later process stages. Pharmaceuticals and fermentation broth contaminants are often polar, which makes them highly soluble in water. This can lead to poor LLE recovery, but SPE is an efficient separation method for the removal of organic compounds from dilute aqueous solutions with the feed material containing as little as 10% compound weight per resin weight (Maity and Payne, 1991). SPE is, therefore, a viable or preferable alternative purification method to LLE (Hennion, 1999).

This chapter discussed the key parameters of the SPE process and the development of the microscale SPE process, which was compared to the established laboratory scale process for the purification of 6-aminopenicillanic acid (6-APA). The aim of the experimentation was to develop an adaptable automated microscale SPE process for quantitative adsorption experimentation in multiwell plates, which should facilitate rapid process optimisation. The results from the SPE experimentation are reviewed in section 5.2 and discussed by comparison with published scientific findings (section 5.3).

5.2 SPE Results & Discussion

The solid phase extraction process was investigated to recover 6-APA from an aqueous solution. The process characteristics (section 5.2.1) were investigated by selecting a

suitable adsorption resin, adsorbate and an appropriate extraction format. The development of the automated microscale SPE process (section 5.2.2) investigated the method of preparation of the extraction vessel using manual and automated slurry handling equipment or the automated solid dosing station to prepare the reagents and solid-liquid mixing techniques to achieve an efficient microscale SPE process. The automated SPE process was used to generate adsorption kinetics for a selection of adsorbents (section 5.2.3) and activated carbon concentration adsorption isotherms (section 5.2.4). The automated SPE process was also used to investigate the effect of pH conditions (section 5.2.5) and develop supported microscale SPE experimentation (section 5.2.6). The data from the microscale SPE experimentation was compared in each case to the laboratory scale process to assess their correlation.

5.2.1 SPE Process Characteristics

The development of a microscale SPE process methodology initially considered various characteristics of the SPE process (section 5.2.1). The characteristics included the adsorbent resin (section 5.2.1.1), adsorbate (section 5.2.1.2) used to assess the SPE process format (section 5.2.1.3). The structure and nature of the adsorbate itself must also be considered when selecting the SPE resin (appendix 14). The use of a low mass adsorbent bed or a SPE disk format can reduce the elution solvent volume to as low as 30 μL (Hennion, 1999), which is financially and environmentally beneficial. The development of the microscale SPE process considered the SPE adsorbent resins, packing material and device diameter (tubes, cartridges, 96-well plate).

5.2.1.1 Adsorbent Resins

There is currently a great diversity of adsorbent resins used in SPE processes. The adsorbents are categorized into five descriptions: reverse phase; polymeric; ion exchange; mixed mode or immuno-extraction adsorbents (Seader and Henley, 1998). Each of these adsorbent classes were designed to adsorb a specific range of compounds according to their chemical natures and physical properties (Table 5.2.1.1.1). The key physical properties of SPE resins include physiochemical stability, ease of regeneration

Adsorbent Types	Activated Alumna	Silica Gel	Activated Carbon	Molecular Sieve organic (Sephadex) Inorganic (Zeolites)	Molecular Seize Zeolites	Polymeric Adsorbents	Amberlite XAD 7	Amberlite XAD 16
Nature of resins	Hydrophilic amorphous	Hydrophilic/ hydrophobic amorphous	Hydrophobic amorphous	Hydrophobic	Polar hydrophobic	crystalline	Neutral polymeric	Hydrophobic polyaromatic
Pore diameter (μm)	10 - 75	22 to 26, 100 to 150	10 – 25 >30	2 - 10	3 - 10	25 - 40	10-15	10-15
Particle porosity (Angstrom)	0.50	0.47 0.71	0.4 - 0.6	NA	0.2 - 0.5	0.4 - 0.55	0.09	0.1
Density ($g.cm^{-3}$)	1.25	1.09 0.62	0.5 – 0.9 0.6 – 0.8	0.98	NA	NA	1.24	1.08
Surface area ($m^2.g^{-1}$)	320	750 - 850 300 - 350	400 – 1200 200 - 600	400	600 - 700	NA	450	900
Capacity for water ($mL.g^{-1}$)	7	11	1	20 - 25	20 - 25	NA	1.14	1.82

NA = Information not available.

Table 5.2.1.1.1. Characteristics and physical properties of solid phase adsorbent resin types. Data compiled from suppliers' data sheets detailing their physical properties and from Seader and Henley (1998).

Adsorbent Types	Activated Alumna	Silica Gel	Activated Carbon	Molecular Sieve organic (Sephadex) Inorganic (Zeolites)	Molecular Seize Zeolites	Polymeric Adsorbents	Amberlite XAD 7	Amberlite XAD 16
Nature of resins	Hydrophilic amorphous	Hydrophilic/ hydrophobic amorphous	Hydrophobic amorphous	Hydrophobic	Polar hydrophobic	crystalline	Neutral polymeric	Hydrophobic polyaromatic
Pore diameter (μm)	10 - 75	22 to 26, 100 to 150	10 – 25 >30	2 - 10	3 - 10	25 - 40	10-15	10-15
Particle porosity (Angstrom)	0.50	0.47 0.71	0.4 - 0.6	NA	0.2 - 0.5	0.4 - 0.55	0.09	0.1
Density ($g.cm^{-3}$)	1.25	1.09 0.62	0.5 – 0.9 0.6 – 0.8	0.98	NA	NA	1.24	1.08
Surface area ($m^2.g^{-1}$)	320	750 - 850 300 - 350	400 – 1200 200 - 600	400	600 - 700	NA	450	900
Capacity for water ($mL.g^{-1}$)	7	11	1	20 - 25	20 - 25	NA	1.14	1.82

NA = Information not available.

Table 5.2.1.1.1. Characteristics and physical properties of solid phase adsorbent resin types. Data compiled from suppliers' data sheets detailing their physical properties and from Seader and Henley (1998).

and incompressibility (Seader and Henley, 1998). Good adsorbents are selective, have a high capacity for the adsorbate and a porous structure that gives them a large surface area. The initial resin screening will quantify the gross specificity for the compound of interest and adsorption kinetics.

There are a number of adsorbent resins used to purify 6-APA from aqueous solutions, including activated carbon, Amberlite XAD-7 and Amberlite XAD-16. These adsorbent resins are described in section 5.2.1.1.1 and section 5.2.1.1.2. The resins were investigated for the adsorption of 6-APA to show which of them was the most suitable resin for the development of the microscale SPE experimentation (section 5.2.1.1.3).

5.2.1.1.1 Activated Carbon

There are various kinds of carbon adsorbents available, including activated carbon, carbon sieves, porous carbon and graphitised carbon black, which have different chemical and physical characteristics. Activated carbons have been used since the late 18^{th} century in industrial applications for the adsorption of gases, organic pollutants (Matisova and Skrabakova, 1995) and coloured contaminants (McKay, 1983). The commercial sources of activated carbon are from biological biomass: wood; coconut shells and fossilised materials. The material is carbonised and activated by boiling in water prior to its use as an adsorbent or bought pre-activated, which increases its porosity and surface area.

Activated carbon has a complex surface chemistry containing phenolic, carboxylic, aldehydic, etheric and peroxidic groups. The mechanism of binding adsorbates occurs primarily by hydrophobic interactions, charge transfer complexation, hydrogen bonding and cation exchange. It has a high adsorption capacity and the multiple interactions make activated carbon an efficient adsorbent (Matisova and Skrabakowa, 1995). Therefore, activated carbon has been used for a wide range of applications (McKay,

1983). Activated carbon has been previously reported to be efficient for the SPE of 6-APA (Dutta et al, 1997b).

5.2.1.1.2 Amberlite XAD

Adsorbents within the Amberlite XAD range of neutral polymeric micro particles contain a series of different chemistries that make them suitable for the adsorption of a diverse range of compounds (Seader and Henley, 1998). These adsorbents are copolymers of styrene and divinylbenzene that were developed to provide mechanical strength, high surface areas and appropriate pore sizes for rapid mass transfer (Chaubal et al, 1995).

5.2.1.1.3 Adsorbent Selection

The range of adsorbent resins investigated for the adsorption of 6-APA (4.0 $g.L^{-1}$) from aqueous solutions included granular activated carbon, Amberlite XAD-7 and Amberlite XAD-16. These resins were used in initial laboratory scale adsorption experimentation to investigate the adsorption kinetics, adsorbent concentration isotherms and their relative specificity for 6-APA. The results were used to select the most suitable resin for the development of the microscale SPE process.

The kinetics of 6-APA adsorption onto two adsorbent resins (granular activated carbon resins and Amberlite XAD-16) were investigated over a 24 hour period at the laboratory scale (100 mL) using the laboratory SPE method (section 2.4.2.1). The changing 6-APA concentrations of the liquid phase samples were analysed and plotted against time (Figure 5.2.1.1.3.1). The kinetics of the investigated adsorbent resins showed that both resins adsorbed 6-APA, although at different rates. Activated carbon ($Y = 2.6 + 1.4e^{(X\ 538)}$) adsorbed 6-APA at a faster rate than XAD-16 ($Y = 2.5 + 0.5e^{(X/530)}$). The adsorption kinetics reached equilibrium after an initial period of adsorption of *circa* 400 minutes for activated carbon and 240 minutes for XAD-16. Activated carbon adsorbed more 6-APA from the liquid phase within 24 hours than XAD-16, reducing the liquid phase 6-APA concentration to 2.65 $g.L^{-1}$ compared to

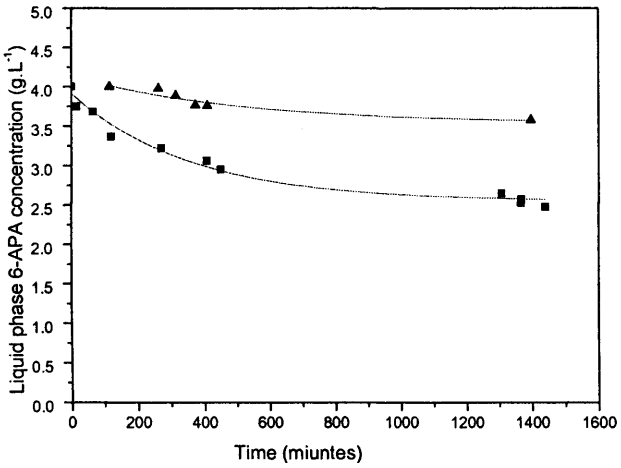

Figure 5.2.1.1.3.1. Adsorption kinetics of 6-APA (4.0 $g.L^{-1}$) dissolved in phosphate buffer (0.2 M, pH 4.5) against time at laboratory scale (100 mL) onto a range of adsorbent resins: (■) granular activated carbon (4.0 $g.L^{-1}$) and (▲) Amberlite XAD-16 (1.36 $g.L^{-1}$) over 24 hours with liquid phase samples analysed on HPLC. Method detailed in section 2.4.2.1.

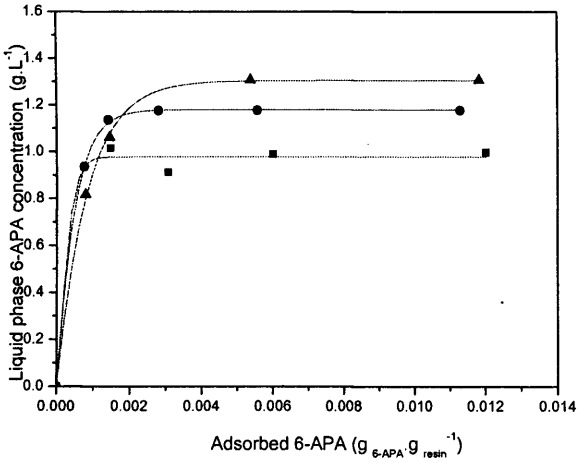

Figure 5.2.1.1.3.2. Adsorbent concentration isotherms for the laboratory scale (50 mL) SPE of 6-APA (4.0 $g.L^{-1}$) with a range of adsorbent resins (0.2 $g.L^{-1}$ to 4.0 $g.L^{-1}$): (■) Amberlite XAD-16, (●) Activated carbon and (▲) Amberlite XAD-7. Method detailed in section 2.4.2.1.

3.58 $g.L^{-1}$. This indicated that the adsorption kinetics for activated carbon were faster than the other adsorbents, despite the lower resin mass used. The related adsorbed 6-APA per gram of resin value for activated carbon (0.38 $g_{6\text{-}APA}.g_{resin}^{-1}$) was higher than that for XAD-16 (0.003 $g_{6\text{-}APA}.g_{resin}^{-1}$) and this indicated its higher specificity for 6-APA.

The adsorbent concentration was investigated using a range of adsorbent resins at laboratory scale (50 mL) using the resin selection method (section 2.4.2.1) to generate adsorbent concentration isotherms for the SPE of 6-APA from aqueous solutions. The SPE of 6-APA with granular activated carbon, Amberlite XAD-16 and XAD-7 adsorption resins was investigated over a range of adsorbent concentrations (0.2 $g.L^{-1}$ to 4.0 $g.L^{-1}$) (Figure 5.2.1.1.3.2). The adsorbent isotherm data for each adsorbent fitted sigmoidal (Boltzmann) curves, indicating that they all fitted the type V isotherm (appendix 14: Figure A14.1). However, the isotherms had different equations: granular activated carbon ($Y = \frac{0-16.7+1.2}{10+e^{(-0.001X/0.0005)}}+1.2$), Amberlite XAD-16 ($Y = \frac{0-0.69+1.0}{1+e^{(-0.00007X/0.0002)}}+1.0$) and XAD-7 ($Y = \frac{0-156+1.3}{1+e^{(-0.004X/0.0008)}}+1.3$), indicating their specificity for 6-APA. The regression analysis of these data showed a good closeness of fit, generating R^2 values of 0.10, 0.992 and 1.00 respectively. The activated carbon resin adsorbed 6-APA at a median adsorbed 6-APA per gram of adsorbent value (1.2 $g_{6\text{-}APA}.g_{resin}^{-1}$) compared to that for XAD-16 (1.0 $g_{6\text{-}APA}.g_{resin}^{-1}$) and XAD-7 (1.5$g_{6\text{-}APA}.g_{resin}^{-1}$). The trend in the equilibrium data agreed with that generated from the adsorbent selection kinetics data above, although the adsorbed 6-APA per gram values were higher.

The adsorbent selection results showed that activated carbon had faster kinetics than XAD-16 and the high use, cost efficiency and availability of activated carbon supported its use in SPE processes (section 1.5.2). Activated carbon was, therefore, the adsorbent resin selected for the development of the automated microscale SPE process.

5.2.1.2 Adsorbate

The adsorbate used to develop the microscale SPE process methodologies was 6-APA, the product of the penicillin G bioconversion by penicillin acylase (section 1.6.2.4), which was used in the development of the microscale LLE process. During the initial experimentation, it was observed that the compound degraded over time. Degradation of 6-APA occurred spontaneously and formed penillic acid or penicilloic acid if the 6-APA solution was alkaline (Grant et al, 2001, Vandamme & Voets, 1974). The effect of pH on degradation was similar to that seen for the degradation of Penicillin G (section 4.2.1.4.1).

The degradation of 6-APA (0.27 $g.L^{-1}$) was investigated over 25 hours at different temperatures: fridge (5 °C) and room temperature (20 °C). The 6-APA concentration was quantified over time using the UV/Vis spectrometer at 257 nm (section 2.5.2). The mean (n = 3) 6-APA concentration data was plotted against time (Figure 5.2.1.2.1) with 2SE error bars, which were relatively small and indicated that both data sets had good reproducibility (2SE < 0.003). The data for each of the temperatures showed similar trends and were fitted to exponential decay curves. The room temperature data fitted the curve ($0.24 + 0.03\ e^{(-X/113)}$) with a R^2 value of 0.907 and the 5 °C data fitted the curve ($0.21 + 0.07\ e^{(-X/94)}$) with a R^2 value of 0.995. The regression analysis of the data indicated that the 5 °C data fitted more closely to the exponential decay curve than the 20 °C data, indicating that the data was more reproducible.

The end point concentration of the 5 °C samples was higher than the 20 °C samples, indicating that the degradation occurred at a slower rate for lower temperatures, which was expected. The spontaneous degradation of 6-APA reduced the 6-APA concentrations at 5 °C to 89.2% and at 20 °C to 75.3% of the original 6-APA concentration after 25 h. The SPE experimentation was therefore, carried out at 20 °C.

5.2.1.3 SPE Process Formats

The SPE process was carried out at a variety of scales (section 1.5.2.1) using a range of appropriate SPE formats. The development of the microscale SPE methodology for use

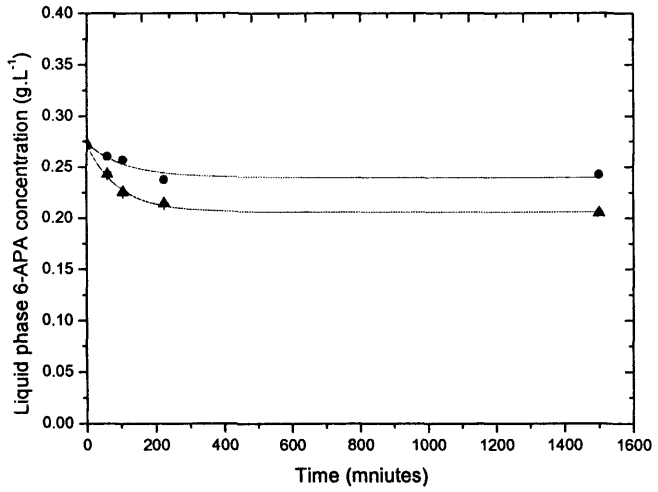

Figure 5.2.1.2.1. Degradation of 6-APA (0.27 $g.L^{-1}$) dissolved in phosphate buffer (0.2 M, pH 4) over 24 hours at (●) 5 °C and (▲) 20 °C. Samples analysed on UV/ Vis spectrometer at 257 nm and mean data (n = 3) plotted with 2SE error bars (+/- 0 to 0.03) against time. Method described in section 2.4.5.1.

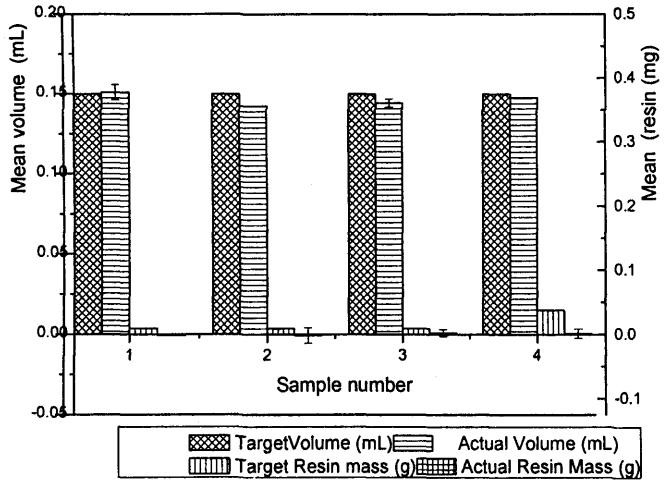

Figure 5.2.2.1.1.1. Effect of pipette tip internal diameter on manual slurry handling accuracy using the manual 1 mL pipette fitted with a variety of pipette tips: (1) 0.85 mm, (2) 1.1 mm, (3) 1.2 mm and (4) 1.22 mm to transfer 150 µL of the granular activated carbon slurry (25 $g.L^{-1}$ or 100 $g.L^{-1}$) prepared in phosphate buffer (0.2 M). Mean values (n = 4) plotted with 2SE error bars. Method detailed in section 2.4.2.2.1. See table 5.2.2.1.1 for statistical details of performance.

in optimisation experimentation considered the suitability of commercially available devices, which included pre-filled SPE tubes, cartridges and 96-well plates.

The commercially available non-polar application development kit (IST Isolute, Jones Chromatography, UK) contained pre-filled 1 mL square cross-sectional tubes with an array of adsorbents (25 mg), which were arranged in a 96-well formatted system. The adsorbents: Octadecyl (non end-capped) functionalised silica manufactured using trifunctional silanel (C18); Octadecyl (end-capped) functionalised silica manufactured using trifunctional silanel (C18 MF); Octyl (non end-capped) functionalised silica, manufactured using trifunctional silanel (C8); Hexyl (end-capped) functionalised silica manufactured using trifunctional silanel (C6); Butyl (end-capped) functionalised silica manufactured using trifunctional silanel (C4); Ethyl (non end-capped) functionalised silica manufactured using trifunctional silanel (C2); Phenyl (non end-capped) functionalised silica (PH) and Hydroxylated polystyrene-divinylbenzene (CN), as described in section 2.4.2.1.1 were assessed for the adsorption of aqueous 6-APA (4.0 $g.L^{-1}$, pH 4.5). These SPE resins showed poor adsorption for 6-APA, adsorbing 9% to 24% of the initial adsorbate (Table 5.2.1.3.1).

The Phenyl (PH) resin had the highest specificity for 6-APA. However, the purification of the adsorbate could have been enhanced by optimising the conditions used to prepare adsorbent with the resin cartridges in the methodology, such as the adsorbent mass. The major limitation of the cartridge format was that it required relatively large sample volumes, which would not always be available in the early stages of developing a purification route for a new compound. The fixed mass of adsorbent resin within the cartridges restricted the generation of isotherm data, preventing the analysis of the adsorbent concentration isotherms. Analysis of the isotherm data is important for the scale-up of the process (section 1.5.2.1). Therefore, the pre-filled cartridge format was not further investigated for use in the microscale SPE methodology.

The empty SPE formats were investigated together with methods of their preparation using slurry handling and solid dosing equipment to assess their suitability for the

IST Isolute Adsorbent Resins (25 mg)		Percentage Absorbed 6-APA
C18	Octadecyl (non end capped)	18%
C18 MF	Octadecyl (non end capped)	14%
C8	Octyl	10%
C6	Hexyl	11%
C4	Butyl	12%
C2	Ethyl	9%
PH	Phenyl	24%
CN	Cyanopropyl	17%

Table 5.2.1.3.1 Percentage 6-APA (4.0 $g.L^{-1}$, pH 4.5) adsorbed by a range of adsorbent resins (25 mg) in the pre-filled 1 mL cartridges supplied in the IST Isolute non-polar (basic pharmaceutical) application development kit from Jones Chromatography, UK. Method detailed in section 2.4.2.1.1.

development of the microscale SPE process (section 5.2.2). Suitable formats were selected from a diverse selection of multiwell plates (section 1.3.1) with a range of characteristics. The selected plates included the 96-deep well and 24-well plates, which contained suitable extraction volumes. These empty formats can be filled with specific quantifies of a range of resins that can be used to develop an adaptive microscale SPE method.

5.2.2 Microscale SPE Method Development

The microscale SPE methodology was developed by investigating the use of the manual slurry handling equipment, the automated slurry handling equipment and the solid dosing station for the preparation of the extraction vessels. The performance of the manual slurry handling equipment was evaluated for transferring the granular activated carbon resin slurries (section 5.2.2.1). The automated equipment was evaluated for its slurry handling capability, investigating the automated slurry handling performance of the liquid handling workstation (section 5.2.2.2) and the solid handling capability of the solid dosing equipment (section 5.2.2.3). The automated liquid handling equipment was also used to achieve solid-liquid mixing within the extraction vessel (section 5.2.2.4) to develop the automated microscale batch SPE process (section 5.2.2.5).

The performance of the automated equipment (section 3.2.1.) investigated by the manufacturers generated customer specifications of 2.0% inaccuracy and 0.5% CV for dispensing 100 µL aliquots using the workstation fitted with disposable tips (appendix 7.1). These performance values were shown to be a little ambitious for the actual operation of the laboratory equipment used in this research, which achieved at best 2.5% inaccuracy and 2.1% CV (section 5.2.4.3.). The performance of the manufacturer's analysis of the solid dosing station's performance showed a 0.9% inaccuracy and 0.09% CV for dispensing 10 mg of starch (appendix 7.3), although the performance of the dosing station dispensing activated carbon resin particles generated 10% inaccuracy. The standard acceptable inaccuracy values used in engineering are +/- 10% of the mean value. The ideal set-up of the equipment for the microscale SPE

experimentation would transfer accurate and precise volumes of the slurry containing significant quantities of resin or quantities of granular solids.

5.2.2.1 Manual Slurry Handling

The manual slurry handling equipment was assessed for dispensing slurry aliquots under a variety of different conditions (section 2.4.2.2.1). The manual pipette was fitted with disposable pipette tips to dispense aliquots of conditioned activated carbon slurry from the bulk slurry (100 mL) mixed using a Rushton turbine fixed to an overhead motor (1000 rpm). The performance of the manual slurry handling equipment was investigated when fitted with different pipette tips and operated under different scenarios. The slurry aliquots were transferred into pre-weighed tubes, which were gravimetrically measured to generate data (section 2.4.2.2) in order to quantify the volume and mass of the transferred slurry aliquots.

The manual slurry handling equipment (section 2.4.2.2.1) was investigated to assess the suitability of a laboratory pipette fitted with disposable pipette tips of different internal diameters (section 5.2.2.1.1). The selected equipment was used to analyse its performance in transferring aliquots of water or granular activated carbon slurries (section 5.2.2.1.2). The performance of the manual slurry handling equipment was also investigated over a range of aliquot volumes (section 5.2.2.1.3). The manual slurry handling equipment was assessed for dispensing a range of powdered activated carbon slurry concentrations (section 5.2.2.1.5) and with a variety of resin slurry preparations consisting of a range of particle sizes (section 5.2.2.1.6). The performance of the manual slurry handling equipment under each of the scenarios was compared (section 5.2.2.1.4) as a preliminary investigation prior to the development of the automated microscale SPE methodology (section 5.2.2.2).

5.2.2.1.1 Manual Slurry Handling Equipment Pipette Tips

The manual slurry handling pipette was fitted with pipette tips of different internal diameters, which were used to transfer aliquots (150 μL) of the aqueous conditioned

granular activated carbon slurry (25 $g.L^{-1}$). The pipette tips investigated were generated in-house or were commercially available and had internal diameters of between 0.85 mm and 1.22 mm. The effect of the internal diameters of the pipette tips on manual slurry handling was illustrated by the percentage target values for each of the pipette tips investigated (Table 5.2.2.1.1.1). The percentage target volume was highest for the smallest internal diameter (0.85 mm) pipette tip (101% target volume), but this sample aspirated only the liquid fraction of the slurry without transferring the solids (0%). The percentage target volume values for the larger internal diameter pipette tips were lower than the values for the smallest diameter pipette tip. This was due to the d_{Tip} being smaller than d_{Resin} for some particles and the aggregated particles.

The percentage target resin mass values for the larger bore pipette tips (26% for 1.2 mm tip and 4% for 1.22 mm tip) were better than the smaller pipette tips, which indicated their benefit for slurry handling. However, the data for the 1.22mm pipette tip was more accurate (2SE = 0.003) than that for the 1.2 mm pipette tip (2SE = 0.223). Therefore, the 1.22 mm pipette tip, which was commercially available and generated the highest volume accuracy of the wide bore pipette tips (99.8% target volume), was used with the manual slurry handling equipment for subsequent experimentation investigating the manual solids transfer.

Each of the pipette tips used with the manual slurry equipment dispensed significantly lower resin mass values than the target value. The data indicated the errors associated with the manual pipette, the pipetting technique and gravimetric analysis equipment (section 3.3).

5.2.2.1.2 Analysis of Manual Slurry Handling Equipment

The performance of manual slurry handling equipment, fitted with 1.22 mm internal diameter pipette tip was assessed for transferring water or slurry samples (100 $g.L^{-1}$) (section 2.4.2.2.1). The conditioned granular activated carbon slurry concentration was higher than that used in previous experiments (section 5.2.2.1) to assist its performance.

Pipette Tip Internal Diameter (mm)	0.85	1.1	1.2	1.22
Target volume (%)	101	95	96	98
2SE Volume	-	0.011	0.223	0.004
CV Volume (%)	NA	46	12	NA
Target resin mass (%)	0.0007	0	26	4
2SE resin mass	-	0.480	0.223	0.003
CV resin mass (%)	NA	4	1002	NA

Table 5.2.2.1.1.1. Performance of manual slurry handling equipment fitted with disposable pipette tips of different internal diameters to transfer 150 μL aliquots of granular activated carbon slurries (25 $g.L^{-1}$). (NB 100 $g.L^{-1}$ granular activated carbon slurry used with 1.22 mm pipette tip). Method detailed in section 2.4.2.2.1.

The slurry handling data for both the liquid and resin fractions were presented with 2SE error bars (Figure 5.2.2.1.2.1).

The actual target volume of water dispensed using the manual pipetting equipment had sub-optimal accuracy (11% inaccuracy), but this was only just outside the acceptable rule of thumb limit for laboratory equipment (10% inaccuracy). This data indicated the inaccuracy of the 1 mL pipette in pipetting 150 µL, which was used outside its designed volume range (200 µL to 1000 µL) due to the limited commercial availability of the wide bore pipette tips, which may have contributed to the inaccuracies. Larger bore (1.4 mm), lower volume (20 µL to 200 µL) pipette tips were commercially available for the automated workstation and they were investigated for their efficient slurry handling capability (section 5.2.2).

The activated carbon slurry volume data was more accurate (0.1% inaccuracy). The actual experimental data for the slurry samples showed that the volume data varied a little from the target volume (0.94% RCV), but the actual mass data varied considerably (632% RCV). The percentage mass of the dispensed slurry was low (-3.4% target resin mass), which was insignificant as it was within the error of the pipette itself and balance. The poor performance data for the manual slurry handling equipment has instigated further investigations (section 5.2.2.1.3 and section 5.2.2.1.6).

5.2.2.1.3 Manual Slurry Handling Volume

The manual slurry handling equipment was fitted with the wide bore (1.22 mm internal diameter) pipette tips and investigated for transferring a range of conditioned granular activated carbon slurry (25 $g.L^{-1}$) over a range of aliquot volumes (200 µL to 1000 µL) to see if it increased the equipment's performance. Each of the slurry volumes (200 µL, 400 µL, 800 µL and 1000 µL) were transferred from the stirred vessel into pre-weighed tubes and the samples were prepared (section 2.4.2.2). The mean values of the dispensed volume and resin mass were plotted with the target values for each of the aliquot volumes (Figure 5.2.2.1.3.1).

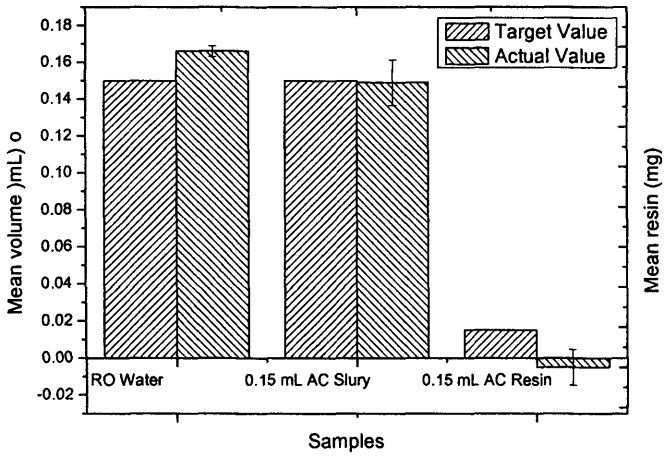

Figure 5.2.2.1.2.1. Performance of the manual slurry handling equipment fitted with disposable pipette tips (d_i = 1.22 mm) to transfer the target and actual liquid and resin fractions within the 150 µL aliquots of water or granular activated carbon slurry (100 $g.L^{-1}$) prepared in phosphate buffer (0.2 M). Mean data (n = 15) plotted with 2SE error bars. Method detailed in section 2.4.2.2.1.

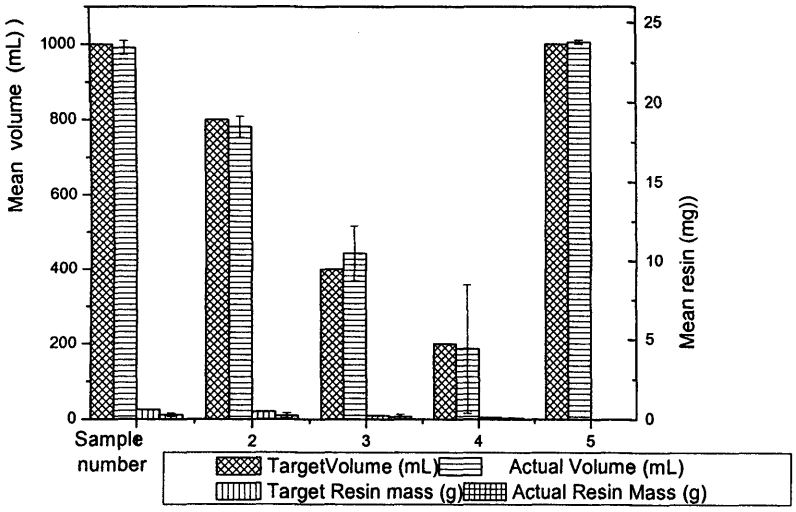

Figure 5.2.2.1.3.1. Effect of aliquot volume on manual slurry handling accuracy of dispensing conditioned granular activated carbon slurry (100 $g.L^{-1}$) prepared with phosphate buffer (0.2 M). Samples: (1) 1000 µL RO water, (2) 200 µL slurry, (3) 400 µL slurry, (4) 800 µL slurry and (5) 1000 µL slurry. Slurry transferred using a 1 mL pipette fitted with wide bore pipette tips (1.2 mm). Mean values (n = 5) plotted with 2SE error bars. Method detailed in section 2.4.2.2.1.

The actual volume dispensed increased with the target volume and was 98% to 111% of the target volume over the aliquot volume range, which represented acceptable accuracy. These results had similar accuracy to the water sample data (111%) displayed in Figure 5.2.2.1.3.1. The volume inaccuracies were accounted for by random pipetting errors or discrepancies in the gravimetric measurements of the analytical balance. The actual dispensed slurry volume, calculated from the gravimetric measurements of the sample tubes, assumed that the density of the liquid was 1000 $kg.m^{-3}$ (i.e. the specific density of water). However, the actual density of the slurry would be higher due to the resin particles, but this was not quantified due to the variable resin content in the dispensed slurry aliquots. For example, the 400 μL slurry sample dispensed 111% target volume, which was expected to be closer to the target volumes than the 150 μL and 200 μL slurry samples that dispensed 100% target volume.

The target resin mass increased proportionally with the target slurry volume, however, the actual resin mass did not follow this trend. The actual dispensed slurry resin mass increased with the target slurry volume from 57% to 74% target resin mass over the lower aliquot range (200 μL to 400 μL).The percentage target resin mass decreased for aliquots above 400 μL to 45% for the 1000 μL aliquot data. This suggested that the increased number of resin particles in the larger slurry volumes blocked the pipette tip, limiting the amount of solids transferred. This may have been due to clumping of the resin particles and occlusion of the orifice. The precision and accuracy of the data varied with the slurry aliquot volume as expected, with greater variation in the smaller volumes. For each of the slurry volumes the percentage target resin mass was below 75%, which was better than previous experiments, but not suitable for setting up reproducible microscale methodologies.

The manual slurry handling volume experimentation was an extension of previous investigations (Lander, 2002) that showed good correlation between the slurry volume pipetted and the dry resin mass over a variety of aliquot volumes (10 μL to 1000 μL) and concentrations (5 $g.L^{-1}$ to 100 $g.L^{-1}$) for a range of adsorbent resins including XAD-4 and Amberlite 563. The manual slurry data had a high degree of accuracy, which was

not matched in this manual slurry handling volume data. The particle size of Amberlite 563 resin (mesh size 20 to 50) was smaller than XAD-4 and XAD-16 (mesh size 20 to 60), as well as granular activated carbon (mesh size 20 to 300). Therefore, the accuracy of dispensing slurries of these smaller resin particles was better than that achieved for granular activated carbon. The use of smaller resin particle sizes of activated carbon was investigated with the use of the manual slurry handling equipment to try to improve its accuracy (section 5.2.2.1.5 and section 5.2.2.1.6).

5.2.2.1.4 Manual Slurry Handling of Powdered Activated Carbon

The performance of the manual slurry handling equipment was assessed transferring powdered activated carbon slurry to investigate the effect of smaller resin particle sizes. The powdered slurry was mixed in a vessel by a Rushton turbine attached to a motor (1000 rpm). Samples of the slurry were removed at different heights in the vessel (0 mm, 15 mm and 20 mm) to identify the optimum sampling position. The gravimetric measurements of the samples were displayed in Figure 5.2.2.1.4.1.

The target and actual slurry volume and resin mass data for the powdered activated carbon slurry (Table 5.2.2.1.5.1) indicated that the sampling height of 15 mm above the bottom of the vessel produced the best percentage target values (88% target volume and 46% target resin mass). The smaller resin particle slurry did not significantly enhance the performance of the manual slurry handling equipment compared using the granular activated carbon data. The percentage target volume was lower than that achieved with the granular activated carbon (100%), but this may have been due to occlusion of the pipette tips by the smaller particles clumping together, which indicated that these smaller particles were also a challenge for manual slurry handling. The powdered activated carbon slurry concentration was limited by physical constraints and the percentage resin mass transferred was affected by the sampling height with the best results achieved with sampling from 1.5 mm off the vessel bottom.

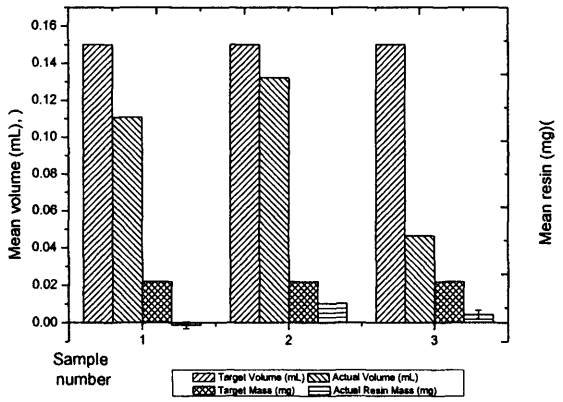

Figure 5.2.2.1.4.1. Manual slurry handling of 150 µL powdered activated carbon slurries (0.15 $g.L^{-1}$) sampled at different heights in the vessel: (1) 0 mm off the vessel bottom; (2) 15 mm off the vessel bottom and (3) 20 mm of the vessel bottom. Method detailed in section 2.4.2.2.1.

SPE Resin	**XAD-7**	**XAD-16**	**Granular Activated Carbon**	**Powder AC 15 mm**	**Water**
Target volume (mL)	0.15	0.15	0.15	0.15	0.15
Actual volume	0.159	0.165	0.145	0.132	0.169
% Target volume	106	110	96	88	113
2SE volume	6.9E-5	7.6E-5	6.9E-3	2.38E-4	1.82E-5
Slurry concentration ($g.L^{-1}$)	100	100	100	0.150	-
Target resin (mg)	15	15	15	0.0 23	-
Actual resin (mg)	0.2	0.2	2.2	0.01	-
% Target resin mass	1.3	1.3	14.6	46	-
2SE resin	0.003	0.007	5.8	0.00001	-

Table 5.2.2.1.5.1. Performance of manual pipetting equipment fitted with wide bore (1.22 mm) pipette tips dispensing aliquots (150 µL) of a range of adsorbent slurries: Amberlite XAD-7; Amberlite XAD-16; granular activated carbon and powdered activated carbon slurries (100 $g.L^{-1}$) or RO water. Method detailed in section 2.4.2.2.1.

The error bars (2SE) indicated that the 15 mm data had the lowest error associated with the dispensed powder slurry volume and resin mass. Analysis of the data indicated that the resin mass data taken at a height of 15 mm in the vessel also had the best precision (0.01% RCV, 0.08% RSE) of the sample height data. The precision data for the powdered activated carbon samples compared favourably with the granular activated carbon data (section 5.2.2.1.6).

5.2.2.1.5 Manual Slurry Handling Particle Size Performance

The manual slurry handling equipment, fitted with the wide bore pipette tips, was assessed for its performance in dispensing a range of SPE resin preparations of different particle sizes (10 μm to 2000 μm). The conditioned resins investigated included Amberlite XAD-7 (100 $g.L^{-1}$), Amberlite XAD-16 (100 $g.L^{-1}$), granular activated carbon (100 $g.L^{-1}$) and powdered activated carbon (0.15 $g.L^{-1}$). The performance of the slurry handling equipment for dispensing these resin slurries (Table 5.2.2.1.5.1) illustrated the
mean percentage values for the dispensed volumes and resin solids for each of the resins investigated.

The best percentage target volume was achieved in dispensing granular activated carbon (96% target volume). The granular activated carbon slurry data showed acceptable results compared to data presented in Table 5.2.2.1.1.1 (96% target volume for the 1.2 mm tip), although the accuracy of the gravimetric method showed a degree of variation. The water data indicated similar performance data to that in the experimentation for Figure 5.2.2.1.2.1, which produced 111% percentage volume with a 2SE value of 0.003. This indicated that there was a degree of random error associated with the manual pipetting technique. The granular activated carbon data in this experiment was less accurate at dispensing the percentage volume (96% compared to 100% (Table 5.2.2.1.6.1)), but both indicated acceptable accuracy and the percentage slurry resin mass for both data sets showed a degree of variation that made this slurry handling technique unacceptable.

a)

Manual Slurry Handling Performance	1.22 mm Pipette Tip	Water (Control Data)	0.15 mL Granular Activated Carbon (100 $g.L^{-1}$)	Volume Data (0.4 mL)
Target volume (mL)	0.15	0.15	0.15	0.4
Actual volume (mL)	0.144	0.166	0.1502	0.443
Figure	5.2.2.1.1.1.	5.2.2.1.2.1	5.2.2.1.3.1	5.2.2.1.4.1
% Target volume	96	111	100	111
% RCV	7.9	0	94.4	42.3
2SE	0.223	0	0.012	0.074

b)

Manual Slurry Handling Performance	1.22 mm Pipette Tip	0.15 mL Granular Activated Carbon	Volume Data (0.4 mL)
Target resin mass (mg)	3.75	15	10
Actual resin mass (mg)	0.1	-5.14	7.08
Slurry concentration ($g.L^{-1}$)	25	100	25
Target resin mass (%)	26	-3.2	71
% RCV	11.9	632	0.124
2SE	0.223	9.6345	5.562

Table 5.2.2.1.6.1. Performance of manual slurry handling equipment at dispensing conditioned granular activated carbon slurry fractions: (a) slurry volume and (b) slurry resin mass under different scenarios investigated. Statistical analysis of the best results from each experiment displayed: 1.22 mm pipette tips 150 µL data; 150 µL water data (control); 150 µL conditioned granular activated carbon data and 400 µL granular activated carbon data. Method detailed in section 2.4.2.2.1.

The percentage target resin masses ranged between 0% to 46.0% with the best results from the powdered activated carbon data, which had the smallest particle size (10 μm to 200 μm, average 45 μm). The statistical analysis showed good precision with the powdered activated carbon data generating 2SE of 0.00001 compared to 2SE of 5.8 for the granular activated carbon data. However, neither of the activated carbon slurry preparations produced accurate or reproducible results, as the manual slurry handling equipment was not reproducible. Therefore, the performance of the automated slurry handling equipment was investigated (section 5.2.2.2).

5.2.2.1.6 Manual Slurry Handling Equipment's Performance

The statistical analysis of all the manual slurry handling experimentation data (Table 5.2.2.1.6.1) assessed each of the elements of slurry handling investigated (a = slurry volume, b = resin mass). The highest percentage volume was achieved with the 150 μL aliquots of granular activated carbon slurry (100 $g.L^{-1}$), which were dispensed using the manual slurry handling equipment fitted with 1.22 mm pipette tips (100% percentage volume). However, this data did not have the highest precision (94.4% RCV), but the data had low relative uncertainty (4.1% RSE), compared to the other scenarios investigated. The best precision for the percentage slurry volume was seen with the slurry volume data (1000 μL: 2% RCV, 1% RSE), which was expected with decreased significance of errors as volume increased.

Analysis of the water sample data quantified the error associated with the manual slurry handling equipment, which had a high degree of error and low precision. The most accurate dispensed slurry mass was achieved by dispensing 400 μL aliquots of conditioned granular activated carbon slurry with a 1.22 mm pipette tip (71% target resin mass). The precision of this data was good (0.1% RCV). The higher slurry concentration samples produced the worse precision, although the data had lower uncertainty (0.01% RSE). The statistical analysis of the data indicated that the manual slurry handling method was not suitably precise to prepare the SPE vessels so manual

slurry handling of alternative activated carbon preparations (section 5.2.2.1.5) and automated slurry handling equipment were investigated (section 5.2.2).

5.2.2.2 Automated Slurry Handling

The development of the automated slurry handling equipment for the preparation of the microscale SPE process investigated the use of the liquid handling workstation (Multiprobe II Ex®(section 3.2.1)) to automatically dispense resin slurries into vials prior to their transfer to microwell plates to prepare the microscale SPE format. The workstation was fitted with a range of commercially available pipette tips of different internal diameters (section 5.2.2.2.1) and used to develop the automated slurry handling procedure (section 5.2.2.2.2), which investigated the effect of the resin particle size (section 5.2.2.2.3). The automated SPE procedure was used to investigate suitable slurry concentrations for preparing the automated microscale SPE process (section 5.2.2.2.4) and the effect of the operation of the workstation, controlled by performance files, on performance (section 5.2.2.2.5). The automated liquid handling workstation was assessed for its slurry handling experimentation by analysing the gravimetric measurements of the vials pre and post dispensing the slurry aliquots.

5.2.2.2.1 Automated Slurry Handling: Pipette Tips

The automated liquid handling workstation was fitted with commercially available small conductive disposable (200 µL) pipette tips of a range of internal diameters to assess their suitability for automated slurry handling. The pipette tips investigated with the workstation were the standard (0.62 mm) and wide bore (1.4 mm) tips. The geometries of these pipette tips were similar to those used in the manual slurry handling experiments, which showed that the accuracy of the dispensed slurry resin mass increased with the increase in the internal diameter of the pipette tip (section 5.2.2.1.1). The dry resin mass of the slurry samples prepared using the automated slurry handling methodology was measured for a number of repeated samples (n = 12) to monitor the slurry handling performance of the workstation.

The mean and target values of the dispensed slurry fractions were displayed with statistical analysis of the data for each of the pipette tips (Table 5.2.2.2.1.1). This illustrated that the standard tips (93% target volume) were more accurate at dispensing the slurry volume compared to the wide bore tips (72% target volume). However, this trend was reversed for the resin mass with wide bore pipette tips (3% target resin mass) dispensing more slurry resin mass than the standard tips (–0.5% target resin mass), although both values were lower than expected. The dispensed slurry volume results were similar to the manual slurry handling results achieved for the range of pipette tips (95% to 101% target volume). This indicated that the automated workstation had difficulty in transferring the slurry. The dispensed resin mass values for both the manual (-19% to 26% target resin mass) and automated (-5% to 8% target resin mass) slurry handling experiments were low, although there were potential improvements that could be achieved by modifying the operation of the workstation, such as altering the automated slurry handling procedure (section 5.2.2.2.2).

The performance of the dispensed slurry volume data for the standard pipette tips (27% RCV) was better than that for the wide bore pipette tips (42% RCV). The performance of the resin mass data for both tips was poor with the performance of the standard pipette tips being slightly worse than the wide bore pipette tips. The performance of the wide bore pipette tips was poor for both of the slurry fractions dispensed using the automated method compared to the manual slurry data (11.9% RCV). Therefore, this was unacceptable for generating reproducible experimentation. The current automated workstation operation required optimisation and a range of parameters was investigated to improve the performance of the automated slurry handling.

5.2.2.2.2 Automated Slurry Handling: Procedure

The automated slurry handling procedure investigated the effect of the equipment's ergonomics and the configuration of the beaker containing the bulk slurry on the performance of the liquid handling workstation. The automated workstation was used

Pipette Tip	Standard		Wide Bore	
Internal Diameter (mm)	0.62		1.4	
Target Volume (µL)	165		165	
	Slurry	Water	Slurry	Water
Actual Volume (µL)	153.8	151.9	119.2	161.9
% Volume	93	101	72 or 93	105
CV (%)	13.5	0.6	52 or 29	16.4
2SE Volume	0.26	0.7	0.03 or0.003	15.5
Slurry Concentration ($g.L^{-1}$)	91		91	
Target Resin Mass (mg)	15		15	
Actual Resin Mass (mg)	-0.8		1.5	
% Resin Mass	-5		10	
CV (%)	-1290		320	
2SE Resin	67		3	

Pipette Tip	Standard		Wide Bore	
Internal Diameter (mm)	0.85		1.4	
Target volume (µL)	165		165	
	Slurry	Water	Slurry	Water
Actual volume (µL)	153.8	153.9	119.2	161.9
% volume	93	102	72	108
2SE volume	0.22	0.011	0.14	0.009
CV (%)	0.7	0.00101	0.146	0.015
RSE (%)	14	1	21	4
Slurry Concentration ($g.L^{-1}$)	91		91	
Target Resin Mass (mg)	15		15	
Actual Resin Mass (mg)	-0.8		1.5	
% Resin Mass	-5		8	
RCV (%)	203018		1584951	
2SE Resin	6		3	

Table 5.2.2.2.1.1. Performance of automated slurry handling using standard (0.85 mm) and wide bore (1.4 mm) pipette tips to transfer 165 µL aliquots of granular activated carbon slurries (100 $mg.L^{-1}$). Method detailed in section 2.4.2.2.2.

to transfer 150 µL aliquots of the activated carbon slurry (100 $g.L^{-1}$) from a stirred beaker into pre-weighed vials. The configuration of the beaker was modified to increase the homogeneity of the slurry by adding four glass baffles (d_B = 2 mm). The automated slurry handling was assessed using visual analysis and gravimetric measurements of the dispensed slurry aliquots.

The pipette of the workstation was positioned at different sampling locations in the beaker containing the bulk powder slurry and at different sampling heights to achieve a suitable procedure for automated slurry handling. Slurry aliquots were aspirated from a central or off-centre position and from a variety of pipetting heights ranging from 0% to 20% above the vessel's bottom. The accuracy of the dispensed resin mass increased from 27% at the 20% vessel height position at 1200 $\mu L.ms^{-1}$ aspirating and dispensing speeds to 57% slurry resin mass at the 15% vessel height position at 800 $\mu L.ms^{-1}$ aspirating and dispensing speeds. The accuracy of these methods was still below that acceptable for the preparation of the microscale SPE formats (90%). However, the performance of the automated equipment was good, achieving a 9% CV and 1% RSE at 20% vessel height and 4% CV and 1% RSE at 15% vessel height. These values were better than the performance of the manual slurry handling. These results were generated for the powder activated carbon slurry, which was expected to be more reproducible than the granular activated carbon slurry as shown by the manual slurry handling (section 5.2.2.1.6) due to its smaller particle size. The most accurate data for the automated slurry handling was achieved at 15% vessel height by sampling from the off-centre position, as this avoided the liquid vortex. The poor accuracy of these data indicated that further development of the automated slurry handling method was required and a variety of scenarios were investigated, such as the resin particle size, slurry concentration and the workstation's performance files.

5.2.2.2.3 Automated Slurry Handling: Resin Particle Size

The activated carbon resin was commercially available in a number of different preparations: granular and powdered, which have different particle size ranges. The

activated carbon preparations were assessed using the Malvern particle sizer (section 2.4.3) to determine the particle size ranges, which were illustrated in Figure 5.2.2.2.3.1. The particle size of granular activated carbon was 200 μm to 2100 μm (Figure 5.2.2.2.3.1 a) and powdered activated carbon was 10 μm to 105 μm (Figure 5.2.2.2.3.1 b). The mean diameters of the granular activated carbon particles were approximately 800 μm for granular activated carbon and 350 μm for powdered activated carbon. The resin particle size is important to the SPE process as it affects the specific surface area of the adsorbent material for adsorption of the adsorbate (appendix 14.1).

An intermediate activated carbon particle size was prepared by grinding the granular material using a pestle and mortar to generate a ground granular activated carbon sample. This reduced the size of the larger particles, creating a particle size range of 200 μm to 2000 μm with a mean diameter of 600 μm, (Figure 5.2.2.2.3.1 c). The reduced particle size of the ground activated carbon was still difficult to pipette accurately as slurry.

The granular activated carbon sample was analysed post dispensing with the solid dosing station (section 3.2.2) to show the effect on the automated dosing station. The dosing station dispensed granular activated carbon sample had a mean particle size diameter of 600 μm (Figure 5.2.2.2.3.1 d). This was smaller than the mean particle size diameter of granular activated carbon of 800 μm. The difference in the mean particle size of the samples indicated that the automated solid dosing equipment may have selectively aspirated the smaller particles in the slurry, or damage to the particles may have been incurred during transportation and storage of the samples.

The activated carbon preparations were prepared as slurries at 147 $g.L^{-1}$ or 300 $g.L^{-1}$ and the performance of the automated slurry handling equipment was assessed for dispensing aliquots (165 μL) of the slurries. The automated slurry handling methodology was used to transfer aliquots (165 μL) of activated carbon slurries (100 $g.L^{-1}$) containing specific particle size ranges. The performance of the automated slurry handling equipment was asssessed by recording the target and actual dispensed slurry

(a)

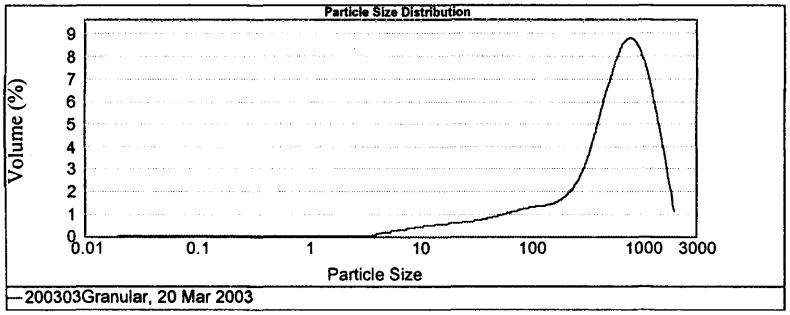

(b)

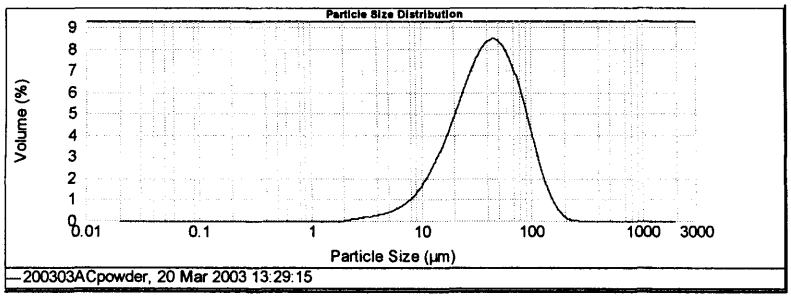

(c)

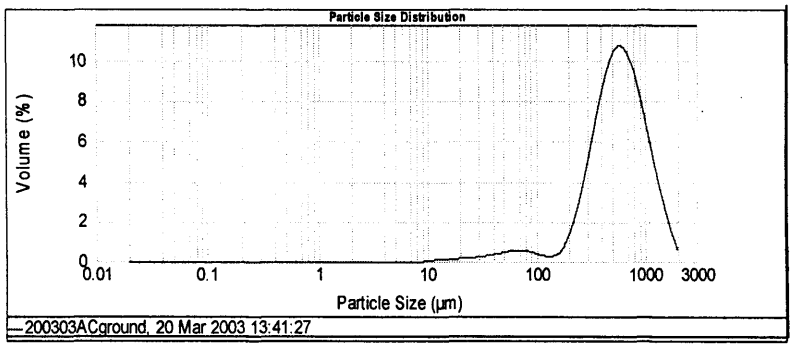

(d)

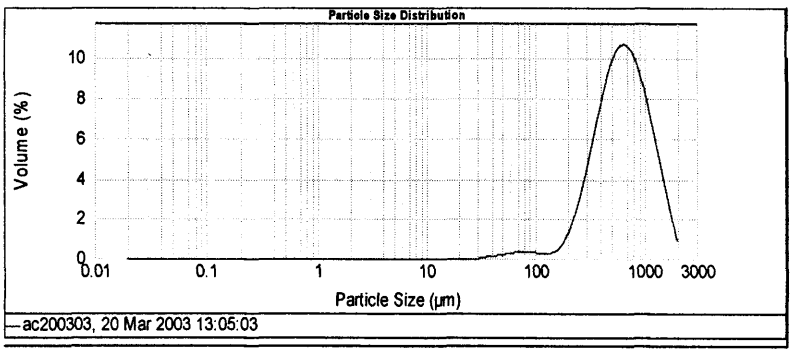

Figure 5.2.2.2.3.1. Particle size distribution of different activated carbon preparations: (a) granular; (b) powder; (c) ground and (d) dosing station dispensed granular. Particle size distributions measured on a Malvern particle sizer. Method detailed in section 2.4.3.

resin masses to calculate the percentage target resin mass dispensed (Figure 5.2.2.2.3.2). The target resin mass was plotted against the actual dispensed mass (Figure 5.2.2.2.3.2), which illustrated how the different activated carbon preparations affected the automated slurry handling capability. The actual data showed that the particle size affected the accuracy of the automated slurry handling, decreasing from 34% target resin mass for the powdered activated carbon to 19% target resin mass for the granular activated carbon. This trend was expected as the larger particle size increased the risk of the particles occluding the efficient transfer of the slurry.

The powdered activated carbon preparation (Samples 1 & 2) had the smallest particle sizes and produced the most accurate slurry resin mass dispensed (both 34% target resin mass) regardless of the slurry concentration. The accuracy of dispensing the powdered activated carbon slurry (34% target resin mass) was better than the accuracy of activated carbon preparations with larger particle sizes. This supported the findings generated using the manual powdered activated carbon slurry handling (section 5.2.2.1.6), which dispensed 16% target resin mass and was equivalent to the automated granular activated carbon slurry dispensed (16%%). The powdered material proved difficult to separate from the liquid phase by filtration, which made it unsuitable for use in the microscale SPE process.

The ground granular activated carbon (Sample 3) automated slurry handling dispensed 25% target resin mass. The ground activated carbon slurry data was more accurate than the granular activated carbon (Sample 4) and had smaller errors associated with it (2SE = 0.016 compared to 0.028). However, the use of the ground granular activated carbon in the automated SPE process would require an additional preparation stage that could not currently be automated.

The ground and granular activated carbon slurries were prepared at different concentrations (150 $g.L^{-1}$and 300 $g.L^{-1}$, respectively). The lower slurry concentration generated better accuracy (25% target resin mass) than the higher slurry concentration (19% target resin mass), although the slurries were prepared with resins of different

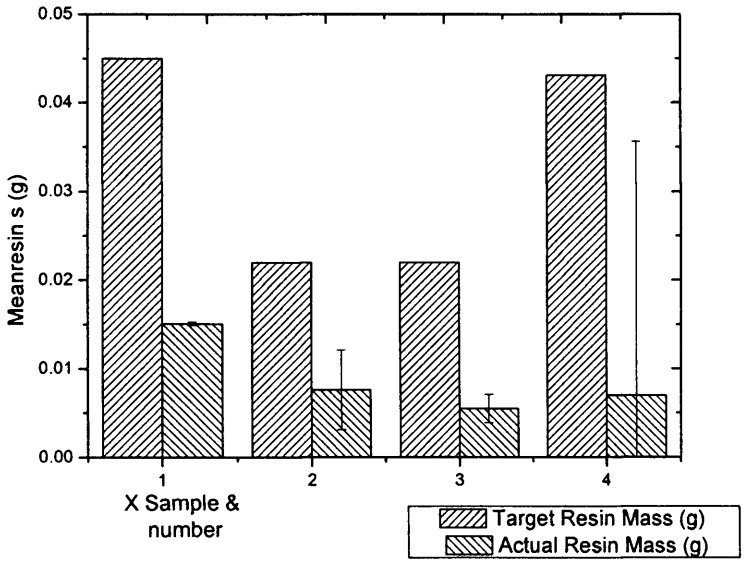

Figure 5.2.2.2.3.2. Target and actual dispensed slurry resin mass of a range of activated carbon slurry preparations transferred using the automated liquid handling workstation: (1) 300 $g.L^{-1}$ powder; (2) 147 $g.L^{-1}$ powder; (3) 147 $g.L^{-1}$ ground and (4) 300 $g.L^{-1}$ granular. Mean data (n = 12) plotted with 2SE error bars. Method detailed in section 2.4.2.2.2.

particle size ranges. The difference in accuracy may have been due to the larger resin particles occluding the orifice of the pipette tip. The ground granular resin particle generated the highest accuracy (72% target resin mass), although this result was irreproducible in subsequent experiments and had large error bars (2SE). The granular activated carbon preparation was recommended for use in further automated liquid handling experimentation for the preparation of multiwell plates for their use in the microscale SPE process (section 5.2.2.2.2)

5.2.2.2.4 Automated Slurry Handling: Slurry Concentration

The automated slurry handling capability of the liquid handling workstation was assessed over a range of granular activated carbon slurry concentrations (13.3 $g.L^{-1}$ to 300 $g.L^{-1}$). The concentration of the activated carbon slurry was increased to reduce the required slurry volume in order to achieve the required mass for the microscale extraction. The slurry concentration and volume values (Table 5.2.2.2.4.1) were selected to achieve the required $_{Qmax}$ value of 0.3 (Dutta et al, 1997a). The increased concentration may facilitate the automated preparation of the microscale SPE format by reducing the required volume and hence the speed of delivery. The increased slurry concentration was anticipated to improve the probability of the particles being aspirated within the aliquots into the pipette tips and transferred to a specific well. This may enhance the performance of the automated solid handling equipment. The dispensed slurry aliquots were recorded using gravimetric measurements and the dispensed slurry volumes and masses were calculated. The actual and target dispensed slurry volumes were plotted with the resin mass values (Figure 5.2.2.2.4.1). In addition, the experimentation investigated the effects of the workstation's operational parameters on slurry handling performance.

The gravimetric data showed accurate liquid handling over the volume range with similar actual dispensed slurry volumes to the target volumes for the range of slurry concentrations and volumes (95% to 108% target volume). The percentage dispensed

	Experimental Scenarios				
Solid phase activated carbon concentration ($g.L^{-1}$)	**0**	**13.3**	**26.67**	**66.67**	**156.67**
Slurry volume (mL)	0.15	0.15	0.1	0.05	0.025
Liquid phase 6-APA concentration ($g.L^{-1}$)	4.0	4.0	4.0	4.0	4.0
Q_{max} ($G_{6\text{-APA}}.G_{resin}^{-1}$)	0	0.3	0.3	0.3	0.3

Table 5.2.2.2.4.1. Automated slurry handling concentration and volume values investigated to generate Figure 5.2.2.2.4.1. Method detailed in section 2.4.2.2.2.

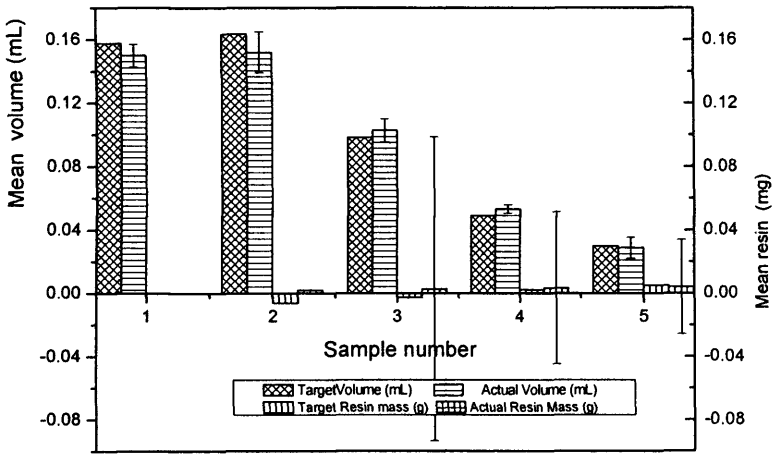

Figure 5.2.2.2.4.1. Effect of slurry concentration and volume on the automated slurry handling performance using the Multiprobe II Ex® fitted with wide bore disposable pipette tips: (1) RO water; (2) 13.3 $g.L^{-1}$ granular activated carbon; (3) 26.6 $g.L^{-1}$ granular activated carbon; (4) 66.7 $g.L^{-1}$ granular activated carbon and (5) 156.7 $g.L^{-1}$ granular activated carbon. Mean values (n = 12) plotted with 2SE error bars. Method detailed in section 2.4.2.2.2.

slurry resin values showed inaccuracies over the range of scenarios (-96% to 159% target resin mass). This poor accuracy indicated the limitations of the automated liquid handling workstation in slurry handling, which made this method of preparation of the microscale SPE format unsuitable under these default operational parameters. Therefore, the performance files of the workstation were modified to improve its performance (section 5.2.2.2.5).

5.2.2.2.5 Workstation Performance Files for Automated Slurry Handling

The automated method was used to transfer samples with a range of activated carbon slurry concentrations to assess the workstation performance file settings. Performance files were generated with specific aspirating and dispensing speeds (1 $\mu L.s^{-1}$ to 1866 $\mu L.s^{-1}$), as well as delay periods before aspirating and dispensing aliquots (10 ms to 300 ms). These parameters were selected to optimise the performance of automated slurry handling which were in excess of those achieved for manual slurry handling (section 5.2.2.1).

The dispensed slurry volume and resin mass values were plotted alongside the target values with 2SE error bars (Figure 5.2.2.2.5.1). The actual and target dispensed slurry volume values for each scenario showed acceptable percentage accuracy values (90% to 99%), which were similar to the results from previous automated slurry handling experiments. The actual dispensed resin mass values showed worse percentage accuracy values than those achieved by investigating the slurry concentration (section 5.2.2.2.4). The best performance for transferring the granular activated carbon was found using the 'slurry' performance file (Table 3.2.1.4.1), which initially had an aspirating speed of 1200 $\mu L.s^{-1}$ and dispensing speed of 1000 $\mu L.s^{-1}$. However, these values were altered to improve the performance of the workstation by modifying the aspiration speed to 10 $\mu L.s^{-1}$ with a 30 μL blowout air volume. This slower aspirating speed achieved complete dispensing of the resin into the wells rather than leaving a significant proportion attached to the disposable tip when removed after the dispensing step. However, the mass of dried adsorbent (average = 51%) was still less than the

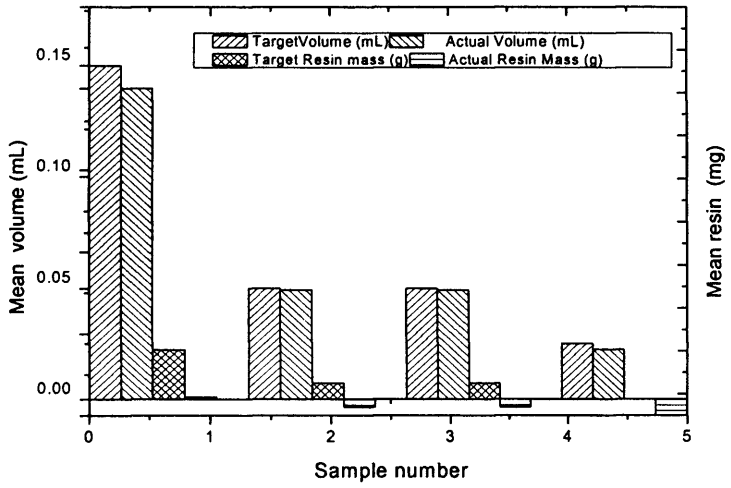

Figure 5.2.2.2.5.1. Effect of the liquid handling workstation's performance files on the automated slurry handling performance using the Multiprobe II Ex® fitted with wide bore disposable pipette tips to dispense granular activated carbon slurries (100 $g.L^{-1}$): (1) 150 µL Waste; (2) 50 µLBlowout; (3) 50 µL Waste; (4) 25 µL RO water. Mean data (n = 12) plotted with 2SE error bars. Method detailed in section 2.4.2.2.2.

target value of that in the original slurry. This may have been due to the size of the particles occluding the disposable tip orifice or their electrostatic attraction to the disposable tips. The reduced aspirating and increased dispensing speeds achievable using the automated liquid handling workstation produced better performance than the manual slurry handling. This was possibly due to the reduced variation in the aspirating and dispensing speeds used to operate the automated slurry handling equipment compared to the manual slurry handling equipment.

The automated slurry handling performance under each of the scenarios investigated did not produce reproducible or accurate dry dispensed resin masses. Neither the automated slurry handling equipment nor the manual slurry handling method were therefore suitable for the preparation of the microscale SPE formats with granular activated carbon. Alternative methods of preparing the microscale SPE experimentation were thus investigated (section 5.2.2.3).

5.2.2.3 Solid Dosing Equipment

The Accelerator™ solid dosing station and the DryPette™ dry powder pipette solid dosing devices were assessed for their suitability for accurately dispensing a known mass of a range of reagents. These reagents included granular activated carbon and Eupergit beads prepared with immobilized penicillin acylase. The equipment was kindly loaned from GlaxoSmithKline, (Tonbridge, UK) and Zinsser Analytic (UK), respectively.

The solid dosing station (section 3.2.2) dispensed the dry activated carbon particles, but not the reagents with increased moisture (conditioned granular activated carbon, Eupergit beads). The solid dosing station had limitations in its use with selected reagents and this must also be considered when assessing its suitability for the microscale SPE methodology. An additional stage must also be incorporated to condition the resin to prepare the microscale SPE format. The dry powder pipette generated a vacuum to hold the powder within a pipette tip and was then expelled under negative pressure. The dry powder pipette could only handle dry reagents

(unconditioned activated carbon) and its lowest mass of solids (min 2 mg) was unable to dispense the required masses for the preparation of the microscale SPE experimentation.

The performance of the Accelerator™ dosing station was analysed for dispensing starch and silica gel (appendix A7.3), which used the manufacturer's performance data. The performance of the Accelerator™ was acceptable and was described in section 3.2.2. This automated equipment was used with respect to microscale SPE to dispense unconditioned granular activated carbon and its performance was assessed to quantify its accuracy (Appendix A10.4.1) and precision (Appendix A10.4.2).

The dosing station dispensed less resin mass than that programmed and the data (Table 3.4.2.1.1) showed the discrepancy between the mass measured from the dosing head balance and that dispensed into the receptacle (52% to 104% accuracy, 13% to 309% CV) over the dispensed mass range. This was due to difficulties in aligning the dosing head over the receptacle, causing some of the solids to be wasted. Careful re-weighing of each sample allowed their use in the preparation of the SPE experimentation in the 96-well and 24-well plate formats. The dosing station should be further developed to overcome the realignment problems to make the equipment more suitable for its direct use in the preparation of microscale SPE formats.

5.2.2.4 Microscale SPE Solid-Liquid Mixing

The microscale SPE process investigated the requirement for solid-liquid mixing (section 2.4.4.1) using a horizontal shaker (1000 rpm). The 24-well plate format (6000 μL) contained conditioned granular activated carbon (13.3 $g.L^{-1}$ at 20 °C), which was contacted with the liquid phase containing 6-APA (4.0 $g.L^{-1}$, pH = 4.5). The adsorption kinetics were monitored by analysing the liquid phase 6-APA concentration, which was plottted against time (Figure 5.2.2.4.1). The different mixing conditions generated kinetic data that fitted exponential decay curves. The static kinetic data fitted the equation $Y = 2.6 + 1.4\ e^{(-x/349)}$ with an R^2value of 0.976 and the mixed kinetic data

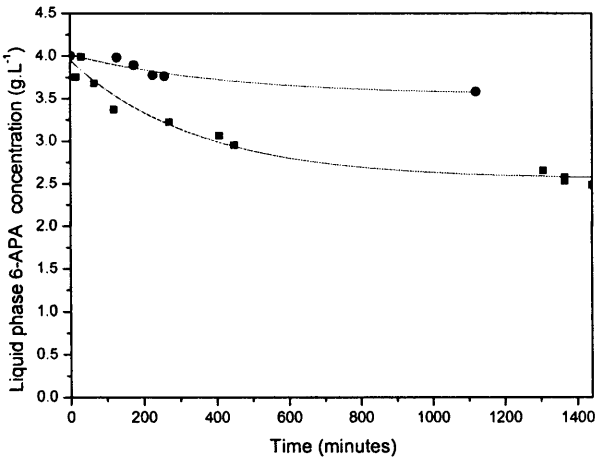

Figure 5.2.2.4.1. Effect of solid-liquid mixing on the manual 24-well microscale SPE process (6000 μL) for the extraction of 6-APA (4.0 $g.L^{-1}$, pH 4.5) with conditioned granular activated carbon (13.3 $g.L^{-1}$) at 20 °C over 24 hours: (■) static and (●) mixed using a horizontal shaker (1000 rpm). Method detailed in section 2.4.4.1.

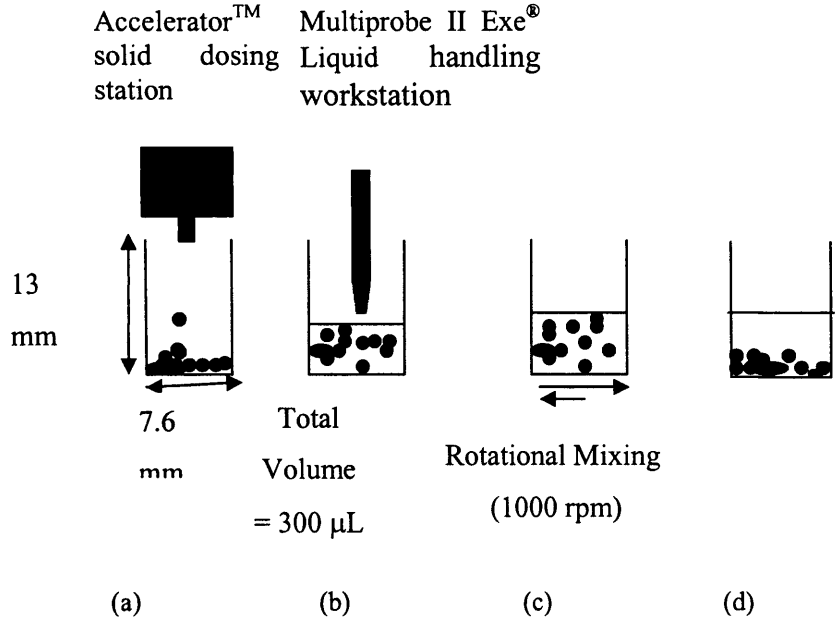

Figure 5.2.2.5.1. Schematic representation of the automated batch microscale solid phase extraction of 6-APA with granular activated carbon in a 96-well plate: (a) dispensing solid phase resin; (b) dispensing liquid phase 6-APA solution; (c) solid-liquid mixing and (d) phase separation under gravity followed by removal of the supernatant for analysis. Method detailed in section 2.4.4.

fitted the equation $Y = 3.5 + 0.5\ e^{(-x/430)}$ with a R^2 value of 0.911. The mixed kinetic data illustrated faster adsorption of 6-APA than the static kinetic data and greater adsorption at equilibrium. Mixing thus ensured the homogeneity of the suspension and facilitated good mass transfer between the liquid and solid phases. This clearly indicated the requirement for solid-liquid mixing during the SPE process at the 24-well scale and this method of mixing was also used at the 96-well microscale.

5.2.2.5 Automated Microscale SPE Process

The automated microscale SPE process was designed using the automated solid dosing station (Accelerator™) and the liquid handling workstation (Mulltiprobe II Ex®). The microscale SPE process was adapted from the laboratory process and previously published laboratory SPE method (Dutta et al, 1997a&b). The calculated Q_{max} value of 0.3 $g_{6\text{-APA}} \cdot g_{Adsorbed}$ (Dutta et al, 1997a) was maintained in the preparation of the automated microscale SPE batch process. The extraction process was carried out using the 96-deep-well plate format (1500 µL) or the 24-deep-well plate format (3000 µL).

The automated microscale SPE process methodology was developed by the initial analysis of the laboratory SPE process, which contained four main stages. These were: conditioning of the adsorbent resin; application of the liquid phase; washing the adsorbent samples adsorbed onto the resin and desorption of the adsorbate (Hennion, 1999). The automated equipment was investigated to achieve each of these SPE stages and different methodologies were assessed to prepare the SPE formats with adsorbent resins (section 5.2.1 to section 5.2.4).

The microscale SPE process used the automated equipment to develop and implement the experimental methodology. The automated solid handling was operated under optimised conditions for handling unconditioned granular activated carbon (section 3.2.2.2), which was transferred to the multiwell format. The workstation rapidly dispensed the liquid phase, operated under the 'Fst' performance file (Table 2.2.1.2.2). The microscale SPE process was illustrated schematically in Figure 5.2.2.5.1. There are four main stages within the automated microsale SPE process: dispensing the solids;

dispensing the liquid phase; mixing the phases and separating the phases. Once the phases were separated samples of the aqueous phase could be removed and analysed on the HPLC (section 2.5.1) to quantify the adsorbate concentration.

The automated platforms were assessed for their accurate and precise liquid and solids dispensing (chapter 3). The performance of these pieces of equipment affected the performance of the automated SPE process. The liquid handling workstation produced an accuracy of 2% to 10% RSD and the precision for dispensing 200 μL to 1000 μL of 0.5% SE (Parker et al, 1996). The workstation was used in the microscale SPE method (section 2.4.4) to characterize the adsorbent ('SPE 24W ACconc', 'SPE 96W ACconc'), adsorbate ('SPE 24W 6APA conc', 'SPE 96W 6APA conc') and pH ('SPE pH') isotherms detailed in Table 2.2.1.2.2.

The microscale SPE process utilised both the 96-well and 24-well formats, which was validated against laboratory scale experiments. The 96-well microscale SPE process was used to investigate the kinetics of the adsorption process, adsorbent concentration isotherm, adsorbate concentration isotherm and the effects of pH conditions on the adsorption of 6-APA with granular activated carbon. The 24-well microscale and laboratory scale SPE process investigated the kinetics of the granular activated carbon adsorption of 6-APA, as well as the adsorbent concentrations isotherm and liquid phase pH conditions.

5.2.3 Activated Carbon Adsorption Kinetics

The kinetics for the adsorption of 6-APA on activated carbon were carried out at the 24-well and laboratory SPE process scales. The laboratory scale kinetics were investigated at different adsorbent concentrations and pH conditions. The kinetics of the SPE process were investigated over 24 hours at different process scales for the adsorption of 6-APA (4.0 $g.L^{-1}$, pH 4.5) with conditioned granular activated carbon. The 24-well microscale SPE process kinetics (Figure 5.2.3.1) and the laboratory scale SPE process kinetics (Figure 5.2.3.1) showed a similar, expected trend of decreasing 6-APA concentration over time. The 24-well microscale data fitted the exponential decay

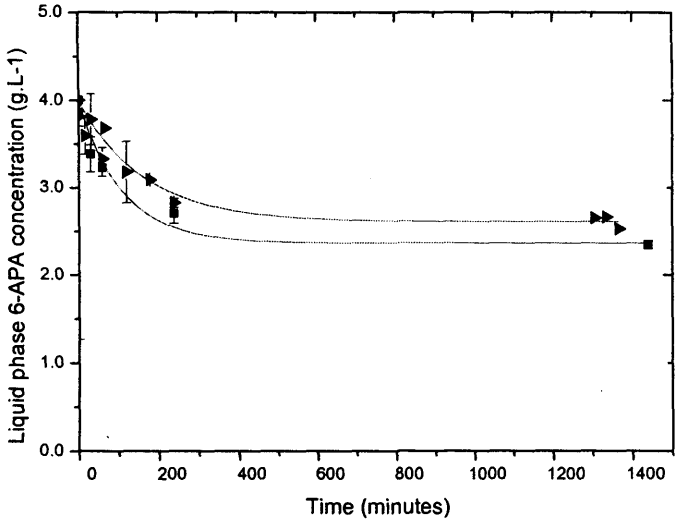

Figure 5.2.3.1. Kinetics of solid phase extraction of 6-APA (4.0 $g.L^{-1}$, pH 4.5) adsorbed onto conditioned granular activated carbon (13.3 $g.L^{-1}$) at 20 °C over 24 hours at (■)24-well microscale (3000 µL) and (▶) laboratory scale (100 mL). Solid line represents an exponential decay curve fitted to the mean data (n = 3) and displayed with 2SE error bars. Method described in section 2.4.4.2.

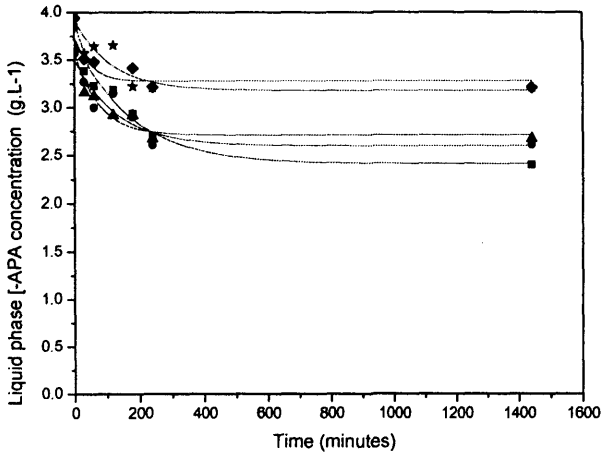

Figure 5.2.3.2. Effect of adsorbent concentration on the kinetics of laboratory scale (50 mL) solid phase extraction of 6-APA (4.0 $g.L^{-1}$, pH 4) onto conditioned granular activated carbon: (★) 0.25 $g.L^{-1}$, (◆) 0.5 $g.L^{-1}$, (▲) 1.0 $g.L^{-1}$, (●) 2.0 $g.L^{-1}$ and (■) 4.0 $g.L^{-1}$ at 20 °C. Solid lines represent exponential decay curves fitted to the data. Method detailed in section 2.4.5.1.

curve $Y = 2.56 + 1.\ e^{(-x/165)}$ with a R^2 value of 0.994. The laboratory process data fitted the exponential curve $Y = 2.4 + 1.5\ e^{(-x/109)}$ with a R^2 value of 0.946. Both sets of data showed that the equilibrium mass transfer and maximum loading (Q_{max}) were reached after 240 minutes (4 hours). The efficiency of the 24-well automated microscale SPE process achieved a 36% w/w adsorption of 6-APA and the laboratory scale process achieved a similar efficiency (41% w/w). These values were much lower than the literature value (90% w/w) (Dutta et al, 1997a), indicating that the process required optimization.

The 24-well and laboratory data indicated the phases should be contacted with each other for 240 minutes to reach equilibrium. This time period was used for subsequent experiments to investigate the effect of temperature and pH on SPE. Previous studies into microplate SPE process kinetics for the extraction of impurities from crude samples, carried out using a 96-deep well plate with a liquid phase volume of 600 μL were mixed using a shaker (Welch et al, 2002). This procedure was assumed to reach equilibrium within 15 minutes, although there was no published kinetics data for the adsorption of these pesticides. This research might have allowed insufficient time to achieve maximal adsorption of the impurities or for the extraction to reach equilibrium.

The kinetics of the SPE process were investigated for the extraction of 6-APA (4.0 $g.L^{-1}$, pH 4.5) with conditioned granular activated carbon at the laboratory scale over a range of adsorbent concentrations (0.25 $g.L^{-1}$ to 4.0 $g.L^{-1}$). The liquid phase 6-APA concentration was plotted against time for each of the adsorbent concentrations (Figure 5.2.3.2). The data fitted exponential decay curves with the fastest rate of adsorption (0.16 $g.g.Lh^{-1}$ to 0.06 $g.Lh^{-1}$) generated by the higher adsorbent concentrations. The faster adsorption rates generated rapidly decreasing liquid phase concentrations. The data matched the expected trend and all data had good fits with the trend lines. It was observed that equilibrium was reached after 4 hours, as previously seen with the microscale and laboratory kinetics data.

The effect of the pH conditions on the kinetics for the extraction of 6-APA (4.0 $g.L^{-1}$) with conditioned activated carbon (13.3 $g.L^{-1}$) was investigated over a pH range. The liquid phase was prepared at a variety of pH conditions (pH 4.5 to pH 7.5) and the adsorption was assessed at the 24-well microscale. The liquid phase 6-APA concentration was plotted against time for each of the pH conditions (Figure 5.2.3.3). The data indicated that the adsorption of 6-APA from the liquid phase onto conditioned granular activated carbon was affected by the pH conditions. The rate of adsorption increased as the pH value decreased from 0.34 $g.g.L.h^{-1}$ at pH 4.5 to 0.15 $g.g.L.h^{-1}$ at pH 7.5. All the data generated at the various pH conditions fitted an exponential decay curve with a good closeness of fit. This illustrated that the liquid phase pH conditions affected the mass transfer, which was due to the more acidic conditions affecting the surface charges of the adsorbate increasing hydrophilic interactions with the adsorbent, facilitating favourable binding with the adsorbent. The equilibrium percentage recovery increased from 15% at pH 7.5 to 45% at pH 4.5 (data taken from Figure 5.2.3.3).

The activated carbon concentration isotherms for the adsorption of 6-APA (4.0 $g.L^{-1}$) were determined at the microscale and laboratory scale. The microscale experimentation used unconditioned adsorbent due to the limitations of the solid dosing equipment, whereas the laboratory experimentation used the conditioned adsorbent as this was manually dispensed. The microscale SPE process was carried out using the 96-well format (section 5.2.4.1) and 24-well format (section 5.2.4.2), which were prepared using the automated solid dosing station and the liquid phase (4.0 $g.L^{-1}$ 6-APA, pH 4.5) was contacted with the adsorbent using the liquid handling workstation. The laboratory SPE process (section 5.2.4.3) was carried out using 20 mL tubes prepared using manual methods (section 2.4.5.3). All the formats were sealed and the reagents mixed on a horizontally rotating platform for 24 hours. Analysis of the samples was carried out on the HPLC (section 2.5.1) and the 6-APA concentration data was used to calculate $g_{6\text{-}APA}.g_{Adsorbent}^{-1}$ values to compare the process scales.

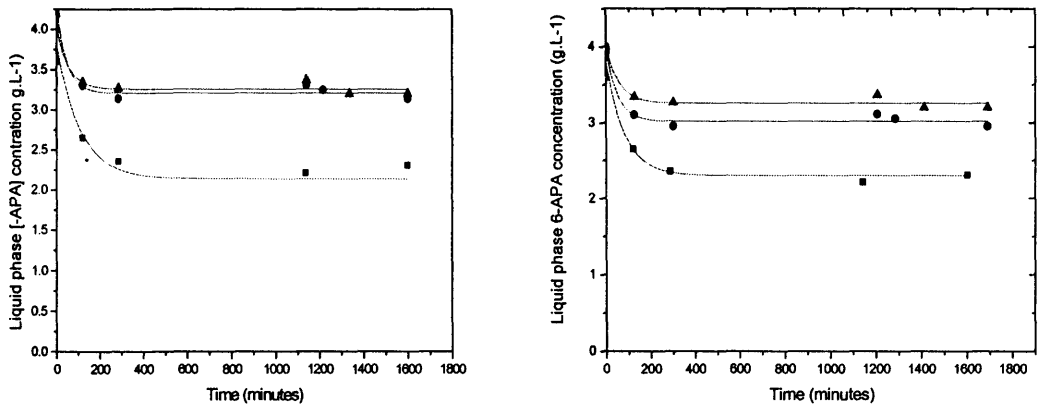

(a) (b)

Figure 5.2.3.3. Effect of liquid phase pH conditions on: (a) 96-well microscale (1500 μL) and (b) 24-well microscale (3000 μL) solid phase extraction kinetics of 6-APA (4.0 $g.L^{-1}$) onto conditioned activated carbon (0.01 $g.L^{-1}$): (■) pH 4.5, (●) pH 6.5 and (▲) pH 7.5. Solid lines represent exponential decay curves fitted to the data. Method described in section 2.4.4.3.

5.2.4 Activated Carbon Concentration Adsorption Isotherms

The activated carbon concentration isotherms for the adsorption of 6-APA (4.0 $g.L^{-1}$) were determined at the microscale and laboratory scale. The microscale experimentation used unconditioned adsorbent due to the limitations of the solid dosing equipment, whereas the laboratory experimentation used the conditioned adsorbent as this was manually dispensed. The microscale SPE process was carried out using the 96-well format (section 5.2.4.1) and 24-well format (section 5.2.4.2), which were prepared using the automated solid dosing station and the liquid phase (4.0 $g.L^{-1}$ 6-APA, pH 4.5) was contacted with the adsorbent using the liquid handling workstation. The laboratory SPE process (section 5.2.4.3) was carried out using 20 mL tubes prepared using manual methods (section 2.4.5.3). All the formats were sealed and the reagents mixed on a horizontally rotating platform for 24 hours. Analysis of the samples was carried out on the HPLC (section 2.5.1) and the 6-APA concentration data was used to calculate $g_{6\text{-}APA}.g_{Adsorbent}^{-1}$ values to compare the process scales.

5.2.4.1 Microscale 96-well Activated Carbon Concentration Isotherm

The microscale 96-well activated carbon adsorption isotherm experimentation was carried out in a 96-deep well plate (1500 µL) over a range of adsorbent concentrations (0.125 $g.L^{-1}$ to 4.0 $g.L^{-1}$ granular activated carbon). The amount of 6-APA adsorbed on the resin particles per gram of resin was plotted against the equilibrium liquid phase concentration (Figure 5.2.4.1.1). The data fitted a linear trend, which was expected for the initial part of a Langmuir isotherm (appendix 14: Figure A13.3 (I)). The gradient of this trend line (Y = 0.19X -0.40) should have passed through the axis origin, but the results did not due to the unconditioned nature of the adsorbent. On contact with the liquid phase the unconditioned adsorbent initially adsorbed the water molecules from the 6-APA solution, which increased the actual dissolved reagent concentration. The variation in the liquid phase concentration affected the 96-well adsorbent concentration isotherm more significantly than the 24-well isotherm data due to the lower extraction volumes, which generated increased scatter of the data around the trend line. The trend

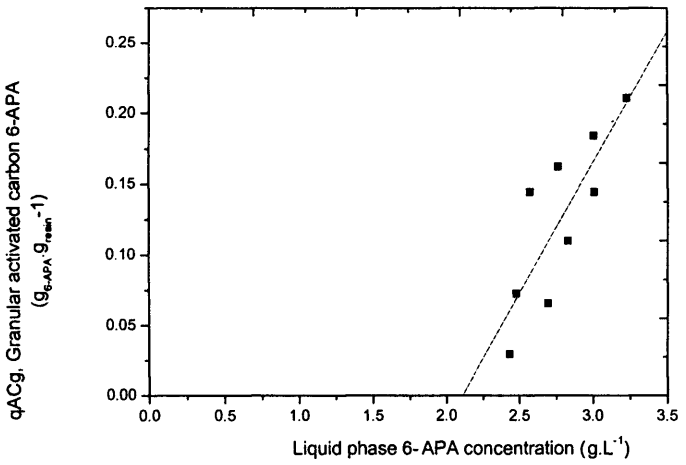

Figure 5.2.4.1.1. Activated carbon concentration isotherm for the 96-well microscale (1500 µL) solid phase extraction of 6-APA (4.0 $g.L^{-1}$, pH 4.5) adsorbed onto unconditioned granular activated carbon (1 $g.L^{-1}$ to 120 $g.L^{-1}$) at 20 °C. Solid line represents linear regression fitted to the data. Method detailed in section 2.4.4.4.

line deviated from the data generated at the 24-well scale (section 5.2.4.2) and laboratory scale (section 5.2.4.3), which was accounted for by the increased significance of any experimental errors seen at the smaller, 96-well scale. These errors may have occurred due to small variations in the operation of the automated equipment causing random experimental errors that were previously discussed (chapter 3) or degradation of 6-APA (section 5.2.1.2) during the experiment prior to HPLC analysis.

5.2.4.2 Microscale 24-well Activated Carbon Concentration Isotherm

The microscale 24-well activated carbon adsorption isotherm experimentation was carried out using a deep 24-well plate (3000 μL) with a range of adsorbent concentrations
(0.125 $g.L^{-1}$ to 4.0 $g.L^{-1}$). The liquid phase (4.0 $g.L^{-1}$ 6-APA, pH 4.5) was contacted with the unconditioned granular activated carbon. The amount of 6-APA adsorbed on the resin particles per gram of adsorbent was plotted against the liquid phase 6-APA concentration (Figure 5.2.4.2.1). The data fitted a linear trend ($Y = 0.149X - 0.26$), which was expected for the initial part of a Langmuir isotherm. The gradient for the 24-well data was similar to the laboratory scale data (section 5.2.4.3), but the 24-well data should have passed through the axis origin. The deviation of the trend line was attributed to the use of unconditioned adsorbent in the 24-well scale SPE, as seen in the 96-well adsorbent concentration isotherm (Figure 5.2.4.2.1). The deviation between the 24-well and 96-well SPE data was considered to be due to the increased significance of experimental errors at the smaller scale that affected the gradient.

5.2.4.3 Laboratory Scale Activated Carbon Concentration

The laboratory scale activated carbon adsorption isotherm experiments were carried out at the 10 mL scale in 20 mL tubes with a range of adsorbent concentrations (0.125 $g.L^{-1}$ to 4.0 $g.L^{-1}$). The liquid phase (4.0 $g.L^{-1}$ 6-APA, pH 4.5) was adsorbed onto conditioned granular activated carbon, which was dispensed manually. The amount of 6-APA adsorbed on the resin particles per gram of adsorbent was plotted against the liquid

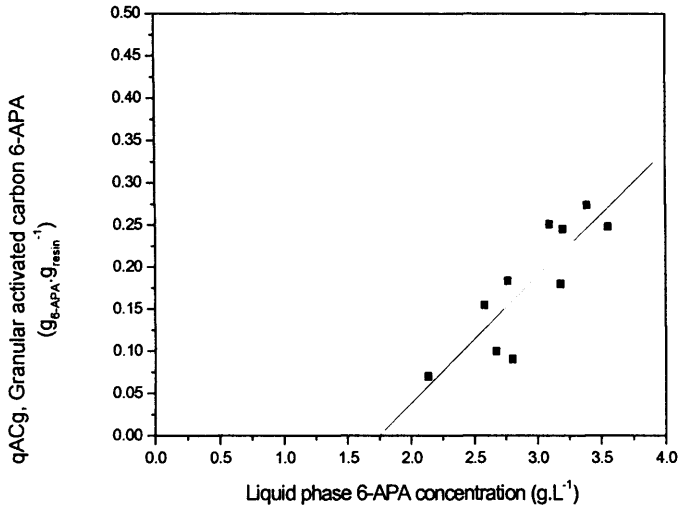

Figure 5.2.4.2.1. Activated carbon concentration isotherm for the 24-well microscale (3000 μL) solid phase extraction of 6-APA (4.0 $g.L^{-1}$) adsorbed onto unconditioned granular activated carbon (1.0 $g.L^{-1}$ to 120.0 $g.L^{-1}$) at pH 4.5 and 20 °C. Solid line represents linear regression fitted to the data. Method detailed in section 2.4.4.4.

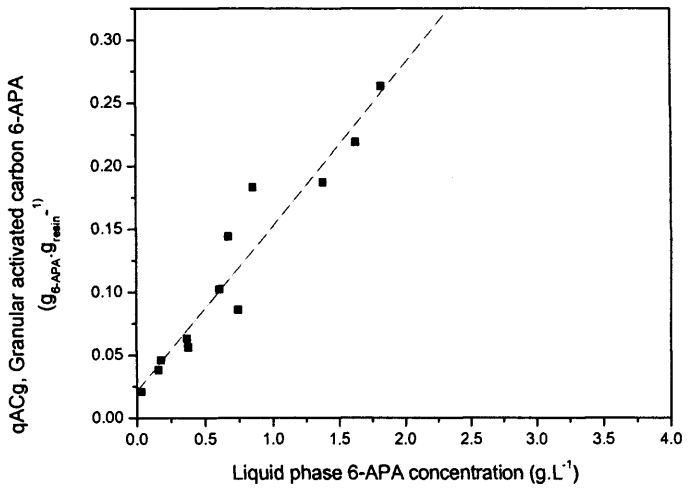

Figure 5.2.4.3.1. Equilibrium adsorption isotherm for the laboratory scale (100 mL) solid phase extraction of 6-APA (4.0 $g.L^{-1}$) onto conditioned granular activated carbon (1.0 $g.L^{-1}$ to 120.0 $g.L^{-1}$) at 20 °C and pH 4.5. Solid line represents linear regression fitted to the data. Method described in section 2.4.5.3.

phase concentration (Figure 5.2.4.3.1). The gradient of the trend line (Y = 0.13X + 0.02) fitted the initial linear part of the Langmuir isotherm. The gradient matched that of the 24-well microscale data and literature value of Y = 0.2X (Dutta et al, 1997a). The position of the data was at the lower liquid phase concentration range due to physical limitations in accurately dispensing low resin masses. The conditioned adsorbent generated data that fitted a trend that passed near the axis origin and the liquid phase concentration was not significantly affected on contact with the adsorbent. The larger volume of this scale ensured that the concentration analysis was more accurate than the microscale data.

5.2.4.4 Adsorbent Concentration Isotherm Data: Comparison of Scale

The adsorbent concentration isotherm was analysed at the 96-well and 24-well microscale, as well as laboratory scale for the adsorption of 6-APA with granular activated carbon. Each of the process scales produced a linear isotherm over the investigated adsorbent concentration range. The amount of 6-APA adsorbed onto the solid phase particles increased with the amount of adsorbed 6-APA per mass of adsorbent (Table 5.2.4.4.1).

The adsorbent concentration isotherm gradient represents the binding affinity of the adsorbent and varied between each of the process scales due to variations in the preparation of the reagents. The laboratory scale adsorbent concentration isotherm used conditioned adsorbent and the gradient (0.13) was lower than the 96-well microscale gradient (0.19) and 24-well microscale gradient (0.15). The microscale processes used unconditioned adsorbent due to the limitation of the automated dosing station, which altered the isotherm gradients by initially adsorbing the water from the liquid phase (*c.* 30%) that increased the actual 6-APA concentration. This variation affected the 96-well SPE process more significantly than the 24-well process due to the reduced relative extraction volumes, and affected the mass transfer onto the solid phase with the actual maximum adsorption being lower than that calculated. Therefore, the microscale data isotherm gradients were higher than the laboratory scale data and the trend line did not

Process Scale	Microscale 96-well (1500 µL)	Microscale 24-well (3000 µL)	Laboratory scale (10 mL)
Isotherm Equation	Y = 0.19X – 0.4	Y = 0.15X - 0.26	Y = 0.13X + 0.02

Table 5.2.4.4.1. Isotherm equations for the microscale 96-well, microscale 24-well and laboratory scale extraction of 6-APA(4.0g.L^{-1}, pH 4.5) with granular activated carbon (1.0 mg to 40.0 mg, 1.0 mg to 80.0 mg or 0.001 g to 2.5 g, respectively) at room temperature over 24 hours. Data from figures 5.2.4.1.1, 5.2.4.2.1 and 5.2.4.3.1. Method detailed in section 2.4.4.4 and section 2.4.5.3.

pass through the axis origin. The supported microscale SPE process (section 5.2.6) was developed to overcome this experimental limitation.

The solid dosing station could dispense 1 mg of solids but this was equivalent to 0.7 $g.L^{-1}$ in the 96-well microscale extraction, 0.3 $g.L^{-1}$ for the 24-well microscale extraction or 0.1 $g.L^{-1}$ for the laboratory scale extraction. This made the adsorbent concentration range more sensitive for the laboratory scale SPE process than that of the microscale SPE process.

5.2.5 Effect of pH Conditions

The effect of the liquid phase pH conditions (pH 4.5 to pH 7.5) on the SPE of 6-APA (4.0 $g.L^{-1}$) with unconditioned granular activated carbon (13.3 $g.L^{-1}$) was investigated at the 96-well and 24-well microscale (section 5.2.2.5), as well as the laboratory scale. The adsorption data from each of these scales (Table 5.2.5.1) showed similar maximum adsorption values ($g_{6\text{-APA}}.g_{Adsorbent}^{-1}$), which decreased with the increase in pH. The observed trend was similar to that seen in the kinetic data (section 5.2.3: Figure 5.2.3.1). However, the laboratory data values were slightly lower than those of the microscale data. This could be due to the higher adsorbent mass, use of unconditioned adsorbents or the increased significance of degradation of the liquid phase 6-APA at the microscale (section 4.2.1.4.1). This general trend of increasing adsorption with decreasing pH has been previously observed (Chaubal et al, 1995).

5.2.6 Supported Microscale SPE Experimentation

The supported microscale SPE process was adapted from the standard batch microscale SPE process (section 5.2.2.5) and the method by Janiszewski et al (1997), together with additional experimentation was used to generate an automated supported microscale SPE process. This process used a filter plate to support the adsorbent particles on a matrix to allow the addition and removal of liquids. The method development investigated membrane pore sizes (section 5.2.6.1) and non-specific solute membrane

Maximum Adsorption ($g_{6\text{-}APA} \cdot g_{Adsorbent}^{-1}$)	SPE Process Scale		
	96-well Microscale	24-well Microscale	Laboratory Scale
pH 4.5	0.053	0.104	0.013
pH 6.5	0.143	0.079	0.039
pH 7.5	0.060	0.023	0.027

Table 5.2.5.1. Maximum adsorption data for 96-well, 24-well microscale and laboratory scale SPE of 6-APA (4.0 $g.L^{-1}$) over a pH range (pH 4.5 to pH 7.5) with activated carbon (0.01 $g.L^{-1}$). Method detailed in section 2.4.4.3 and 2.4.5. Microscale data from figures 5.2.4.1.1, 5.2.4.2.1, and 5.2.4.3.1.

retention (section 5.2.6.1.1) to identify a commercially available filter plate as a suitable support matrix. The automated supported microscale SPE process used the automated platforms (section 5.2.6.2) to facilitate both resin conditioning and the adsorption and desorption of the adsorbate.

The supported microscale SPE process was developed from published research, which used the 96-well formatted SPE blocks (Janiszewski et al, 1997) or filter plates (Zweigenbaum et al, 1999). The 96-well SPE block contained 96 mini cartridges (1.2 mL) with pre-filters and particle loaded membranes that contained fixed adsorbent resin masses. The mini cartridges were used with a total SPE volume of 1.15 mL, which was the smallest SPE process used at the laboratory scale (section 1.5.2.1.2) and microscale (section 1.5.2.1.3). The 96-well filter plates used to purify urine samples prior to bioanalysis (Zweigenbaum et al, 1999) required a higher total extraction volume (2.4 mL) and the wells contained a fixed resin mass. The supported microscale SPE process (section 2.4.6.3) required a total extraction mass of 800 μL and was used to investigate key process parameters to optimise the purification process. Some of these SPE formats were prepared using automated liquid handling equipment. This increased the sample throughput which enhanced its performance (Jemal et al, 2000).

The automated supported microscale SPE process delivered a flexible approach to process optimisation using the 96-well plate and automated platforms to deliver a high throughput method of screening conditions to optimise the process. This process was used to generate high throughput data to analyse adsorbent capacity (section 5.2.6.3) and efficiency (section 5.2.6.4). The automated supported microscale SPE process demonstrated greater application for the rapid analysis of resin conditioning, adsorption and desorption of the adsorbate (6-APA) onto activated carbon.

5.2.6.1 Membrane Pore Size

Filter membranes with different pore diameters (0.2 μm to 1.0 μm) were investigated at the laboratory scale for retention of granular activated carbon particles (Figure 5.2.6.1.1). This demonstrated that the filters with pore sizes below 0.45 μm produced

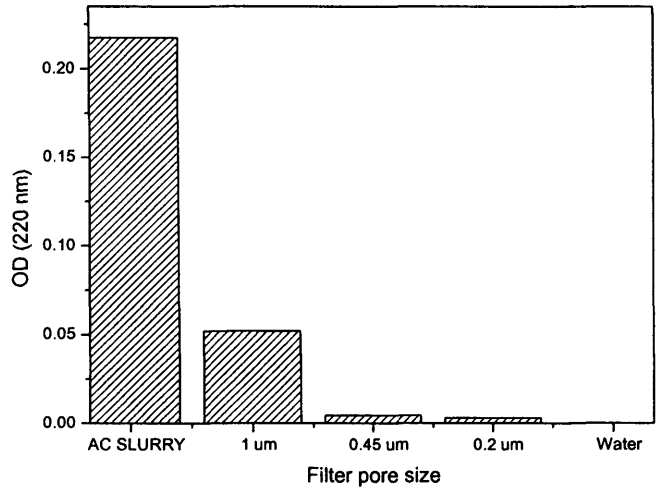

Figure 5.2.6.1.1. Clarification of activated carbon slurry samples with membranes of different pore sizes (0.2 μm to 1.0 μm). Optical density (OD) at 220 nm of the permeate from filtered granular activated carbon slurries (13.3 $g.L^{-1}$) carried out at the laboratory scale. Method described in section 2.4.6.1.

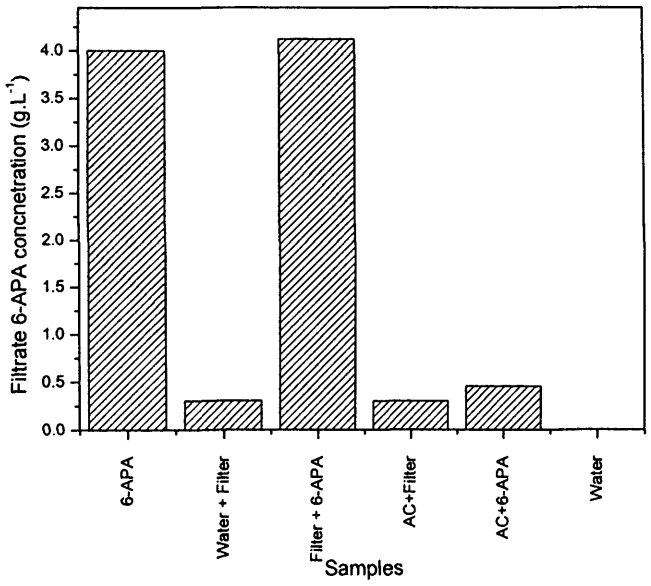

Figure 5.2.6.1.1.1. Retention of water and aqueous 6-APA (4.0 $g.L^{-1}$, pH 4.5) by the 96-well filter plate membrane (0.45 μm). The mean filtrate 6-APA concentration values (n = 3) plotted with 2SE error bars. Method described in section 2.4.6.2.

significant clarification of the granular activated carbon slurry samples (13.3 $g.L^{-1}$) and the best clarification was achieved using membranes with 0.2 μm pores (99.99% clarity).

Two commercially available filter plates, kindly provided by their suppliers, were investigated for their suitability as the matrix for the supported microscale SPE process and their compatibility with granular activated carbon and aqueous 6-APA. These filter plates were in the 96-well (Millipore, UK) and 24-well (Perkin Elmer) formats. The 96-well filter plate contained a polyvinylidene membrane (0.45 μm) and the 24-well filter plate contained a glass fibre membrane. The 24-well filter plate was not expected to be suitable as a support matrix for the activated carbon particles because the glass fibre membrane had 1.0 μm pores and the laboratory testing of this membrane (section 5.2.6.1) demonstrated that the activated carbon particles were present in the filtrate.

5.2.6.1.1 Non-specific Solute Retention on Filter Membranes

The retention of water and 6-APA on the membrane and its effects on the SPE process was investigated for the 96-well filter plates. The 96-well filter plate absorbed water and the filtrate contained particulate material from the membrane (Figure 5.2.6.1.1.1). This indicated that an initial membrane wash was a requirement for the preparation of the membrane prior to the addition of the adsorbate. The filter did not significantly absorb 6-APA from the liquid phase, which indicated that minimal water was lost from the liquid phase, so this did not affect its concentration nor deleteriously affect the SPE process. Therefore, the 96-well Durapore filter plate (Millipore, UK) used with an initial filter washing stage prior to adsorption was deemed suitable for use in the supported microscale SPE process.

5.2.6.2 Automated Supported Microscale SPE Process

The automated supported microscale SPE process (section 2.4.6.3) was developed utilising commercially available 96-well filter plates, with a suitable filter membrane that excluded the granular activated carbon particles, which were selected based on the pore size data (section 5.2.6.1). The multiwell plates were washed to remove any

particles from the membrane prior to experimentation as the retention of water by the membrane was previously indicated (section 5.2.6.1.1). The SPE format was prepared with activated carbon resin dispensed using the dosing station, the particles were contacted with various liquid reagents using a workstation and these reagents were separated from the adsorbent using a filtration rig and manifold to supply a vacuum to the filter plate in order to speed the separation of the solid and liquid phases. A schematic illustration of the supported microscale SPE process format (Figure 5.2.6.2.1) illustrated its key features.

The automated supported microscale SPE process method contained five key stages to prepare and carry out the experimentation (Figure 5.2.6.2.2). The unconditioned activated carbon adsorbent (13.3 $g.L^{-1}$) was initially dispensed into the wells using the automated solid dosing station (section 2.2.2). The adsorbent was conditioned and the membrane hydrated with the conditioning buffer (200 μL water) using the liquid handling workstation, which was later removed under vacuum. The adsorbent resin was then contacted with the liquid phase feed material (200 μL), containing 6-APA (4.0 $g.L^{-1}$). The vacuum filtration unit was used with a filtration manifold to supply a vacuum to the filter plate in order to separate the solid and liquid phases. The adsorbate was eluted from the adsorbent by the addition of an aliquot (200 μL) of the elution buffer (Methanol), which was removed under vacuum into a clean collection plate. The vacuum was supplied to the filter plate by the filtration rig fitted to a filtration manifold. This separated the solid from the liquid reagents. The adsorbate was eluted from the adsorbent by the addition of an aliquot (200 μL) of the elution buffer (Methanol), which was removed under vacuum into a clean collection plate. The vacuum was supplied to the filter plate by the filtration rig fitted to a filtration manifold. This separated the solid from the liquid reagents. The adsorbent was then washed with water to capture any remaining 6-APA.

The automated supported microscale SPE process (total volume = 800 μL) offered an adaptable system that could contain a range of adsorbent resins and masses. This microscale SPE process offered the opportunity for analysis of the conditions for

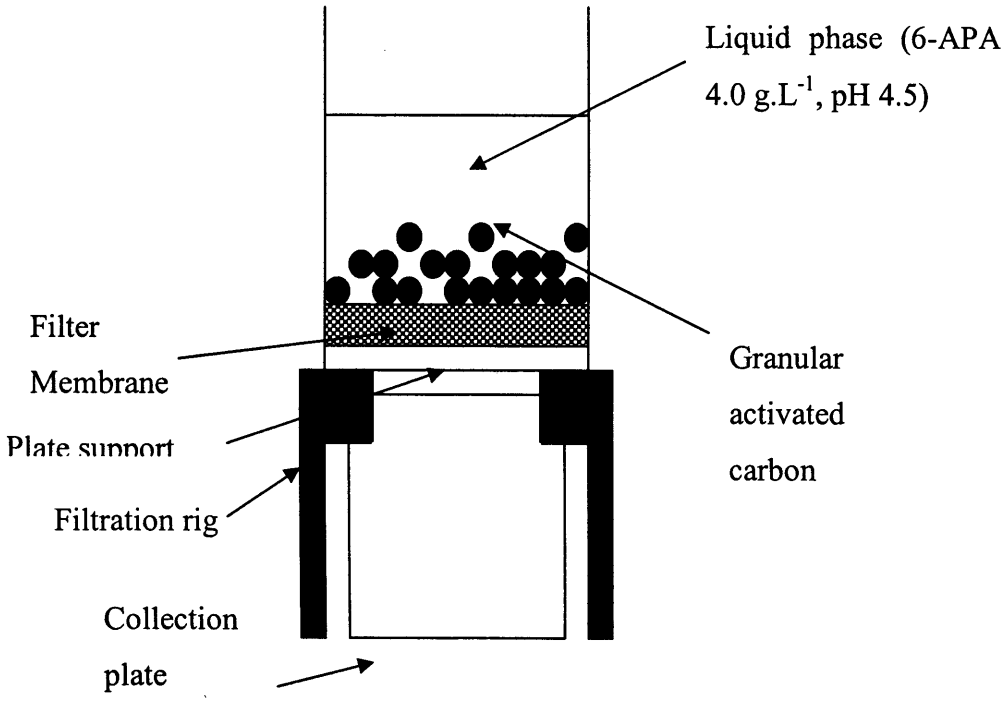

Figure 5.2.6.2.1 Schematic of a well in the 96-well plate used in the automated supported SPE process indicating the adsorbent resin, liquid phase, membrane matrix and plate support. Method detailed in section 2.4.6.

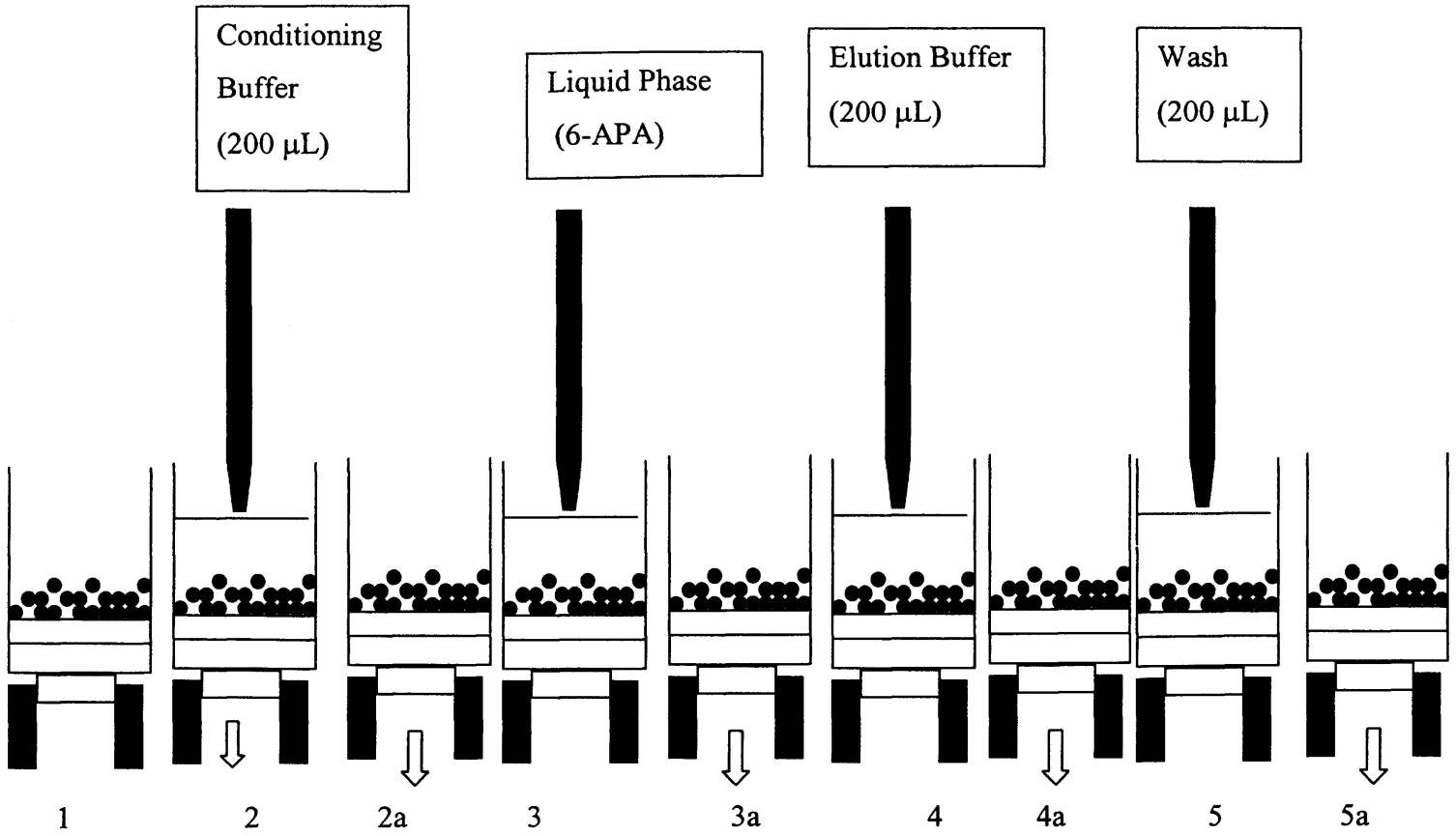

Figure 5.2.6.2.2. Schematic representation of the supported microscale SPE process stages: (1) dispense adsorbent; resin, (2) conditioning the adsorbent and membrane support; (2a) removing the conditioning buffer under vacuum; (3) contacting the liquid phase with the phase using the liquid handling workstation; (3a) removing the liquid phase under vacuum; (4) eluting the adsorbate from the solid phase and (4a) removing the elution buffer under vacuum; (5) washing the solid phase and (5a) removing the liquid wash under vacuum (total extraction volume 800 µL). Method detailed in section 2.4.6.3.

adsorbent conditioning, adsorption, washing the samples adsorbed onto the resin and elution of the adsorbate. The supported microscale SPE process was used to screen the adsorbent capacity for 6-APA (section 5.2.6.3) and process efficiencies (section 5.2.6.4).

5.2.6.3 Adsorbent Capacity

The capacity of the granular activated carbon for the adsorption of 6-APA was assessed using the 96-well supported microscale SPE process. The adsorption of 6-APA onto the activated carbon particles was assessed over time by the sequential addition of liquid phase aliquots (300 μL) to the wells, contacting the phases for 15 minutes before separating them under vacuum. Analysis of the filtrate's 6-APA concentration was plotted against the total liquid phase volume or total 6-APA added to the well (Figure 5.2.6.3.1). The data trend lines illustrated the mass transfer between the solid and liquid phases. The data had a good fit with the exponential decay and growth curves ($1.5\ Y + 1.5\ e^{(X/8.3)}$, $-1.6\ Y + 5.6\ e^{(X/2.0)}$), which illustrated the mass transfer between the liquid and solid phases. The liquid phase had an acceptable regression analysis value of 0.981 and the solid phase showed a closer fit of the data with a R^2 value of 0.993. The data indicated that the resin had not adsorbed the maximum adsorbate due to the limitations of the volumes investigated. This experimentation should be expanded to validate the supported microscale SPE process, but time restrictions prevented this occurring.

The 96-well supported SPE process data did not cover the 6-APA volume range to saturate the activated carbon ($1.13\ g.L^{-1}$) adsorbent. The maximum capacity of the adsorbent for 6-APA was 0.6 $g_{6\text{-}APA}.g_{Adsorbent}^{-1}$, which was higher than the previously reported value of 0.3 $g_{6\text{-}APA}.g_{Adsorbent}^{-1}$ (Dutta et al, 1997a). The variation may have been a result of variation in the experimental conditions, such as increased temperatures causing degradation of the liquid phase 6-APA concentration or the mixing conditions on the concentration which was higher than that achieved using the batch 96-well microscale SPE process (79%). The difference in these recoveries was expected due to

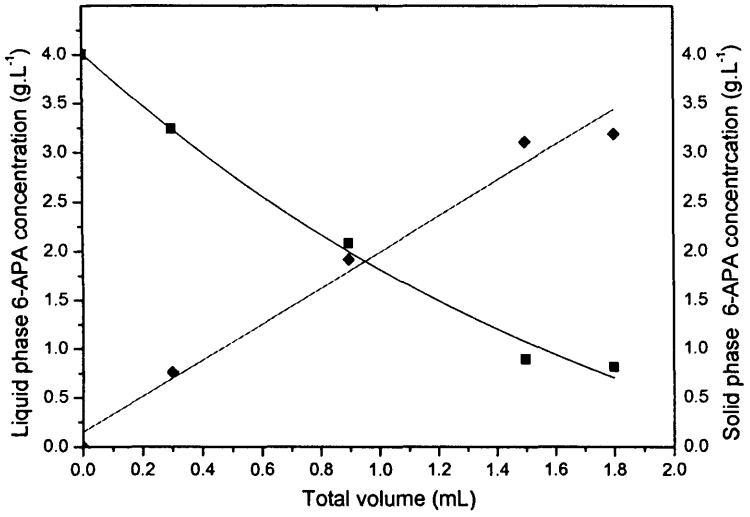

Figure 5.2.6.3.1 Granular activated carbon (13.3 $g.L^{-1}$) capacity for 6-APA (4.0 $g.L^{-1}$, pH 4.5) at the 96-well microscale showing the concentration of 6-APA in the (■) liquid phase and (♦) bound to the solid phase. Solid lines represent Gaussian curves fitted to the data as the adsorbate is adsorbed onto the resin. Method detailed in section 2.4.6.4.

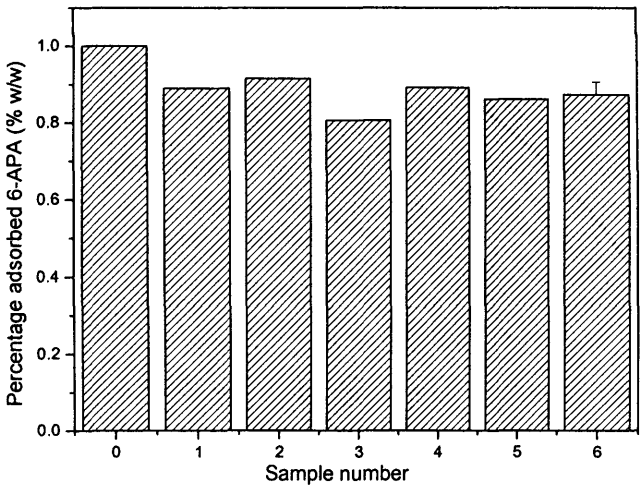

Figure 5.2.6.4.1. Percentage adsorbed 6-APA for replicate samples using the 96-well supported microscale SPE of 6-APA (4.0 $g.L^{-1}$, pH 4.5) onto conditioned granular activated carbon (13.3 $g.L^{-1}$). Samples: (0) feed material. (Samples 1 to 5) individual SPE data and (6) mean data (n = 5) with 2SE error bar. Method detailed in section 2.4.6.5.

the pre-conditioning of the horizontal shaker, which affected mass transfer. To fully validate this process further investigation would be required to assess these variations.

5.2.6.4 Efficiency of the Supported SPE Process

The supported microscale SPE process was used to quantify the efficiency of the adsorption of 6-APA (4.0 $g.L^{-1}$) onto granular activated carbon particles (13.3 $g.L^{-1}$). The 0.45 μm polyvinylidene fluoride membrane 96-well filter and granular activated carbon adsorbent were washed with an aliquot of reverse osmosis water prior to their contact with the liquid phase. The equilibrium liquid phase concentrations for a number of samples were used to calculate the percentage of 6-APA adsorbed by the adsorbent used in the supported microscale SPE process (Figure 5.2.6.4.1). These showed that a high degree of 6-APA adsorption (average = 87.3% w/w) was achieved using this method. The maximum efficiency (100% adsorption) of these process conditions was not expected because 6-APA may degrade (section 5.2.1.2) during the process, as previously discussed in chapter 4 (section 4.2.1.4.1). The utility of the 96-well microscale supported SPE process was demonstrated in these experiments. However, it was considered that the 96-well microscale supported SPE process was capable of further reduction in extraction volume, but time did not allow for these comprehensive experimentations to be carried out.

5.3 Conclusion

The solid phase extraction process was developed at the microscale and a range of experiments were carried out to investigate the key process parameters, which were replicated at the laboratory scale. The SPE process characteristics were investigated for the development of the automated microscale SPE process and this data was used to assess the suitability of the automated equipment for the preparation and implementation of the microscale SPE experimentation. The automated microscale SPE process was used to investigate the SPE kinetics, adsorbent concentration and pH isotherm. The supported microscale SPE process was developed for investigating the

in-situ adsorbent conditioning, SPE experimentation and adsorbate elution to facilitate the automation of the process. The automation of the entire SPE process will be integrated with additional automated purification processes to generate rapid analysis of suitable purification routes.

The characteristics of the SPE process were initially investigated to find suitable adsorbent resins, adsorbate and SPE formats for the development of the microscale SPE process. The commercially available application development kit was used to screen the adsorbents housed within pre-filled 1 mL cartridges (8 adsorbent resins) for the adsorption of 6-APA, but the adsorption efficiencies of these resins were poor (< 25%). A variety of adsorbent resins (activated carbon, XAD-7, XAD-16) were investigated for the extraction of 6-APA at laboratory scale, which all had high efficiencies (80% to 90% adsorbed 6-APA). Activated carbon was recommended for the development of the microscale SPE process, as it showed good efficiency for the adsorption of 6-APA, was widely available and has been extensively used at a variety of scales. The degradation of the adsorbate was influenced by the experimental conditions, with increased degradation at 20 °C, but this was not considered significant enough to require experiments to be carried out at lower temperatures. This was advantageous as the automated equipment is large and would have required a refrigerated room. The SPE formats were assessed for their suitability for the development of adaptable, quantitative SPE experiments using 96-well and 24-well plate formats. The activated carbon adsorbent resin was selected for the SPE of 6-APA from an aqueous feed with the 96-well and 24-well plates selected for the development of the microscale SPE process.

The manual and automated slurry handling equipment was investigated for their capability to dispense activated carbon slurry, investigating performance over a range of pipette tips, reagents, slurry volumes and activated carbon preparations. The performances of these scenarios were not suitably accurate or precise to reliably and reproducibly dispense the adsorbent samples to prepare the microscale SPE formats. The automated solid dosing equipment was assessed for dispensing a range of

adsorbent solids. The automated dosing station was used in conjunction with additional manual weighing of the resin solids to prepare the extraction wells in the microscale SPE formats.

The implementation of the automated microscale SPE experimentation was achieved in 96-well and 24-well plates using the automated liquid handling workstation fitted with a filtration rig. The requirement for solid-liquid mixing was investigated and it was shown that the phases were suitably mixed in the extraction wells using a horizontally rotating platform. The automated microscale SPE processes were prepared using the automated solid-dosing station to prepare the adsorbent solids and the liquid handling workstation to contact the liquid phase with the adsorbent. The phases were contacted and mixed on a horizontal shaker for up to 24 hours before they were separated under a vacuum using the filtration rig. The 6-APA concentrations of the samples were quantified by the HPLC (section 2.5.1) and used to assess the SPE process. The microscale and the laboratory process scale SPE processes were used to characterize the SPE of 6-APA with activated carbon by investigating the extraction kinetics, adsorbent concentration isotherm and pH isotherm.

The kinetics and isotherms of 6-APA extraction with granular activated carbon was carried out at the 24-well and laboratory SPE process scales over 24 hours. The kinetics was also measured over a range of adsorbent concentrations and liquid phase pH conditions. They were similar to kinetic data generated at the 24-well and laboratory scales, which validated these experiments. The kinetics were accelerated using more concentrated adsorbent extractions and at lower pH conditions, which enhanced the purification of 6-APA.

The granular activated carbon concentration isotherms were carried out at the 96-well, 24-well microscale and laboratory scale for the adsorption of 6-APA. There was a good correlation between the 24-well microscale and laboratory scale data, which had similar isotherm gradients. The microscale adsorbent isotherms were generated using unconditioned adsorbent, which absorbed water from the liquid phase prior to

adsorption of the adsorbate, modifying 6-APA concentrations and shifting the isotherm from the axis origin. This identified a limitation of the microscale SPE process. The 6-APA concentration isotherms experimentation was carried out with granular activated carbon at the 96-well microscale, 24-well and laboratory scale to validate the adsorbent concentration isotherm data, but these results were not reliable enough to be presented and time restrictions prevented further experimentation.

The pH conditions of the liquid phase were investigated at the 96-well, 24-well and laboratory scales for the equilibrium adsorption of 6-APA with granular activated carbon to identify Q_{max}. The Q_{max} values increased with the decreased liquid phase pH conditions, however, the laboratory values were slightly lower than the microscale data. This trend agreed with that previously observed by Chaubal et al (1995) of the adsorption increasing with decreasing pH. The trend was replicated at each scale, although the laboratory data values were slightly lower than the microscale data. This could be due to the higher adsorbent mass, use of unconditioned adsorbents or the increased significance of degradation of the liquid phase 6-APA at the microscale (section 4.2.1.4.1). The Q_{max} values for the different scales were similar and validated the experimental processes, which matched the published data (Q_{max} = 0.3) for the laboratory scale SPE (Dutta et al, 1997a).

The microscale SPE process was adapted to generate the supported microscale SPE process, which used a support matrix to hold the adsorbent particles. This supported microscale SPE process was developed for the 96-well format, which used commercially available filter plates to provide a support matrix for the adsorbent and adsorbate during contact between the phases. The filter membranes were assessed for retention of the activated carbon particles and the membrane with 0.45 μm pores was considered the most suitable. This filter plate was investigated for retention of the adsorbate and it was demonstrated that after its initial hydration it did not significantly adsorb the adsorbate and so was considered a suitable support matrix. This experimental technique utilised the solid dosing station to prepare the various resin

masses and the liquid handling workstation to prepare the liquid phase of the SPE experimentation.

The supported microscale SPE process facilitated the screening of conditions for adsorbent conditioning, adsorbate adsorption and elution of the adsorbate from the adsorbent. This allowed the characterisation and optimisation of the SPE process for the extraction of 6-APA. The supported microscale SPE process was used to quantify the adsorbent's capacity and efficiency for 6-APA. The supported microscale SPE process was 87% efficient and was demonstrated to adsorb more 6-APA than the microscale SPE process. This process facilitated the investigation into the complete adsorption and desorption process, which could be used for the screening of adsorption solvents or conditioning reagents in order to optimise the entire SPE process. This increased utility made this experimental process the SPE process of choice.

The supported SPE process would enable the automation of the entire SPE process and so facilitated the integration of sequential purification processes. The supported microscale SPE process used a total extraction volume of 800 μL, which was below that of any published SPE methods. However, it was considered that the extraction volume could be reduced to 400 μL by reducing each of the aliquots to 100 μL, which was not expected to have any detrimental affects on the performance of the SPE process. Investigations to validate this and further reduction of the process volume limits was not permitted due to the restrictions of time. The supported microscale SPE process could be used to investigate this further, focussing on the washing and elution stages of the SPE process.

The SPE experiments used a pure aqueous 6-APA liquid phase that did not contain any contaminants. If the liquid phase used was from a real feed stream, for example one that had been taken directly from the bioconversion or after a primary purification stage, it would have contained additional contaminants. These contaminants could have interfered with the 6-APA binding to the adsorbent, reducing the recovery of the SPE process and could bind irreversibly, in turn wasting the adsorbent.

In this chapter the microscale SPE process was developed, validated and used to generate kinetics and isotherm data. The previous chapters discussed the suitability of the commercially available automated equipment for the development of microscale purification processes (chapter 3) and the development of the microscale LLE process (chapter 4). In the next chapter the microscale research will be assessed for its commercialisation and business potential (chapter 6).

Chapter 6: Commercial Potential of Research

6.1 Executive Summary

During the course of this research funds were obtained from the Centre for Scientific Enterprise (a collaboration between UCL and the London Business School) to carry out a three month evaluation of microscale process optimisation in relation to the establishment of a new technology venture. This chapter gives a summary of the evaluation generated in 2003 and is included here as one of the requirements for the Centre of Scientific Enterprise funding.

Pharmaceutical companies, and in particular biopharmaceutical companies, are under extreme pressure to increase the throughput of their drug pipelines. In so doing, product development and clinical trials dictate the project's critical path to getting the pharmaceutical to market. Tight deadlines are often achieved at the detriment of process development.

Strict regulation means that manufacturing processes are fixed early in the development cycle, often before they are fully optimised. Plant and production efficiencies remain sub-optimal for the lifetime of the drug as the costs and risks associated with changing an approved process are too great. Smart Screening for Process Design Optimisation (SS-PDO) offers a better way forward. Process optimisation can be carried out in the laboratory at a smaller scale, in a shorter time and at lower cost than before. Two developments make this possible: (i) research work carried out as part of this thesis has demonstrated the scientific validity of the approach; (ii) a system architecture has been defined which integrates standard laboratory equipment to provide a fully automated path to an optimised process.

It is believed that incumbent automated laboratory equipment manufacturers are best placed to take this new technology to market. They have access to large customers and have total control over their existing product portfolios on which the SS-PDO concept depends. However, manufacturers will depend on the unique collection of knowledge and skills of UCL researchers to commercialise the concept. It is recommended a consultancy venture be formed to partner this knowledge with the strategic resources of an operational equipment manufacturer (OEM).

6.2 Introduction

Most chemical and pharmaceutical manufacturing process development is done at pilot plant scale. Whilst smaller than full scale manufacture, pilot plant trials are expensive and time consuming.

What if manufacturing processes could be optimised on the laboratory bench? What if the optimisation could be performed automatically? Smart Screening for Process Development Optimisation promises just that.

Research by the author and others at University College London (Doig et al, 2002, Nealon et al, 2005, Doig et al, 2005) has shown that automated high throughput screening systems can be used to optimise production of molecules at the microlitre scale. Critically, the optimised microscale processes can be possibly scaled up. Bringing such techniques to the market requires the integration of a diverse range of software, equipment, scientific understanding and experimental results. While the concept is simple, its delivery is not.

During the course of this evaluation, the greatest challenge has been to define the technology sufficiently clearly to allow the development of possible business models to gain an insight into the potential market. Primary research has validated the concept and indicated a strong level of interest from our selected initial market. The challenge remains in the formulation of the mechanisms to deliver the real advantages of SS-PDO to clients.

6.3 Technology Summary

Smart Screening for Process Design Optimisation relies on experimental results, which demonstrate that processes identified and optimised at the microscale can be scaled up to litre scale experiments at the same yields and product quality. The implication of this research is that companies seeking to optimise production processes of large molecules, such as proteins, may do so in an automated laboratory, saving time and money. The approach is applicable to many liquid or soluble products, including pharmaceuticals, foodstuffs, healthcare and beauty products.

6.3.1 How the Technologies are Currently Used

The knowledge is applied through the integration of three existing technologies: factorial design software, automated equipment with experimental analysis and windows of operation software. Figure 6.3.1.1 illustrates the relationships between these components.

Factorial design software is used to design experiments to investigate particular conditions of a chosen process parameter that are affected by multiple factors, such as concentration and temperature. High and low values of this parameter are tested, to determine specific effects and interactions. A trained operator, who understands the experimentation, can select the data inputs must program this software.

Many pharmaceutical companies have installed automated liquid handling workstations (section 1.3.2.1.1), auto-sampling analysis tools and other automated equipment (section 1.3.2). Such equipment allows multiple experiments to be carried out in a rapid and repeatable way, reducing the reagent volume and manual labour and increasing quality of results.

Equipment manufacturers have developed devices and software programs, which allow a variety of production processes and purification steps to be used in the experimental design. These include precipitation, crystallisation, chromatography, liquid-liquid extraction, solid phase extraction, centrifugation and filtration together with a variety of bioanalysis techniques (section 1.4.3.2). Standard 96-well plate formats allow multiple experiments to be performed essentially simultaneously on a microscale. Pharmaceutical production lines use the same production and purification steps to manufacture target molecules, only on a far larger scale.

Other manufacturers have developed systems that connect 'islands of automation', such as liquid handling workstations and autosampling analysis tools. For example, Zymark's CLARA™ software co-ordinates the operation of automated equipment, such as Twister II a robotic arm, linking a simple interface with over 60 different laboratory devices. Figure 6.3.1.1 illustrates the use of a robotic arm to move samples between equipment units.

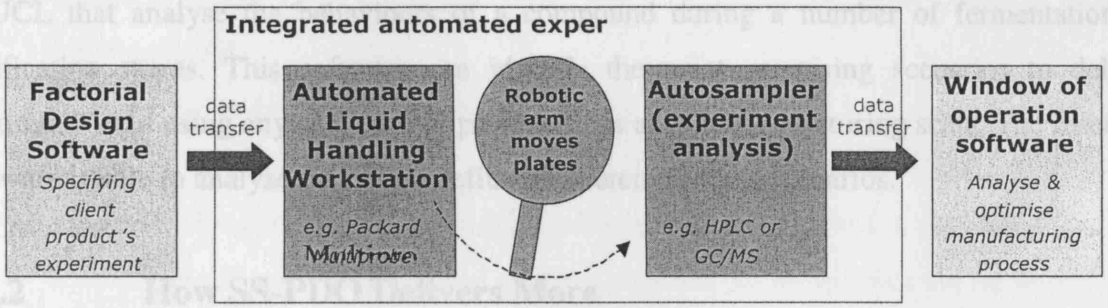

Figure 6. 3.1.1. Overview of existing technologies.

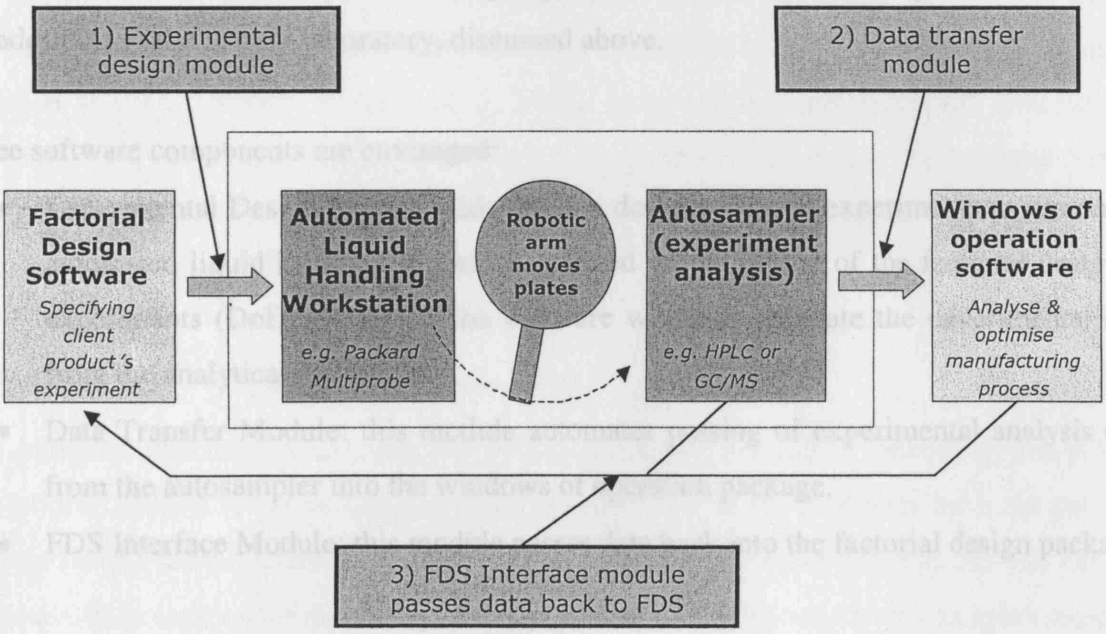

Figure 6.3.2.1. Overview of SS-PDO.

The automated equipment must be programmed to run a particular experiment using the operational software provided by the manufacturer and used to develop optimisation experimentation by a trained operator.

Windows of operation software: experimental data has been used to construct software tools at UCL that analyse the behaviours of a compound during a number of fermentation or purification stages. This software can identify the most promising scenarios to deliver maximum yield using any sequence of process steps at full manufacturing scale. The research software is able to analyse the cost benefits of different process scenarios.

6.3.2 How SS-PDO Delivers More

SS-PDO has been conceived as a suite of software tools that will integrate the three existing technologies, discussed above, to deliver automated process design optimisation. No single experiment run on a liquid handling workstation will deliver an optimised process. Multiple experiments must be conducted with analysis of results and subsequent experiment design modification. Performed manually, such work is time consuming and costly. It is proposed that the iterative element of process design optimisation be automated. Figure 6.3.2.1 shows the additions to the current laboratory, discussed above.

Three software components are envisaged:

- Experimental Design Module: this module designs a set of experiments to run on the automated liquid handling workstation based on the output of the factorial design of experiments (DoE) software. The software will also integrate the experimental data from the analytical instrument.
- Data Transfer Module: this module automates passing of experimental analysis data from the autosampler into the windows of operation package.
- FDS Interface Module: this module passes data back into the factorial design package.

Installed and configured, the complete system is designed to run several experimental iterations automatically. Once the analysis results from the autosampler meet the specified success criteria, the iterative cycle is ended. The final experiment design produced by the experimental design Module constitutes the optimised microscale process.

6.3.3 Key Benefits of SS-PDO

There are several key benefits to automated process design optimisation:

- Superior process designs deliver higher product yields at lower cost, once in production.
- Reduced labour costs: reprogramming and redesigning of experiments is handled automatically.
- Higher productivity: automation may be scheduled to work 24 hours a day, 7 days a week.
- Parallel tasking: many experimental conditions may be screened in tandem.
- Lower reagent costs: quantities of reagents required per experiment are far lower.

6.3.4 Current Status of SS-PDO

6.3.4.1 Experience with the Technology

At the present time, SS-PDO does not exist, even in prototype form. In essence, the offering is at the conceptual stage. Scientific research has proven the validity of the approach only for key parameters for certain processes. These include: kinetics, phase mixing, solvents and pH for liquid-liquid extraction; kinetics, substrate concentration, aeration and pH for fermentation (Doig et al, 2002), kinetics (Nealon et al, 2005), phase mixing; and adsorbent concentration for solid phase extraction. . The pieces of interacting software are required to turn the concept into reality have been identified, and the architecture has been set out. However, no detailed design for a working system has been developed.

6.3.4.2 Uncertainties of the Technology

The scientific principles underlying the use of automated laboratory technology for process design optimisation are at an early stage of development. Many processes have not yet been analysed using the automated approach. Development of experimental programs and analysis of results from such experiments will take significant further effort. Other processes requiring full investigation include fermentation, solid phase extraction, filtration, and centrifugation. The goal is to carry out whole microlitre production and purification processes successfully.

The process parameters that have been investigated have only been demonstrated to scale up to the millilitre scale. There is no proof that microscale experiments may be scaled up to manufacturing scale (1000 mL and above) without significant redevelopment.

6.3.4.3 Software Interfacing

There exists a wide variety of automated and analytical equipment. A large selection is required to carry out automated microlitre experimentation. In the first instance, the integration task required to deliver SS-PDO, as a system will be made easier by the adoption of a single equipment supplier.

Leading manufacturer in 2003, Perkin Elmer offers the widest range of equipment, allowing a greater diversity of experiment design. It is envisaged that development of an initial SS-PDO system would be based around Perkin-Elmer instruments. Many pharmaceutical companies favour this manufacturer (the initial target market for SS-PDO).

6.4 Potential Markets for SS-PDO

6.4.1 Processing and Manufacturing Industries

Many industries manufacture products that are in liquid form. Many could benefit from SS-PDO technology. Examples include the bulk chemicals industry, healthcare, beauty products, food and beverages. However, bulk chemicals are not a particularly attractive market for SS-PDO. Processes are already well understood, reagents costs are generally low and many process steps cannot be performed at ambient temperatures (20 °C) supported by the laboratory equipment. Many modern pharmaceuticals, biopharmaceuticals, require a gentle production route and this is a growing submarket to the pharmaceutical industry that would be suited to this technology (section 6.4.2).

The food and beverage industry, like healthcare and beauty products, is highly competitive and so the opportunity to reduce manufacturing costs would be welcome. These industries show a modest amount of innovation that could provide an entry opportunity for SS-PDO.

6.4.2 Biopharmaceutical Industry

The most significant market for this technology is likely to be the biopharmaceutical industry. This industry operates in a heavily regulated environment. New products require extensive pre-clinical and clinical trials before reaching the market. Currently only 1 in 10 candidate drugs that enter clinical trials are approved by the regulatory agencies (Food and Drug Administration (USA), Medicines Control Agency (UK), European Medicines Evaluation Agency (Europe). On average, it takes 5 to 12 years before a new product generates a dollar of revenue. Figure 6.4.2.1 shows the typical clinical trial process for a new pharmaceutical product.

Biopharmaceutical companies are often focused primarily on product development and innovation. The pressure to push candidate molecules through the drug development pipeline often limits the time spent on process development and optimisation. The logic behind this approach is clear: only a small fraction of candidate molecules succeed in moving from concept stage to market. Time spent on extensive process development would risk limiting flow through the drug pipeline, thus cutting off the industry's future supply of cash.

Research examined 23 major development projects at 11 American and European biopharmaceutical companies (Pisano and Wheelwright, 1995). They showed that many faced unexpected problems in process development, which delayed product launch or limited the commercial success of the product. These problems were the direct result of the belief that process development was a relatively low priority.

In comparison with industrial synthesis of traditional chemical pharmaceuticals, biopharmaceutical manufacturing processes are much more complex and expensive. As a result, the cost of goods for biopharmaceutical drugs is typically, 20% to 30% of sales prices (Farid, 2003).

Before a product can be used, the manufacturing process must be approved by the relevant regulatory agency to establish that it will consistently produce a high quality and safe products (FDA, 2002). Process modifications after a drug is launched normally require re-approval and new clinical data. The effect of these regulatory requirements is to lock in the manufacturing process early (Foo et al, 2001). Engineers are required to develop

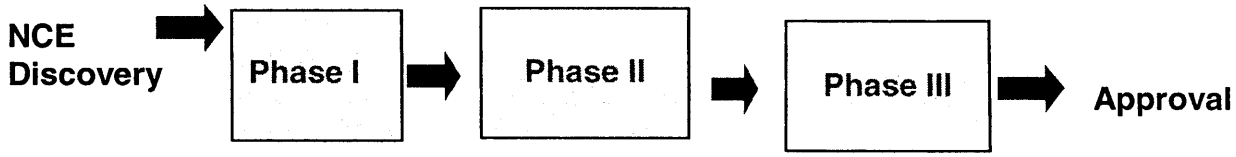

Description	Tests on 20 - 100 healthy volunteers	Efficacy testing on 100 - 300 patient volunteers	Efficacy testing on 1000 - 3000 patient volunteers
Cost	$58 million	$42 million	$117 million
Entering Phase	100%	70%	36%
Time	1 - 1.5 years	2 years	2.5 - 3 years

Figure 6.4.2.1. Clinical trial stages of new chemical entities (NCE) from Pisano and Wheelwright, 1995.

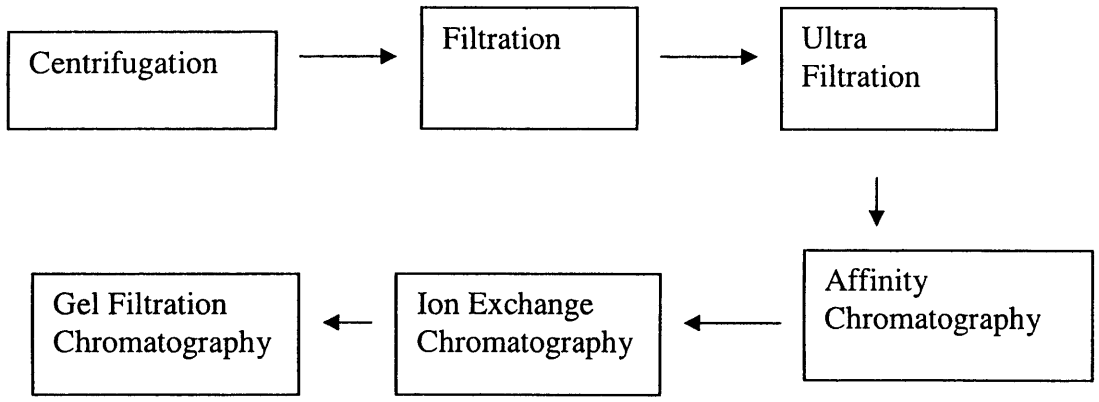

Figure 6.5.1.1. Process steps in production of monoclonal antibodies.

manufacturing processes with limited time and resources at their disposal (Bryon, 1999). Typically, processes that emerge from such rushed development are sub-optimal, resulting in low product yields.

A product that offered the means to optimise processes quickly at low cost using minimal starting materials, could provide substantial cost benefits to biopharmaceutical companies. It would enable them to focus on process development in tandem with product development, getting the product onto the shelf sooner, with higher yields and reduced development costs.

6.5 Market Focus for SS-PDO

It is believed that the biopharmaceutical industry is the best market to target with the SS-PDO technology. It is also believed that in the future, the predominant emerging biopharmaceuticals will be proteins. Therefore, the market research demonstrated the need for protein purification processes. Purification can use a variety of process steps: chromatography; centrifugation; liquid extraction; dialysis and filtration to name only a few. Scientific validation of the SS-PDO approach has been completed for chromatography and liquid extraction, so any processes using only these parameters could currently be improved with SS-PDO. Over time, more parameters will be researched and added to the standard capabilities of SS-PDO, increasing the benefits and potential market size.

6.5.1 Case Study: Production of Monoclonal Antibodies

In this section the commercial potential of SS-PDO is shown to be significant by calculating anticipated cost benefits and savings in a real life example. The case study examines the processing of a class of biopharmaceuticals known as monoclonal antibodies. The process is shown in Figure 6.5.1.1.

The fermentation of cells that produce the selected protein are grown to high concentrations and the cells are separated from the fermentation broth using a filtration system. An ultra-filter with molecule-sized holes has then used to separate proteins (which include the monoclonal antibody product) from other smaller molecules, such as sugars and salts. Next, three chromatography steps are used to purify the antibody and remove contaminants, ending

up with the desired pure monoclonal antibody. This process has been simplified, ignoring many additional steps, such as storage.

The process was programmed into a bioprocess cost analysis package called SuperPro Designer[13] (Intellegen, 2003), which is an example of the process design software discussed above. This package calculates the NPV of project to manufacture monoclonal antibodies, based on the following inputs:

- Capital investment: setting up the plant – $11,500,000 outlay in year one.
- Annual operating costs: operating costs (made up of the direct materials, direct labour, plus general and administrative expenses) are estimated to be $4,500,000 per year, starting next year.
- Annual revenues: manufacturing capacity was estimated to be 2.24 kg/year. The selling price of the monoclonal antibody is around $2,500 per gram in 2002 when this report was written ($300 in 2007), so total annual revenues from the plant would be $5,600,000 per year, starting in year two.

This gives a gross margin of 20.6%, generally deemed low for a pharmaceutical product. Looking only at the first 5 years of plant operations, and using a 7% discount rate, the project has a net profit value (NPV) of $6.9 m. On this basis, the project would not be undertaken.

Research has shown that fermentation conditions can be analysed in ultra-scaled down experiments (Doig et al, 2002). During the chromatography steps, analysis can be carried out to determine the best operating conditions (these are both typical of the optimisations that SS-PDO can deliver). The original process has relatively average performance. If it is compared with the best in its class, a number of potential improvements are apparent.

Fermentation performance: currently the fermentation is producing only 0.06 $g.L^{-1}$ of product. Initial optimisation of the media and fermentation conditions could improve the performance by 65%.

[13] SuperPro Designer is a tool for engineers and scientists used to aid process design for development and manufacturing.

Improved Fermentation and chromatography steps: each chromatography step has product recoveries of 80%. Comparing this performance with that of experimental systems in the literature, it is believed that the product recovery in this process could be improved to between 90% and 95%.

Reduced downtime and maintenance: improved integration of the process reduces the amount of downtime required to change filter membranes and chromatography matrices, which could increase uptime by 13%. Table 6.5.1.1 indicates the project economics for various combinations of the possible improvements.

SS-PDO acts in all three identified areas of process improvement. With SS-PDO process improvements, the project becomes positive NPV. This analysis illustrates the basis for selection of the pharmaceutical industry as the primary target market for the product offering.

6.5.2 Market Size

The pharmaceutical industry, and in particular the biopharmaceutical industry, is concerned about the availability of sufficient manufacturing capacity for the production of drugs, especially the more complex proteins ('large molecules') based drugs. Increasingly, costs are becoming an issue, as the 'tap that was wide open' in the 90s is now dripping investment money sparsely. As an example of this, Figure 6.5.2.1 shows how the number of new chemical licence biopharmaceuticals has increased since 1990 to 2002, which reflect the opportunity for SS-PDO and their increasing popularity has been reflected in recent conference held on biopharmaceuticals manufacturing, such as ?.

The programme states: "Protein manufacturing presents the pharmaceutical industry with a new set of challenges that must be addressed to reap the rewards of biotechnology. In addition to the complexity of large molecule production and purification, the development of biological therapeutics often entails greater investment risk than traditional small molecule drugs. The manufacturing strategy for biologics must be determined early in the development process, typically before Phase III clinical trials, to avoid costly changes in the manufacturing process, delays in product launch timing, or both."

Base case: NPV ($6.9 m) (Gross) margin 20.6%	**Improved Fermentation**	**Improved Chromatography**	**Reduced Downtime**
No Other change	NPV $10.9m Margin 52.4%	NPV $8.8m Margin 49.96%	NPV -$3.64 million Margin 26.7%
Improved fermentation and…		NPV $35.3m Margin 70%	NPV $15.9 million Margin 56%
Improved chromatography and…			NPV $13.5m Margin 53.8 million
All three improved	NPV 43.7m Margin 72.3%		

Table 6.5.1.1. Financial benefits of process optimisation.

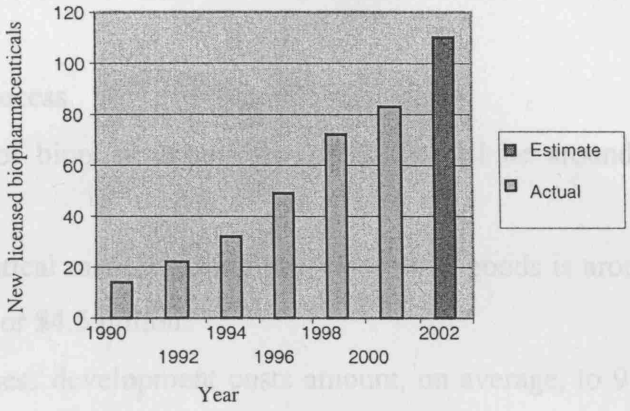

Figure 6.5.2.1. New licensed biopharmaceuticals per year from. from Pisano and Wheelwright, 1995.

SS-PDO is aimed precisely at this: optimising the manufacturing strategy during the development process. It is estimated that the market for SS-PDO is of the order of $400 million per year. The market lies in two main areas: in saving costs during the screening process and in reducing the cost of the manufacturing process. The derivation of this number is outlined below:

A - Screening process

- The number of new licensed biopharmaceutical products, per year, is at least 110 (Amersham Plc, 2003).The average total cost of a biopharmaceutical development process is around $500 m (Drews, 2000).
- Biopharmaceutical screening costs on average up to 49% of total costs, comprising Biological screening, and Clinical (Phase I, II, III, and IV) screening (Drews, 2000).
- So, per new (successful) product, an amount of nearly $250 million is spent on screening. It is estimated conservatively that SS-PDO can save at least 10% of these costs. This gives $500 million x 49% x 10% x 110 million = $269.5 million per year.

B – Manufacturing Process

- Global sales of biopharmaceuticals for, 2003 will be around $18 billion (Branch, 2002).
- Biopharmaceutical manufacturing process cost of goods is around 25% of sales price (Farid, 2003), or $4.5 billion.
- Of these, process development costs amount, on average, to 9.9% (Drews, 2000), or $446 million.
- SS-PDO can reduce the costs of these by at least 30%, giving savings of ~$134 million per year. As SS-PDO is developed further, more process parameters can be handled and the percentage will increase beyond 30%.

The approach of the company taking SS-PDO to market will be to target selected parameters and selected drug design processes to provide companies in this market with a whole product solution: increased efficiency for their screening process and savings on the manufacturing design process (Table 6.5.2.1).

A - Reducing costs of screening, per successful drug	
Estimated reduction in costs of screening (pre-C, I, II, III, IV)	10%
On the development of one successful drug savings can amount to	$25 million
Estimated number of new licensed biopharmaceuticals ("successful drugs") in 2002	110
Total market for SS-PDO in biopharmaceutical screening, per year	$271million
B - Reducing costs of manufacturing process development	
Estimated reduction in costs of process development	30%
Total market for SS-PDO in biopharmaceutical process development, per year	$134 million
Overall total market for SS-PDO, per year	$404 million

Table 6.5.2.1. Estimating the potential market size for SS-PDO.

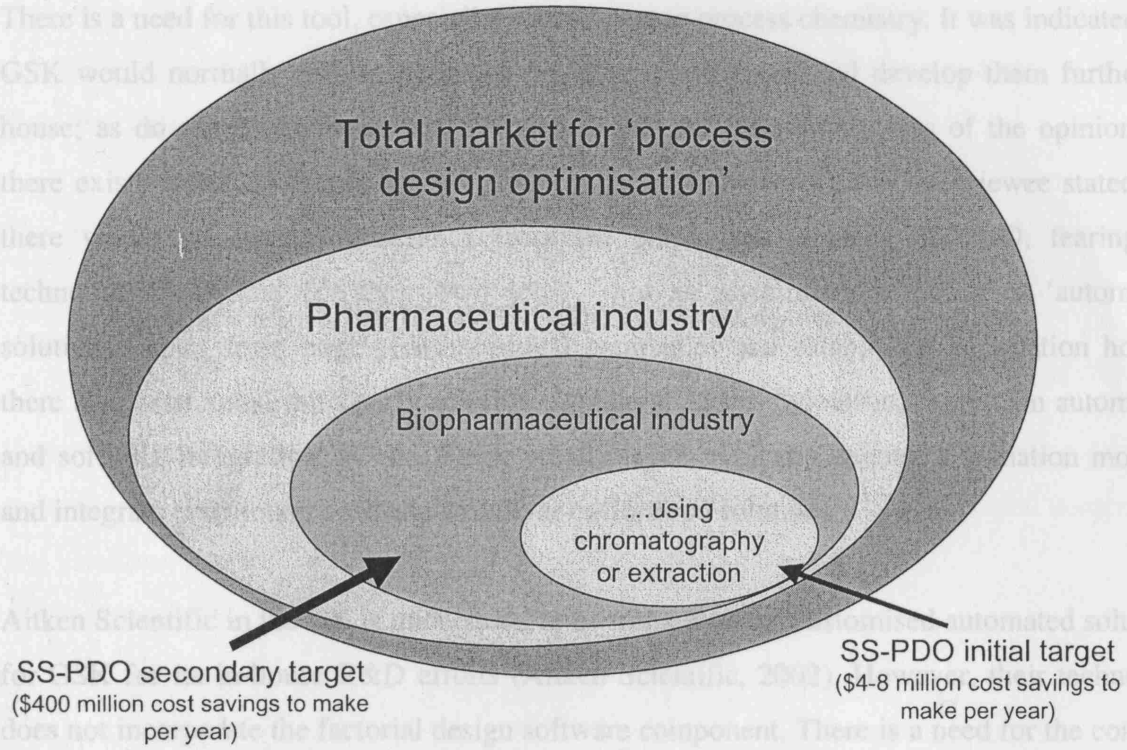

Figure 6.5.2.2. 'Niche' starting market for SS-PDO.

The primary research was undertaken, speaking with industry leaders to seek their views on the viability of the SS-PDO approach. Although, they would not be drawn on figures, there was general agreement that significant savings would be achieved by implementation of the SS-PDO approach.

As mentioned above, initially targeting only the market for chromatography and extraction screening, which constitutes around 1-2% of this total market. This gives an initial 'niche' market of $4-8 million per year. At this time, it is anticipated that launch of this product would enjoy first mover advantage in this market (Figure 6.5.2.2).

6.6 Customer Validation

At least four large pharmaceutical companies are keenly interested and currently engaged in implementing integrated liquid handling automation solutions (similar to the SS-PDO concept, but lacking key statistical experiment design and data acquisition components): GlaxoSmithKline (GSK), Eli Lilly, Merck, AstraZeneca.

There is a need for this tool, especially with respect to process chemistry. It was indicated that GSK would normally buy in potential enabling technologies and develop them further in-house; as do other pharmaceutical companies, but the interviewee was of the opinion that there exists room for a commercial product/ package. However, the interviewee stated that there would be marked reluctance from the employees to using SS-PDO, fearing the technology itself and for their own jobs – not an uncommon response to 'automated' solutions. Apart from large-pharmaceutical companies and established automation houses, there also exist small third party solution providers. Aitken Scientific, experts on automation and software integration, is one. These small players typically acquire automation modules and integrate proprietary software to deliver customised solutions.

Aitken Scientific in the UK is understood to be implementing customised automated solutions for GSK for its in-house R&D efforts (Aitken Scientific, 2002). However, their technology does not incorporate the factorial design software component. There is a need for the concept. He underlined the importance of statistical design of experiment software to the chemistry and critical manufacturing processes in the pharmacy industry, which is served by the Automation

sector. Though there is a large market on the application side, the key deterrents identified were:

- Developing, troubleshooting and optimising the interfacing parameters for each module (which may be customised to individual customer requirements).
- Automating each module, integrating the whole system and developing protocols to discover and characterize factor effects. Such work is extremely laborious and time-consuming.
- Establishing the robustness of the models and control systems.

Aitken Scientific does not currently employ factorial design software.
Another large-pharmaceutical company, Eli Lilly, is working in association with Perkin-Elmer and Chemical Research Science Robotics to set-up indigenous automated stations for its pilot plant. It was indicated that the concept is promising, but would involve a lot of time and money to set-up and simulate the process. Interestingly, the interviewee noted that to integrate discrete automation elements with statistical software called for specific technical skills that Eli Lilly do not currently possess. On a positive note, the interviewee mentioned that if such a system were in operation it would benefit tithe interviewee industry in terms of both development times and economics.

The SS-PDO concept remains distinct in the sense that our proprietary process technology offers a highly efficient and rapid solution with multivariate comparability analyses, by identifying the most optimal experiment and development model.

One of the key concerns over the process development is the substantial lead-time anticipated on account of process optimisation, software integration (i.e. both statistical and automation) and validation, which was estimated to require 30 man years to complete[14].

[14] 30 man years to complete automation process fermentation of a process x (10 processes (purification + fermentation) + 20 man years for process integration, software development and data retrieval.

6.7 Intellectual Property

The integration of factorial design software with chemical synthesizer and the feedback for process optimisation is already disclosed under US Patent US6044212, filed by Anachem. This software selects parameters to optimise chemical processes. The system is based on combinatorial chemistry; automation technology and computer controlled design. The software can select from a number of experimental test screening parameters, such as temperature, pressure and concentration. Samples are analysed and the data used to determine the product yields. This is achieved using a chemical synthesiser, analyser and robotic arm and computer communication.

The Anachem patent is clearly very similar to the SS-PDO concept, but specific to chemical processes. Are there many key differences that might allow SS-PDO a route to protect its IP? Processes themselves are difficult to the patent, as they are hard to defend and easily changed to allow their use in industry. The best opportunity is to seek to protect some of the experimental parameter knowledge, i.e. the results of the laboratory work, which indicate exactly how microscale behaviours can be scaled-up. However, work done to date on this topic has already been disclosed and is in the public domain.

The software controlling the liquid handling workstation already exists – WinPrep™ (owned by Perkin-Elmer). Users of this software for process parameter screening are able to define particular applications (i.e. experimental procedures to be run on the equipment). Such a collection of process parameter screening applications could minimally be protected by copyright. Similar considerations apply to the factorial design software, which already exists (e.g. StatEase).

The main difficulty in protecting the IP of SS-PDO arises from its reliance on third party software packages. The output of each stage is transparent to the equipment operator: they can observe exactly how each iteration of the experiment has been designed and the data file can be saved for later use. Scientists would in any case demand and require a high degree of transparency in order to gain regulatory approval for processes resulting from microscale optimisation.

In summary, SS-PDO poses some very significant challenges in terms of intellectual property protection. It is unclear at this stage that it will be possible to prevent the knowledge diffusing through the industry.

6.8 Business Models

One of the key problems in commercialising this technology is determining a suitable business model. The venture could be delivered through three alternatives, System Integrator, Licensing model and consultancy. Each has particular advantages and disadvantages.

6.8.1 Systems Integrator

This option considers the acquisition of laboratory equipment from OEMs, integration of the operating systems of the different devices using in-house developed software, and the sale of the integrated solution to end customers. Calibration, training and basic consultancy would be included in the set-up fee and a margin would be charged on resold equipment. The selling process finishes when the bundle is commissioned and ready to be used by the customer. Partnership agreements would be required with OEMs.

In this way, the customer purchases an integrated solution with a single point of contact. Target customers would need SS-PDO functionality on a regular basis, e.g. large pharmaceutical or biotechnology companies testing several alternative drugs. The customer owns the technology, which could be adapted to test as many product developments as desired.

This model would require SS-PDO to be developed and manufactured as a standard product, and to sell it in several markets, affording growth opportunities that are absent in the alternative business models (section 6.8).

Disadvantages include the need to develop distribution channels, high investment in R&D (particularly development of software integration modules) and expensive marketing requirements. A large sales force would be required. Reselling agreements with OEMs could be difficult to negotiate. Large volume customers of OEMs would likely be reluctant to pay higher prices to a small systems integration house for resold equipment. There is a risk that

the added value of SS-PDO would be disguised by the attempt to supply what is by and large standard laboratory equipment.

6.8.2 Licensing Model

The concepts of automated experimentation, factorial design software and processes optimisation are not novel, nor is their integration. Such integration has already been achieved for chemical synthesis. SS-PDO is aimed at biological synthesis and purification of drugs based on large molecules, such as proteins. A patent is not appropriate as the idea is not novel and there is 'prior art'.

However, the programs for the liquid handling workstation, written using Perkin-Elmer WinPrep™ software, are novel. These programs can be copyrighted, but this will not afford much protection, as the programs source cannot be protected from scrutiny. Moreover, it is likely that this concept would be viewed as too difficult by practitioners, who wish to pursue science, not software engineering.

6.8.3 Consultancy Model

This model will involve the purchase of the necessary automated equipment by the company and the development of the software required to integrate the different devices. This bundle will not be sold on, but would be used to provide service and support to clients. The offer is targeted to customers that will use the functionality on an infrequent or one-off basis. Small biotechnology ventures are typical customers of this service.

This model is less detailed than the other options: there is no need to develop distribution channels, a sales force or to stock inventory.

The greatest disadvantage of this model is that, if successful, it is very difficult to replicate and gain scale. Researchers with the requisite knowledge, who are interested in working at a consultancy, are scarce. Growth would be constrained by this limiting factor.

6.8.4 Business Model Selection

The best model is a combination of the system integration and consultancy . In the short term, a consultancy of sorts will be required to demonstrate that the technology and the people behind it can deliver. This approach will be useful to start the venture. Hopefully, satisfied customers would purchase a complete system to optimise processes themselves. In the longer term, as soon as the company builds market share and reputation, it can begin to focus its attention on the first model. The combination of both models (consultancy first, systems integration later) has been used by several start-up companies of this nature. The approach balances risk and capital requirements with the opportunity to move up the learning curve.

6.9 Competition

6.9.1 Equipment Manufacturers

Most notable amongst key automation package suppliers is Tecan, a Swiss company. Their product, Genesis® Freedom™ automated workstation, has an open architecture which enables the workstation to integrate a wide range of modules. It is gaining wide acceptance in the industry. Another key player is the working alliance between Qiagen and Zymark Corp. Their BioRobot™ systems, with innovative arm robotics, have demonstrated novel automation applications, but are weak on flexibility to integrate discrete modules.

Both Tecan and Qiagen are very strong on the automation front, but are currently not exploring the incorporation of DoE elements.

Another key player is Perkin-Elmer, which offers a wide range of products to automate liquid handling. Their Gripper Integration Platform system (GRIPS) uses proprietary WinPrep™ software. Its intrinsic architecture affords the flexibility to adapt to a host of different modules. As noted above, Perkin-Elmer's automation design provides the most suitable starting point for the further development of SS-PDO. as initial experimentation had been carried out using their equipment. It aims to interface and integrate with DoE components and enable seamless data acquisition and exportability across various platforms for subsequent analyses – exactly the functionality required for SS-PDO.

6.9.2 Large Pharmaceutical Firms

Most large pharmaceutical firms already have programs underway to develop technology similar to SS-PDO. These firms are the largest customers of the equipment manufacturers and, on the whole, already own the relevant apparatus and software. While in-house developments do not necessarily obviate the market need for SS-PDO, they may impact severely on overall demand.

6.10 Marketing and Business Development

A variety of marketing approaches would be required to ensure adoption of SS-PDO.

Product awareness would be increased by presentations at selected conferences, including LabAutomation and other chemical processing conferences.

The initial research would need to be presented in scientific papers or seminars and in research discussion groups with industry representatives. While this would inevitably disclose some of the experimental detail of the microscale experimentation techniques, it is essential to demonstrate the validity of the system and its relevance to larger scale process.
Advertisements should be placed in specialist journals, such as Today's Chemist at Work, Drug Discover Today or the Journal of Automated Methods and Management in Chemistry that are read by potential users of the technology. Rate of adoption by pharmaceutical companies will be increased by building awareness of a technique that might be saving a competitor's time and money already.

6.11 Conclusion and Recommendations

Large equipment manufacturers such as Perkin-Elmer are best placed to commercialise this technology. They have access to two critical strategic resources: high spending customers in the pharmaceutical sector and their own product ranges. Therefore, at this stage, a number of recommendations for the development of this venture would be:

- Seek additional advice on the options available to protect the experiment design IP that have been developed.

- If suitable IP protection can be put in place, a company should be formed around the consultancy business model.
- Partnership with a large equipment manufacturer is essential. Select one to work with on an exclusive basis initially, as recommended Perkin-Elmer.
- The equipment manufacturers are unlikely to have the unique combination of understanding and skills possessed by the university researchers in this field. The presentation and definition of this skill set needs to be improved in order to sell the partnership, and indeed, the whole SS-PDO concept to customers.
- ~30 man-years[14] of work are needed to characterize all parameters required for pharmaceutical production processes. Once formalised as a consultancy venture, the new firm must broaden its access to other research resources. Unless SS-PDO can address more than the starting 'niche', the concept will have limited application.

In the final chapter, the results presented in this thesis will be discussed in light of the business evaluation, described in this chapter, and areas for future work will be detailed.

Chapter 7: Conclusions and Future Work

7.1 Introduction

This chapter discusses the results from the research detailed in this thesis. The discussions and conclusions from each chapter are drawn upon to consider their implications on the future direction of research. The main areas of research investigated the automated platforms (section 7.2) and their use in developing microscale equilibrium separation processes (section 7.3), which included liquid-liquid extraction (section 7.3.1) and solid phase extraction (section 7.3.2). These research areas were considered together as part of a new technology venture and its business potential was discussed, highlighting the challenges it might face (section 7.4). The analysis of how the research areas relate to each other and additional experimental tools are discussed in relation to the pharmaceutical industry (section 7. 5).

Automated equipment (section 1.3.2) had been integrated into research laboratories of the large pharmaceutical companies for use in a range of applications including combinatorial chemistry and high throughput screening. The adoption of this technology into laboratories by industry leaders increased the speed and numbers of experiments carried out. Many problems of the pharmaceutical industry (section 1.2.3) were expected to be solved by the use of automation (section 1.2.4). However, limitations of these automated approaches to drug discovery have been identified and the disjointed automation of the R&D process has generated alternative challenges, such as optimising the purification processes to accelerate the scaling-up of the process to manufacture new chemical entities. The research in this thesis focussed on the creation of automated purification processes to tackle this problem by developing microscale purification processes and correlating the results with a larger process scale. This used commercially available automated equipment, owned by pharmaceutical companies, to rapidly integrate these research findings, making the research relevant to them as it could be directly

transferred into their laboratories. This could reduce the time period required to scale-up the processes for manufacturing.

The aim of this research was to investigate the development of automated platforms and assess their suitability for microscale equilibrium stage extraction processes. This was achieved for the LLE and SPE process and the microscale data was compared to the manual microscale and laboratory scale data, as well as literature data to validate this process scale. These microscale processes were used to screen their key parameters to optimise the purification of the 6-APA from a simulated penicillin acylase bioconversion product stream. The automated microscale processes rapidly generated high sample numbers for investigating key process parameters. Statistical analysis of the data indicated that it was of acceptable accuracy and precision, making microscale suitable for the overall bioprocess research and development. The automation of the equilibrium separation processes demonstrated the potential benefits of using the automated platforms in automated microscale experimentation by generating rapid results and large data sets.

7.2 Conclusion on Automated Platforms

The automated platforms used in this research comprised of a liquid handling workstation (Multiprobe II Ex®) and a solid dosing station (Accelerator™). The liquid handling and solid handling capability of the automated platforms used within this research were investigated by assessing their operating characteristics. A range of operational parameters were investigated using gravimetric measurements of dispensed liquid aliquots or solid masses. Statistical analysis of these data quantified the performance of the equipment (chapter 3). The accuracy and precision of the data provided an insight into the impact of the equipment on the automated microscale process methods. The performances of the automated platforms compared well with the manufacturer's published data (section 3.2.1.6).

Analysis of the manufacturer's performance and familiarisation with the operation of the automated platforms identified the types of error encountered, as well as key issues

related to their operation. These issues included selecting: suitable multiwell plates with the required characteristics; commercially available automated equipment and operating parameters for the automated platforms to achieve the level of performance required by the automated microscale experimentation.

The multiwell plates were carefully selected with suitable characteristics prior to experimentation to prevent problems occurring and allow their use for specific applications (section 1.4). The automated microscale experimentation was successfully developed using a variety of multiwell plate formats (section 1.3.1), which had appropriate volumes and number of wells, together with the automated platforms. The materials of composition of these plates (appendix 1) were selected according to the required experimental application and their interaction with the reagents. Some composition materials adsorb charged compounds (proteins), chemically react with reagents (organic solvents) or are effected by static electricity that may affect their use in the automated experimentation. Borosilicate multiwell plates were selected for use in the automated LLE experimentation (section 4.2.1) to avoid adsorption of charged compounds and reaction with organic solvents. Polypropylene plates were used in the automated SPE experimentation (section 5.2.2.5) to reduce the effect of static electricity within the plate on solid handling as it can effect the transfer of adsorbent resins. The supported SPE experimentation investigated a range of filter plates and polystyrene collection plates.

The automated platforms were selected due to their operation, adaptability, performance, commercial availability and acceptability by the pharmaceutical industry. The Multiprobe II Ex® liquid handling workstation was selected from the vast range of commercially available workstations (section 1.3.2.1.1) due to its operation, versatility and high performance assessed by the manufacturers (appendix 7). This instrument is widely used in industry (section 1.8). Many of these researchers assumed the accuracy of the automated platforms' dispensed volumes and only quoted precision values for the experimental methods. The liquid handling workstation was evaluated (section 3.2.1) to quantify the achievable performance. The Accelerator™ solid dosing station was selected

based on its operation and availability. The actual performance achieved by these individual pieces of equipment was good and they were used to generate reliable microscale processes.

The performance of the individual automated platforms required good accuracy and precision to ensure that it is a robust technology, which dispensed the programmed reagent quantities to allow its use in the development of reliable experimental methods. The automated equipment required high accuracy and precision values, which indicated any systematic or random errors associated with the equipment. Accuracy is more important for assessing the performance of the automated platforms as a high value would indicate the limited occurrence of systematic errors, making it an acceptable technology, whereas a degree of variation in the precision is acceptable and can be improved by operational settings or changes in the methodology. However, precision is more important for assessing the performance of the experimental methods as a low value would indicate the limited occurrence of random errors which can be minimised by good laboratory practice.

Accuracy is required for delivering the programmed liquid volumes or solid masses into the receptacles to ensure that the experimental conditions are consistent and reproducible. Accuracy is the most significant performance measurement in assessing the automated platforms and experimentation methods as the bioprocess engineer has the most control over this value. Precision is required to generate data that is reproducible and repeatable, with close correlation to the mean. Random errors are introduced in all experiments due to the slight variation within reagents and equipment operations, but they are minimised by good laboratory practice. The use of the automated platforms was anticipated to reduce the occurrence of random errors. Random errors could occur even if a systematic error occurred and can easily be minimised. Therefore, accuracy is the most important method of analysing the performance of the automated platforms as it relates directly to the experimental method developed for LLE and SPE processes.

The performance of the automated platforms was individually assessed over a range of operating parameters prior to the development of the automated microscale processes. The liquid handling workstation was used to dispense liquid aliquots over a range of volumes, pipette tips, operational modes and reagents (section 3.2.1.3). The solid dosing station dispensed a range of resin masses for a variety of reagents (section 3.2.2). All of these quantities were gravimetrically measured and statistically analysed to quantify the performance of the automated platforms.

The performance of the automated platforms was improved by its initial optimisation to generate high accuracy and precision, which validated its operation. Once optimised, the automated platforms were used in experimental methods and the performance of the experimental methods was assessed. This focussed on the precision as the accuracy of the methods was related to that of the automated platforms, which was considered to have the highest accuracy achievable. The precision of the methods should be high, reflecting that little variation occurs and it can be used to generate reproducible experimentation.

7.2.1 Performance of Liquid Handling Workstation

The performance of the liquid handling workstation used in this research was assessed under a variety of operational settings to investigate its performance related to different pipette tip volumes, operational modes and dispensing speeds. It was observed that the performance of the workstation improved by its operation with disposable pipette tips (1.7% inaccuracy) compared to that with fixed pipette tips (2.0% inaccuracy) at dispensing 100 μL RO water, despite the pipette tips having the same internal orifice diameters. This may have been due to the differences in the composition material of the pipette tips affecting the fluid dynamics. The precision showed the reverse trend (disposable tips 2.1% CV, fixed tips 0.1% CV). However, the accuracy of the data is more important in setting up the operation of the equipment as the parameters can be changed to limit the occurrence of systematic errors. In addition, the use of disposable tips offers protection against the cross-contamination of the bulk reagents, or between the

wells. The disposable pipette tips were selected for use in the microscale experimentation.

Dispensing larger volumes enhanced the performance of the workstation. This trend was seen for both types of pipette tips and also in the manufacturer's data. The best performance was achieved for the largest volumes and so aliquots of >150 μL were used in the development of the microscale experimentation. The automated platforms were designed for dispensing high performance lower nanolitre volumes, but this required additional modification of the equipment.

The accuracy values for dispensing the range of volumes (1 μL to 100 μL) were similar to the values quoted by the manufacture for their customer specification accuracy (2% inaccuracy) and the literature for the Cyberlab C-400 workstation (4.1% CV) (Astle and Akowitz, 1996) and the Quadra 96 workstation (1.25% CV) (Bateman et al, 1999). This indicated the suitability of using 150 μL aliquots in the microscale equilibrium separation experimentation so this volume was selected for each of the phase volumes used in the microscale LLE experimentation (chapter 4) and similar volumes for microscale SPE experimentation (chapter 5).

The operational mode of the workstation influenced its performance with the best performance achieved using the waste mode (0.6% inaccuracy and 0.5% CV) to dispensing 150 μL RO water. This improved upon its performance for dispensing 175 μL using the blowout mode (0.11% inaccuracy, despite 2.2% CV). The performance of the workstation operated at a variety of dispensing speeds and showed that the performance increased with the dispensing speed. The standard dispensing speed of many performance files for dispensing water (Water Waste FT.prf and Water Blowout Small.prf) was 400 $\mu L.s^{-1}$, which generated good performance (1.6% inaccuracy, 3.2% CV) and this speed was used in many of the bespoke performance files. The performance of dispensing butyl acetate using the workstation (0.3% inaccuracy, 0.4% CV) was better than for water (0.6% inaccuracy, 0.5% CV) due to the different rheologies and performance files of the liquids. This validated the use of the workstation in the

microscale LLE process fitted with disposable tips, dispensing 150 μL when operated in the waste mode. The dispensing speed was dependent on the speed of operation of the workstation and could only be accelerated by removing the aspirated air gap step between the aspirating and dispensing aliquot steps, which would require major reprogramming of the hardware.

The workstation encountered small systematic errors that were minimised by the careful selection of suitable performance files. Any random errors encountered by the workstation were caused by variation in the workstation calibration (section 4.2.8.1) or poor alignment of the pipette tips, which introduced air into the system. These errors were minimised by the effective maintenance of the workstation, regular calibration and strictly following the standard operating procedure (appendix 9). This would ensure that the workstation has accurate liquid handling and movement between the labware to enable its use in a vast array of experiments.

7.2.2 Performance of Dosing Station

The performance of the solid dosing station was investigated for dispensing a variety of reagents. The operating parameters of the dosing station were selected using the Accelerator™ application software prior to its use in experimentation to generate its optimum performance for dispensing specific reagents. The manufacturers quoted that the solid dosing station could handle 95% of reagents, but it was only able to dispense a selection of the reagents used in processes studied here. These reagents were limited to dry crystalline solids. This limitation of the equipment required the modification of the experimental design and formats used in the automated microscale SPE process to include an adsorbent conditioning step. This instigated the development of the supported microscale SPE process (section 5.2.6).

The manufacturer of the Accelerator™ provided performance data for dispensing starch (10 mg) and silica (200 mg) using optimum operation parameters. The manufacturer of the solid dosing station showed good performance with accuracy and precision values of

less than 1%. However, the actual performance of the solid dosing station dispensing granular activated carbon produced poorer results. This suboptimal performance may have been due to errors caused by the set up parameters controlling the dispensing mechanism of the solid dosing station. There was no other established commercially available solid dosing station to compare its performance against, although subsequent products have now been launched, so the manufacturer's data was used as the performance standard.

The solid dosing station used the selected operating parameters to dispense unconditioned granular activated carbon over a range of masses. Analysis of the actual mass dispensed showed variation between the replicate samples across the range of resin masses and with the predicted masses. This may have been caused by the dosing head of the solid dosing station unreliably aligning with the receptacle to collect the dispensed solids, which resulted in solid loses. The receptacle used had increased orifice diameters to reduce spillages and minimise these losses, but the significance of these losses increased with the reduction in dispensed mass. Modification of the dispensing head by the addition of a funnel device or the addition of a weight to correct the misalignment of the dosing head may facilitate the accuracy of the solids delivery, but this was not investigated in this research.

The actual performance of the solid dosing station had low percentage accuracy values (44% to 1103% accuracy) over the range of solid masses dispensed, which compared poorly to the predicted masses, quantified by the equipment. The performance of the solid dosing station was expected to decrease as the mass increased as errors become less significant with the increase in mass, but this data showed no clear trend. The best performance of the solid dosing station was achieved when dispensing the second largest mass investigated (40 mg), dispensing an actual mass of unconditioned granular activated carbon (40.12 mg) with 0.3% inaccuracy, although the data showed great variation. The performance of the dosing station dispensing granular activated carbon was worse than the manufacturer's data for dispensing silica or starch.

7.2.3 Recommendations for Microscale Experimentation

The performance of the automated platforms used in this research identified that the workstation had acceptable accuracy and precision, which compared favourably with the manufacturer's data. This performance was better than that for larger laboratory scale equipment (*circa* 10%) and the workstation was recommended for use in the development of the microscale equilibrium stage separation processes (chapters 4 and 5). The dosing station had a more variable performance that made the samples unreliable for their direct use in the microscale experimentation. Therefore, these solids were manually weighed prior to their use in microscale SPE experimentation (chapter 5) to ensure the accuracy of the results. These automated platforms provided a rapid method of preparation and implementation of experimentation (section 7.3). The performance of the dosing station and its incompatibility with the multiwell plate format indicated future work required for the development of the automated platforms (section 7.2.4).

The performance of the automated workstation and solid dosing station both effected the outcome of the experimental methods, as did the performance and precision of the laboratory equipment (analytical balance, pH meter) used to prepare the reagents. The performance of the automated platforms indicated their suitability for developing microscale experimentation to assess the microscale LLE and SPE processes. The experimental methods developed using the automated platforms were expected to have good performance, reflecting the performance of the automated platforms compared to the manual methods. However, the experimental methods used additional laboratory equipment to the workstation for preparing and analysing the reagents. This possibly introduced random errors throughout the method, each of which influenced the overall performance of the experimental methods. Therefore, the accuracy of the experimental method was expected to be lower than the performance of the automated platforms alone. The overall performance will reflect the performance of each of the instruments used and care should be taken in their selection and utilisation in the method for the preparation of the reagents, the actual experimentation method and the analysis of the samples to generate the results. The performance and development of the microscale equilibrium purification processes are discussed below.

7.2.4 Automated Platforms Future Work

The performance of the automated platforms will require further investigation as they are used for an increasing number of applications:

- Each of the commercially available automated platforms used in the automated laboratory must be individually assessed for their performance specific to the equipment for automated experimentation. This will make the experimentation robust and provide awareness of and minimise related errors. In addition, the speed of operation may have to be varied for time dependent reactions by modification of the operation parameters.
- The liquid handling workstation is capable of dispensing a wider range of liquid volumes than those investigated in this research. These larger quantities may be required for use in other automated processes. Therefore, it is recommended that analysis of the performance of the workstation be investigated over the extended volume range. This experimentation will generate a window of operation for the selection of multiwell plates, experimental volumes and different reagents.
- Improve the performance of the solid dosing station by modifying the operating parameters to set up the instrument and alignment of the dosing head to reduce reagent waste. Program the dosing station to be compatible with a range of multiwell plate configurations to accelerate the preparation of microscale experimentation. Integrate the dosing station with other automated platforms.
- The solid dosing station is capable of dispensing a wider range of solid masses and solid types than those investigated in this research. The larger quantities and different solid preparations (powder, beads with immobilised enzymes) may be required for use in other automated processes. Therefore, analysis of the different solids over an extended range of masses should be investigated and the performance of the solid dosing station be analysed to generate a window of opportunity for its operation to expand its versatility.

- Investigate the performance of additional automated weighing platforms for their ability to dispense a range of solid materials and a range of masses suitable for microscale experimentation.
- New experimental applications will demand the development of new equipment, devices or new functions of the existing equipment, such as compatible calorimeters, accurate heaters or refrigerators compatible with the multiwell format. This may require the automation of manual microscale or small scale equipment and devices, which may require greater performance from these instruments.
- The automated laboratory contains many automated instruments and these will be required to easily communicate physically and electronically so that they can be controlled by one operating system on one PC that schedules and sequences their operation. Therefore, a universal programming language will be required.
- Additional software to support the rapid analysis of the results generated from the automated equipment must be set up using Excel macros or bespoke programs to accelerate data processing.

7.3 Equilibrium Stage Separation Processes

7.3.1 Liquid-Liquid Extraction

The microscale LLE process (chapter 4) was developed using the automated platforms with the experimentation carried out in a 96-well borosilicate plate. The plate was selected for its chemical stability with organic solvents and the well volume, which allowed enough space for adequate mixing. The microscale LLE process was developed as a batch process with a total extraction volume of 300 μL dispensed in two 150 μL aliquots and the workstation was operated in the waste mode with disposable pipette tips to minimise contamination and achieve high accuracy (section 3.2.1). The automated microscale LLE process consisted of four stages: dispensing of heavy phase; dispensing and dispersing the light phase; phase mixing by repeated aspirating and dispersing an aliquot of the disperson; and final phase separation. The liquid handling workstation was

used to identify suitable phase mixing by repeated pipetting. The automated microscale LLE process allowed the rapid investigation of the extraction kinetics, a range of aqueous phase pH conditions, suitable organic phases and dispensing speeds. The results of this could be used for optimising process conditions and scale up the process to the manufacturing scale for new pharmaceuticals.

During the development of the microscale processes, performance files were written for the workstation to deliver different liquids and they were used in automated methods, which were designed incorporating the positioning of the pipette tips, their tracking and the mixing parameters. This process was then assessed generating mass balance data to determine the percentage recovery of PAA. The experimental data that achieved the best LLE mass transfer (90.6%) used 30 mixing cycles (142 s), 0% tracking and was dispensed from 2% above the well bottom, these settings were used in the microscale LLE automated methods. The microscale mass balance data was compared to different scales using percentage recovery values. The microscale data showed good comparison with the laboratory data (75% recovery), which was used as a control. The laboratory scale percentage recovery data was 2% higher than the microscale data, but this difference was deemed acceptable. These results compared favourably with the laboratory scale and the manual microscale LLE processes data, which validated this process scale.

The liquid handling workstation has a liquid level sensing function that detects the level of the liquid within the well by detecting the conductivity of the liquid. This is used to detect the liquid air boundary and this must be passed before aspirating the liquid, which allowed the accurate transfer of liquid volumes. The liquid level sensing function can also detect the boundary between the two immiscible phases, accurately separating one phase from another. The performance of this workstation function was found to be dependent on the actual liquids used. Specific performance files were written for the accurate transfer of each organic solvent and sampling of the two separated phases using the calculated well heights of the liquids. This resulted in smaller samples removed from the well to ensure that they were uncontaminated and larger wasted phase volumes, ensuring

sample purity. It was important that the organic phase did not contaminate the aqueous phase PAA samples as it detrimentally interfered with the HPLC analysis.

The extraction aqueous phase samples were aspirated from a position above the well bottom to avoid contamination with the organic phase. The aqueous phase sample volume (100 μL) aspirated from the well and dispensed into the HPLC vials was 50 μL larger than the phase volume in order to achieve a clean and reproducible sample. This excess volume would have significant effects if repeated sampling was required from the same well. Therefore the starting volume influences the choice of the volume and configuration of the wells in the multiwell plate, which would also effect the number of repeated experiments and parameters investigated per plate. The potential for contamination with organic phases effects the HPLC performance. This may significantly effect the development of a microscale counter-current LLE process, which uses the same organic phase throughout the different extraction stages and results in reduced end stage phase volumes due to the losses incurred by sampling.

The parameters investigated were extraction mass transfer kinetics for each of the contaminating compounds, mixing conditions, aqueous phase pH conditions, organic phase solvents and dispensing speeds. The analysis of the mass transfer kinetics of the LLE of both the products and substrates of the penicillin acylase bioconversion revealed that each had their own characteristic kinetics (section 4.2.2). Equilibrium was reached within 2 mixing cycles (16 s) for Pen G and within 30 mixing cycles for PAA (142 s) at pH 4.5. These values reflect the ionisation of the compounds with Pen G having 2 amide groups and a carboxylic acid group within its structure, making it more neutrally charged at low pH conditions compared to PAA with only one carboxylic acid group. The distribution coefficient was 2 for Pen G and 24 for PAA at pH 4.5 (section 4.2.2), which agreed with the pH data (section 4.2.3). The LLE of the synthetic bioconversion product stream used 30 mixing cycles (142 s) to remove both Pen G and PAA. The kinetics of the LLE of PAA using a variety of solvents (section 4.2.4.1) produced similar trends, approaching equilibrium after mixing. It was unclear that equilibrium had been reached for each reagent as the end points should have matched those achieved at different scales

and this should have been further investigated, but time did not allow further investigation into this challenge to generate a generic process.

The aqueous phase pH conditions were screened between pH 2 and pH 8, which revealed the ionisation point (pK) of the individual components (PAA pK = 4.9, Pen G pK = 4.5). These values agreed with those published in the literature (Van der Wielen and Lankveld, 1996, and Rapson and Bird, 1963). The best pH conditions for the purification of 6-APA from the synthetic product stream were at pH 4.5 (section 4.2.3), as this extracted the contaminants from the feed material most effectively.

The operational dispensing speed of the liquid handling workstation was investigated for its effect on the mass transfer during the automated microscale LLE process (section 4.2.5). The microscale LLE process compared favourably with the manual microscale and laboratory scale LLE process data (71% to 75% w/w recovery), which was similar to that found by Jemal et al (1999) who also demonstrated the time savings of the automated LLE process. The experimental kinetic data at each dispensing speed showed that the mass transfer increased with the dispensing speed. The mass transfer rates for the different dispensing speeds were similar for the dispensing speeds above 400 $\mu L.s^{-1}$, achieving a partition coefficient of 36. The dispensing speed data was used to calculate k_La values (section 4.2.6), which showed that k_La values plateaued after this dispensing speed and the maximum mass transfer rate was achieved. The mass transfer achieved using different dispensing speeds was modelled and the corresponding k_La values were calculated.

The automated microscale LLE process was used to screen a range of organic phases, which had different rheologies, for the extraction of contaminants from 6-APA in the simulated bioconversion process stream (section 4.2.4.1). This required the generation of specific performance files for the liquid handling workstation in order to accurately dispense these liquids. The different density and viscosity values for the range of solvents investigated generated different challenges to their liquid handling (section 3.2.1.5). Cyclohexane is more viscous than butyl acetate and this effected the liquid handling by

requiring a slower aspirating speed, aspirating delay, dispensing delay with a larger waste volume and air gap. Ionic liquid is denser than butyl acetate and the aqueous phase, which effected its liquid handling by requiring an increased aspirating speed, aspirating delay, dispensing speed, dispensing delay, air gap with decreased waste volume, blowout volume and transport gap. The increased density changed the experimentation, altering the aqueous phase sampling height, which was aspirated from 1 mm below the liquid surface of the light phase.

The different organic phases generated different extraction kinetics for PAA LLE. The extraction of PAA with cyclohexane and ionic liquid matched the kinetics of butyl acetate. The best distribution constants were achieved using cyclohexane or hexane at pH 4.5, but butyl acetate generated poor results compared to those previously observed. This was possibly due to variation in the well preparation or poor sampling caused by small variations in the operation of the automated workstation.

The automated microscale experimentation had good performance (section 4.2.7), achieving 99.9% accuracy and 99.9% precision. The performance of the automated microscale process was better than the manual microscale (99.5% accuracy, 99.6% precision) and laboratory (85.6% accuracy, 92.8% precision) processes. These results validated the automated microscale process and indicated that the process was robust. Similar performance results were observed by Jemal et al (1999) for the manual and automated LLE processes, which were carried out to compare the speed of operation for these processes. However, the experimental method used by Jemal for the automated LLE process required manual intervention to generate phase mixing and the additional pieces of equipment increased the possibility of experimental errors occurring.

The statistical data used a sample size of more than 12 data points, taken on more than three different days, which was larger than the sample size used by Jemal et al (1999) of 3 runs on 3 different days. The inter-run and intra-run analysis of precision for the manual and automated LLE process by Jemal showed that the intra-run data for the automated LLE process (5.1% to 7.6% CV) was less imprecise than the manual LLE

process (2.4% to 7.6% RSD), but more consistent. This demonstrated that more random errors occurred with the use of the semi-automated LLE process using the Multiprobe automated workstation and manual vortexing. Jemal did not investigate the LLE kinetics for each analyte extracted and no percentage recovery values were published. The research discussed in this thesis showed that the LLE microscale kinetics varied with the extracted analyte (section 4.2.2).

The accuracy and precision of the microscale LLE experimentation data were better than those from Jemal et al (1999) who considered the accuracy and precision values for his data "excellent". However, the inconsistency of the microscale LLE experimentation was cause for concern, as it was expected that the use of the automated equipment would remove human error and increase performance. The errors occurred due to errors associated with the operation of the automated equipment and the variability between runs, which required the use of a larger sample size to ensure the significance of the data.

Observations during the development and use of the automated microscale LLE experimentation identified a number of sources of error associated with the workstation (section 4.2.8). These related to the calibration of the workstation, cleaning of the labware, liquid phase preparation and aqueous phase pH issues. These issues identified limitations in the operation of both the automated and laboratory equipment. Many of these issues could be minimised by good laboratory practice and regular calibration of the equipment carried out uniformly, but others were due to physical restrictions in equipment and reagents.

7.3.1.1 Liquid-Liquid Extraction Future Work

The microscale extraction process needs additional experimentation to supplement this research in order to further validate and develop the process.

Validation of the automated microscale LLE process is important for encouraging the uptake of this technology, which should be achieved by undertaking further work in the following areas:

- The automated microscale LLE process was carried out using simulated bioconversion product stream feed material, but real bioconversion product stream feed material must be used to demonstrate the robustness of the process scale in order to further validate it and approve its direct use for optimising the purification of new products from contaminated product streams.
- Investigate the use and integration of accelerated quantitative techniques, such as on-line HPLC or GC analysis to generate data faster for process analysis.
- Further development of the dispensing speed microscale LLE kinetics experimentation to investigate the k_La values achieved using different solvents with a wider range of viscosity and density values to increase their use in this application.
- Develop a theory for creating performance files for an extended range of solvents.
- Investigate the kinetics of phase separation of the microscale LLE process to streamline and accelerate the experimentation, which will facilitate its use in process optimisation experimentation.
- Further investigation of the dispensing speed microscale LLE kinetics experimentation to investigate the k_La values achieved using different solvents with a wider range of viscosity and density values to increase the breadth of the model and its use in this application.
- Further investigate the kinetics of PAA LLE with a wider range of solvents to ensure that equilibrium is reached with the number of mixing cycles or equivalent time used to generate mass transfer.
- Use the microscale LLE process for the extraction of another process stream to demonstrate that this approach is not specific and the results of which will generate a generic process, which will ensure that it becomes an acceptable process scale that can be used to optimise the LLE of any compound, so that it can be used for the purification of new pharmaceuticals within R&D.

- The automated batch microscale LLE process compared favourably with the laboratory scale process (section 4.2.3.1), which acted as a control. However, further validation of the process scale with larger scale processes is required before it's acceptance as a valid experimental tool. This will require comparison with pilot plant LLE scale data and even manufacturing scale LLE data to establish the relevance of the microscale data to other scales and the data accepted as evidence of regulatory control.
- The automated batch microscale LLE process was successfully developed and used to optimise this extraction process. However, LLE is used commercially as a continuous process or as a counter-current process and this process should be considered for the development of a representative continuous microscale LLE process using the automated platforms.
- Develop a microscale counter-current LLE process, which will operate continuously, reducing the volume of organic solvent required and lowering the hazardous chemicals risk. The recycling of the organic solvent is increasingly important to industry as it reduces its environmental impact and process cost, especially as companies are becoming legally and financially responsible for their waste as environmental concerns increase globally and companies face increasing responsibility for their waste management.
- Develop the microscale counter-current LLE process for an established experimental model, such as purifying lactones from the product stream of the Baeyer Villiger Monooxygenase bioconversion that converts cyclic ketones to lactones. The automated scale down of counter-current LLE has been achieved at 400 µL by Sutherland et al (1989) using a liquid handling workstation. This process could easily be scaled down to further reduce the extraction volume in order to rapidly screen key parameters to optimise the process.
- Use the microscale counter-current LLE process for the extraction of another compound from a bioconversion product stream to generate a generic counter-current technique, which will validate it and enhance microscale LLE as an acceptable process scale.

- Quantify the statistical performance of the automated microscale counter-current LLE process method by repeating individual experiments.
- Compare the operational performance of the automated microscale counter-current LLE process with that at the laboratory scale.

7.3.2 Solid Phase Extraction

The automated microscale SPE and supported microscale SPE processes were successfully developed using the automated platforms. The automated microscale SPE processes used the automated platforms to prepare a variety of multiwell formats, including a polypropylene 96-deep well or 24-deep well plate containing a total extraction volume of 1500 µL or 3000 µL and containing the required solid phase. The supported microscale SPE process used a range of 96-well and 24-well filter plates with different membranes to support the activated carbon adsorbent resin and the liquid phase (200 µL). This process used an automated vacuum manifold with the workstation to apply a vacuum to transfer the liquid phase into a clean multiwell plate. A selection of adsorbent resins were screened and activated carbon has a faster rate of adsorption and greater affinity for 6-APA than Amberlite XAD-16 and XAD-7.

The microscale SPE process (chapter 5) was developed using automated platforms to prepare the microscale formats and carry out the SPE methods. The Multiprobe II Ex® workstation and Accelerator™ dosing station were investigated for their suitability for preparing the extraction wells with liquid, solid and slurry reagents. The preparation method of the SPE formats investigated manual and automated slurry handling, as well as automated solid dosing equipment to transfer adsorbent to the multiwell plates. Manual slurry handling (section 5.2.2.1) and automated slurry handling (section 5.2.2.2) were investigated over a range of different pipette tips, volumes, concentrations and particle sizes. The performance of these slurry handling equipment was poor due to the large particle size of granular activated carbon occluding the pipette tip orifice, but this was expected to be suitable for smaller adsorbent particles, such as Amberlite XAD-4. The automated solid dosing station was better than the slurry handling equipment, but also had poor accuracy at dispensing the small resin masses required by the microscale SPE

processes. The microscale SPE formats were prepared using the adsorbent dispensed by the dosing station, then were manually re-weighed to ensure the required high degree of accuracy and dispensed into the wells of the multiwell plates, prior to the addition of the liquid phase. The workstation accurately dispensing the liquid phase and the adsorbent dispensed by the solid handling station were manually checked to prepare the microscale SPE process. Human intervention was required to transfer vials between solid dosing, workstation and analytical equipment, although the filtration rig was controlled via the WinPrep software, removing any scheduling issues.

The automated microscale SPE process was developed as a batch process, which contained four stages: dispensing the adsorbent slurry, dispensing and dispersion of the liquid feed, phase mixing on rotating platforms, and final phase separation under gravity before sampling.

The automated microscale SPE process was developed from that used by Jemal et al (1999), which used pre-filled 96-well plates with a fixed quantity of C_{18} adsorbent resin. This automated method took 1h 41 min to purify 96 samples, which was similar to their semi automated LLE process and three times faster than the manual LLE process. The requirement of mixing was demonstrated by the increased adsorption compared to a static plate and so a horixontal platform was used in all SPE experimentation. The microscale SPE process was used to characterize the adsorption of 6-APA with granular activated carbon, which was investigated by generating adsorption kinetics, adsorption isotherms and pH adsorption data.

The automated microscale SPE process method was used to investigate the activated carbon adsorption kinetics at the 24-well microscale and laboratory scale. The microscale SPE process (36% w/w 6-APA) showed good correlation with the laboratory SPE process (41% w/w 6-APA), although the adsorbents used at each scale were in different states of conditioning due to the limitations of the solid dosing station, but both achieved equilibrium after *circa* 4 hours.

The adsorbent concentration isotherm was carried out at 24-well, 96-well and laboratory scales, which each produced a linear isotherm over the range investigated. The microscale SPE processes used unconditioned activated carbon due to the limitation of the dosing station, which affected the adsorption isotherm gradients compared to the laboratory adsorption isotherm that used conditioned adsorbent. This indicated that the adsorption of water by the unconditioned adsorbent increased the liquid phase concentration. Ideally, this experimentation should have been repeated at the laboratory scale using the unconditioned adsorbent to achieve real correlation between the scales, but this was not possible due to time restrictions. The liquid phase concentration isotherm was also investigated, but no reproducible results were generated to compare to the adsorbent isotherm.

The liquid phase pH conditions effected the adsorption of 6-APA by activated carbon were investigated at the 96-well microscale, 24-well microscale and laboratory scale. The Q_{max} values increased with the decrease in the liquid phase pH conditions. This trend was previously observed by Chaubal et al (1995) and was replicated at each scale. The Q_{max} values for the different scales were similar and validated the experimental processes, which also matched the published data ($Q_{max} = 0.3$) for the laboratory scale SPE (Dutta et al, 1997a). The laboratory data values were slightly lower than the microscale data possibly due to the higher adsorbent mass, use of unconditioned adsorbents or the increased significance of degradation of the liquid phase 6-APA at the microscale (section 4.2.1.4.1).

The performance of the SPE process was influenced by the performance of the automated platforms used within the experimentation. The liquid handling workstation was previously shown to be accurate and precise. There was no accuracy or precision data for any of the microscale SPE processes because of the difficulty of repeating identical conditions due to the imprecision of the solid dosing station, difficulty in manually dosing due to the amorphous nature of the adsorbent and difficulty in identical conditions of the laboratory scale. The performance of the automated SPE process used by Jemal et al (1999) generated a 0% to 7.8% inaccuracy, inter-run precision of 0.3% to 4.3% RSD

and intra-run precision of 3.1% to 9.6% RSD. The performance values quoted in the literature for SPE processes were for the performance of the liquid handling workstation rather than for dispensing solids or the SPE experimentation.

The supported microscale SPE process was developed using the automated platforms with a filtration rig using the 24-well and 96-well filter plates to support the adsorbent resin. The process required a total reagent volume of 800 μL. The supported microscale SPE process was operated as a pseudo continuous process with five stages: dispensing the solid phase in the filter plate wells; conditioning the solid phase and membrane; dispensing the liquid phase to contact the resin; phase separation; eluting the adsorbate from the solid phase and washing the solid phase. Each of these stages were programmed into the Winprep software and linked to the controller device of the filtration rig to co-ordinate their operations. The workstation dispensed the aliqots using the 'Fst' performance file to accelerate the process operation. This process was suitable for investigating the key parameters: adsorbent conditioning; adsorption; phase mixing; phase separation; elution characteristics of the SPE system; adsorbent washing and regeneration. The results of these experiments could be used to optimise the process.

The supported microscale SPE process adsorption yield (87%) was greater than that seen using the batch microscale SPE process (75%) due to the use of conditioned adsorbent. The supported SPE process demonstrated the high capacity of the adsorbent for 6-APA (*circa* 0.6 $g.L^{-1}$). The washed filter membrane absorbed some 6-APA (filtrate = 90% feed 6-APA concentration), which may have been retained within the membrane rather than adsorbed onto the membrane fibres as subsequent washing of the filter released the remaining 6-APA. This indicated that the filter membrane was a suitable support matrix, as it would not affect the adsorption of the reagent. The support matrix was tested with the adsorbent resin (mean adsorbate 6-APA concentration = 87% w/w).

7.3.1 Solid Phase Extraction Future Work

The microscale solid phase extraction process requires additional research in order to further validate and develop the process. This should focus on the validation of the

microscale membrane supported SPE process, as it also showed increased versatility for investigating all aspects of the SPE process. This made it suitable for investigating the comparison of key process parameters with the laboratory scale, which could validate this process scale, as well as determine the robustness of both microscale processes. Currently there is no laboratory scale supported process.

The automated batch microscale SPE process compared favourably with the laboratory scale process (section 5.2.4.3). However, the automated microscale SPE processes were carried out using individual, analytical grade reagents. Therefore, the process requires further validation before its acceptance as a valid experimental tool by:

- Use of real feed material direct from biotransformation or LLE purification containing trace contaminants to assess the performance of the selected adsorbent to see if the contaminants effected the SPE process deleteriously, such as by causing adsorbent inhibition or preventing its regeneration.
- Further validating the process using another experimental system, such as the BVMO bioconversion product, ketone, separated from lactone to validate its use as a generic process.
- Assessment of the microscale SPE process performance using statistical analysis for quantitative comparisons using resins of smaller particle size.

The use of the supported SPE process to screen parameters to fully investigate the conditioning, adsorption and elution stages of the solid phase extraction process would require:

- Use of the supported microscale SPE process to optimise the adsorbent conditioning, elution and regeneration conditions for the extraction of 6-APA using activated carbon to indicate the time saving of carrying out automated experimentation to generate this data.
- Use of experimentation to use real feed material direct from biotransformation or post LLE purification material containing trace contaminants to assess the performance of the selected adsorbent and the supporting filter to see if this

effected the SPE process deleteriously, such as membrane fouling, adsorbent inhibition or regeneration inhibition.

- Assessment of this SPE method to investigate the regeneration of the adsorbent and the breakthrough of the adsorbent with a specific adsorbate.
- Demonstration of the automated microscale supported SPE process to be an effective microscale technique. This process could be used to screen a range of adsorbents, adsorbates and liquid phase pH conditions. This process could be used to assess the desorption conditions, investigating the desorption buffer, pH and desorption kinetics. This would expand its utility and further validate this experimental tool.
- Screening of a number of other adsorbents for the purification of 6-APA, such as Amberlite XAD-7 and XAD-16 (Dutta et al, 1997a), which was used for the purification of another compounds, such as 7-ACA, cephalexin and cefadroxyl. This would facilitate further characteristic analysis of these adsorbents and investigate automated slurry handling using the workstation to prepare the multiwell plates for microscale SPE process.
- Development of a laboratory supported SPE process that matches the geometry and has an equivalent pressure drop to compare with the microscale supported SPE process and the laboratory SPE process.
- Validation of the membrane supported SPE process for the comparison with other process scale data (laboratory scale) to compare their purification. Validate both the microscale and laboratory scale supported SPE processes with larger SPE process scales (pilot plant and manufacturing scales).
- Quantification of the statistical performance of the automated microscale supported SPE process method by repeating identical experiments by using resins of smaller and uniform particle size.

At the laboratory and larger scales there are an increasing number of pieces of automated equipment that are controlled by PC software, such as the monitoring and control systems of the conditions within the extraction vessel. This automation is common, especially in pilot plant equipment where the vessel cannot be opened to investigate the conditions in

the media to prevent contamination of its contents. To control the extraction conditions, on-line monitoring is used and the vessel is designed with sampling ports that do not effect its sterility and an eyeglass to monitor the conditions inside the vessel. This uses the integration of automated hardware with interpretational software, which has been achieved in the chemical industry by Camile Products. This company was purchased by Argonaut (Argonaut Inc, 2002) and these systems are working at a larger experimental scale which increases their productivity and accelerates the drug development process, whilst reducing their costs. This approach of integrating automated synthesisers with software has been extended to create experimental design and process optimisation software that links all the pieces to make an automated chemical laboratory. Ideally, these processes will integrate with the equipment within automated laboratories.

7.4 Conclusion of Commercial Potential of Research

The commercial potential of the research investigated in this thesis was analysed (chapter 6) to evaluate the microscale process optimisation technology called Smart Screening for Process Design Optimisation (SS-PDO). The scientific validity of the microscale experimentation was demonstrated in the previous chapters. The microscale automated platforms and the development of system architecture was defined to integrate additional pieces of standard automated laboratory equipment with experimentation and scheduling software to provide a fully automated path to an optimised process. The bespoke experimental software rapidly screens process parameters of the production and purification routes for new pharmaceuticals to increase their efficiencies. SS-PDO generates faster and more accurate results at a smaller scale at lower cost than before and accelerates the securing of regulatory approved routes early in the development cycle.

Analysis of the technology and potential customer needs identified the potential markets for SS-PDO, which included the pharmaceutical industry and the specific sub-market focused on was the biopharmaceutical industry due to its high value products and potential growth. The total estimated potential market for SS-PDO was estimated to be $404 million. The 5 large pharmaceutical firms already use automated equipment for

drug discovery, which reduces the barriers to entry and this technology. Discussions with key players in the industry expressed a need for such technology, and they have budgets to invest in new technology, so are ideally placed to become customers. However, they have existing links with the automated equipment manufacturers, so there will be competition from companies such as Tecan, who are the most notable automated equipment suppliers that have their own software product ranges. SS-PDO had limited protection of its intellectual property as there were competing patents identified and the developed software is only protected by copyright, which makes it a weak technology to have as a core product. The business models developed for a new venture using this technology were investigated identifying: a systems integrator; licensing; and consultancy models.

It is believed that incumbent automated laboratory equipment manufacturers are best placed to take this new technology to market. They have access to large customers and have total control over their existing product portfolios on which the SS-PDO concept depends. However, manufacturers will depend on the unique collection of knowledge and skills of UCL researchers to develop and commercialise the concept. It is recommended that a consultancy venture be formed to partner this knowledge with the strategic resources of an operational equipment manufacturer.

It is recommended that SS-PDO requires additional work before it is commercially viable and the following recommendations were made:

- Seek further advice on the options available to protect the experiment design IP that has been developed.
- If suitable IP protection can be put in place, a company should be formed around the consultancy business model.
- Partnership with a large equipment manufacturer is essential for compatibility with and supply of industrial equipment. One of these should be selected to work with on an exclusive basis, initially with Perkin-Elmer as recommended.

- The equipment manufacturers are unlikely to have the unique combination of engineering understanding and skills possessed by the university researchers in this field. The presentation and definition of this skill set needs to be improved in order to sell the partnership and the whole SS-PDO concept to customers.
- Additional research of ~50 man-years of work are needed to characterize all parameters required for pharmaceutical production processes. Once formalised as a consultancy venture, the new firm must broaden its access to other research resources. Unless SS-PDO can address more than the initial 'niche' market, the concept will have limited application.
- A comprehensive business plan should be written to gain funding to finance further research required to validate this technology.

7.5 Future Developments in Pharmaceutical Industry

The pharmaceutical industry contains automated laboratories with high throughput equipment that are being combined to increase sample throughput for seamless experimentation. This had been developed in order to combat some of the current problems of the pharmaceutical industry, namely the limited number of drug discoveries and delays in transferring the process to manufacture. This research has shown the potential of using an automated laboratory to investigate the processes within biochemical engineering. This would require the development and investigation of further unit operations at the microscale such as fermentation or chromatography, as well as the enhancement of these automated platform functions by adding microscale pH control, or their manipulation to achieve increased performance of the equipment and experimentation. The business potential of using such a laboratory for process screening and optimisation showed that this would achieve cost savings, but this technology would be best developed by one of the automation instrument manufacturers (chapter 6).

The pharmaceutical industry, like other industries, is constantly searching for ways to increase its profitability. Ten years ago, this was achieved by a series of cost cutting measures related to the production of pharmaceuticals. Now, their focus is on increasing

the number of drug candidates entering the market by increasing innovation and integration of new technology. The integration of automated equipment has achieved this by increasing the sample throughput for candidate screening.

Automated experimentation rapidly generates precise and accurate data. The HTS approach has generated a number of possible drug candidates, but this has transferred the bottleneck in the R&D process mainly to the manual process development stages (Conner, 1999). This identified that the next area to become automated is process scale up in order to decrease the pre-clinical R&D time to 12 months. The automated platforms will become essential within R&D of new chemical entities to rapidly scale up their production to produce compounds for clinical trials and then manufacturing. This could save development time, which could accelerate the product to market by reducing the time at pilot plant experimentation.

The pharmaceutical industry is using this automated equipment in drug discovery for combinatorial chemistry, high throughput screening and bioanalysis in order to accelerate the generation of experimental data on new drug candidates, facilitating research and development process. The automated process optimisation could also save the pharmaceutical companies both time and money, which could deliver therapeutics to the patients quicker, whilst improving the profits and productivity of the pharmaceutical companies.

As the pharmaceutical industry develops it will become of increasing importance for multidisciplinary teams to work together on the development of a product. This may even require a good understanding of the technologies used in the industry at the higher management business levels to understand the limitations and aspirations of the researchers using the automated approach. It is important that everyone is conversant with the design of experimentation software so that information can easily be shared and discussed, reducing time lags in translating it to real applications.

The requirements of the pharmaceutical industry are varied, but must comply with good laboratory practice and good manufacturing practice. A new pharmaceutical must clear 4 phases of clinical trials and gain approval from the regulatory authorities, which all take time. To integrate this technology into the pharmaceutical industry, the automated microscale research and its data must be accepted by the regulatory authorities as a research tool that is a suitable alternative to the traditional laboratory methods for generating information in support of the application for the approval of process applications. This will require the proof of the engineering principles behind the processes and validation with other process scales using a variety of experimental models.

Appendices

Index of Appendices

Appendix 1: Multiwell Plates and Automated Equipment

The multiwell well plate has changed greatly during its brief history in respect to its composition, format and other specialist characteristics that were adapted to increase its versatility. The multiwell plates have all been developed to facilitate their use with automated equipment for a diverse range of applications (section 1.4).

A1.1 Multiwell Plate Composition

Microwell plates are produced from a variety of different plastics by injection moulding into a cast, which make them lightweight, cheap and disposable (Johnson 1999). The selection of the plate's composition material depends upon its end use and the material properties required. For example, those made from thermosetting plastics are resistant to high temperatures, which makes then suited to PCR applications. The composition of the plates also effects its absorbent properties, effecting the suitability of the plate at certain UV wavelengths, IR or gamma radiation to measure optical density or for scintillation counts. Most of the plates are manufactured from either polystyrene or polypropylene.

A1.1.1 Polystyrene

Polystyrene is the most popular plastic used to manufacture bottles, petri dishes and multiwell plates due to its glass-like properties, which makes it ideal for microscopy and spectrometry. However, this material property makes the products brittle so they shatter easily when subjected to a torque force, such as that experienced in a centrifuge. In addition, the hydrophilic nature of polystyrene adsorbs hydrophobic molecules, especially DNA and proteins. Therefore, the quantification of these compounds requires the use of disposable polystyrene cuvettes to avoid cross-contamination. The spectrophotometer readings are affected by the radiation absorbance of these plates below 250 nm. As polystyrene also emits fluorescence readings taken below this wavelength, the samples must be contained in quartz plates or glass cuvettes to avoid any interference.

To overcome this problem, polystyrene is mixed with cellulose acetate and a dye to create a black plastic. This creates plates suitable for fluorescence measurements, as the cross-talk between the wells is minimised. Polystyrene is also mixed with titanium oxide to create white

opaque plastic plates. The white plates are suitable for luminescence measurements, as the signal is not distorted within the well.

A1.1.2 Polypropylene

Multiwell plates are also manufactured from polypropylene, which is a flexible and chemically inert plastic. Polypropylene is often the composition material of containment vessels designed for materials containing organic solvents or used to produce eppendorf ^{TM} tubes as its flexibility allows a hinged top.

A1.1.3 Other Materials of Plate Compositions

Multiwell plates can be manufactured from other plastics, including polyethylene tetrachloride (PET), polycarbonate, polytetrafluoroethyl (PTFE), polyvinylchloride (PVC) and polyacrylamide. Multiwell plates are also manufactured from borosilicate. These plates are both resistant to organic solvents and are re-usable, which makes them ideal for research into liquid extraction.

Polycarbonate combines the best characteristics of polystyrene and polypropylene. It is lightweight and cheap. This material is typically used in the manufacture of plates with tapered wells for polymerase chain reaction (PCR) applications. The polycarbonate plates are not resistant to organic solvents, so would not be suitable for many chemical applications. The polytetrafluoroethyl plates are resistant to organic solvents, making them suitable for liquid-liquid extraction experimentation. The limited durability of these plates would restrict their use with automated equipment that uses a gripper arm due to their increased flexibility. The choice of the composition material of a microwell plate will, therefore, greatly depend upon the reagents required and the automated handling of the plates in the specific experimentation.

A1.2 Plate Footprint

The multiwell plate's footprint dimensions were initially different during their development by various manufacturers, which caused problems for the companies developing and manufacturing automated equipment. Agreement of these industry leaders generated multiwell plates that were designed and manufactured to the standard footplate (80 mm x 130 mm) detailed by the Society for Biomolecular Screening (SbS). This allowed their use in most automated instruments without any modifications.

A1.3 Plate Properties

The multiwell plate was altered from its original standard 96-well format to alter the number of wells, their volume, geometries, shape, configuration and the well coatings to facilitate different applications.

A1.3.1 Well number

The number of wells in a multiwell plate was modified for a variety of specific uses. Tissue culture demanded a series of vessels to gradually scale up the replication of a mammalian cell clones and this inspired the 48, 24, 12 and 6-well plates to sequentially grow up cells in larger wells to achieve staggered growth. This allowed the cell line to achieve confluence before being transferred from the 96-well plate to the next larger size before the cell number was great enough for the cell line to survive in a 50 ml tissue culture flask. However, not all applications required larger well volumes. The needs of HTS for increased number of wells lead to the development of the 384 and 1536-well plates to cope with the generation of large numbers of compounds. This was important as assays became further miniaturised. These samples were screened in 384 and 1536-well plates, which increased the plate's sample capacity and allowed ultra-high throughput screening (UHTS) to occur. This facilitated the automated storage and retrieval of drug discovery libraries (Hudson Control Group 2002).

A1.3.2 Plate Geometries

The shape of the well has increased to round and square in cross-sections. The round wells aided mixing when placed on an oscillating table. The well's volume was increased from the standard 339 mm^2 by creating a deep well plate, which is used in fermentation to limit the effects of evaporation. The well bottom was also varied from a flat bottom to a U, V or C shaped bottom to aid material retrieval and increase material contact and mixing. Plates even changed the composition of the well bottom to ensure light transductance, so that they could be read on a spectrophotometer at the ultra-violet wavelengths to detect DNA or contained membranes to allow filtration to occur.

A1.3.3 Plate Configurations

The wells in a standard 96-well plate were arranged in 8 rows and 13 columns, with each well neighbouring up to 8 wells. The configuration of the wells was altered to reduce cross-

contamination by arranging the wells with skewed alignment, neighbouring up to 6 wells. Another well configuration was to arrange the wells in a circle, so that each well neighboured only 2 wells.

A1.3.4 Plate Coatings

The multiwell plate was adapted by adding a surface coating to facilitate its use in new applications like tissue culture, which was first designed in 1988 by Xenopore using streptavadin to enhance the cell adhesion to the well walls. The success of this led to the creation of a number of chemical and biological coatings of the plates for a variety of applications. This further widened the scientific fields using these plates, which has increased emerging plate designs.

A1.4 Automated Equipment

The automated laboratory contains a number of pieces of automated equipment that are often linked together by a robotic arm (section 1.3.2.1). Details of the automated equipment and their manufacturers are presented in table A1.4.1. The most widely used piece of automated equipment is the liquid handling workstation. A variety of these workstations have been developed by a number of manufacturers (section 1.3.2.1.1).

A1.5 Automated Devices

Automated equipment are compatible with many devices that expand its utility (section 1.3.2.2). These devices include the plate stacker and the robotic arm, to be used for an expanding number of applications. Details of the devices, their manufacturers and product names are presented in table A1.5.1.

Automated Equipment	Manufacturers		Function
Liquid handling workstation	Various – see table 1.3.2.1.1		Pipetting Diluting, Mixing
Parallel synthesis	GenVac Robbins –	Flexichem Chemspeed	Chemical synthesis
Concentrator	Porvair Scientific Ltd		Reduce sample vol.
Centrifuge	Qiagen Beckman Coutler	Sorvall	Solid-liquid separation
Plate washers	Bio-Rad Colibri Robotics Flush division of Digital Instruments Labsystems Molecular Devices	Tecan Titertek Tomtec Tri Continent Bio-Tex	Cleaning the plate of reagents used in ELISA etc.
Rotary evaporators	GenVac		Solvent evaporation
Thermocyclers	Biotech Europe MWG Biotech AG	GMI IT Biochem	PCR
Plate stackers	CCS Packard Hudson Control Group Tecan	TekCel Titertek Tomtec Velocity 11 Zymark	Storage of plates, tip boxes
Analytical instruments	See table 1.4.4.1		Analyse sample
Automated samplers	Spark Perkin Elmer	Auora Biomed Alcottt Tech Inc.	Deliver sample to analytical instruments
Robotic arms	Beckman Coulter CCS Packard CRS Hudson Control Group	TekCel Titertek Tomtec Velocity 11 Zymark	Moves plate between robotic equipment

Table A1.4.1. Automated equipment categories found in an automated laboratory with their major manufacturers and functions (information from company websites).

Devices	Manufacturers	Product Names
Incubator	Radleys	Microtherm shaker incubator
Temperature controlled mixing	Eppendorf	Thermomixer
Shaker	Radleys	Roto mix
Stirrer	Radleys	Magnetic stirrers & fleas
Plate warmer	Wolflabs	Plate warmer
SPE cartridge rig	Phenomenex Whatman ISI Millipore	Vacuum manifold
Plate sealer film & roller	Radleys	Aluminium foil, Duraseal, membrane, thermal bond film, Prafilm
Plate Lids	Radleys	PTFE. Polypropylene, Polystyrene
Filtration rig	Radleys	UniVac SPE manifold
Water bath	Grant Instruments	Water bath
Optic probes	Anglia Instruments Ltd. Cordis Corporation Ocean Optics	FOXY A1 fibre optic oxygen probe pH probe
Calometric probe	TopoMetrix Corporation SeBolt	Platinum rhodium resistance probe Narayansdwamy-Moynithan
Microscope probe	Thermomicroscopes	Scanning/Proximal/ Nearfield optical scanning microscope
Balance	Zinsser Analytical	Balance with data collector

Table A1.5.1. Devices compatible with multiwell plates and automated equipment, their manufacturers and product names (information from company websites).

Appendix 2: Comparison of Biocatalytic Properties

	Penicillin Acylase	***Baeyer-Villiger* Monooxygenase**
Organisms	Bacteria, fungi, animal, plant, actinomycetes *P.chrysogenum* *E.coli*	Bacteria & Fungi Acinobacter - pathogenic, toxic substrate gm Baker's yeast, b-phenethyl alcohol gm-*Ascinomyces*
Enzyme availability	Whole cell Free enzyme Immobilised on Eupergit C & other carriers	Whole cell, higher yield cofactor regeneration Immobilised on Eupergit C requires cofactor regeneration
Reaction	Penicillin G -> 6 amino penacillanic acid + Phenyl acetic acid (figure 1.6.2.4.1)	Cyclohexanone -> caprolactone ketone -> ester cyclic ketone -> lactone
Cofactors	N/A	NADPH
Conditions	pH 7.8	Cleavage under mild conditions
Enantiomer specificity	Specific	Specific
Substrate	Penicillin G Penicillin V	Ketones: cyclobutanones cyclopentanones Cyclohexanones bicyclic ketones
Kinetics	Characterized	Uncharacterized
Inhibition	Substrate & product	Substrate & product
Biocatalyst Cost	Free enzyme: £37.20 for 750U Immobilised: £22.55 for 500U	Purified enzyme unavailable
Reagent Assays		
Gas Chromatography	GC for PAA	GC
Colourimetric	6APA Hydroxylamic hydrochloride p-dimethylaminobenzaldehyde (415nm)	340nm Glycerol3Phosphate dH Glutamic Oxaloacetate Transamase Alcohol dehydrogenase
Potentiometric	PH stat for PAA	N/A
HPLC	HPLC 225/ 260nm for 6APA & PAA, Pen G	N/A
Fluorescence	PAA, Pen G	N/A
Mass Spectroscopy	PAA. 6-APA. Pen G	N/A
UV/Vis/IR spectroscopy	PAA. 6APA. Pen G	N/A
NMR	PAA. 6-APA. Pang	N/A
Process	Batch Continuous	Batch

Appendix 3: Immobilised Enzyme Activity

Immobilised enzymes are covalently bonded to the support molecules. The immobilisation on carrier beads effects the enzyme's activity as the diffusion of the substrate to the catalytic site and the removal of the products is limited. This creates micro pockets of high concentrations of these reagents within the support matrix, which enhances their inhibitory effects (Kasche et al, 1983). The concentration and pH gradients established within the carrier may decrease the effectiveness of the enzyme, as it drives a less favourable equilibrium. A mathematical model has been used to explain the diffusional effects on kinetics (Kumar et al, 1996).

Immobilisation restricts the diffusion of molecules around the catalytic site. This reduces the diffusion of the products from the enzyme, which creates pockets of localised high concentration, increasing their inhibitory effects. Fick's law states that the mass flux is proportional to the concentration gradient (equation A3.1) and describes the diffusion of these ionic compounds within the carrier.

$$J_A = N_A - D_{AB}\frac{dC_A}{dy}$$

[A3.1]

where J_A is the mass flux, N_A is the rate of mass transfer of the solute, A is the interfacial area where mass transfer occurs, D_{AB} is the diffusion coefficient or diffusivity of component A in a mixture of A and B, dC_A is the change in concentration of solute A and dy is the change in distance (Doran, 1998). This equation also relates to the mass transfer between town immiscible phases for LLE (appendix 13) and SPE.

Fick's law assumes that the buffer is evenly distributed over the carrier so that the buffer is not transported within the carrier. Thieles modulus is a measure of diffusion at the catalytic site and Kumar et al (1996) calculated it at 1.67 to 9.8, which implies that the diffusional effects are significant. The substrate and products are electrolytes and perform under thermodynamic laws, which also effect their access to the catalytic site. Diffusion limitations reduce the intrinsic kinetic ability of the enzyme as the limited removal of the products reduces the binding of new substrate.

The concentration of penicillin determines the effective diffusion velocity within the immobilised enzyme, as it is slower to associate with the enzyme than for the products to disassociate. This is because the substrate can not diffuse through the entire particle (particle porosity), the pores are entangled, ever changing the path of diffusion (particle tortuosity) and the pores are of similar size to the substrate (restricted diffusion). The internal surface chemistry and charge also effect the mass transfer rates.

The diffusion limitations within the carrier molecule create pockets of high product concentration (PAA), which effects the localised pH. The average pH gradient within the Eupergit C carrier is 1 pH unit below the bulk pH with the use of buffers because of the localised higher concentration of PAA during penicillin hydrolysis (Spiess et al, 1999). The use of buffers with pK values similar to the bulk pH reduces the scale of the pH gradient created within the immobilised enzyme. "Low pH zones cause optimal reaction rates, reduced equilibrium conversion and reduced enzyme stability" (Kasche, 1983).

It is essential that the bioconversion reactor is well mixed to generate the maximal efficiency of the immobilisation process. Fick's law assumes that the reactors housing the immobilised enzymes have plug flow and are ideally mixed to create a homogeneous solution. However, the stirrer speed selected must not cause shear damage to the immobilised enzymes nor create fine particles.

Appendix 4: Characteristics of the substrate and products of Penicillin Acylase

Characteristic	Penicillin G	6-Amino penicillinic acid	Phenyl acetic acid
Formula	$C_{16}H_{18}N_2O_4S$	$C_6H_{12}N_2O_3$	$C_8H_8O_2$
Molecular weight	334.38	216.28	136.14
Nature	Powder	Non-microscopic crystals	Macroscopic crystals
Key functional groups	Benzyl Carboxylic acids Methyl x2 Aldehyde	Amine NH2 Carboxylic acid Aldehyde Methyl x2	Benzene ring Carboxylic acid
Boiling point	N/A	198-200 °C	76.5 °C
Melting point	N/A	N/A	265.5 - 97 (760-1) °C
Aqueous solubility	Potassium salt freely soluble	Freely	Freely in hot, sparingly in cold Sat sol 0.131 N
Organic solubility	Methanol Ethanol Glycerol	Alcohol	Alcohol Ether
Thermal stability	RT, 20°- 25 °C	1 - 5 °C few days	RT, 20 - 25 °C
pH stability	Aqueous: pH 5-8 pH decomposition rate constant 3% aqueous solution 5-7.5	3% aqueous solution 5 - 7.5 pH	
Degradation	Spontaneous hydrolysis -> 6APA and penillic acid (dissociation of carboxyl group)	Spontaneous degradation Acid solution: -> penillic acid Aqueous solution -> penicilloic acid Alkaline solution -> penicilloic acid	
pKa	2.75	2.3, 4.91 (Rapson & Bird 1963)	5.56 x 10-5
Hazards	Irritant to eyes, skin & breathing	Sensitization if inhaled avoid eye contact Consumption Strong oxidising agents	Irritant to eyes & skin Affects breathing

Appendix 5: Multiprobe Terminology Definitions

Terminology	Explanation
Blowout mode	Dispensing mode that aspirates exactly the volume of liquid required, dispenses it and subsequently dispenses a volume of air to ensure that the entire aliquot is dispensed
Deck	Working area of the workstation onto that equipment or racks to hold disposable labware are fixed
Mixing cycles	Sequential aspiration and dispension of an aliquot of liquid from the same location
Multiprobe	Liquid handling workstation made by Packard Instruments/Perkin Elmer containing 4 independent automated pipettes
Labware	Equipment, devices or consumables used on the deck within the test
Performance file	Instructions to control the operation of the liquid handling workstation detailing the pipetting speeds, air gaps, delays, pump ramp etc. (section 2.2.1.4.1)
Procedure	Action consisting of a series of individual steps e.g. Flush/Wash
RAMP	Random access motor precision, incremental increase in movement of piston
Rak	Fitting to secure labware onto the deck
Reagent trough	35mL, 50 mL or 100 mL square or rectangular cross-sectional container made of PTFE that fits within the metal frame rak.
Step	Individual task e.g. pick up disposable tip from tip rack
Test	Series of procedures to carry out an experimentation method
Test outline	Details of the composite procedures within the test and the layout of the labware on the deck
Tracking	Vertical movement of the pipette tip during aspiration or dispension following the liquid level
Waste mode	Dispensing mode that aspirates more liquid than required to dispense exactly the volume specified, wasting the excess liquid
WinPrep	Software controlling the operation of the Multiprobe liquid handling workstation

Appendix 6: Multiprobe Tests

Layout of labware on the deck and an overview of the procedures in the bespoke tests written for the Multiprobe II^{EX}, which are detailed in table 2.2.1.2.1 and 2.2.1.2.2 are illustrated below:

Test: Dispense

Dispense RO water aliquots into HPLC vials to assess performance.

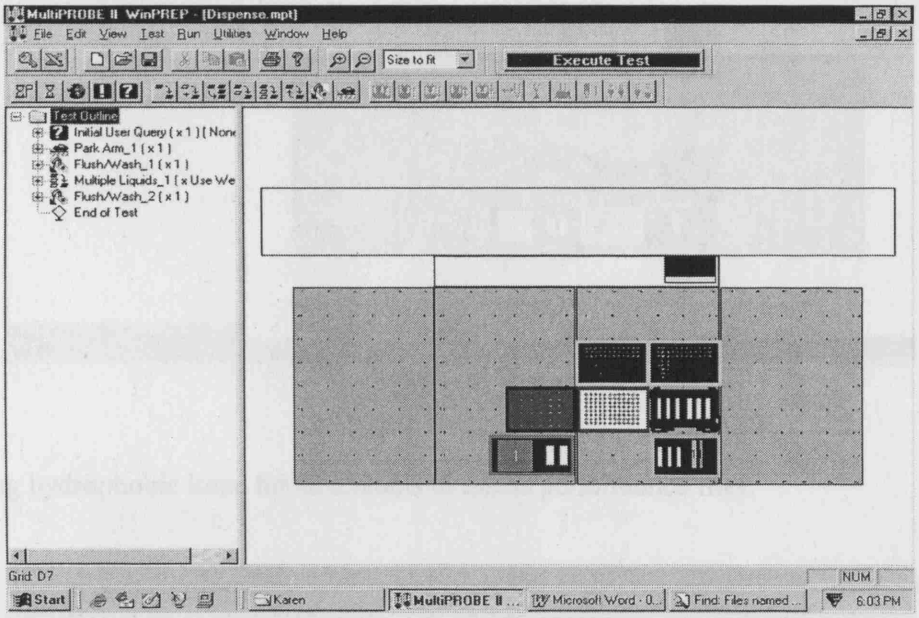

Test: Dispense BA

Dispense butyl acetate aliquots into HPLC vials to assess performance.

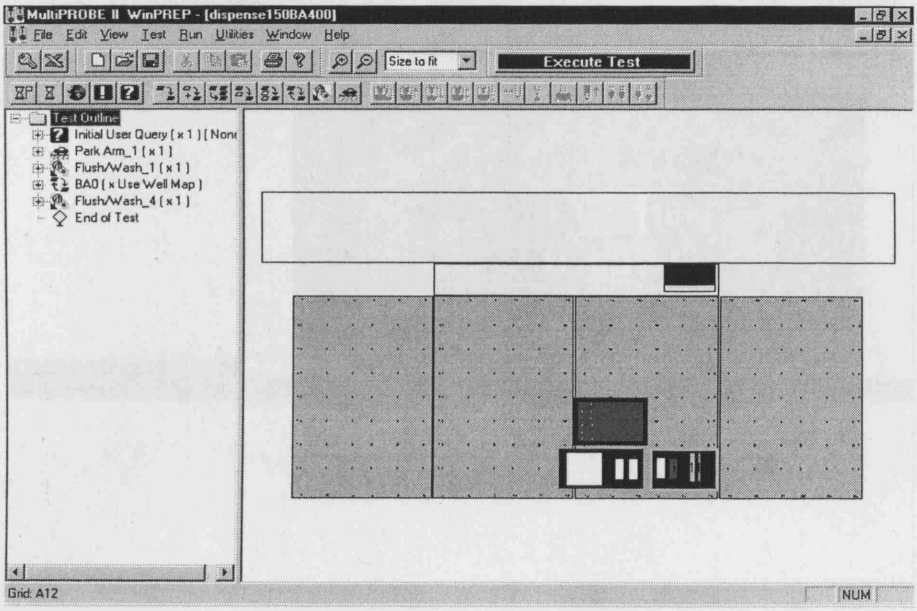

Test: Exp1

Dispense RO water aliquots to assess performance files.

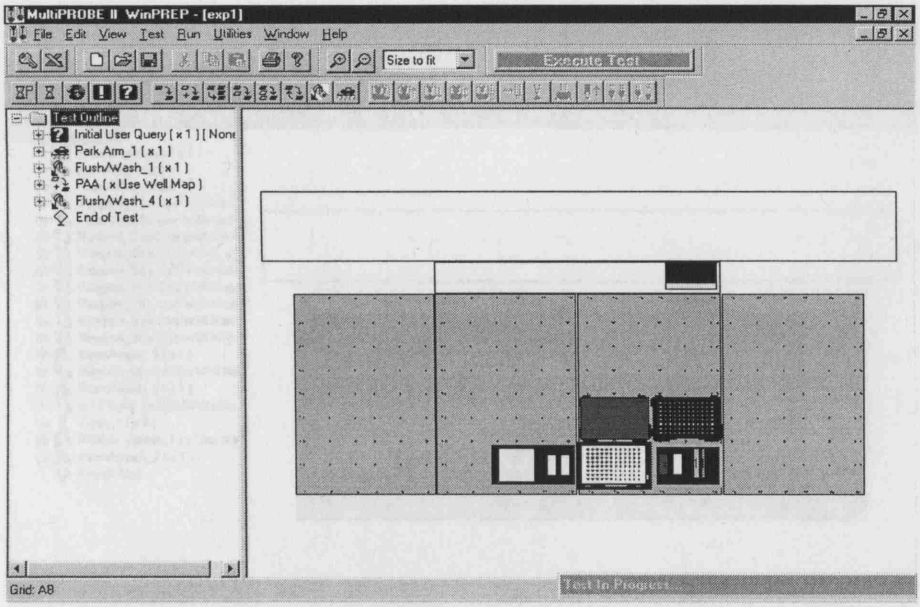

Test: Hpi

LLE using hydrophobic ionic liquid aliquots to assess performance files.

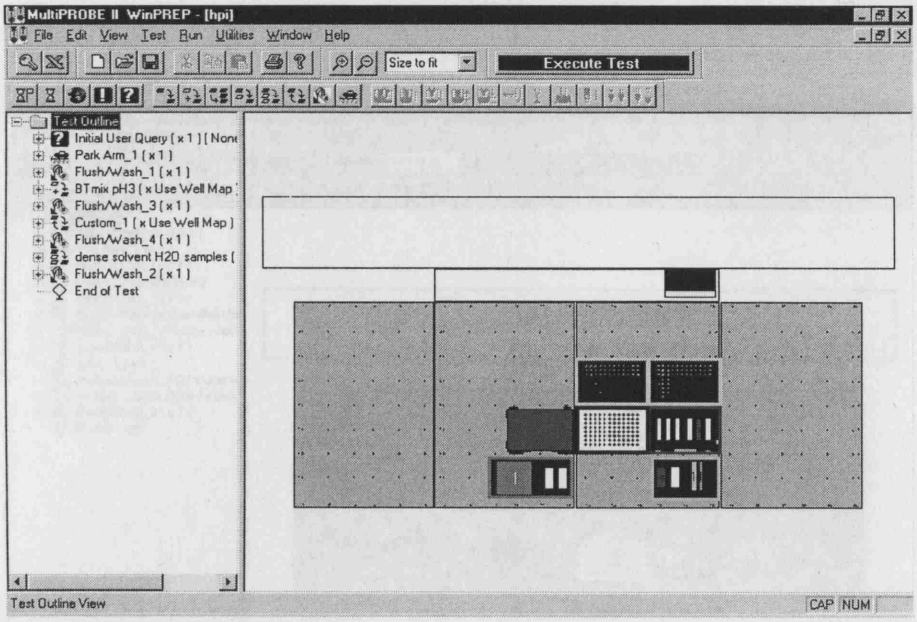

Test: LLE 9pH

LLE using 9 different aqueous phase pH conditions.

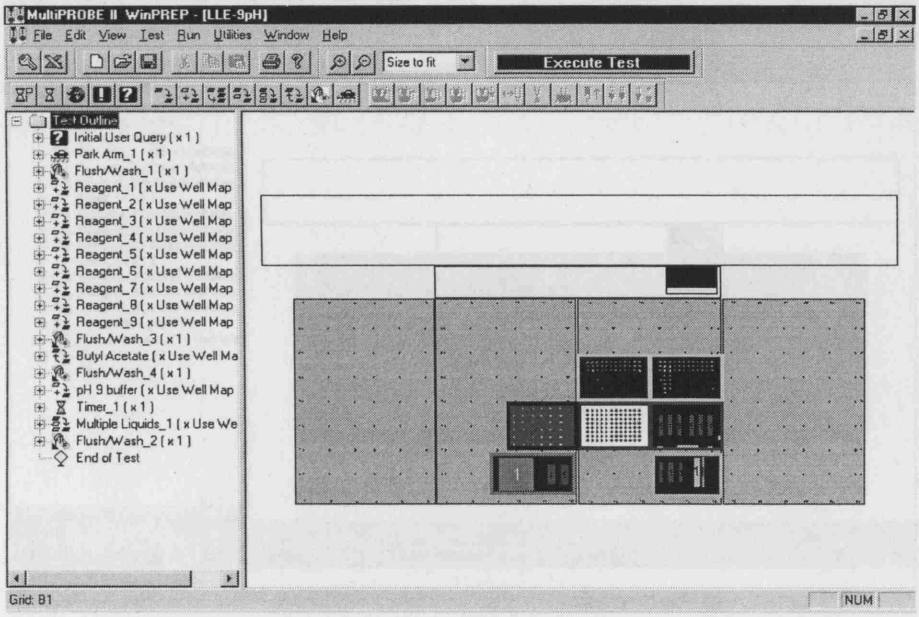

Test: LLE mass balance 1pH

LLE at 1 pH with sampling of the aqueous and organic phases.

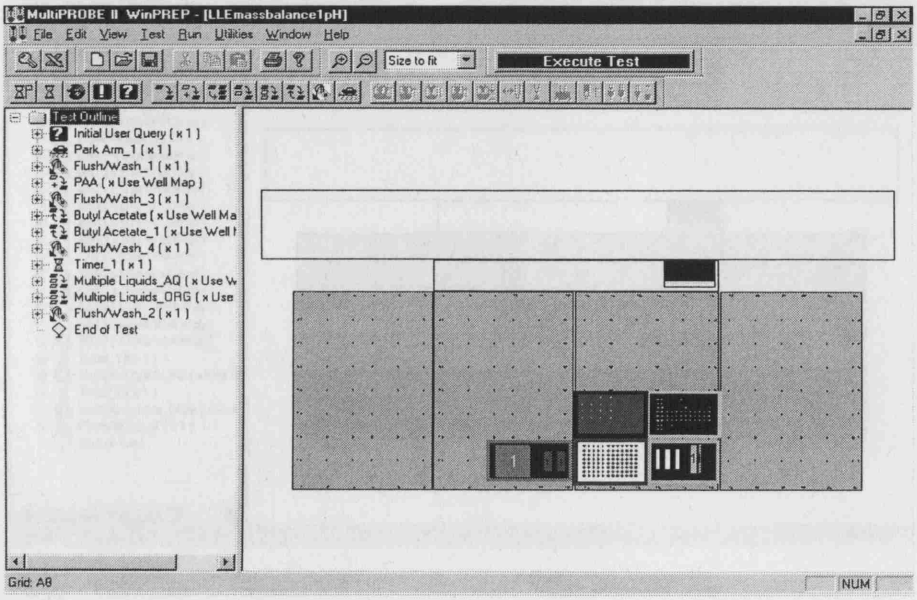

Test: LLE PH-HPLC

LLE at 9 different pH conditions and transfer of the aqueous phase samples to HPLC

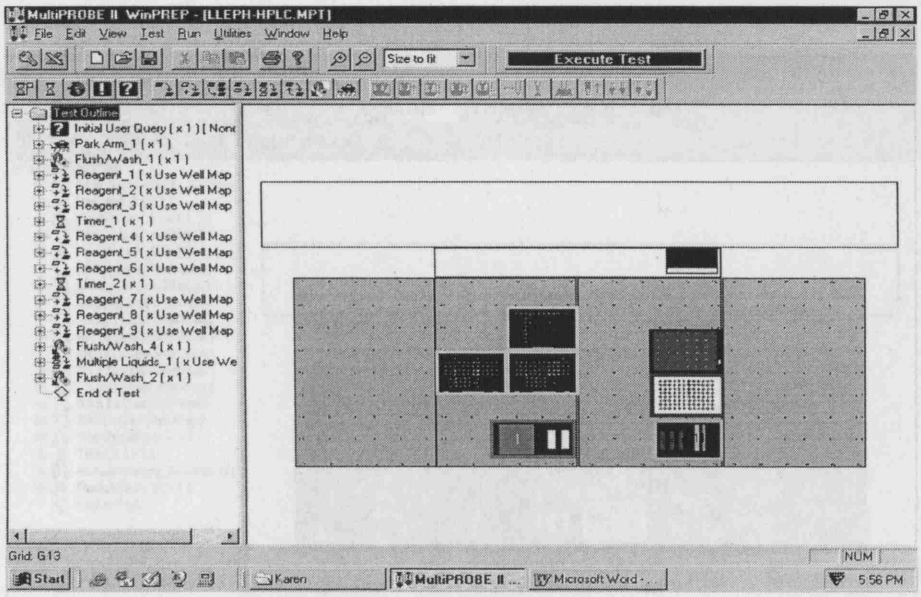

vials.

Test: LLE Static v Move

LLE with static and mixed phases.

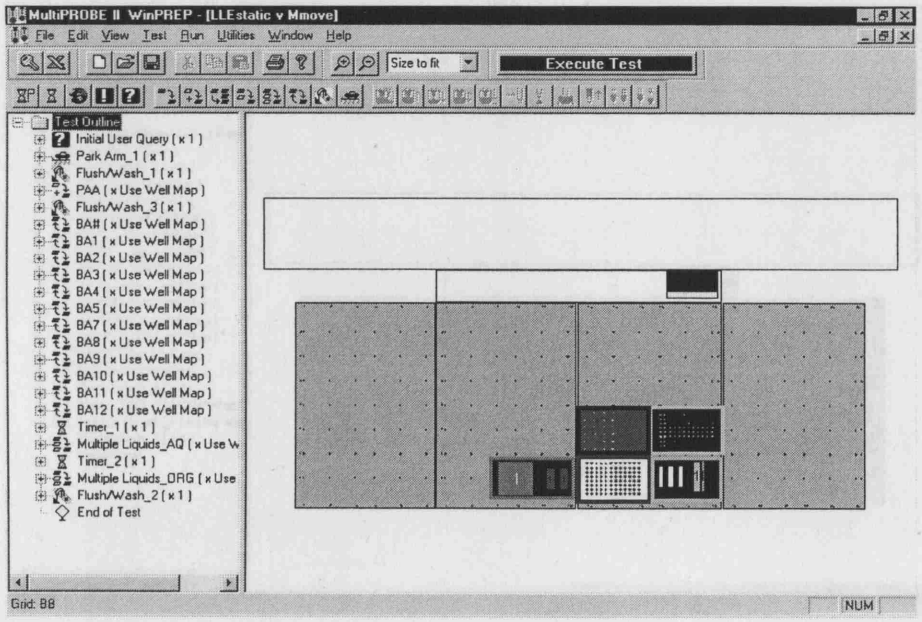

Test: Mix150

LLE with 150 µL phases mixed at a range of mixing cycles.

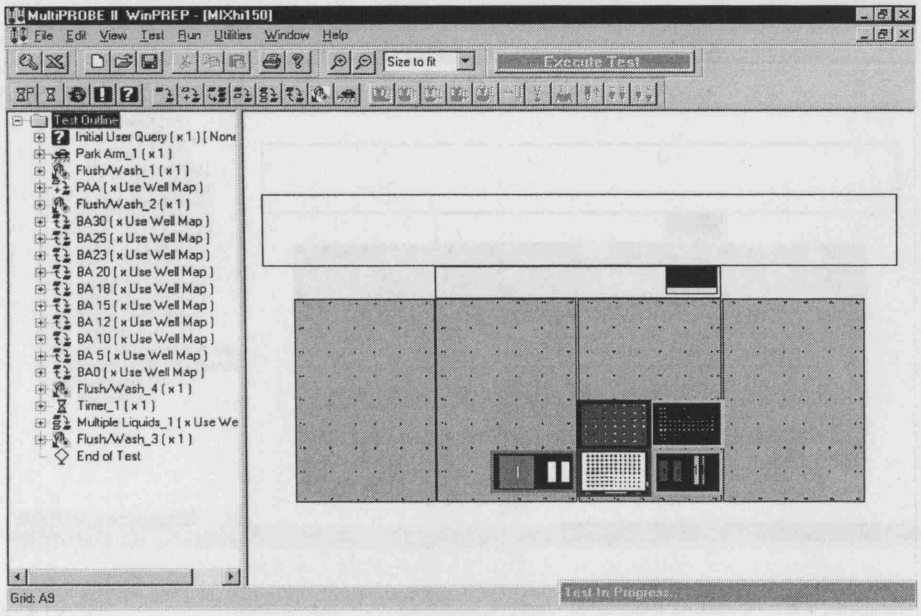

Test: MIX HI 150PG

LLE of Pen G with phases mixed at a higher selection of mixing cycles.

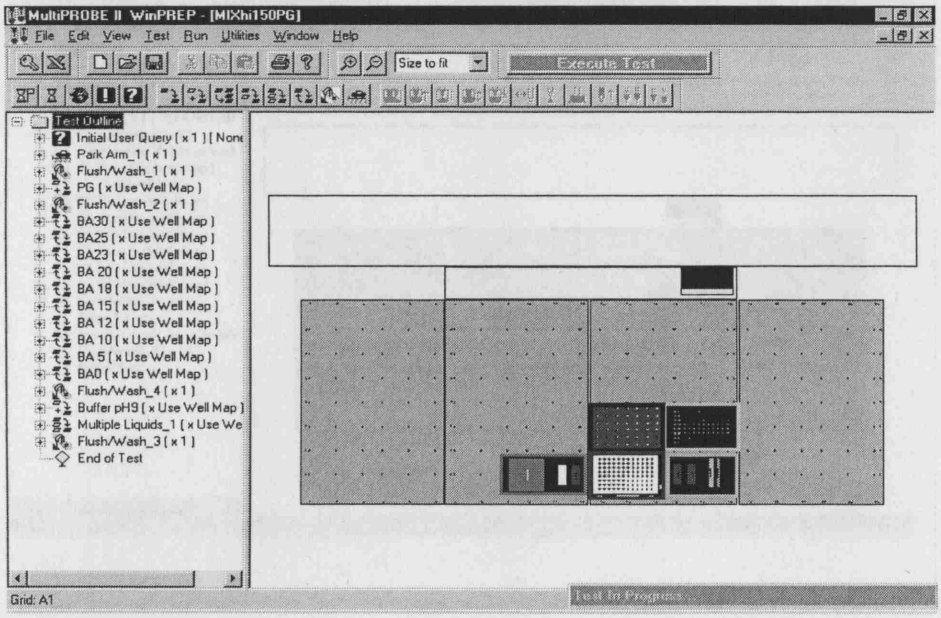

Test: MIX LO 150PG

LLE of Pen G with phases mixed at a lower selection of mixing cycles.

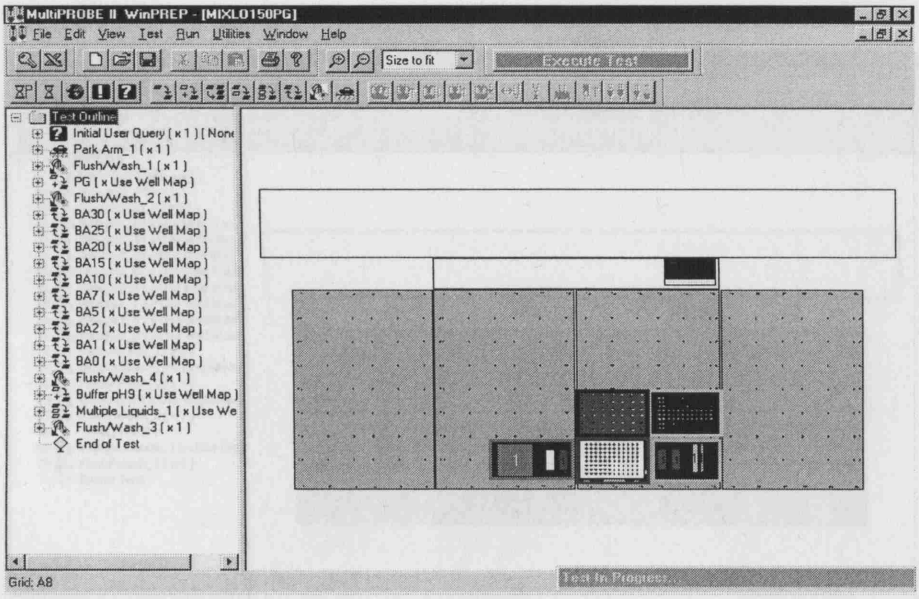

Test: MIX & WAIT

LLE at range of mixing cycles and transferring samples to HPLC vials.

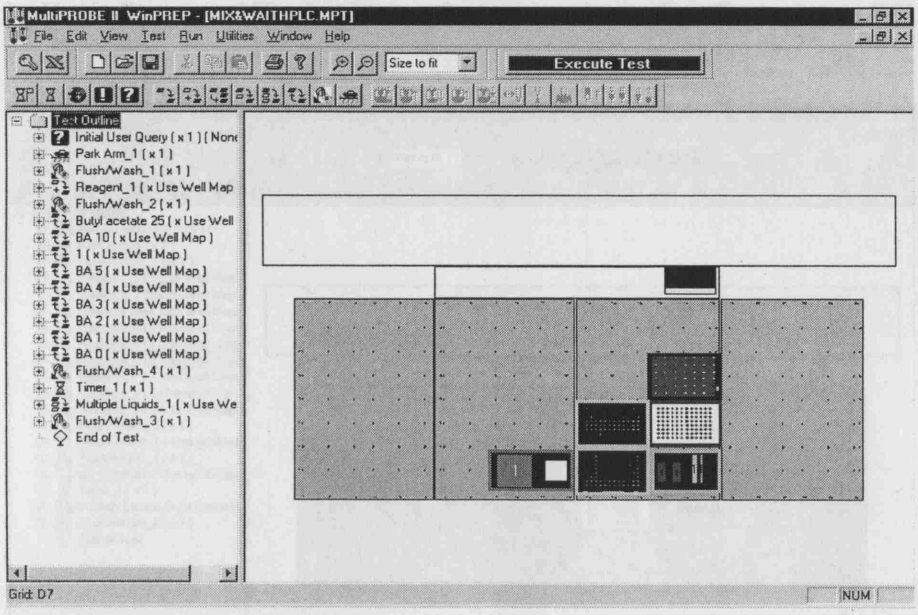

Test: PG PH LLE

LLE of Pen G at a higher selection of mixing cycles.

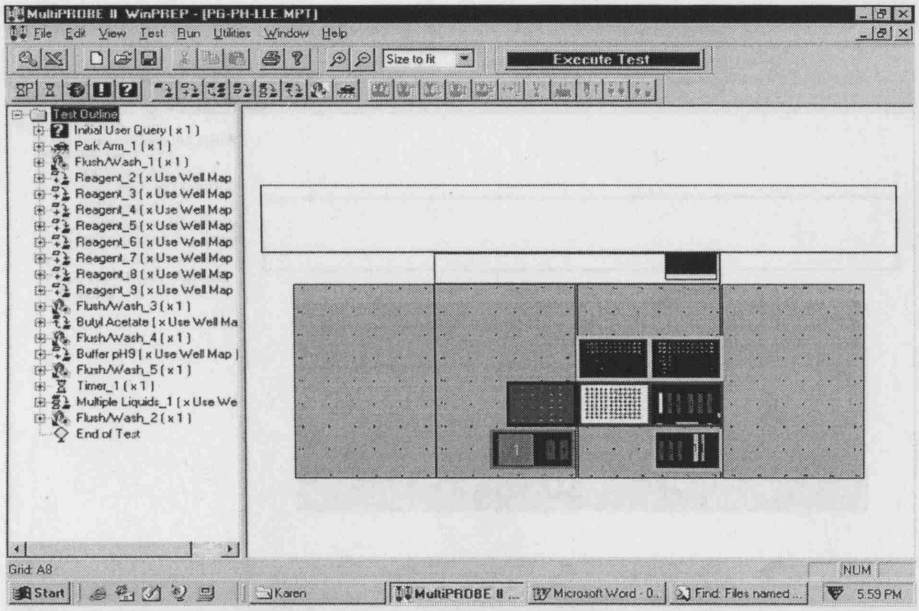

Test: PH-LLEHPLC350-010201

LLE of PAA at 9 pH conditions at 350 µL with butyl acetate and transfer of samples to HPLC vials.

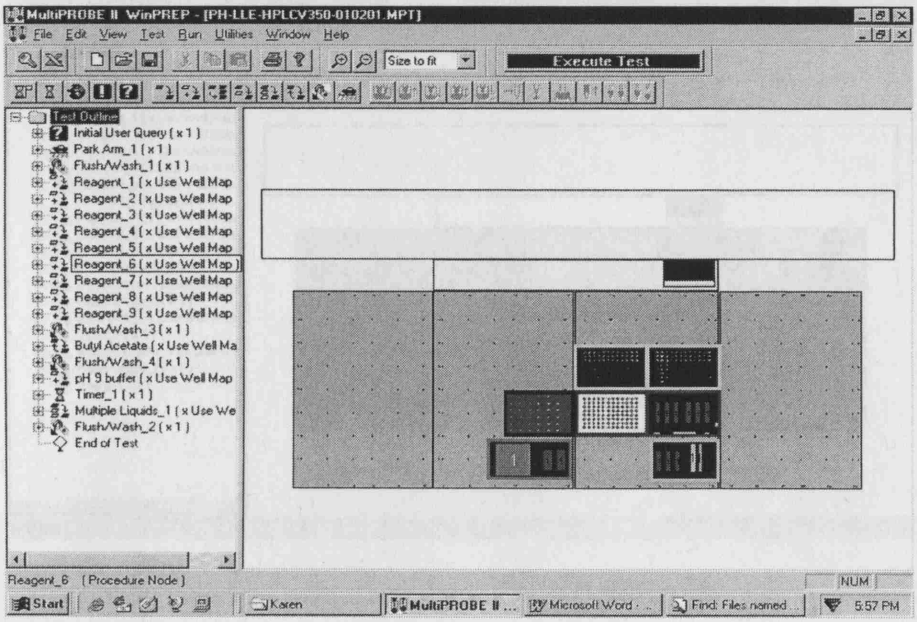

Test: PH1-solventsFeb test

LLE at range of mixing cycles using different organic phases.

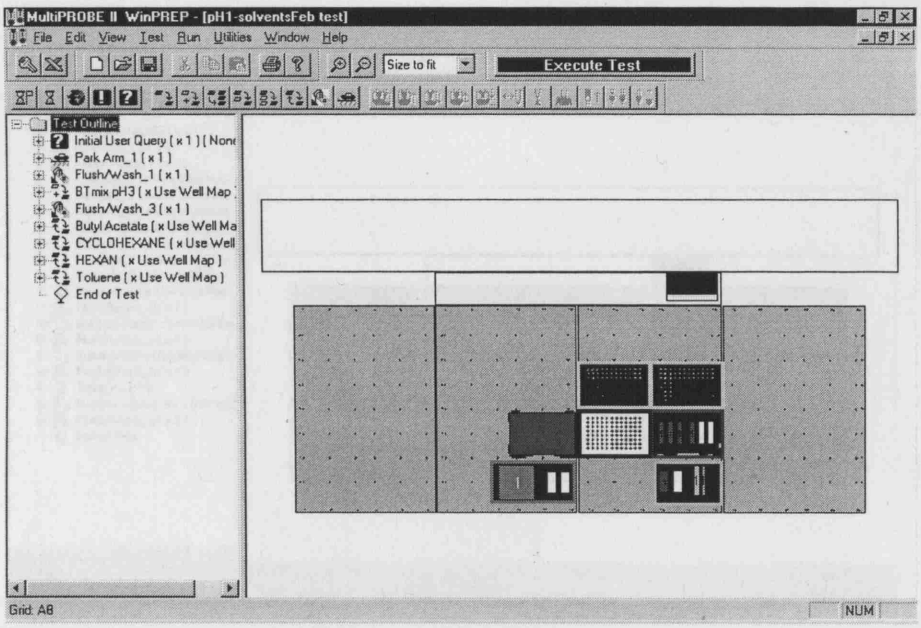

Test: PH HPLC BTmix

LLE of synthesised bioconversion product stream at 9 pH conditions.

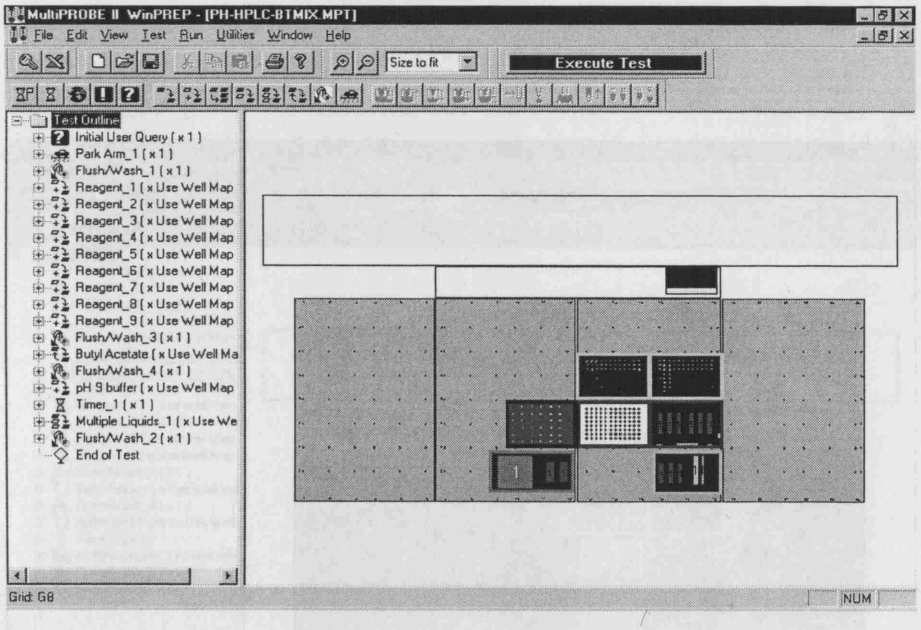

Test: PH LLE PG

LLE of Pen G with butyl acetate at 9 different pH conditions.

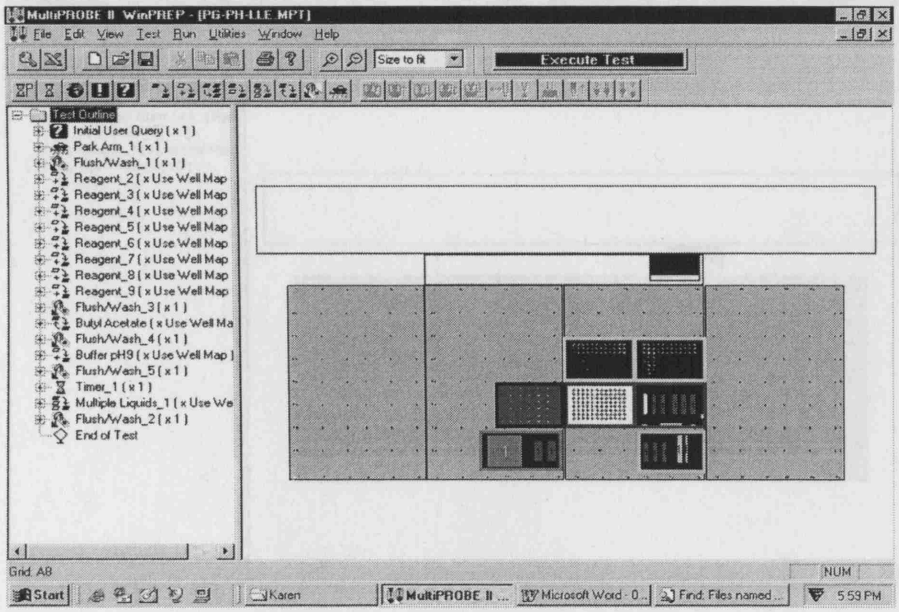

Test: PH LLE PG2

LLE of Pen G with butyl acetate over 9 pH conditions.

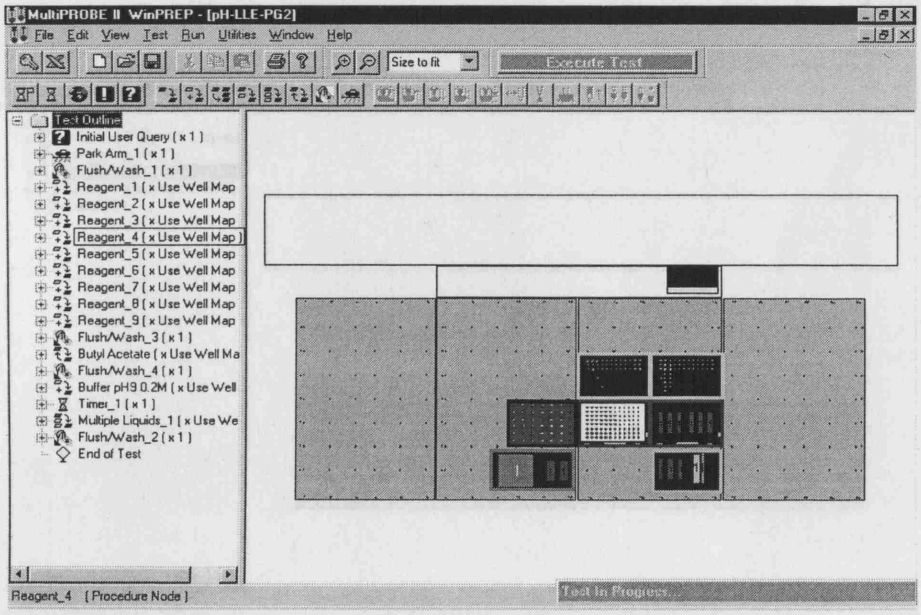

Test: Slurry

Dispense activated carbon slurry for the preparation of SPE adsorbents.

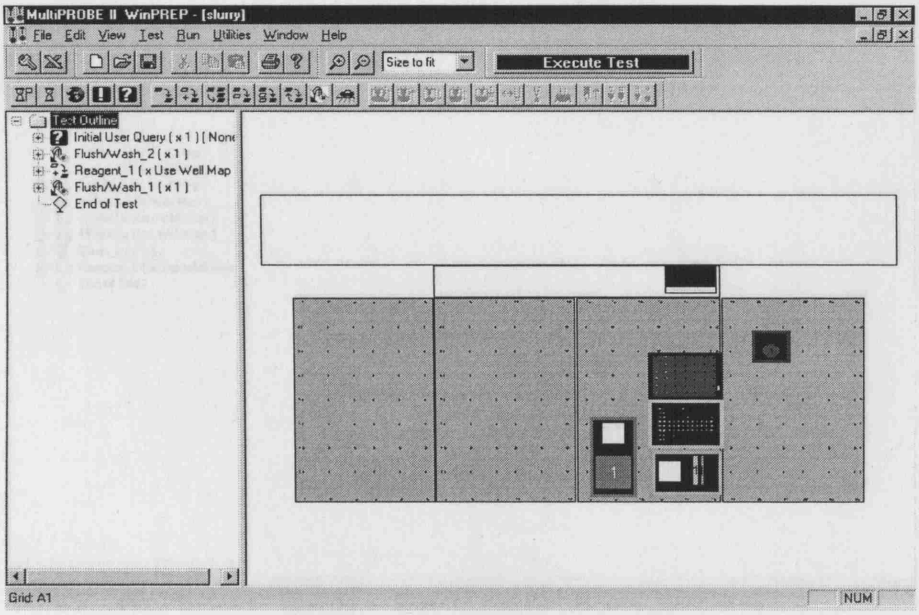

Test: SPE 24W ACconc

SPE of 6-APA using a range of activated carbon concentrations in a 24-well plate.

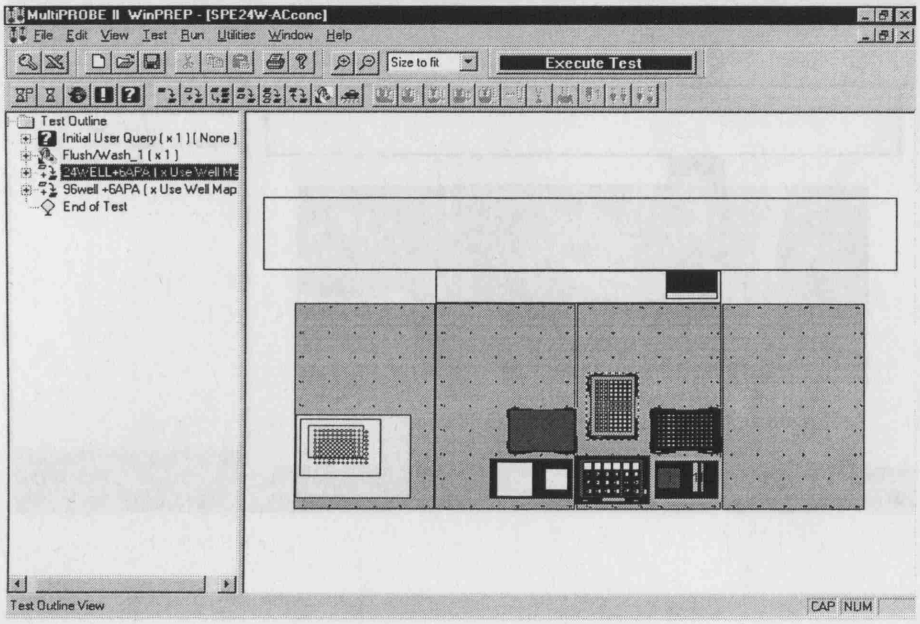

Test: SPE 24wellACmixKinetics

Kinetics of SPE of 6-APA using activated carbon

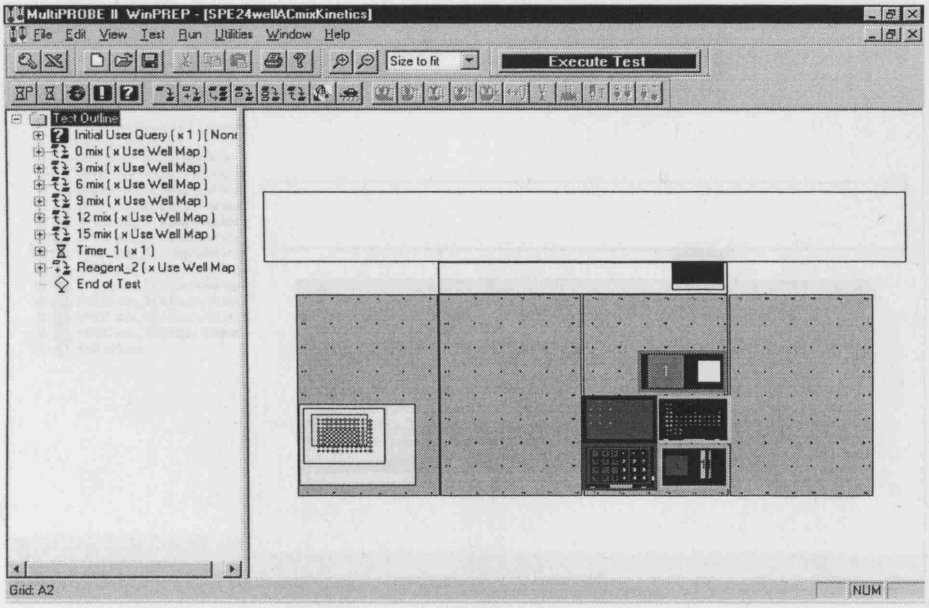

Test: SPE24WELL6APACONC3EXPTS

SPE of range of 6-APA concentrations using activated carbon

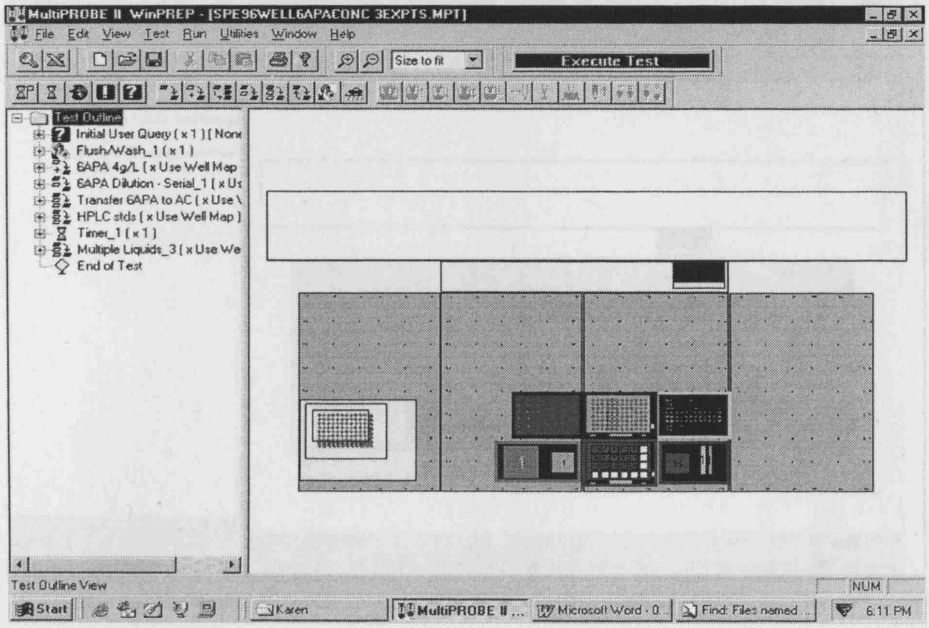

Test: SPE 24well KINETICS

Kinetics of SPE of 6-APA using activated carbon in a 24-well plate.

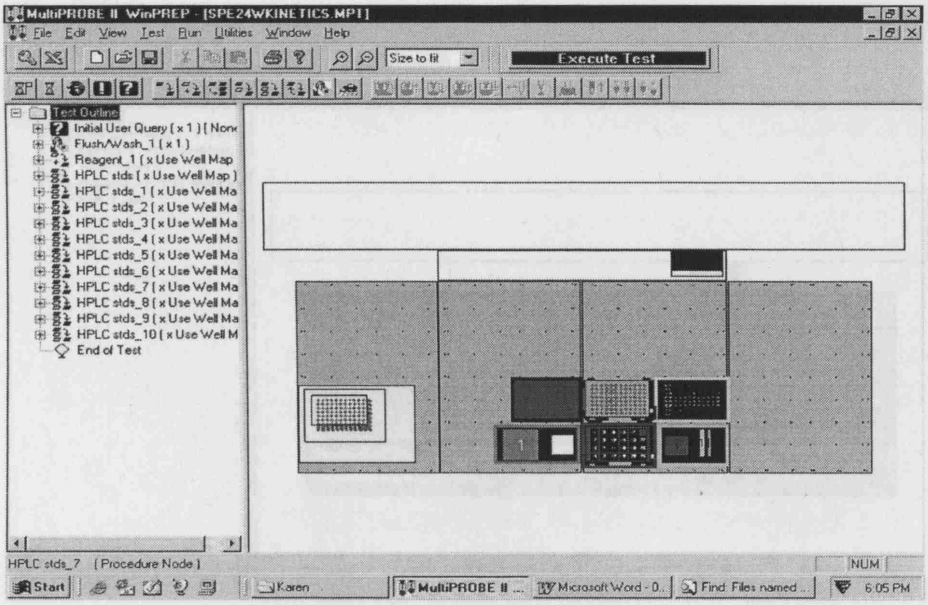

Test: SPE 96well 6APA conc

SPE using activated carbon at a range of 6-APA concentrations.

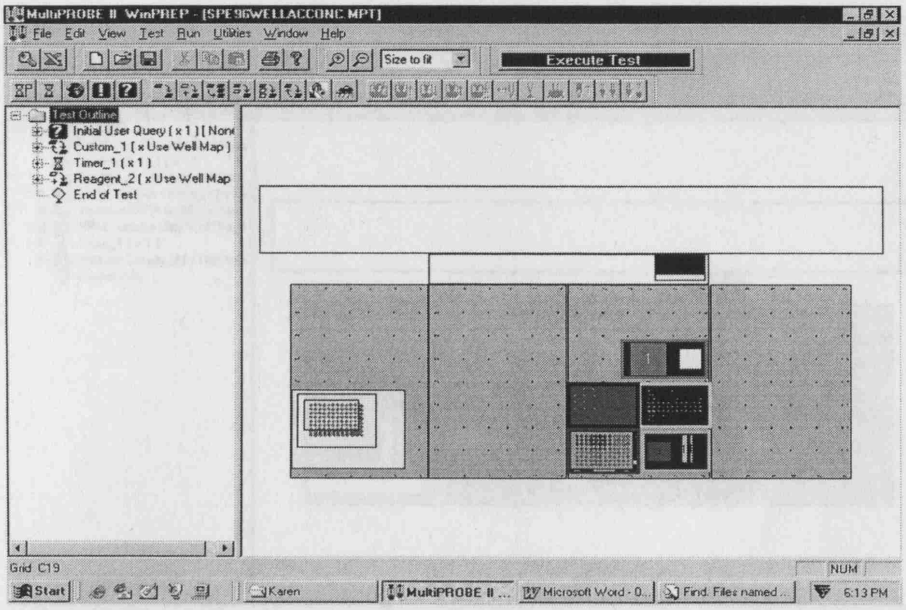

Test: SPE 96wellACconc

SPE of 6-APA using a range of activated carbon concentrations in 96 well plate.

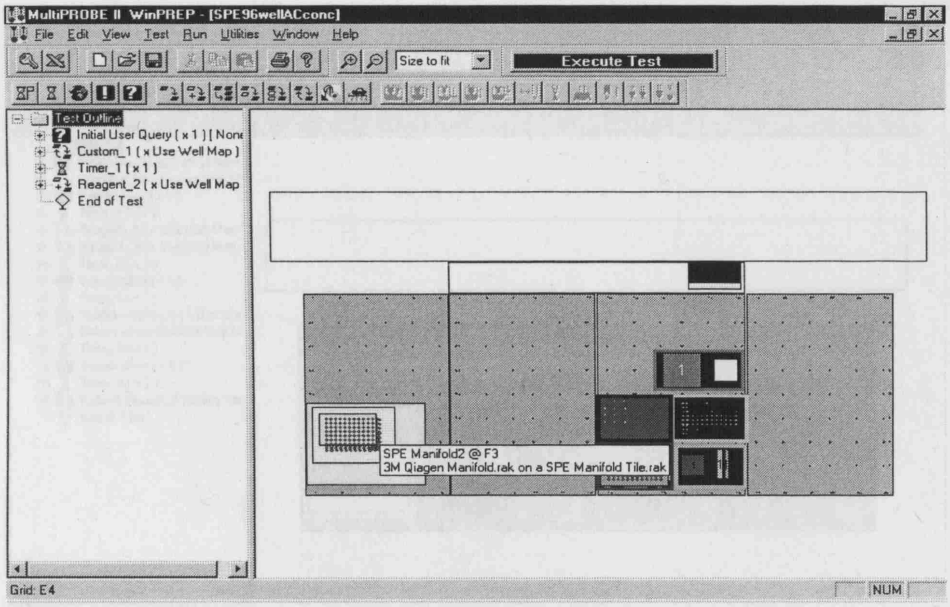

Test: SPE 96wellACconc 3EXPTS

SPE of 9-APA at a range of activated carbon concentration in a 96 well plate

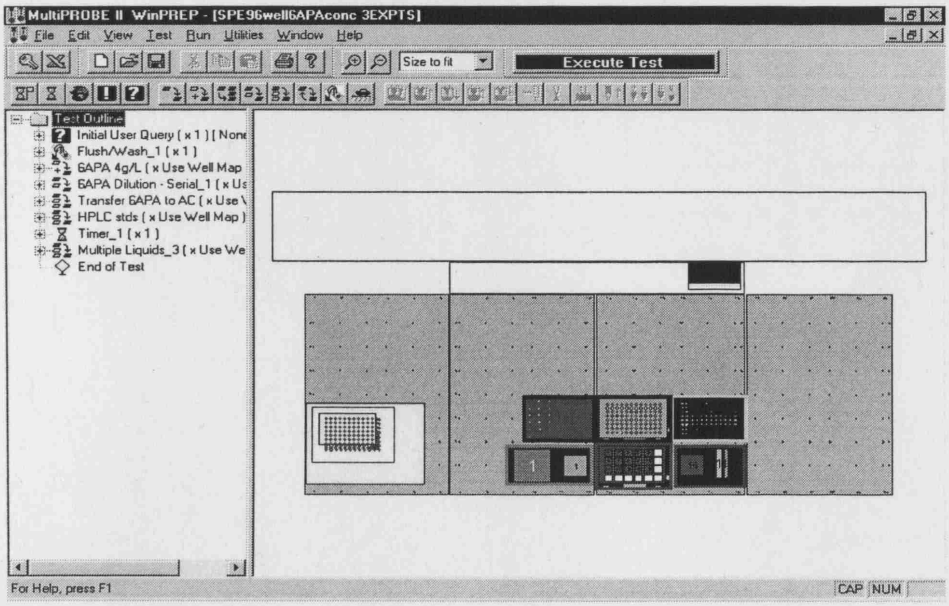

Test: SPEtestKEW

SPE of 6-APA with activated carbon using filtration to separate the phases.

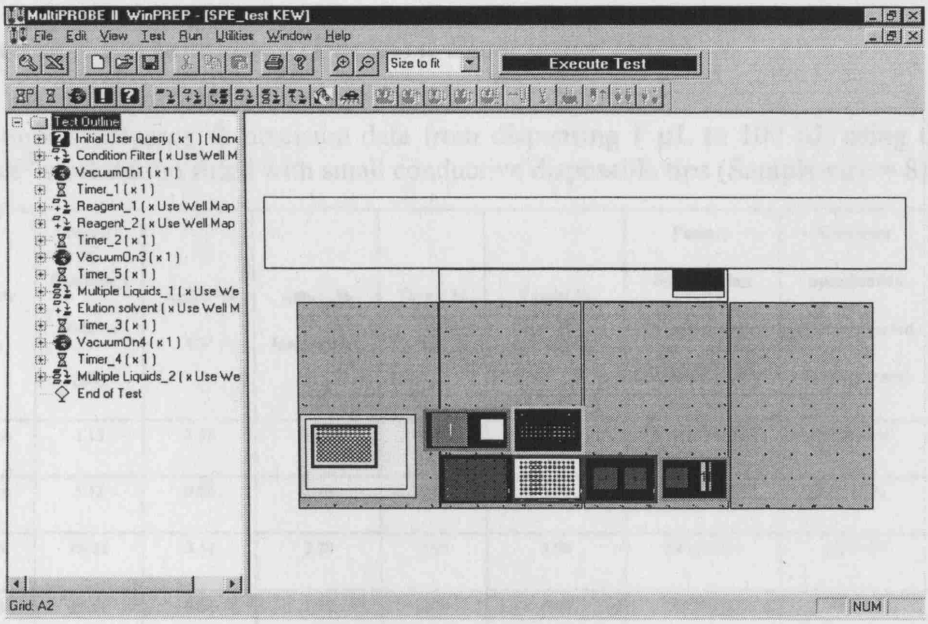

Appendix 7: Manufacturer's Analysis of the Automated Platform's Performance

A7.1 Multiprobe's Performance (Packard Bioscience 2003).

A7.1.1.Manufacturer's accuracy & precision data from dispensing 1 µL to 100 µL using the Multiprobe II Exe® workstation fitted with small conductive disposable tips (Sample size = 8).

Volume (µL)	Pipette Tip	Mean Dispensed Volume (µL)	Actual % CV	Actual % Inaccuracy1	Target % CV	Target % Inaccuracy	Factory Specification (Recommended % inaccuracy)	Customer Specification (Recommended % inaccuracy)
1	Micro	1.15	3.83	14.6	5.00	6.00	1 +/-24%	1 +/-28%
5	Micro	5.12	0.86	2.40	3.00	5.00	5 +/-4.5%	5 +/-5%
10	Micro	10.22	0.52	2.20	2.00	5.00	10 +/-3.5%	10 +/-4%
50	Small	49.42	0.27	1.16	1.00	1.00	50 +/-2%	50 +/-3%
100	Small	99.28	0.25	0.72	0.50	0.50	100 +/- 1.5%	100 +/- 2%

A7.1.2.Manufacturer's accuracy & precision data from dispensing 1 µL to 100 µL using the Multiprobe II Ex® workstation fitted with fixed tips (Sample size =8).

Volume (µL)	Mean Dispensed Volume (µL)	Actual % CV	Actual % Inaccuracy2	Target % CV	Target % Inaccuracy	Factory Specification (Recommended % inaccuracy)	Customer Specification (Recommended % inaccuracy)
1	0.99	5.34	1.0	5.00	6.00	1 +/-11%	1 +/-17%
10 (Blowout)	10.02	0.75	0.2	3.00	5.00	10 +/-2%	10 +/-2.5%
100 (Waste)	100.58	0.53	0.58	0.50	0.50	100 +/- 2%	100 +/- 2.5%
Comparison to Small Tips	Smaller at low vol but bigger at high vol	Bigger	Smaller	Bigger	Same	Smaller % at low vol bigger % at high vol	Smaller % at low vol bigger % at high vol

[1] % Inaccuracy = (volume/mean) x 100

[2] % Inaccuracy = (volume/mean) x 100

A7.2 Accelerator's Performance (Chem Speed, 2003a).

A7.2.1.Manufacture's accuracy and precision data from dispensing solids using the Chem Speed Accelerator™ dual dosing system.

	Target Mass (mg)	Mean Dispensed Mass (mg)	% Accuracy	2SE	% CV
Starch	10	9.91	99.1	0.03	0.5
Silica gel	200	200.7	100.4	1.3	0.4

Appendix 8. Categories of Automated Laboratory Equipment and Liquid Handling Workstations.

(a) Categories of automated laboratory equipment.

Equipment Category	Manufacturer	Application
Liquid handling workstation	Various: see table A8b or table 1.3.2.1.1.1	Pipetting, diluting, mixing
Parallel synthesis	GenVac Robbins Flexichem Chemspeed	Solvent evaporation Chemical synthesis Chemical synthesis Liquid & solid dispenser
Concentrator	Porvair Scientific Ltd	Reduce sample volume
Centrifuge	Qiagen Beckman Coulter Sorwall	Centrifugation
Plate washers	Bio-Rad Tecan Colibri Robotics Flush div of DI Labsystems Molecular Devices Titertek Tomtec Tri Continent Bio-Tex	Cleaning the plate of reagents used in ELISA

(b) Liquid Handling Workstations.

Liquid Handling Workstations	**Manufacturers**
Multiprobe	Perkin Elmer
Platemaate	Matrix Technologies
Hydra 96	Robbins
Biomek 2000	Beckman
Quadra 96	Tomec
Gemini Genesis	Tecan
Microlab STAR Microlab 2200	Hamilton
Rapid Plate	Zymark

Appendix 9 Standard Operating Procedure for Multiprobe II Ex®

SOP No: XX

Title: Operation of Multiprobe IIE in Biotransformation Lab, room 2.21

WRITTEN BY	DATE	OPERATING HEAD	DATE	DOC. REF.
K. E.WILLSON	03.10.00	C. ORSBORN	03.10.00	SOP.XX
S. C. R. PICKERING		Signature:		
Signatures:				

A9.1.0 Introduction

The Multiprobe is an automated liquid pipetting robot designed for volumes between 1 mL and 10 μL (volumes between 1 μL and 10 ml can be used, but with reduced accuracy). The Multiprobe consists of 4 independently moving heads that can use fixed or disposable tips. Programming, operation and control is achieved through a serial-linked PC using running WinPrep over Windows NT 4.0.

A9.2.0 SOP for Multiprobe II Automated Pipetter

Describes the procedure to safely carry out the operation programming and cleaning – you must be trained by Sam Pickering (x2494) or Karen Willson (x2494) before you can use this equipment.

A9.3.0 Safety precaution

I) Always wear protective eyewear and white lab coats.

II) Regular safety checks should be carried out to ensure that the Multiprobe is in good working order (ESPECIALLY SYSTEM LIQUID LEVEL CHECKS).

III) **NEVER** put any part of your body within the safety barrier whilst the machine is in operation.

IV) Always supervise the operation of the Multiprobe (don't leave it to work by itself, as accidents can happen).

A9.4.0 Booking Procedure

I) Open Multiprobe Booking Outlook program from the desktop PC attached to the Multiprobe.

II) Select the day and time required. Type your name and the equipment required:

MP = Multiprobe

SC = Spectracount

FC = Fluorocount

LT = Laptop computer

TM = Thermomixer

FU = Filtration Unit

HC = Heater/Chiller Unit

III) Bookings are to be made per hour and time should be included for routine sessional maintenance procedures in addition to experimentation.

IV) Please show consideration for other users and email all other trained Multiprobe users prior to block booking this equipment.

A9.5.0 Maintenance Logbook

Complete the logbook, remembering to include the following sections:

- Operators Name
- Date
- Maintenance (list all actions and tests carried out)
- Tests Used (you may also find it useful to note the file names of any data associated with this test)
- Labware
- Reagents (highlighting any that are hazardous)
- Detector (Spectracount or Fluorocount), noting template used, starting and finishing numbers.
- Shutdown maintenance.

A9.6.0 Multiprobe Initialisation

I) Fill out Multiprobe logbook checklist recording all actions taken.

II) Turn on PC and Multiprobe.

III) Open Desktop using **your** allocated user name and password (issued on completion of training).

IV) Open WinPrep on the desktop of the PC.

V) Check System Fluid, refill with Purite water.

VI) Run Utilities, Random Move Test.

VII) Run Utilities, Flush/Wash Test. Check syringes and syringe-outlet tubing for air bubbles. If the bubbles persist, re-run test until the tubing and syringes are clear.

A9.7.0 Running Existing Test

I) Open directory and select chosen test.

II) Add tiles and labware to deck in specified locations. Check thoroughly the location and alignment of tiles.

A9.8.0 Programming of Multiprobe

I) Open NEW TEST (click 'NONE') and then save immediately in your own folder specifying a unique file name.

II) Add the required labware for your experimentation on the deck view, checking the correct position.

III) Add procedures to the test to build up your experimental operations from:

- Timer: allows timed pause to be inserted into the procedure
- User procedure: create your own
- Custom: create your own procedure
- Dilution Procedure: serial/direct or custom
- Flush/Wash: for cleaning the fixed tips
- Multiple Liquids: Many liquids to many wells

- Reagent: one liquid to many wells, order dependent
- Single Liquid: one liquid to many wells
- Allocate labware and wells to your procedures

For further information please refer to the manuals (volumes 1 & 2).

During test development the 'REUSABLE TIPS' should be used with the 'TEST PLATES' for trials of the test with H_2O.

A9.9.0 Operating the Multiprobe

I) Only use new tips for experimental work and reuse 'REUSABLE TIPS' for experimental test design work (use **water** instead of reagents).

II) Execute test to run your saved test procedure.

III) Check labware set-up on desktop and the deck.

IV) Check tip box set-up.

A9.10.0 Closing down Multiprobe

I) Run Utilities, Flush/Wash (10ml x 3).

II) Shutdown WinPrep (remembering to save your test first) and turn-off Multiprobe.

III) Save your data files to disk.

IV) Clean deck with a very small amount of TEGO and rinse with water.

V) Remove ALL labware and replace in appropriate storage location.

VI) Wash reagent troughs thoroughly and leave to drain.

VII) Replace reusable-tips into labelled box/dispose of used experimental tips.

VIII) Close all programmes. Shutdown PC.

A9.11.0 Monthly Maintenance

I) Calibrate the arm to the deck every month.

II) Decontaminate system liquid & waste tubing.

III) Test syringes, tip pickup & liquid level sense.

Appendix 10: Types of Error

The type and cause of experimental errors are discussed in this section with relation to both microscale and laboratory scale experimentation and equipment. There are three main types of error: gross error (section A10.1); systematic error (section A10.2) and random error (section A10.3). These are generated by different causes and they each have different effects on experimental results. The methods of evaluation error used statistical values to assess performance (section A10.4).

A10.1 Gross Errors

Gross errors are serious errors that cause experimentation to be aborted (Miller and Miller, 1988). These errors are mostly produced by human error, such as preparing the wrong compound, dropping or destroying the sample. However, gross errors can also be caused by equipment failures or the experimentation method itself. These errors can be easily detected and prevented by good laboratory practice of careful preparation, experimental operation and equipment maintenance so shall not be discussed further.

A10.2 Systematic Errors

Systematic or determinate errors occur as a result of inherent problems with the experimental techniques or equipment. The systematic errors associated with experimentation are due to poor methodologies, techniques or the use of false assumptions about the accuracy of the analytical equipment. An example of a systematic error incurred by using equipment is its poor calibration that causes all readings to differ from the real value by a fixed amount. These errors are not detected by repetition as they produce the same errors for all the data points, but can be easily detected by comparison with standards from statutory bodies' control samples or published data. In addition, human bias also effects the accuracy of experimental data by introducing systematic errors due to operator visual problems, which may effect the reading of data from equipment and observations (Miller and Miller, 1988). Systematic errors were assessed by calculating the percentage accuracy[11] of the data (sectionA10.4.1).

[11] Definition of statistical terminology in appendix 11

Systematic errors can be easily reduced by a number of different precautions relating to the equipment, sampling and procedures. The likely sources of systematic error should be identified as early as possible and removed prior to experimentation. The analysis of the experimental design can reveal possible sources of contamination or gravimetric errors. All pieces of equipment should be calibrated prior to use in experimentation. Gravimetric errors can be reduced by weighing the receptacle before and after the transfer of solids into the container for the preparation of a solution. The calibrated analytical equipment must have a positive control to calculate the reagent's concentration to reduce the effect of any systematic errors. The use of standard reference materials and methods can also be used to reduce the occurrence of systematic errors caused by impure reagents. If systematic errors are occurring the experimentation should be repeated, carried out using an entirely independent procedure.

A10.3 Random Errors

Random or incidental errors are individual errors that are produced spontaneously and generate random differences (scatter) within a set of results. There are numerous random errors associated with experimentation or equipment (Miller and Miller, 1988). Weighing and pipetting errors in the preparation of the experimental reagents generate random errors. The random errors associated with equipment are caused by minute misalignments that generate experimental differences. These errors can not be avoided, but can be minimised by the use of good laboratory practice and repetition of samples or sample measurements. The random errors can be detected by statistically analysing the data[1]. The degree of scatter reflects the occurrence of random errors and effects the precision[4] of the mean, which can be assessed using statistical methods (section A10.4.2). The statistical assessment of the precision of a method can be assessed for the repeatability and reproducibility by analysing the within-run (intra-run) precision or between-run (inter-run) precision (Miller and Miller, 1988). The readings varied with the experimental conditions and the random variation for the automated equipment was evaluated in chapter 3.

[1] Methods of statistical analysis (aAppendix 11)

A10.4 Methods of Evaluating Errors

The performance of experimental methods and equipment were assessed using a variety of methods to quantify their accuracy[1] (section A10.4.1) and precision[1] (section A10.4.2). These values are used to estimate the systematic and random errors, which allow the comparison between the performances of similar equipment. The reliability of the equipment was evaluated using component failure rates (section A10.4.3).

A10.4.1 Accuracy

The accuracy of data describes how well it conforms to fact, indicating if it deviates only slightly or within acceptable limits from a standard, which provides a correct reading or measurement (Miller and Miller, 1988). The analysis of the accuracy of experimental data quantifies the systematic errors within the experimental procedures and equipment. The accuracy of the individual pieces of automated equipment used here has been assessed (section 3.2). Accuracy can be analysed by assessing gravimetric data and calculating the percentage inaccuracy[1] quantifying any systematic errors (section 2.6). This analysis indicates how well the mean values fit the true value, which is especially important during the automated process method development.

All experimental calculations of accuracy used within this research compared the sample to the standard feed stream (control), which reduced any systematic errors. It is important that the experimental methods and equipment are accurate in order to generate robust processes that are not significantly affected by external factors, such as differences in the reagent batch preparation and the labware used. The experimental data was generated at different scales to allow productivity comparisons. Additionally, the microscale LLE experimentation was carried out using manual microscale, automated microscale and laboratory scale experimentation. The data from these experiments were compared using parity plots of the mean values with their associated errors, which illustrated their respective accuracies (section 4.2.7).

A10.4.2 Precision

The precision of data describes the scatter of the data and its distribution around the mean. The statistical analysis of the experimental precision quantified the random errors within the

[1] Methods of statistical analysis (Appendix 11)

experimental procedures, plus the automated and analytical equipment. This can be quantified by analysing the variance[1], standard deviation[4] and coefficient of variance[1] of the data. There are two types of precision that are calculated: within-run data or between-run data, which describe the method's repeatability or the reproducibility of the data (section A10.4. 2.1 and A10.4.2.2, respectively).

A10.4.2.1 Repeatability

The repeatability of a series of data indicates the within-run precision of the experimentation, which is achieved by the use of replicate samples (Miller and Miller, 1988). The precision of an experiment is often dependent on ancillary equipment used during the experimentation, such as analytical balances, pipettes and pH meters. The precision of these pieces of laboratory equipment is dependant on their initial calibration and inherent number of significant figures displayed. However, during experimentation, losses can occur in the transportation of both solid and liquid reagents. The automated equipment generated high numbers of replicate data from the same microscale experimentation to quantify the precision of the experimental method, which indicated the similarity of the four pipette tips on the workstation. This analysis of precision determined the repeatability of the experimentation.

A10.4.2.2 Reproducibility

The reproducibility of data quantifies the analysis of between-run precision, which reflects its ability to produce a counterpart or copy of the data on a different occasion (Miller and Miller, 1988). The microlitre and laboratory scale experimental data were repeated to generate large sample numbers, which increased the significance of the accuracy and precision, generated from a series of replicate experiments that were repeated on consecutive days. The reproducibility of the microscale experimentation data is important for assessing the suitability of the liquid handling workstation and dosing station for this research (chapters 4 and 5). The experimentation was repeated four times within the experiment and at least three times to generate higher numbers of samples in order to ensure that there was good compatibility between them to achieve a high probability that the calculated mean was the true mean.

[1] Methods of statistical analysis (Appendix 11)

A10.4.3 Reliability

Reliability is the "*characteristic of an item expressed by the probability that it will perform a required function under stated conditions for a stated period of time*" (Dummer, 1974). The reliability of automated equipment is important to their manufacturers and users because they need to know that the equipment will not breakdown and cause gross experimental errors. Therefore, the manufacturers investigated both the components and equipment for failure rates to assess their reliability before releasing the equipment into the market.

Reliability is an estimate of the failure rate of electronic and mechanical equipment, which quantifies the mean time before failure (MTBF) of the components or equipment and the reciprocal is the failure rate. Equipment fails due to environmental factors, such as humidity, temperature, dust and radiation. Reliability of an instrument can be estimated from that of its components. For example, the reliability of a television is 5,000-10,000 hours, which is less than that of individual components: capacitors (0.01% to 0.05% per 1000 hours) and resistors (being 0.2% to 0.6% per 1000 hours) (Dummer 1974).

The reliability of the automated equipment used in this research was unavailable from the relevant manufacturers. Reliability information on the valve components used in the liquid handling systems indicated that they had between one and seven failures per million cycles (Grant et al, 2001), which is an acceptable reliability level for the equipment. This information is useful to the manufacturers in preparing their guidelines for maintenance and repair.

Manufacturers, such as Perkin Elmer, recommend a yearly service to check the operation and performance of the equipment. In addition, the daily, weekly and monthly maintenance programs were recommended and were routinely followed using the standard operating procedure that was generated based on them (appendix 9).

Appendix 11: Statistical Methods of Assessing Performance

Statistical methods were used to assess the performance of the automated platform and experimental methods. The automated platforms generated gravimetric data (section 2.2.3) to quantify its performance by statistically analysing the data to quantify its accuracy (section 10.4.1) and precision (section 10.4.2).

A11.1 Analysing Accuracy

The accuracy or inaccuracy of experimental data is assessed by its comparison with a standard, such as the target values for gravimetric data, which are used to calculate the percentage accuracy (equation A11.1) or percentage inaccuracy (equation A11.2) or percentage error (equation A11.3):

$$\%A = \frac{b}{T}.100 \qquad [A11.1]$$

$$\%I = \frac{\sqrt{(b-T)^2}}{T}.100 \qquad [A11.2]$$

$$\%E = \frac{b-T}{T}.100 \qquad [A11.3]$$

where %A is the percentage accuracy, *%I* is the percentage inaccuracy, *%E* is the percentage error, b is the mean volume or mass and T is the target volume or mass. The percentage inaccuracy is similar to the percentage errors, which are both calculated from the difference between the value and the target value as a percentage of the target value. However, percentage inaccuracy is a positive number, whereas percentage error is either a positive or negative value. This quantifies any systematic errors occurring due to the equipment or experimental procedures that are effecting the measurements, such as misalignments, miscalibration or operation errors of the equipment.

A11.2 Statistical Analysis of Precision

The statistical analysis of the precision of experimental and gravimetric data was used to assess the repeatability and reproducibility of the experimental methods and equipment used in this research using the equations in table A11.2.1. The statistical analysis describes the distribution of the data (section A11.2.1). If only two data points were plotted it may not be very representative. Therefore, a large sample number (section A11.2.2) is used and all the data points are plotted to illustrate their distribution around the mean (section A11.2.4). The large sample number allows the calculation of the confidence interval of the data (section A11.2.3), which describes the confidence in the mean value to be the true mean (section A11.2.4). The variance (section A11.2.5), standard deviation (section A11.2.6), and coefficient of variance (section A11.2.7) are different ways of commenting on the precision. The statistical analysis of standard error (section A11.2.8) and the coefficient of standard error (section A11.2.9) are related to the standard deviation, but are dependent on the sample number and so are measurements of accuracy. The statistical analysis is valid for both normally distributed data and populations deviating slightly from this distribution, which covers most analytical data (Miller and Miller 1988). The systematic errors associated with these automation platforms were assessed and minimised prior to microscale experimentation.

A11.2.1 Sample Distribution

A sample distribution describes how the full collection of data of a group being analysed (population) or a subset of this collection (sample) is distributed. The frequency distribution of the sample data displays the number of observations in each 5% interval, which indicates the population distribution. If the observations have a Normal distribution, the frequency distribution forms a symmetrical bell-shaped curve around the mean (equation A11.4) where y is the distribution accuracy, x_i is an individual data measurement, $\bar{x}$ is the theoretical mean value of all the x_i values and σ is the standard deviation (Miller and Miller, 1988).

Analytical & Statistical Expressions	Equations	Equation Numbers
Sample distribution	$y = \frac{\exp(-(x_i-\bar{x})^2/2\sigma)^2}{\sigma\sqrt{2\pi}}$	A11.4
Sample Number	$\bar{x} - t_\alpha \frac{s}{n} \leq truevalue \geq \bar{x} + t_\alpha \frac{s}{n}$	A11.5
Sample Mean or Population Mean	$\bar{x} = \frac{\Sigma(x_i)}{n}$ or $\bar{X} = \frac{\Sigma(x_i)}{N}$	A11.6
Population Variance$_1$ (V_1)	$V = \frac{\Sigma(x_i - \bar{X})^2}{N}$	A11.7
Sample Variance$_2$ (V_2)	$v = \frac{\Sigma(x-\bar{x})^2}{n}$	A11.8
Standard Deviation$_1$ = σ_1	$s = \sqrt{\frac{\Sigma(x-\bar{X})^2}{N}}$	A11.9
Standard Deviation$_2$ = σ_2	$s = \sqrt{\frac{\Sigma(x-\bar{x})^2}{n-1}}$	A11.10
Coefficient of Variance	$CV = \frac{s}{\bar{X}}$	A11.11
Relative Coefficient of Variance	$RCV = \frac{CV}{\bar{x}}.100$	A11.12
Standard Error	$SE = \sigma/\sqrt{n}$	A11.13
Relative Standard Error	$RSE = \frac{SE}{\bar{x}}.100$	A11.14

Table A11.2.1.Analytical and statistical expressions defined by their equations that quantify accuracy and precision, taken from Miller and Miller, (1988).

Terminology: x_i are individual data measurements, $\bar{x}$ is the mean value of all x_i values; σ or s is the standard deviation (squared variation of x_i from the mean); V_1 is the population variance; V_2 is the sample variance; $\bar{X}$ is the true mean of the population; $\bar{x}$ is the mean of x_i values; i is the independent value; α is the confidence value; n is the sample number or sample size; n is the sample number; N is the population number; v is the sample variance; CV is the coefficient of variation and SE is the standard error of the mean.

A11.2.2 Sample Number

The sample number is the number of repeated measurements or data taken from experimentation. Repetition is important to generate enough data to detect clear trends within the data set to have statistical significance. A large sample size of 50 is considered to be theoretically infinite provided that the measurements are independent and if there are no systematic errors the mean is considered the true value of the sample (Miller and Miller, 1988). The estimate of the mean becomes more uncertain as the sample size decreases and the selection of the sample size can be calculated by equation A11.5 where $\overline{X}$ is the mean, the independent, t_α is the confidence, s is the standard deviation, n is the sample number and *true value* is the population's true mean. Therefore, for a normally distributed sample with 95% confidence is achieved when t_α is 1.96 (taken from a probability table of critical values for an acceptable standard deviation of 5% of the mean).

A11.2.3 Confidence Interval

The confidence interval is defined by the sample values, which fall within a certain range of the mean indicated by the sample distribution. The size of the confidence interval reflects the confidence in the mean value being close to the true mean, which is determined by the confidence or probability (1 confidence). This is determined by the population mean ± variance and is related to the standard deviation for a population or the standard error for a sample. The extremes of this range are termed the confidence limits, where the true mean is not believed to lie.

A confidence interval is formed by one standard deviation on either side of the mean ($\bar{x}$), which contains about 68% of the sample for data that has a normal distribution. The confidence interval formed of the mean ± two standard deviations contains 95% of the sample and the confidence interval formed of the mean ± three standard deviations contains 99.5% of the sample. The confidence interval containing 95% of the population is also achieved by the range determined by the mean ± two standard errors (Miller and Miller, 1988) when using a sample rather than a population.

A11.2.4 Sample Mean

The sample mean is the average value or arithmetic mean ($\overline{X}$), abbreviated to mean, which is the sum of all individual measurements (x_i) divided by the sample number (n) (table A11.2.1, equation A11.6). The sample mean is calculated using the sample number (n), a subset of the population, rather than the population mean from the population number (N). The sample mean is unlikely to be exactly equal to the true value of the population mean, so it is expressed as a range of values that have a 95% confidence of the mean being within two degrees of freedom or significance levels from the mean, which is estimated by the sample mean ± 2 standard errors (Miller and Miller, 1988).

A11.2.5 Variance

The variance (V) is the degree of spread or scatter of a sample or population around the mean, which is the average of the squared deviations around the mean, which is calculated for the population using equation A11.7 and for the sample using table A11.2.1, equation A11.8. Variance is the average of the squared difference between the individual x_i values and the mean. The variance of data taken from a population or sample is equal to the population or sample variance, respectively, divided by the population or sample size to generate the average variation of the observations from the mean. This value is used in the calculation of other statistical analyses including standard deviation and standard error (Miller and Miller, 1988).

A11.2.6 Standard Deviation

Standard deviation (s, SD or σ) is a measurement of the spread of rational number values of measurements from the mean value, which is the average absolute difference between the individual data points and the mean (table A11.2.1, equation A11.9 or A11.10). This value quantifies the precision of a population and is the square root of variance.

The unbiased estimate of the population mean uses n - 1, but this assumes a large sample size therefore σ was calculated for the experimental data using n, which is used by many calculators and software packages. SD does not reflect how the results are distributed, so outliers can not be easily identified. Therefore standard error (section A11.2.9) and relative standard deviation (section A11.2.10) must be calculated to assess the sample distribution (Miller and Miller, 1988).

A11.2.7 Coefficient of Variance

The coefficient of variance (CV) or relative standard deviation (RSD) are an absolute measurement of the distribution of data. The CV values are calculated using the standard deviation relative to the mean (table A11.2.1, equation A11.11), which indicates the precision of data. It is used to compare population distributions that vary by an order of magnitude as the size of the observations themselves makes direct comparison meaningless (Miller and Miller, 1988).

A11.2.8 Relative Coefficient of Variance

The relative coefficient of variance, like the coefficient of variance, is calculated on the sample distribution, which is dependant on the standard deviation of the population. The coefficient of variance is a percentage of the mean (table A11.2.1, equation A11.12). The percentage RCV quantifies the relative precision of the data samples in the data set, whether that is within-run or between-run data. This standardisation allows the comparison with different sample sets as the RCV value is not dependant on the mean values, which may vary in their order of magnitude (Miller and Miller, 1988).

A11.2.9 Standard Error

Standard error (SE) is a measurement of the uncertainty in estimating the true value from the sample mean and is calculated from the standard deviation divided by the root of the sample number. The SE value represents the error encountered by repeated sampling from the same experimental conditions (table A11.2.1, equation A11.13). SE is independent of the way the observations are distributed around the mean and effects the accuracy of the data, which assumes normal distribution. In order to capture 95% of the data, the sampling distributing should include the mean ± 2SE (Miller and Miller, 1988).

A11.2.10 Relative Standard Error

The relative standard error (RSE), like standard error, is calculated from the sample distribution. RSE is dependant on the standard deviation of the population, which expresses the standard error as a percentage of the mean (table A11.2.1, equation A11.14). This allows its comparison with different observation samples, which have means that vary in their order of magnitude (Miller and Miller, 1988).

A11.3 Statistical Analysis of Comparative Data

A11.3.1 Calculating the Error Associated with the Workstation

Analysis of the standard deviation related to the individual equipment used in generating gravimetric data to assess the performance of the liquid handling workstation pipetting can be achieved by using the standard deviation values for the Multiprobe II liquid handling workstation (section 3.2.1) and the analytical balance (appendix 12) in equation A11.115:

$$SD^2_{Pipetting} = SD^2_{Workstation} + SD^2_{Balance} \quad [A11.15]$$

where $SD^2_{Pipetting}$ is the variance of the pipetting data for dispensing 100µL RO water, $SD^2_{Workstation}$ is the variance due to the precision of the liquid handling workstation (section 3.2.1.2) and $SD^2_{Balance}$ is the variance due to the precision of the analytical Balance (section 3.2.1.1).

A11.3.2 Chi^2 Statistical Analysis

The chi^2 statistical analysis of the performance data generated by the liquid handling workstation for dispensing 100 µL aliquots of RO water with both disposable small conductive and fixed pipette tips (equation A11.16):

$$Chi^2 = \frac{(n-1).s^2}{\sigma^2} \quad [A11.16]$$

where n is the number of samples used to generate statistical data, s is the standard deviation for the actual dispensed aliquots using laboratory data and σ is the standard deviation for the manufacturer's data (appendix 7.1).

A11.3.3 Normal Test

The results of equation A11.5 were used in testing the mean and the estimate of precision using equation A11.17:

$$X = \frac{|\bar{x} - T| - A}{\frac{\sigma}{\sqrt{n}}} \qquad [A11.17]$$

where X is the?, $\bar{x}$ is the mean for dispensing 100 µL, T is the target volume, A is the manufacturer's accuracy for dispensing the volume σ is the standard deviation for the manufacturer's data and n is the sample number.

Appendix 12: Evaluation of the Analytical Balance

Evaluation of the performance of the analytical balance (HLDAS Hereause Instruments, UK) was assessed by generating gravimetric data for its performance repeatedly weighing a number of reagents: a polypropylene weighing boat, paper and activated carbon (Sigma Chemicals, UK). The variations of the masses were illustrated in figures A12.1 and A12.2, which illustrated the degree of error associated with an absolute measurement and the measurements of the difference between the boat and the reagent. These data were used to statistically analyse the random errors associated with the analytical balance. The mean mass of the weighing boat was 2.2324 $\pm$ 0.0058 g, the paper weighed 1.7 $\pm$ 0.1 mg and the activated carbon particle weighed 0.9 $\pm$ 0.3 mg. The precision values for the weighing boat data (0.02% CV) and paper sample (6.1% CV) were excellent, but the activated carbon sample had a 30% CV due to the variation encountered caused by its adsorption of atmospheric moisture. Ideally the balance should be calibrated and its stability checked using a standard calibrated weight, as it is not susceptible to hygroscopic variation.

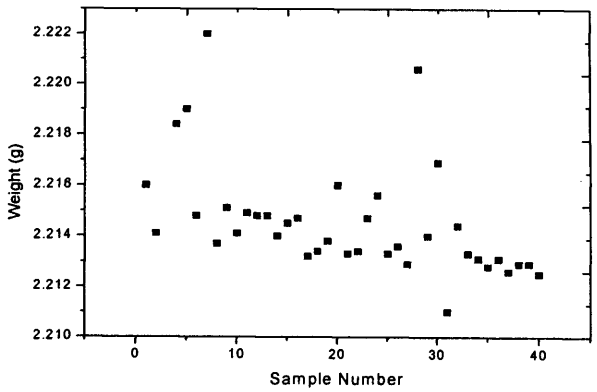

Figure A12.1 Plot of gravimetric data used to assess the performance of the analytical balance for repeated weighing (n = 39) of a polypropylene weighing boat.

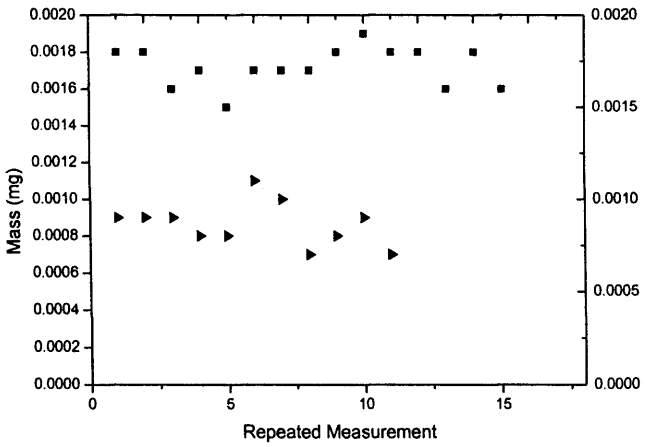

Figure A12.2 Plot of gravimetric data used to assess the performance of the analytical balance for repeatedly weighing (■) paper (n = 15) and (▶) activated carbon (n = 11).

Appendix 13: Principles of Liquid-Liquid Extraction

A13.1 Equilibrium Processes

Equilibrium processes reach a steady state within a system over time in relation to its concentration, temperature, pressure or chemical potential properties. These properties become uniform throughout the system and do not change over time. This occurs when the opposing driving forces are equally balanced so there is no net mass transfer in separation equilibrium processes, such as liquid-liquid extraction (LLE).

A13.2 Quantifying LLE Efficiency

The methods of analysis to quantify the efficiency of a LLE process can be described by the distribution constant and yield or percentage recovery. The equilibrium distribution constant (K_D) is defined in equation A13.1. This quantifies the partitioning of a compound between two immiscible liquid phases at equilibrium:

$$K_D = \frac{C_{org}^*}{C_{aq}^*} \qquad [A13.1]$$

where C_{org}^* is the equilibrium concentration in organic phase and C_{aq}^* is the equilibrium concentration in aqueous phase. If $K_D<1$ the compound is more concentrated in the aqueous phase.

The distribution ratio (D) is defined in equation A13.2. This quantifies the partitioning of a compound between two immiscible liquid phases at time t:

$$D = \frac{C_{org}}{C_{aq}} \qquad [A13.2]$$

where C_{org} is the concentration in organic phase at time t and C_{aq} is the concentration in aqueous phase at time t. If $D<1$ the compound is more concentrated in the aqueous or heavy phase.

The yield (Y_D) of the compound purified using the LLE process is defined in equation A13.3:

$$Y_u = \frac{V_u}{1 + \frac{V_U}{K_D}} \qquad [A13.3]$$

where Y_u is the yield of upper phase, V_u is the volume of the upper phase, V_L is the volume of the lower phase and K_D is the equilibrium distribution constant. The yield value is similar to the percentage recovery value of the solute partitioning. If it is very low a good product yield can still be achieved by the use of a high volume of the phase preferred by the solute.

The percentage recovery in the extracting (organic) phase defines the percentage of the component from a mixture during the LLE process, which is defined in equation A13.4:

$$\%R = \frac{C_{org}}{C_{Total}} \qquad [A13.4]$$

where $\%R$ is the percentage of compound removed, C_{Org} is the concentration of compound in organic phase at equilibrium and C_{Total} is the total concentration of compound in the bulk phase.

A13.3 Mass Transfer

A13.3.1 Film Theory

The film theory describes the mass transfer between two immiscible liquid phases and the formation of a stagnant thin fluid film either side of the interfacial boundary (Lewis, 1916, Whitman, 1923). The mass in the bulk phase is transferred by convection and crosses the film boundary, moving along the concentration gradient by diffusion.

A13.3.2 Convective Mass Transfer

Convective mass transfer is driven by the net energy gained by the system, caused by movement of the liquid by mechanical mixing or pipe flow. Fluid flow through the pipe nozzle or pipette orifice forms a jet, mixing with the bulk phase as the jet contacts the phase boundary breaking up into droplets, which increase the interfacial area. The nozzle diameter and the fluid velocity effect the size of the droplets, which influences the mass transfer.

A13. 3.3 Liquid Diffusion Theory

The diffusion theory of mass transfer describes the molecular diffusion of a component within the biphasic system. The system contains molecule 'A', which is non-uniform and varies in concentration (C_A) from C_{A1} to C_{A2}. The concentration gradient is a function of distance and forms a negative exponential curve. The concentration gradient drives the diffusion of the component from the region of high concentration until equilibrium is achieved. The time required to achieve equilibrium is dependent on the degree of mixing, temperature and pressure. If a method of mixing (*e.g.* stirring) is not used, the sole mixing occurs by random molecular movements (diffusion) (Doran, 1998). However, as shown, mixing can increase the formation of equilibrium.

The mass transfer of component A describes its movement across an area (a) perpendicular to the direction of diffusion. Fick's first law of diffusion (equation A3.1), which describes the rate of mass transfer in a single phase system is due to molecular diffusion. This law states that the mass flux (J_A) or rate of mass diffusion is proportional to the concentration gradient. For binary systems the mass flux of each component must be considered using the diffusivity values for the component relative to the mixture, assuming that the components in the system are non-reacting.

A13.3.4 Partition Theory

The first law of thermodynamics states that energy can be changed from one form to another, but it can neither be created nor destroyed (Ramsden, 1985). Mass is also conserved within a system despite chemical reactions so that the input and output can be calculated in a stoichermetric mass balance. Therefore, the partitioning of a compound between two phases can be quantified and analysed using the partition theory, which states that the mass of the system is conserved during mass transfer (equation A13.5):

$$C_1V_1(0) = C_1V_1(t) + C_2V_2(t) \qquad [A13.5]$$

where $C_1(0)$ is the concentration of the reagent in phase 1 at the start (time = 0), $V_1(0)$ is the volume of phase 1 at the start(time = 0), $C_1(t)$is the concentration of the reagent in phase 1 at time (t), $V_1(t)$ is the volume of phase 1 at time t), $C_2(t)$ is the concentration of the reagent in phase 2 at time (t), $V_2(t)$ is the volume of phase 2 at time (t).

The partition equation (equation A13.6) was combined with the distribution ratio (equation A13.2) and the mass flux (equation A3.1) to generate equation A13.6:

$$\frac{dC_1(t)}{dt} = -\frac{KLa}{V_1}\left((1+mVr).C_1(t) - mVr.C_1(0)\right) \qquad [A13.6]$$

where $dC_1(t)$ is the change in concentration in phase 1 at time t, dt is the change in time, K_La is the combined overall solute mass transfer coefficient, V_1 is the volume of phase 1, m is the distribution ratio, V_r is the volume ratio and C_1^* is the concentration of PAA in the aqueous phase at time 0.

This equation can be rearranged to form an algorithmic solution (equation A13.8) that was used in the analysis of dispensing speeds to quantify the mass transfer kinetics (section 4.2.6).

$$C_1(t) = C_1(0)e^{-\frac{K_La}{V_1}.(1+mV_r)t} + \frac{mV_r}{1+mV_r}.C_1(0) \qquad [A13.7]$$

where $dC_1(t)$ is the change in concentration in phase 1 at time t, C_1^* is the concentration of PAA in the aqueous phase at time 0, K_La is the combined overall solute mass transfer coefficient, V_1 is the volume of phase 1, m is the distribution ratio and V_r is the volume ratio.

A13.4 Fluid Dynamics

Fluid dynamics is the study of the mathematical phenomenon that describes a fluid in motion, which is based upon the expression of physical laws related to the fluid flow (Welty et al, 2001). The fundamental physical laws include the law of conservation of mass and the first law of thermodynamics. Fluid dynamics covers the analysis of the fluid flow by calculating the Reynolds number, the shear force describing the movement of the liquid, jet fluid flow, drop formation and droplet size distribution.

A13. 4.1 Reynolds Number

The Reynolds number (Re) describes the fluid dynamics of a system and is a dimensionless value that is calculated using rheological and kinematic properties of the fluid. The Reynolds number for pipe flow within the pipette tips (Re_p) is calculated using linear flow (equation A13.8) (Doran, 1998):

$$\mathrm{Re} = \frac{D\rho u}{\mu} \qquad [A13.8]$$

where Re is the Reynolds number, D is the pipe diameter, u is the average linear velocity, ρ is the fluid density and μ is the fluid viscosity.

A13.4.2 Biphasic Rheology

In liquid-liquid extraction the average physical properties of the two phases are normally used. The density of a biphasic mixture is calculated from the density of the dispersed or mobile phase, which contained the majority of the upper phase and the density of the continuous or static phase (equation A13.9):

$$\rho = Q\rho_d + (1-Q)\rho_c \qquad [A13.9]$$

where ρ is the density of biphasic liquid, ρ_d is the density of dispersant phase, ρ_c is the density of continuous phase and Q is the phase ratio (volume of dispersed phase: volume of continuous phase).

Similarly, the viscosity of a biphasic mixture is calculated from the viscosity of the dispersed phase and the viscosity of the continuous phase by equation A13.10:

$$\mu_d = \mu_c(1-Q)^{-2.5} \qquad [A13.10]$$

where μ_d is the viscosity of dispersed phase, μ_c is the viscosity of continuous phase and Q is the phase ratio (volume of dispersed phase: volume of continuous phase in aliquot).

A13.4.3 Jet Mixing Fluid Dynamics

The jet mixing fluid dynamics is a phenomenon of a liquid jetting into an immiscible bulk liquid, which is commonly observed in industrial LLE process equipment. The jet forms when a liquid flows vertically through an orifice or nozzle with a mean linear velocity into another liquid. The diameter of the jet is determined by the nozzle diameter. The length of the jet increases as the dispension velocity increases, until it reaches the maximal length. When the dispensing velocity exceeds the critical velocity of maximal jet length the jet length decreases to zero. The length of the jet mixing is calculated using eA13.11:

$$\frac{d_t}{d_j} = \alpha\left(\frac{\pi l_t}{l_s}\right)^{\beta} + \gamma \qquad \text{[A13.11]}$$

where d_t is the diameter of the nozzle, d_j is the diameter of the jet, l_s is the length of the jet mixing, α and γ are constants (Thornton, 1992). The concentration observed in jets of Newtonian liquids increases with the distance from the nozzle and the flow rates through the nozzle which effect the mass transfer of the system (Thompson, 2002).

A13.4.3.1 Drop Formation

The droplet size is determined by the nozzle diameter, flow rate and physical properties of the liquid. Droplets form at the tip of the nozzle at low linear velocities. The small, individual drops break off once they reach a certain size. The size of the droplets increase with velocity between the velocity of jetting and the velocity of maximal jet length, when a continuous jet of liquid is formed (Thornton, 1992). The droplet size effects the mass transfer from the continuous to the disperse phase (section A13.3).

A13.4.3.2 Drop coalescence

The dispersed droplets coalescence when in close proximity to each other or the same bulk phase and over time the liquids separate into two distinct phases. Coalescence between droplets occurs as the liquid within the drop moves, temporarily forming a point of lowest film thickness as the film is drained, flattening the droplet as the area of the draining film increases and merging them. This is dependent on the force driving the interfaces towards each other, such as viscosity or density, and the capillary forces caused by changes to interfacial tension

enlarge the droplets. The coalescence time increases with drop size increases. The dynamic coalescence at the interface is dependent on the droplet number and size, which effects the coalescence time. A band of droplets first form at the interface and the gravitational force, transmitted through the contacting surfaces, causes the droplets and intervening films to deform and the droplets to coalesce.

Appendix 14: Principles of Solid Phase Extraction

The solid phase extraction process is influenced by various factors related to the adsorbent, including the solid surface structure, specific surface area, adsorption forces, equilibrium mass transfer and thermodynamics. These describe the physical and chemical phenomena that occur in the extraction well during the SPE process, which enables analysis of the process by calculating q_{max} values. This section also describes the types of SPE resins and scales of operation.

A14.1 Structures of Solid Surfaces

The structures of solid surfaces effect the adsorption of molecules onto their surface. The surface structure of a solid depends on the arrangement of the atoms, which is due to their valences. There are three main categories of surface structure: flat surface, mono-atomic stepped surface and the kink surface (Thornton, 1992). The atoms of the flat surface are arranged in the same plane forming a closely packed surface, such as that seen in most transitional metals. The atoms in the stepped surface are arranged in a flat plane (terrace) that forms a new terrace above the previous plane after a distance from the start of the previous terrace (step), creating a staircase effect. The kinked surface has steps that occur randomly over the surface, as seen in a granular structure (Masel, 1996). The surface structure influences the selectivity and capacity of the adsorbent resin for the adsorbate (solute to be adsorbed).

The SPE resin particles can be described according to their structure. Many SPE resins are granular particles that have an uneven external surface with deep superficial cracks that contribute to the internal area together with the pore walls. The resin can contain micro pores (2×10^{-9} m), macro pores (2×10^{-8} m) or transitional pores (0.2 to 2×10^{-8} m). Many modern adsorbent resins are silica based compounds, such as Amberlite XAD, which form crystals with the atoms arranged in a diamond structure. Activated carbon has a polymorphic structure with a multifaceted rough surface, which generates a large surface area. The specific surface area is used to characterize the adsorbent (section 5.2.1.1.1).

During the SPE process, the adsorbate forms a monolayer on the surface of the solid particles. The adsorbate concentration in the monolayer increases over time as the solvent molecules are

displaced from the solid surface until equilibrium is reached. This is dependent on the capacity of the adsorbent for the adsorbate, the initial solute concentration in the liquid phase and the excess in the liquid phase at time *t*.

Langmuir described the geometry of the adsorbed monolayer with the adsorbed solutes (adsorbate) binding on a flat surface at distinct positions directly above a surface atom (linear site) on the solid surface (section A14.1.1). However, rough surfaces have many different sites of adsorption including the linear sites, bridge bound sites between two adjacent atoms and triple co-ordinated sites above a three fold hollow. This generates an increased chance of the adsorbate binding.

A14.1.1 Specific Surface Area of Adsorption

The specific surface area of adsorption is calculated for the classical interpretation of the type I isotherms (section A14.3) (Gregg and Sing, 1967). The specific surface area of adsorption is used in a variety of investigations into the solid surface.

The point of the isotherm where the adsorption is equal to the monolayer capacity (x_m) can be used to calculate the specific surface area of adsorption using equation A14.1:

$$S = \frac{x_m N A_m}{MWT} \qquad [A14.1]$$

where S is the specific surface ($m^2.g^{-1}$), x_m is the monolayer capacity ($g_{adsorbate}.g_{sresin}^{-1}$), N is Avagadaro's number, 6.02 x 10^{23} molecules per mole, A_m is the molecular cross sectional area of the adsorbate (m^2) and MWT is the molecular weight of adsorbate (Gregg and Sing, 1967). The value of A_m is estimated from the mean diameter of the molecule, assumed to be spherical.

A14.1.2 Adsorbent Porosity

The adsorbents are highly porous particles with interconnected, small diameter micropores (<2 x 10^6 m) which create a large surface area (Gregg and Sing, 1967). Therefore, the porosity of the particles is 30% to 85% with an average diameter of 0.01 to 2 x 10^{-8} m (Dutta et al, 1997). Activated carbon and charcoal have extremely large surface areas (1000 $m^2.g^{-1}$) and high

porosity (Masel, 1996). The specific surface area is not significantly affected by the particle size, as the internal surface area is large. The specific surface is a combination of the internal and external surfaces. The internal surface includes the wall area of the pores, whilst the external surface area is due to superficial cracks that increase the total surface area. Adsorbents have high specific surface areas, which are far greater than those of catalysts that typically have a surface area of $100m^2.g^{-1}$ (Masel, 1996). This facilitates the binding of the adsorbate, which is a key property of the adsorbent solids (section A14.1.3).

A14.1.3 Binding of Molecules to Surfaces

During the adsorption process the adsorbate molecules bind at specific sites on the surface of the solid adsorbent, forming a monolayer of tightly packed molecules (Masel, 1996). This phenomenon was first observed during the 1970's and the density of the adsorbate monolayer is similar to that of a liquid. For gas-solid adsorption the monolayer contains 1 to 2 x 10^{15} molecules per cm^2 for a range of gaseous compounds (Masel, 1996). For solid-liquid adsorption the density of the monolayer of the liquid is assumed to be similar to that of water (1 x 10^{15} molecules). To adsorb this number of molecules a surface of 6 x 10^8 cm^2 is required to hold a mole of gas or solute, which equates to the area of a football pitch (2550 m^2). This area is contained within a few cubic centimetres for a good adsorbent, such as activated carbon.

The SPE process adsorbs aqueous molecules onto the solid surface by forming chemical and physical bonds. The chemosorption forms a direct chemical bond between the adsorbent and adsorbate by sharing electrons. The physicosorption forms no direct bond between the components but temporary attractive forces (section A14.3.1). Both types of bond contribute to the adsorption of the adsorbate. This selectively separates compounds from a binary or higher mixture (Masel, 1996), which is driven by a driving force to generate mass transfer (section A14.2).

A14.1.3.1 Adsorption Forces

There are physical and chemical forces involved in the adsorption process causing the binding of the adsorbate to the surface of the adsorbent by transferring electrons between the molecules. This occurs according to the specific geometry of the adsorbent and contributes to the formation of the liquid monolayer on the solids surface. The energy related to each of these adsorption forces is greater for chemosorption (15 to 100 $kcal.mol^{-1}$) than those of physic

sorption (2 to 10kcal.mol^{-1}), but both of these forces contribute to the adsorption of most molecules.

The physic sorption forces include the attractive and repulsive forces. These forces are generated by the molecular interactions of Van der Waal's forces, polarity attractions, dipole interactions and hydrogen bonds (Maity N & Payne G, 1991). The molecular surface charges polarise the molecule, facilitating the attractive bonding forces of the adsorbate to the adsorbent.

A14.2 SPE Mass Transfer

The mass transfer phenomenon involved in equilibrium separation process was discussed in chapter 4, appendix 13 and will be considered briefly here in relation to SPE. Mass transfer from one phase to another is similar regardless of the nature of the phases and involves similar mechanisms. The SPE system is a highly dispersed solid, which is exposed to a liquid phase containing a solute and the solid begins to adsorb the solute. A portion of the initial solute concentration in the liquid phase (x_L) is transferred to the monolayer surface (x_m^1) and the liquid ($x_{L_i^1}$). The liquid-solid mass transfer coefficient describes the rate of transfer (equation A14.2) which is similar to that of the LLE process:

$$\frac{dC}{dt} = -\beta_L . S_S (C_t - C_S) \qquad [A14.2]$$

where $dC.dt^{-1}$ is the change in concentration of the adsorbate in the liquid phase over time (g. Ls^{-1}), β_L is the liquid-solid mass transfer coefficient, S_S is the surface area of adsorbent (m^2), C_t is the concentration of adsorbate in the liquid phase at time t (g.L^{-1}) and C_S is the concentration of adsorbate in the solid phase at time t (g.L^{-1}) (McKay, 1983).

A14.2.1 Adsorbent Capacity

The capacity of an adsorbent for a specific adsorbate is a property that is dependent of the physical characteristics of the adsorbent. This can be determined by loading the adsorbent with

the adsorbate until the liquid phase contains the excess adsorbate and plotting the data to produce a breakthrough curve.

A14.3 Equilibrium Adsorption Isotherms

The equilibrium isotherm is the relationship between the equilibrium concentration in the liquid phase and the concentration on the adsorbent particles or solid phase at a given temperature and pressure (McCabe et al, 2001b). The concentration of 6-APA in the liquid phase (4.0 $g.L^{-1}$) can be used to calculate the adsorbate bound to the resin or the mass adsorbed per unit mass of adsorbent ($g.g^{-1}$). These values were plotted against each other to generate the equilibrium isotherm by varying the concentration of the adsorbent or the adsorbate. The flattening of the isotherm indicates the equilibrium point of the SPE, which generates the q_{max} value. This value is used to determine the capacity of an adsorbent for a compound.

There are over 100 published isotherm equations derived from various physical, mathematical and experimental considerations of the adsorption process (Toth, 2003). There are five characteristic isotherms originally for the solid-gas adsorption, types I - V (figure A14.3.1), which were proposed by Brunauer, Deming, Deming and Teller (Gregg and Sing, 1967). The solid-liquid adsorption isotherms are characterized into four main types: strongly favourable, favourable, linear or unfavourable. The most frequently occurring SPE isotherm is the Langmuir isotherm, type I or favourable isotherm.

The Langmuir isotherm (figure A14.3.1 (I) is a well characterized isotherm that has an adsorption loading described by:

$$W = Q_{\max}\left[\frac{Kc}{(1+Kc)}\right] \qquad \text{[A14.3]}$$

where W is the adsorbate loading (g), Q_{max} is the maximum adsorbate loading (g), K is the adsorption constant and c is the concentration of the fluid ($g.L^{-1}$).

The efficiency of the SPE process was assessed by calculating a percentage recovery value, which is defined by equation A14.4:

$$\%\ \text{Recovery} = \frac{\text{mass of extracted adsorbate on solid (g)}}{\text{total mass of adsorbate originally present in feed } (g)} \qquad \text{[A14.4]}$$

The maximum solute bound to the adsorbent (Q_{max}) is a useful means of comparison of a range of adsorbents and is defined by equation A14.5:

$$Q_{max} = \frac{\text{mass of extracted adsorbate on solid } (g_{Adsorbate})}{\text{total mass of adsorbent resin } (g_{Resin})} \qquad \text{[A14.5]}$$

where Q_{max} is the maximum adsorbate bound (g) per gram of adsorbent.

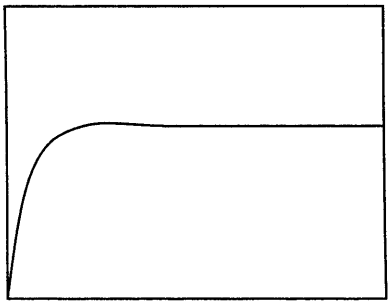

I

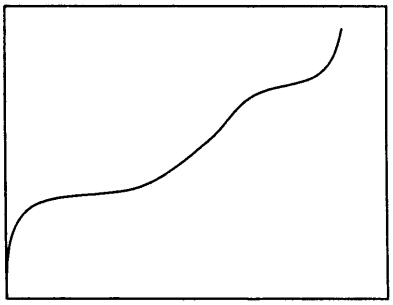

II

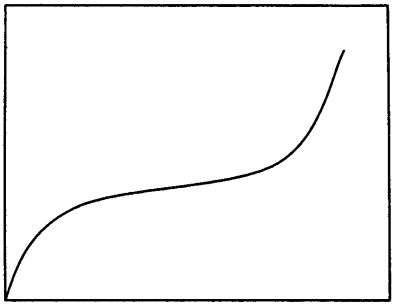

III

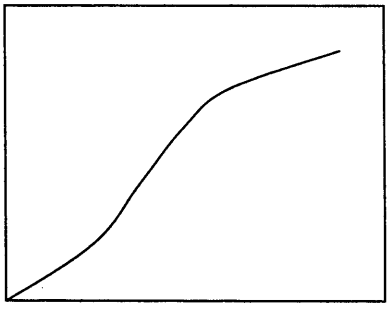

IV

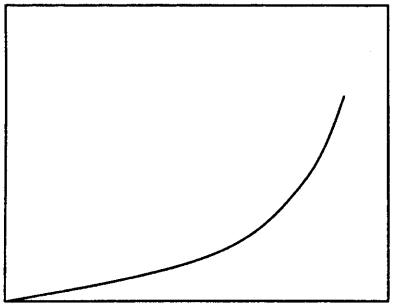

V

Figure A14.1. The five types of adsorption isotherms according to the classification of Brunauer et al (1938), type I – V for gas-solid isotherms plotting equilibrium concentration in the gas against equilibrium concentration in the liquid.

Appendix 15: HPLC trace & Calibration Curves

The HPLC trace for the synthesised bioconversion product stream (figure A15.1) contained Pen G, 6-APA and PAA, as detailed in section 2.1.1.1. Calibration curves measured each of these compounds (figure A15.2 to A15.4) over a concentration range using the HPLC (section 2.5.1) to indicate the linearity of the HPLC quantification. It was observed that the buffer pH conditions effected the gradient of the calibration curve for 6-APA and PAA. Therefore, all experimental data contained a sample of the standard feed material in order to calculate the respective solute concentrations.

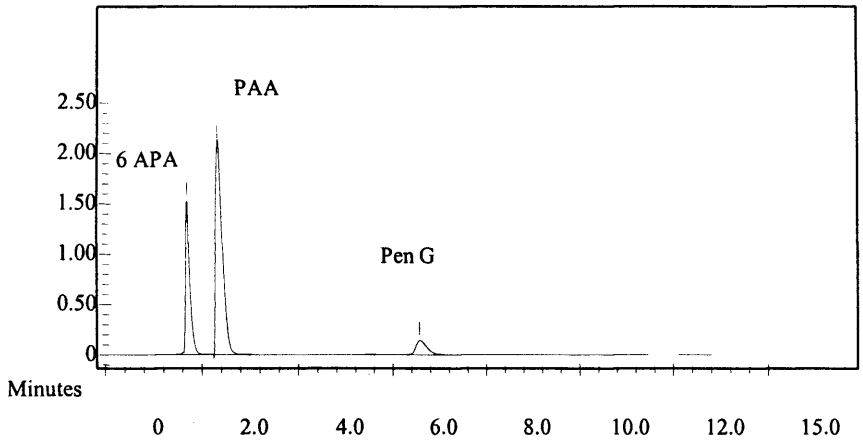

Figure A15.1 HPLC trace for simulated bioconversion product stream on a C18 column. Method described in section 2.5.1.

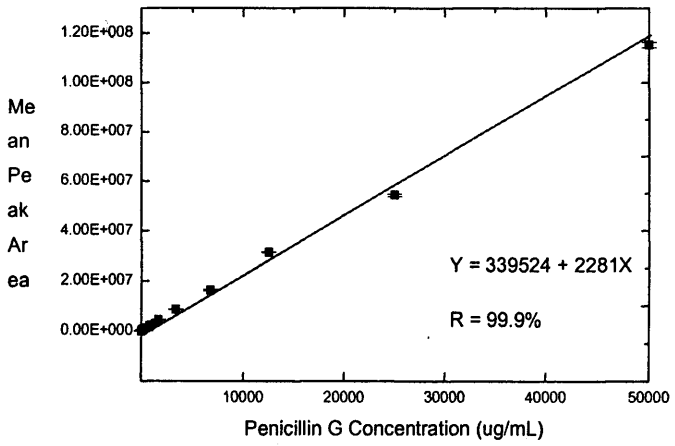

Figure A15.2. Standard Curve of Penicillin at pH 7.8 prepared using the HPLC on a C18 column. Method described in section 2.5.1.1.

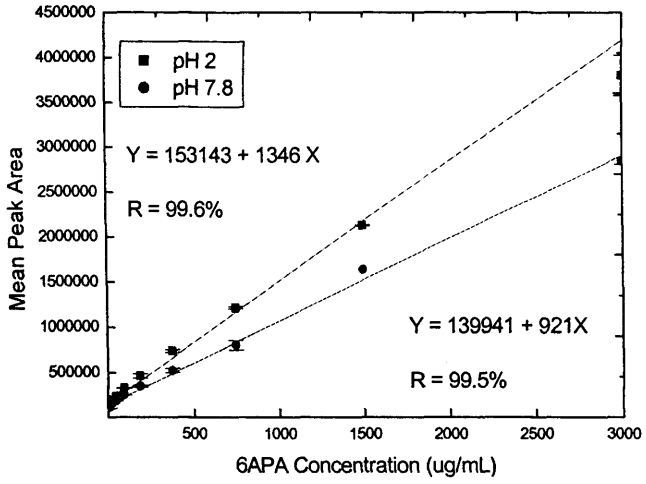

Figure A15.3. Standard Curve of 6-APA at pH 2 and pH 7.8 prepared using the HPLC on a C18 column. Method described in section 2.5.1.1.

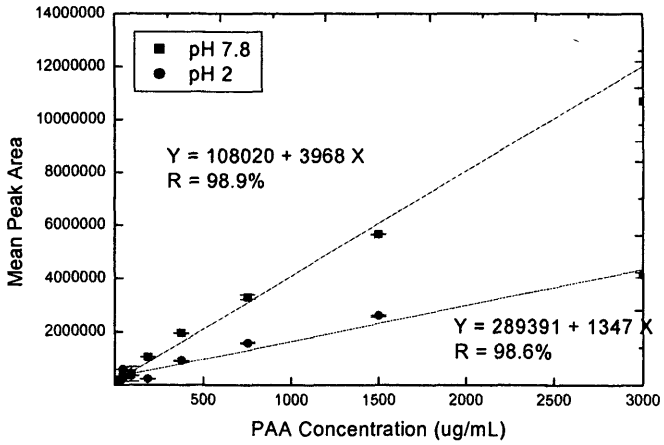

Figure A15.4. Standard curve of PAA at pH 2 and pH 7.8 prepared using the HPLC on a C18 column. Method described in section 2.5.1.1.

Appendix 16: 6-APA Spectrophotometer Calibration Curve

The spectrophotometer calibration curve for 6-APA was generated for the absorbance at 257 nm over a range of 6APA concentrations (0.1 to 4.0 $g.L^{-1}$). The calibration curve (figure A16.1) showed that the absorbance increased linearly with the 6-APA concentration over the concentration range, fitting the equation Y = 0.399 X + 0.01 with a regression of 1.000.

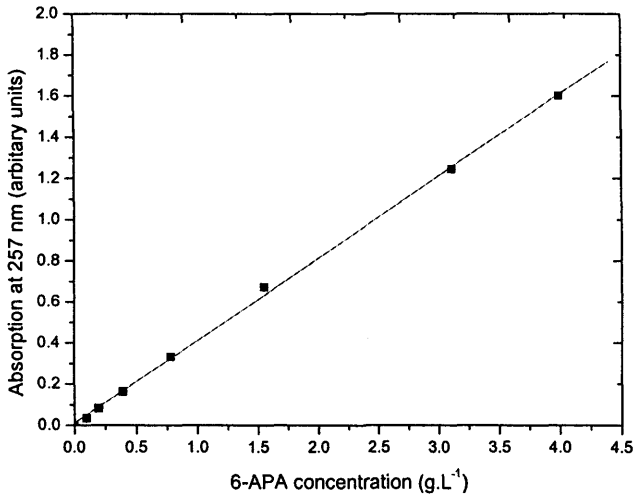

Figure A16.1 Calibration curve for 6-APA analysed on a spectrophotometer at 257 nm over a range of 6-APA concentrations (0.125 $g.L^{-1}$ to 4.0 $g.L^{-1}$) dissolved in phosphate buffer (01. M, pH 7). Method described in section 2.5.2.1.

Appendix 17: Published paper: Use of Operating Windows in the assessment of integrated robotic systems for the measurement of bioprocess kinetics

This paper was generated from research based on my initial research into the reliability of the Multiprobe liquid handling workstation, together with additional experiments developed by other researchers. I highlighted the importance of assessing the statistical performance of the automated platforms, identified the key methods of statistical analysis and designed the initial gravimetric experimentation to assess the performance of the workstation over a range of volumes and reagents, which contributed 30% to this paper.

The accuracy and precision analysed in chapter 3 were repeated and the range of dispensed liquid aliquots was extended to 200 μL, which showed a clearer statistical trend. Further analysis of the reliability of the use of each of the pipette tips on the workstation was made and showed little significant difference between their performance and this quantified the minimal variation, validated observations made in my preliminary research for this thesis. I designed the initial performance files to facilitate the transfer of organic solvents using the workstation and assessed its performance for a range of solvents. The performance of the workstation was analysed for experimentation using a more predictable solvent, dimethyl sulfoxide (DMSO) that was a low viscosity reagent, which showed improved statistical performance over the volume range.

The research in this paper investigated the affects of kinetics for a diverse range of bioprocesses to generate an operating window for the use of integrated robotic systems. These bioprocesses included alkaline cells lysis, aerobic fermentation of Escherichia coli and product recovery using liquid–liquid extraction. I designed and undertook the automated experimentation for the analysis of the kinetics of the liquid-liquid extraction process (chapter 4).

Nealon A., Willson K., Pickering A., Clayton T., O'Kenedy R., Titchner-Hooker N., and Lye G. (2005). Use of Operating Windows in the assessment of integrated robotic systems for the measurement of bioprocess kinetics. Biotechnology Progress. 21: 283-291.

See following pages for paper in full.

Abbott B., Cerimele B., and Fukuda D. (1976). Immobilization of a cephalosporin acetyl esterase by containment within an ultra filtration device. *Biotechnology and Bioengineering* 18: 1033-1042.

Adrian T., Freitag J., and Maurer G. (2001). A novel high pressure liquid-liquid extraction process for down stream processing in biotechnology: extraction of cardiac glycosides. *Journal of Biochemical and Biophysical methods* 69(5): 559-565.

Aitken Scientific. (2002). Webpage: *www.aitken-sci.co.uk.*

Alberts B., Bray D., Lewis J., Raff M., Roberts K., Watson J. (1994). Molecular Biology of the Cell, Garland Publishing Inc., 3rd edition.

Allanson J.P., Biddlecombe R.A., Jones A.E., and Pleasance S. (1996). The use of automated solid phase extraction in the '96 well' format for high throughput bioanalysis using liquid chromatography coupled to tandem mass spectrometry. *Rapid Communications in Mass Spectrometry* 10: 811-816.

Alltech Associates Ltd. (2002). Choosing the right SPE product. Webpage: www.alltechweb.com/productinfo/technical/rdu/spe_product,htm.

Amersham Plc. (2003). Webpage: www.amersham.com/ar2000/Visionaries?08a,htm.

Anachem. (2002). Webpage: www.anachem.com.

Argonaut Inc. (2002). Argonaut technologies Inc. expand product offering with the acquisition of Camile Products. Webpage: www.argonaut.com/.

Asaro M., and Wilson R. (1998). The screen test. *Chemistry in Industry* Oct: 777.

Asenjo J.A. (2003). Separation Processes, Chapter in Biotechnology. Bioprocess technology, M. Dekker.

Astle T.W., and Akowitz A. (1996). Accuracy and tip carryover contamination in 96-well pipetting. *Journal of Biomedical Screening* 1(4): 211-217.

Astra Zeneca. (2006). AstraZeneca - Pipeline Summary - New chemical entities and line extensions. Webpage: www.astrazeneca.com.

Bailey J.E., and Ollis D.F. (1984). Primary Isolation, chapter in Biochemistry Fundamentals, McGraw-Hill Chemical, engineering series, 2nd edition: 738-764.

Bakhtiar R., Lohne J., Ramos L., Khemani L., and Hayes M. (2002). High throughput quantification of the anti-leukemia drug STi571 and its main metabolite (CGP 74588) in human plasma using liquid chromatography tandem mass spectrometry. *Journal of Chromatography B* 768(2): 325-340.

Balsingham K., Warburton D., Dunnill P., and Lilly D. (1972). The isolation of penicillin amidase from *Escherichia coli. Biochemica et Biophysica Acta* 276: 250-256.

Barbel M., Stadler R., and Stadler P. (2001). Generalized topological spaces in evolutionary theory and combinatorial chemistry. Webpage: www.tbi,univie,ac,at~[baer.studla]: 1-9.

Bateman T., Ayers A., and Greenway B. (1999). An engineering evaluation of four fluid transfer devices for automated 384 well high throughput screening. *Laboratory Robotics and Automation* 11(5): 230-259.

Battilotti M., and Barberini U. (1988). Preparation of D-valine from D,L-5-isopropylhydantoin by. stereoselective biocatalysis. *Journal of Molecular Catalysis* 43(3): 343-352.

Bayer AG. (2000). Webpage: http://www.bayer.com/en/History.aspx.

Beschov V., Velizarov S., and Peeva L. (1995). Some kinetic aspects and modelling of biotransformation of D-glucose to keto-D-gluconates. *Bioprocessing Engineering* 13(6): 301-305.

Biddlecombe R.A., and Pleasance S. (1999). Automated protein precipitation by precipitation by filtration in the 96-well format. *Journal of Chromatography B* 764: 257-265.

Blanch H., and Clark D. (1996). Penicillin Fermentation. Biotechnology 4: Microbial Products: 204-211.

Blanch H., and Clark D. (1996a). Product Recovery. Biotechnology 4: Microbial. Products: 453-455.

Blanch H., and Clark D.S. (1996). Penicillin. Case study, chapter 8 in Biochemical Engineering, Dekker: 57-661.

Blanchard B.S., and Fabrycky.W.J. (1981). Systems Engineering and Analysis, Prentice, Hall international, series in industrial and systems engineering, 2nd edition.

Bolden S., Hoke T., Eichhold D., and McCauley-Myers K. (2002). Semi-automated liquid-liquid back extraction in a 96-well format to decrease sample preparation time for the determination of dextromethorphan and dextrotphan in human plasma. *Journal of Chromatography B* 772: 1-10.

Bora M., Ghosh A., Dutta N., and Mathur R. (2000). Reactive extraction of 6-APA with aliquot 336: equilibria and kinetics. *The Canadian Journal of Chemical Engineering* 75: 520-526.

Boyle N., and Janda K. (2002). Formats for combinatorial synthesis: solid phase, liquid phase and surface. *Current Opinion in Chemical Biology* 6(3): 339-346.

Branch. (2002). Industry Canada - life sciences. Webpage: www.strategis,ic,gc,ca/SSG/ph01473e,html.

Braun J., Chanu P., and Goffic F. (1989). The immobilization of penicillin G acylase on chitosan. *Biotechnology and Bioengineering* 33: 242-246.

Brocklebank S., Woodley J., and Lilly M. (1999). Immobalisatied transketolase for carbon-carbon bond synthesis: biocatalyst stability. *Journal of Molecular Catalysis B: Enzymatic* 7: 223-231.

Brunauer S., Emmett P.H., and Teller E. (1938). Adsorption of gases in multimolecular layers. *Journal of American Chemistry Society,* 60, 309-319.

Bruner J., Birkemo L., Jordan K., Smith G., and Ormand J. (2001). Collecting sample weight data on various liquid handling robots. *Journal of Association for Laboratory Automation* 6(5): 64-66.

Brush M. (2002). Automated liquid handlers advance. *The Scientist* 16(3): 38-45.

Bryjak J., and Nowoeyta A. (1993). Kinetic behavior of penicillin acylase immobilized on acrylic carrier. *Bioprocess Eengineering* 9: 37-42.

Byron D. (1999).Rapid process development for biopharmaceuticals. *Pharmaceutical Technology Europe* July 1999: 26–29.

Carlesmith S., Dunhill P., and Lilly M. (1980). Kinetic behavior of immobilized. penicillin acylase. *Biotechnology and Bioengineering* 22: 735-756.

Carter W. jr., and Carter C.W. (1979). Protein crystallisation using incomplete factorial experiments. *The Journal of Biological Chemistry* 254: 12219-12223.

Carter C., Baldwin E., and Frick L. (1988). Statistical design of experiments for protein crystal growth and the use of a precrystalisation assay. *Journal of Crystal Growth* 90: 60-73.

Cascaval D., Tudose R., and Oniscu C. (1998). Study on penicillin G liquid-liquid extraction with and without chemical reaction. *Hungarian Journal of Industrial Chemistry* 26(2): 70-75, 1-146,.

Chaubal M., Payne G., Reynolds C., and Albright R. (1995). Equilibrium for the adsorption of antibiotics onto neutral polymeric sorbents: experimental and modeling studies. *Biotechnology and Bioengineering* 47: 215-226.

Chemspeed. (2003). Solid dosing unit for the accelerator. - solid dosing as convenient and accurate as liquid dosing. Webpage: www.chemspeed.com/content/products/products_vlt100.shtml?

Chempseed. (2003a). Analysis of Accelerator's performance. Information provided by Chemspeed.

Chen Y., Hanson G.D., Jiang X.J., and Naidong W. (2002). Simultaneous determination of hydrocodine and hydromorphone in human plasma by liquid chromatography with tandem mass spectrometric detection. *Journal of Chromatography B* 769: 55-64.

Cheng Y., Neue U.D., and Bean L. (1998). Straightforward solid phase extraction method for the detection of verapamil and its metabolites in plasma in a 96-well extraction plate. *Journal of Chromatography A* 828: 273-281.

Chou C., Yu C., Tseng J., Lin M., and Lin H. (1999). Genetic manipulation to identify limiting steps and develop strategies for high level expression of penicillin acylase in *Escherichia coli*. *Biotechnology and Bioengineering* 63: 263-271.

Cole M., Savidge T., and Vanderhaeghe H. (1975). Hydroxylamine assay, Antibiotic inactivation and modification. *Methods in Enzymology* 43: 698-705.

Conner K. (1999). Automating the process development laboratory is key to future profitability. *Today's Chemist at Work:* 19-34.

Crooks G.E., Rees G.D., Robinson B.H., Svensson M., and Stephenson G.R. (1995). Comparison of hydrolysis and esterification behaviour of *Humicola lanuginosa* and *Rhizomucor miehei* lipases in AOT- stabilized water-in-oil microemulsions. I: Effect of pH and. water content on reaction kinetics. *Biotechnology and Bioengineering* 48(1): 78-88.

Cudney K., and McPherson A. (1994). Screening and optimisation strategies for macromolecular crystal growth. *Acta Crystallisation* D50: 414-423.

Cull S., Holbrey J., Vargas-Mora V., Seddon K., and Lye G. (2000). Room temperature ionic liquids as replacements for organic solvents in multiphase bioprocess operations. *Biotechnology and Bioengineering* 69: 227-233.

Cusack R., and Fremeaux. (1991). Though basically simple, the technique has a surprisingly wide range of useful variations. *Chemical Engineering* 2191: 66-76.

Davies E.K., and Richards W.G. (2002). The potential of internet computing for drug discovery *Drug Discovery Today*. 7(11): S99-S103.

Davies G.C., Hutton R.S., Millot N., Macdonald S.J.F., Anson M.S., and Campbell I.B. (2002). Simultaneous high throughput assessment of thermodynamic and kinetic behaviors of chemical reactions: theory and experimentation. *Physical Chemistry Chemical Physics* 4(10): 1791-1796.

Davies L., Allanson J., Causon R. (1999). Rapid determination of the anti-cancer drug chlorambucil. (Leukeran^{TM}) and its phenyl acetic acid mustard metabolite in human serum and plasma by automated solid phase extraction and liquid chromatography-tandem mass spectrometry. *Journal of Chromatography B* 732: 173-184.

Davis M. (1999). Combinatorial Methods: How will they integrate into chemical engineering? *American Institute of Chemical Engineering Journal* 45 (11): 2270-2272.

Davis P., and Swayze E. (2000). Automation solid phase synthesis of linear nitrogen-linked compounds. *Biotechnology and Bioengineering* 71: 19-27.

Demuth D., Finger K., Hill J., Levine S., Lowenhauser G., and Newsam J. (2002). Developing computational support for high throughput experimentation applied to heterogeneous catalysis. *American Chemistry Society Symposium Series* 814: 147-164.

Dilkin P., Mallmann C., de Almeida C., and Correa B. (2001). Robotic automated clean-up for detection of fumonisins B1 and B2 in corn and corn based feed by high performance liquid chromatography. *Journal of Chromatography A* 925: 151-157.

DiLorenzo M.E., Timoney C.F., and Felder R.A. (2001). Technological advancements in liquid handling robotics. *Association for Laboratory Automation* 6(12): 36-40.

Doig S., Pickering S., Lye G., and Woodley J. (2002). The use of microscale processing technologies for quantification of biocatalytic *B*aeyer-*villager* oxidation kinetics. *Biotechnology and Bioengineering* 80(1): 42-49.

Doig S.D., Pickering S.C.R., Lye G.J., and Baganz F. (2005). Modelling surface aeration rates in shaken microtitre plates using dimensionless groups. *Chemical Engineering Science* 60)10): 2741-2750.

Dong M., and Gant J. (1984). Short three microncolumns: applications in high speed LCLC. *LC GC* 2: 194.

Doran P. (1998). Bioprocess Engineering Principles, Academic Press, 3rd edition.

Drews J. (2000). Drug Discovery: A historical perspective. *Science* 287: 1960-1964.

Driscoll J., Delmendo R., Papan R., and Sewutz D. (1998). Multiprobe nL complements drug discovery assay miniaturization. *Journal of Biomedical Screening* 3(3): 237-239.

Duggleby H., Tolley S., Hill C., Dodson E., and Moody P. (1995). Penicillin acylase has a single amino acid catalytic center. *Nature* 373: 264-268.

W. (1974). An Elementary Guide to Reliability, Pergamon Press, 2nd edition.

Dutta M., Baruah R., Dutta N., and Ghosh A. (1997a). The adsorption of certain semi-synthetic cephalosporin on activated carbon. *Colloids Surfaces A: Physicochemical and engineering aspects* 127: 25-37.

Dutta M., Baruah R., and Dutta N. (1997b). Adsorption of 6-aminopenicillinanic acid on activated carbon. *Separation and Purification Technology* 12: 99-108.

Eichhold D., Baruah R., and Dutta N. (1997). Adsorption of 6-amino penicillanic acid on activated carbon. *Separation and Purification Technology* 12: 99-108.

Enomoto K., Suzoki R., Araki A., Nakajima T., Ohta H., Gohl K., Preaudat M., Seguin P., Mathis G., Kominami G., and Takemoto H. (2002). High throughput miniaturized immunoassay for human interleukin-13 secreted from NK3.3 cells using homogenous time-resolved fluorescence. *Journal of Pharmaceutical and Biomedical Analysis* 28(1): 73-79.

Farid S. (2003). A decision support tool for simulating the process and business perspectives of biopharmaceutical manufacture. *University of London thesis.*

Foo F., Karri S., Davies E., Titchener-Hooker N.J., and Dunnill P. (2001). Biopharmaceutical process development: part 1, information from the first product generation. *Biopharm Europe* June *2001. 58*-64.

FDA. (2002). Code of Federal Regulations. Webpage: www.fda.gov/.

Gauw R., Stoffolano P., and Kuhlenbeck D. (2000). Semi automated 96-well solid phase extraction and gas chromatography- negative chemistry ionization tandem mass spectrometry for trace analysis of floprostenolin. *Journal of Chromatography B* 744: 283-291.

Ghosh A.C., Mathur R.K., and Dutta N. (1997). Extraction and purification of cephalosporin antibiotics. *Advance in Biochemical Engineering and Biotechnology* 56: 112-145.

Gilar M., Belemky A., and Wang B. (2001). High throughput biopolymer desalting by solid phase extraction prior to mass spectrometry analysis. *Journal of Chomayography* A 921: 3-13.

Godoy R.D., Sanabria L.F., Gomez Aguirre A., Giraldo L., Gomez Ordonez A., and Buitrago G. (1996). Reaction heat measurements in the enzymatic hydrolysis of penicillin GK to obtain 6-APA. *Enzyme and Microbial Technology* 19(8): 585-589.

Grant D.C., Chilcote D., Kelly W., and Litchy M.R. (2001). Testing liquid handling system components to ensure purity and reliability. *Micro,* 19(5): 41-52.

Gregg S.J., and Sing K.S. (1967). Adsorption Surface Area and Porosity, Academic Press.

Guisan J.M., Alvara G., and Ferdanandez-Lafauente R. (1990). Immobilisation-stabilization of Penicillin G Acylase, Edited by Okado H, Tranaka A, The New York Academy of Sciences.

Haagensen P., Karlsen L., Petersen J., and Villadsen J. (1983). The kinetics of penicillin V deacylation on an immobilised enzyme. *Biotechnology* 25: 1873-1895.

Hanson K., and Cartwright C. (2001). Evaluation of an automated liquid-handling system (Tecan Genesis RSP 100) in the Abbott LC assay for *Chlamydia trachamatis. Journal of Clinical Microbiology* 39(5): 1975-1977.

Harrison A., and Walker D. (1998). Automated 96-well solid phase extraction for the detection of doramextin in cattle plasma. *Journal of Pharmaceutical and Biomedical Analysis* 16: 777-783.

Hazard Evaluation Laboratories. (2000). Faster, better chemistry. *Chemistry and Industry:* 2-5.

Hennion M. (1999). Solid phase extraction: method development, sorbents and coupling with liquid chromatography. *Journal of Chromatography A* 856: 3-54.

Hicketier M., and Buchholz K. (1990). Investigation on cephalosporin C adsorption kinetics and equilibria. A*pplied Microbiology and Biotechnology* 32: 680-685.

Houston J.G., and Banks M. (1997). The chemical-biological interface: development in automated and miniaturized screening technology. *Current Opinion in Biotechnology* 8(6): 734-740.

Hsieh S., and Selinger K. (2002). High throughput bioanalytical method using automated sample preparation and liquid chromatography- atmospheric pressure ionspray mass spectrometry for quantitative determination of glybenclamide in human serum. *Journal of Chromatography B* 772: 347-356.

Huang N.H., Kagel J.R., and Rossi D.T. (1999). Automated solid-phase extraction workstations combined with quantitative bioanalytical LC/MS. *Journal of Pharmaceutical and Biomedical Analysis* 19: 613-620.

Hubert P., Chap P., Seccato A., and Bechet I. (1992). Determination of verapamil and norapamil in human plasma by LC, comparison between liquid-liquid extraction procedure and an automated liquid-solid extraction method for sample preparation. *Journal of Pharmaceutical and Biomedical Analysis* 10(11-12): 937-942.

Hudson control group. (2002). Trends in lab automation. Webpage: ww.hudsoncontrol.com/lab_automation_ovweveiw_4,htm.

Hughes E.X., Cohen J., Gangi W., Lineen J., and Manard A. (2005). Strategic alternatives in the pharmaceutical industry: Managerial challenges in the pharmaceutical, biotech, and medical device industries. Kellog School of Management (HIMT-453).

Illanes A., Altamirano C., and Zuniga M. (1996). Thermal inactivation of immobilized penicillin acylase in the presence of substrate and produces. Journal of *Biotechnology and Bioengineering* 50: 609-611.

Infoplease. (2004). Webpage: www.infoplease.com/ce6/sci/A0856821.html.

Intellegen. (2003). Webpage: www.intellegen.com/SuperPro.htm.

InvestorWords. (2003). Research and development, Webpage: http://www.investorwords.com/4200/research_and_development.html.

Ivey School of Business. (2000). Diabetagen case study, Richard Ivey School of Business, University of Ontario.

Jandu S. (2000). Automation stations. *Chemistry and Industry: The Supply Line, Biochemical Engineering* 18/9/00: 2-3.

Janiszewski J., Schneider R.P., Hoffmaster K., Swyden M., Wells D., and Fouda H. (1997). Automated sample preparation using membrane microtiter extraction for bioanalytical mass spectrometry. *Rapid Communications in Mass Spectrometry* 11: 1033-1037.

Jansens P., Bruinsma O., and van Rosmalten G. (1995). Optimization and modeling of the crystallization process in a cascade with backmixing. *American Institute of Chemical Engineering Journal* 41(4): 828-837.

Jefferis R.P. (1998). Thoughts on pharmaceutical research coordination. Webpage: http://muse,widenet.edu/-rpj0001/Papers/Research/Research.htm: 1-4.

Jemal M., Teitz D., Ouyang Z., and Khan S. (1999). Comparison of plasma sample purification by manual liquid-liquid extraction, automated 96-well liquid-liquid extraction and automated 96-well solid-phase extraction for analysis by high-performance liquid chromatography with tandem mass spectrometry. *Journal of Chromatography B* 732(2): 501-508.

Jemal M., Huang M., Mao Y., Whigan D., Schuster A. (2000). Liquid chromatography/ electrospray tandem mass spectroscopy method for the quantification of fosinoprilat in human serum using automated 96-well solid-phase extraction for sample preparation. *Rapid Communications in mass* Spectrometry 14: 1023-1028.

Jenkins R. (1999). Purification, Chapter in Product Recovery in Bioprocess Technology, Butterworth Heinemann: 164-199.

Jing Ke, Yancey M., Zhang S., Lowes S., and Henion J. (2000). Quantitative liquid chromatographic-tandem mass spectrometric determination of reserpine in FVB/N mouse plasma using a "chelating" agent (disodium EDTA) for releasing protein-bound analytes during 96-well liquid-liquid extraction. *Journal of Chromatography B* 742: 369-380.

Johnson B. (1999). All's well that ends well: a profile of specialty microwell plates. *The Scientist* 13(19): 16-24.

Jones D.J., Gibson V.C., Green S.M., and Maddox P.J. (2002). Discovery of a new family of chromium thylene polymerisation catalysts using high throughput screening methodology. *Chemical Communications* 10: 1038-1039.

Kalinichenko E.N., Podkopaeva T.L., Kelve M., Saarma M., and Mikhailopulo I.A. (1990). 3'-Fluoro-3'-deoxy analogs of 2–5A 5'-monophosphate: Binding to 2–5A-dependent endoribonuclease and susceptibility to (2'-5') phosphodiesterase degradation. *Biochemical and Biophysical Research Communications* 16(7(1): 20-26.

Karande P., and Mitragotri S. (2002). High throughput screening of transdermal formulations. *Pharmaceutical Research* 19(5): 655-660.

Karri S., Davies E., and Titchener-Hooker N.J. (2001). Biopharmaceutical process development: part 3, A framework to assist decision making. *Biopharm Europe* September 2001:76-82.

Kasche V. (1983). Correlation of experimental and theoretical data for artificial and natural systems with immobilized biocatalysts. *Enzyme and Microbial Technology* 5(1): 2-13.

Kawamoto T., Aoki A., Sonomoto K., and Tanaka A. (1989). Novel photocatalytic NAD^+ recycling system with a semiconductor in organic solvent. *Journal of Fermentation and Bioengineering* 67(5): 361-362.

Kaye B., Herron W.J., Macrae P.V., Robinson S., Stopher D.A., Venn R.F. and Wild W. (1996). Rapid, solid phase extraction technique for the high-throughput assay of darifenacin in human plasma. *Analytica Chemica Acta* 68(9): 1658-1660.

Keightley R. (1986). Principles of automated diluting and pipetting. *The Medical Technologies* 11: 23-24.

Key Notes. (1996). Prescription Pharmaceuticals. Webpage: www.keynotes.com.

Kolb A.J. (1994). The role of microplate selection and assay design in the application of automation and robotics. *Laboratory Information Management* 26: 107-113.

Koo Y. and Chang W. (1999). On-line recovery of large molecules using reciprocating size exclusion chromatography with temperature swing. *Biotechnology Techniques* 13(11): 809-812.

Koshy P., Rowan A., Life P., and Cawston T. (1992). 96 well plate assays for measuring collagenase activity using H^3 acetylated collagen. *Analytical Chemistry* 275: 202-207.

Kristenson E., Haverkate E., Slooten C., Ramos L., Vreuls R., and Brinkman U. (2001). Minimized automated solid phase dispersion extraction of pesticides in fruit followed by gas chromatographic-mass spectrometric analysis. *Journal of Chromatography A* 917: 277-286.

Kumar R., Suresh K., and Shankar S. (1996). Kinetics and reaction engineering of penicillin G hydrolysis, *Journal of Chemistry, Technology and Biotechnology* 66: 243-250.

Kuzmic P., Elrod K., Cregar L., Sideris S., Ral R., and Janc J. (2000). High throughput screening of enzyme inhibitors: simultaneous determination of tight-binding inhibition constants and enzyme concentration. *Analytical Biochemistry* 286(1): 45-50.

Lam K., and Renil M. (2002). From combinatorial chemistry to chemical microarray. *Current Opinion in Chemical Biology* 6(3): 353-358.

Lander K. (2002). High throughputs adsorbent screening, University of London thesis.

Lane A., and Lynn A. (1987). The application of the Tecan 530 liquid handling system to the automation of the Lowry assay. *Biochemistry Society* 15: 696-697.

Lang *RA.*, Schaad U.B., Rüdeberg A., Wedgwood J., Que J.U., Fürer E., and Cryz S.J. jr. (1995). Effect of high-affinity anti-Pseudomonas aeruginosa lipopolysaccharide antibodies induced by immunization on the rate of *Pseudomonas aeruginosa* infection in patients with cystic fibrosis' *The Journal of Pediatrics* 127(5): 711-717.

Langerhof F., Nathorst-Westfelt L., and Ekstrom B. (1964). Production of 6-aminopenicillinanic acid with immobilized *Escherichia coli* acylase. *Methods in Enzymology* 44: 759-768.

Larroche C., Arpah M., and Gros J.B. (1989). Methyl-ketones by Ca-alginate/Eudrasit RL entrapped spores of Penicillium roqueforti. *Enzyme Microbial Technology* 11:106-112.

Lee Cheng-Kang, and Su Wen-Da . (1998). Separation of phenylacetic acid from 6-aminopenicillanic acid via cloud-point extraction with N-decyltetra(ethylene oxide) nonionic surfactant. *Separation and Purification Technology* 33(7): 1003-1012.

Lehman Brothers. (1995). Pharma pipelines report. Webpage: www.lehman.com.

Lewis R. (1997). Liquid handling equipment evolved to suit large scale applications. *The Scientist* 11(1): 18-19.

Lewis W.K. (1916). Laboratory and plant the principles of counter current extraction. *Industrial Engineering Chemistry* 8: 825-833.

Lilly M. (1992). The design and operation of biotransformation processes. .*Recent Advances in Biotechnology*: 47-68.

Lilly M., and Woodley J. (1996). A structured approach to design and operation of biotransformation processes. *Journal of Industrial Microbiology* 17: 24-33.

Lin C., Hsieh J., Matuszeusk B., and Dobrinska M. (1996). An automated sample preparation and high performance liquid chromatographic method for the detection of MK5919 a novel leukotriene biosynthesis inhibitor in human plasma. *Biochemical Engineering* 7: 89.

Lye G.J. (1993). Kinetic studies in the extraction of proteins using reverse micelles. University of Reading thesis.

Lye G.J., and Woodley J.M. (1999). Application of *in situ* product-removal techniques to biocatalytic processes. *Trends in Biotechnology* 17(10): 395-402.

Lye G., Ayazi-Shamlou P., Beganz F., Dalby P., and Woodley J. (2003). Accelerated design of bioconversion processes using automated microscale processing techniques. *Trends in Biotechnology* 21(1): 29-37.

Maity N., and Payne G. (1991). Adsorption from aqueous solutions based on a combination of hydrogen bonding and hydrophobic interactions. *Langmuir* 7: 1247-1254.

Maryott A., Hobbs M., and Gross P. (1949). Electric polarization of association of carboxylic acids III A study of the association of some additional carboxylic acids in benzene solution. *Merck Index* 71: 1671-1674.

Masel R.I. (1996). Principles of Adsorption and Reaction on Solid Surfaces, Wiley, series in chemical engineering.

Mathews H., and Rawlings J. (1998). Batch crystallization of a photochemical: Modeling, control and filtration. *AICHE Journal* 44(5): 1119-1127.

Mathews C., Woolf E., Lin L., Fang W., Hsieh S., Simpson R., and Matuszewski B. (2001). High throughput, semi-automated determination of a cyclooxygenase II inhibitor in human plasma and urine using solid phase extraction in the 96-well format and high performance liquid chromatography with post column photochemical determination-fluorescence detection. *Journal of Chromatography B* 751: 237-246.

Mathews C., Woolf E., and Matuszewski B. (2002). Improved procedure for the detection of rofecoxib in human plasma involving 96-well solid phase extraction and fluorescence detection. *Journal of Chromatography A* 949: 83-89.

Matisova E., and Skrabakova S. (1995). Carbon sorbents and their utilization for the preconcentration of organic pollutants in environmental samples. *Journal of Chromatography A 707: 145*-179.

McBain J.W., and Bakram A.H. (1926). New sorption balance. *Journal of American Chemistry Society* 48: 690-695.

McCabe W.L., Smith J.C., and Harriott P. (2001a). Liquid Extraction, Unit Operations of Chemical Engineering, McGraw-Hill chemical engineering series, 6th edition: 747-767.

McCabe W.L., Smith J.C., and Harriot I. (2001b). Fixed Bed Separations. Chapter in Unit Operations of Chemical Engineering, 6th edition: 812-844.

McKay G. (1983). The adsorption of dyestuffs from aqueous solutions using activated carbon, IV, external mass transfer processes. *Journal of Chemical Technology* 33A: 205-218.

Menke O., Martínez A.G, Subramanian L.R. and Hanack M. (1995). A novel one-step synthesis of γ-lactones from olefins and Phenyliodonium (ethoxycarbonyl) nonafluorobutylsulfonylmethanide catalyzed by copper(II) triflate. *Tetrahedron Letters* 36(23): 405-405.

Merck Index, Mettler Toledo. (1999). Myriad Allex System promotional pamphlet.

Miller J.C., and Miller J.N. (1988). Statistics for Analytical Chemistry, Ellis Horwood, series in analytical chemistry, 2nd edition.

Mintzberg H., Jorgensen J., Dougherty D., and Westley F. (1996). Some surprising things about collaboration—Knowing how people connect makes it work better. *Organizational Dynamics* 25(1):60-71.

Mwangi S., and Garside J. (1987). The applications of 6-APA crystals and the effects of phenoxy acetic acid. *Biochemistry Society* 15: 696-697.

Nealon A., Willson K.E., Pickering S.C.R., Clayton T., O'Kenedy R., Titchener-Hooker N., and Lye G. (2005). Use of Operating Windows in the assessment of integrated robotic systems for the measurement of bioprocess kinetics. *Biotechnology Progress* 21: 283-291.

NewsEdge Corporation. (2005*)*. IFI Patent Intelligence: IFI Issues List of 2005's Top Patent Companies:PR Newswire. Webpage: www.NewsEdge Corporation.com.

Nielsen J. (2002). Combinatorial synthesis of natural products. *Current Opinion in Chemical Biology* 6(3): 297-305.

Ohtsu M., and Sawada K. (2002). High resolution and high-throughput probes. *Springer Series in Optical Sciences* 84: 61-74.

Oliver G., Valle F., Rosetti F., Gomez-Pedrozo M., Gosset G., and Bolivar F. (1985). A common precursor for the subunit of the penicillin acylase from *Escherichia coli* ATCC1105. *Gene* 40: 9-17.

Olsen K.K. (2000). A quantitative study of factors governing automatic pipetting performance. *American Laboratory* 32(14): 49-51.

Oprea T.I. (2002). Chemical space in navigation in lead discovery. *Current Opinion in Chemical Biology* 6(3): 384-389.

Otto S., Furlan R.L.E., and Sanders J.K.M. (2002). Recent developments in dynamic combinatorial chemistry. *Current Opinion in Chemical Biology* 6(3): 321-327.

Packard Bioscience. (2003). Multiprobe II Automated Liquid Handling Systems: Specifications. Information from Packard Bioscience.

Pan Bingfeng, Gu Jianxing, Li Zuyi, and Ward O.P. (1995). Reductive biotransformations of 2-substituted-3-carbonyl butanoate by resting cells and an enzymeatic system of *Geotrichum*. *Enzyme and Microbial Technology* 17(9): 853-855.

Papagianopoulos M., Zimmermann B., Mellenthin A., Krappe M., Maio G., and Galensa R. (2002). Online coupling of pressurized liquid extraction, solid phase extraction and high

performance liquid chromatography for automated analysis. *Journal of Chromatography A* 993: 9-16.

Parandosh Z. (1997). Counterpoint: Cell based assays. *Journal of Biomedical Screening* 2(4): 201-202.

Parker T.D., Wright D.S., and Rossi D.T. (1996). Design and evaluation of an automated solid-phase extraction method development system for use with biological fluids. *Analytical Chemistry* 68(14): 2437-2441.

Peng S., Hensen C., Strojnowski M., and Golebiowski A. (2000a). Automated high throughput liquid-liquid extraction for initial purification of combinatorial libraries. *Analytical Chemistry* 72: 261-266.

Peng S., King S., Bomes D., Foltz D., Baker T., and Natchus M. (2000b). Automated 96-well SPE and LC-MS-MS for determination of protease inhibitors in plasma and cartilage tissue. *Analytical Chemistry: 1913*-1917.

Peng S.X., Branch T.M., and King S.L. (2001). Fully automated 96-well liquid-liquid extraction for analysis of biological samples by liquid chromatography with tandem mass spectrometry. *Analytical Chemistry 75(3): 708-714.*

Perkin Elmer (2002). Webpage: www.perkinelmer.com - now part of Packard www.Bioscience.com.

Pickering S.C.R. (2003). Ultra scale down and automation and biotransformation processes. University of London thesis.

Pisano G.P., and Wheelwright S.C. (1995). The new logic of high-tech R and D. *Harvard Business Review: 93*-105.

Plumb R., Gray R., and Jones C. (1997). Use of reduced sorbent bed and disk membrane solid phase extraction for the analysis of pharmaceutical compounds in biological fluid with applications in the 96-we: format. *Journal of Chromatography B* 694: 123-133.

Pochert J. (2000). Liquid level detection (LLD) in high throughput screening application. *International Biotechnology Laboratory, Oct 2000,* Microlab STAR Hamilton Bonasuz.Ag. poster.

Precision Weighing Balances. (2004). Webpage: www.Precision Weighing Balances - Acculab ALC-80_4 Analytical Balance.htm.

PriceWaterhouseCoopers. (2000). Pharma 2005: An industrial Revolution in R and D. PricewaterhouseCoopers Report.

Ramos L., Bakhtiar R., and Tse F.L.S. (2000). Liquid-liquid extraction using 96-well plate format in conjunction with liquid chromatography/ tandem mass spectrometry for quantitative determination of methylphenidate (Ritalin®) in human plasma. *Rapid Communications in Mass Spectrometry* 14: 740-745.

Rang H.P., Dale M.M., and Ritter J.M. (1999). How drugs act: molecular aspects, chapter in Pharmacology, Churchill Livingstone, 4th edition: 22-46.

Rapson and Bird. (1963). Ionization constant of some penicillins and of their alkaline and penicillinase hydrolysis products. *Journal of Pharmacy and Pharmacology* 15: 222 T-233 T.

Reisman H.B. (1993). Problems in scale-up of biotechnology production processes. *Critical Reviews of Biotechnology* 13(3) 195-253.

Reschke M., and Schugere K. (1984). Reactive extraction of Re-distribution coefficients and degrees of extraction. *The Chemical Engineering Journal* 28: B11-B20.

Reuters. (2001). The drug discovery outlook: Drivers of innovation into the 21st century. Webpage: www.ReutersBusinessInsight.com.

Roche Carolina. (2003). Process Development. Webpage: *www.rochecarolina.com/Business%20Services/Process%20Development,htm.*

Rogers M. (1997). High throughput screening - liquid handling systems for 384-well applications. *Drug Discovery Today* 2(9): 395-396.

Rollins M., and Pochert J. (2000). Accurate automation - Liquid/ liquid phase separation in pharmaceutical HTS. *Screening* 1: 46-47.

Rossi D.T. (2002). Integrating automation and LC/MS for drug discovery bioanalysis`. *Journal of Automated Methods and Management in Chemistry* 24(1): 1-7.

Rouan M., Buffet C., and Masson R. (2001). Practice of solid phase extraction and protein precipitation in the chromatography ultra violet detection. *Journal of Chromatography B* 754: 45-55.

Rouan M., Buffet C., Marfil F., Humbert H., and Maurer G. (2002). Plasma deproteinization by precipitation and filtration in the 96-well format. *Journal of Pharmaceutical and Biomedical Analysis* 25(5): 995-1000.

Ruddick C. (2000). Automation of liquid-liquid extraction processes. *Chemistry Today* July/August: 40-43.

Savidge T.A. (2001). Enzymatic conversions used in the production of penicillins and cephalosporin, chapter 5 in Drugs and the pharmaceutical sciences 22. Dekker,: 171-224.

Schmid E.F., and Smith D.A. (2002). Discovery, innovation and the cyclical nature of the pharmaceutical business. *Drug Discovery Today* 7(10): 563-568.

Schneider I. (1997). Automated liquid handling tools focus on sample size and lab productivity. *Genetic Engineering News:* 34-36.

Seader J.D., and Henley E.J. (1998). Adsorption, ion exchange and chromatography, chapter 15 in Separation Process Principles, John Wiley: 778-847.

Shamrock W.F., Reilly K., and Lloyd D.K. (2000). Automated sample preparation of Roxifiban tablets; transfer of a manual method to an automated workstation. *Journal of Pharmaceutical and Biomedical Analysis* 21: 1225-1232.

Shengshui H., and Zaofan. Z. (1991). Detection of trace 6-aminopenicillanic acid by adsorptive stripping voltammetry. *Analytical Letters* 24(5), 827-836.

Sheridan P. (2000). Testing for scale up. *Chemistry and Industry: The Supply Line 22/5/00:* 2.

Sherwood T.K. (1952). Absorption and Extraction, McGraw-Hill chemical engineering series, 2nd edition.

Shewale J., and Shivaraman H. (1989). Penicillin acylase: enzyme production and application in the manufacture of 6-APA. *Process Biochemistry: 146*-154.

Shimoyama R., Ohkubo T., Sugawara K., Ogasawara T., Ozaki T., Kagiya A., and Saito Y. (1998). Monitoring of phenytoin in human breast milk, maternal plasma and cord blood plasma by solid-phase extraction and liquid chromatography. *Journal of Pharmaceutical and Biomedical Bioanalysis* 17: 863-869.

Shodor . (2002). Penicillin model application. Webpage: www.shodor,org.

Sho Jung *K., and Parkin K.L (1995).* Acetylacylglycerol formation by lipase in microaqueous milieu: effects of acetyl group donor and environmental factors. *Journal of Agricultural and Food Chemistry* 43(7): 1775-1783.

Shou W., Pelzer M., Addison T., Jiang X., and Naidong W. (2002). An automated 96-well solid-phase extraction and liquid chromatography-tandem mass spectrometry method for the analysis of morphine, morphine-3-glucuronide and morphine-6-glucuromide in human plasma. *Journal of Pharmaceutical and Biomedical Analysis* 27(1): 143-152.

Skehan P. (2000). Dealing with the data deluge in high throughput screening. *Journal of Automated Methods and Management in Chemistry* 22(5): 145-148.

Society for Biomolecular Screening. (1996). Footprint dimensions for microplates. Webpages: www.sbsonline.org/., *www.google.com/96-well footplate dimensions.*

Sofer G. (1997). Validation: Ensuring the accuracy of scaled-down chromatography models, *Biopharm Research*: 36-39.

Spiess A., Schlothauer R.C., Hinrichs J., Scheidat B., and Kasche V. (1999). pH Gradients in immobilized amidases and their influence on rates and yields of beta-lactam hydrolysis. *Biotechnology and Bioengineering* 62(3): 267-277.

Steinborner S., and Henion J. (1999). Liquid-liquid extraction in the 96-well plate format with SRM LC MS quantitative determination of methotrexate and its metabolites in human plasma. *Analytical Chemistry* 71(3): 2340-2345.

Stevens M., Bouchard P., Karib I., and Chamg T. (1998). Comparison of automation equipment in high throughput screening. *Biomolecular Screening* 3(4): 305-311.

Sugimori D., Takeguchi M., and Okura I. (1995). Biocatalytic methanol production form methane with Methylosinus trichosporium OB-b: an approach to improved methanol accumulation. *Biotechnology Letters* 17(8): 783-784.

Sutherland I., Siddiqi S., Keightley R., and Fisher D. (1989). A new approach to countercurrent distribution combining separation with analysis in the Biomek automated laboratory workstation, chapter in Separations using Aqueous Phase Systems: Applications in Cell Biology and Biotechnology, Edited by Fisher D., and Sutherland I.A., Plenum: 407-416.

Szita N., Buser R., and Dual J. (2001). Aspiration and dispensing of biological liquids in the micro- and submicrolitre range at high precision. *Biomedical Microdevices* 3(3): 175-182.

Takahashi E., Nakamichi K., and Furui M. (1995). *Micrococcus freudenreichii* FERM-P13221. *Journal of Fermentation and Bioengineering* 80(3): 247-250.

Tavare N.S., Jadhav V.K. (1999). Separation through crystallization and hydrotropy: the 6-aminopenicillanic acid (6-APA) and phenoxyacetic acid (PAA) system. *Journal of Crystal Growth* 198-199(2): 1320-1325.

Taylor P., Stewart F., Dunnington S., Quinn S., Schalz C., Vaidya K., Kurali T., Lane T., Xian W., Sherrill T., Snider J., Terp S., Tanher Tzberg K. (2000). Automated assay optimization with integrated statistics smart robotics. *Journal of Molecular Screening* 5(4): 213-225.

Tecan. (2002). Webpage: www.tecan.com.

Teitz D., Khan S., Powell M., and Jemal M. (2000). An automated method of sample preparation of biological fluids using pier cable caps to eliminate the uncapping of the sample tubes during sample transfer. *Journal of Biochemical and Biophysical Methods* 45(2): 193-204.

Thiericke R. (2000). Drug discovery from nature: automated high quality sample preparation. *Journal of Automated Methods and Management in Chemistry* 22(5): 149-157.

Thompson K. (2002). Virtual wells: combinatorial biology demands ultra-high-throughput. Webpage: *www.netsci.org/science/screening/feature04,html.*

Thornton J. (1992). Science and Practice of Liquid-Liquid Extraction Volume 1, Oxford University Press (The Oxford engineering science series).

Titchener-Hooker N.J., and Zhou Y.H. (2001). Biopharmaceutical process development: part 2, methods of reducing development time. *Biopharm Europe* September 2001: 68-74.

Toth J. (2003). Adsorption: Theory, Modeling and Analysis. *Separation Science and Technology* 38(16): 3905-3926.

Tsai S.W., and Huang C.M. (1999). Enantioselective synthesis of (S)-suprofen ester prodrugs by lipase in cyclohexane. *Enzyme and Microbial Technology* 25(8-9): 682-688.

Tshaen D.P., Abanson L., Cai D., Desmond R., Dolling U.H., Frey L., Karady S., and Shi V.J, (1995). A synthetic synthesis of MK0499. *Journal of Chromatography A* 60: 4324-4330.

Turner R., Felder R.A., and Kealy M. (2000). Comparison of manual and automated liquid handling for PCR. *Nature* UK Product Review 2000/9: 26-27.

University of Western Sydney. (2003). Definition of research. Webpage: *www.uws,edu,au/uws/research_services/RODevelopment/definition,htm.* Definition taken. from DES Higher Education Research Data Collection Guidelines.

US Patent Office. (2002). The use of automated technology in chemical process research and development. Webpage: http: //patft.uspto.gov/netacgi/nph-Parser?Sect1=PTO2andSect2=HITOFFandp=1andu=/netahtml/search-bool.htmlandr=1andf=Gandl=50andco1=ANDandd=ft00ands1=6044212.WKU.andOS=PN/6044212andRS=PN/6044212.

van Brakel J., and Kleizen H. (1990). Problems in down stream processing, chapter in Chemical Engineering Problems in Biotechnology, Elsevier Applied Science, edited by Winkler M, Society of Chemical Industry: 95-165.

Vandamme E., and Voets J. (1974). Microbial penicillin acylase, advances. *Applied Microbiology* 17: 311-369.

van der Hoff R., and Baumann R.A. (1993). On-line combination of automated micro liquid-liquid extraction and capillary gas chromatography for the determination of pesticides in water. *Journal of Chromatography A* 644 (2): 367-373.

van der Wielen L., and Lankveld M. (1996). Anion exchange equilibria of penicillin G, phenylacetic acid and 6-aminopenicillanic acid versus Cl^- on IRA400 ion exchange resin. *Journal of Chemical Engineering Data* 41: 239-249.

Venn R.F., Merson J., Cole S., and Macrae P. (2005). 96-well solid phase extraction: a brief history of its development. *Journal of Chromatography B* 817: 77-80.

Wang A., Fisher A., Hsieh J., Cairns A., Rogers J., and Musson D. (2002). Determination of a B3-agonist in human plasma by LC/MS with semi-automated 48-well diatomaceous earth plate. *Journal of Pharmaceutical and Biomedical Analysis* 26(3): 357-365.

Wagner R.W., Li F., Du H., and Lindsey J.S. (1999). Investigation of cocatalysis conditions using an automated microscale multifactor workstation synthesis of meso-tetramesitylphyrin. *Organic Process Research and Development* 3: 28-37.

Warburton D., Dunnill P., and Lilly D. (1973). Conversion of benzyl penicillin to 6-aminopenicillanic acid in a batch reactor and continuous feed stirred tank reactor using immobilised penicillin amidase. *Biotechnology and Bioengineering: 13*-25.

Watt A.P., Morrison D., Locker K.L., and Evans D.C. (2000). High throughput biocatalysis by an automation of protein precipitation assay using a 96-well plate format with detection by LC-MS/MS. *Analytical Chemistry* 72(5): 979-984.

Weast (1981).

Webb F.C. (1963). Biochemical Engineering, van Nostrand: 541-549.

Welch C.J., Shalmi M., Biba M., Chilenski J.R., Szumigala R.H., Dolling U., Mathre D.J., and Reider P.J. (2002). Microplate evaluation of process adsorbents. *Journal of Separation Science* 25: 847-850.

Welty J.R., Wicks C.E., Wilson R.E., and Rorrer G. (2001). Convective mass transfer between phases, chapter in Fundamentals of Momentum. Heat and Mass Transfer, Wiley, 4th edition: 586-604.

Wess G. (2002). How to escape the bottleneck of medicinal chemistry. *Drug Discovery Today* 7(10): 533-555.

Whitman W.G. (1923). Preliminary experimental conformation of 2-film theory of gas adsorption. *Chemical and Metallurgical Engineering* 29: 146-148.

Wilson K., and Walker M. (1994). Ion exchange chromatography, section in Practical Biochemistry, Cambridge University Press, 4th edition: 471-498.

Woo K., and Kim J. (1999). New hydrolysis methods for extremely small amount of lipids and capillary gas chromatographic analysis as N (O)-tert-butyldimethylsilyl fatty acid derivatives compared with methyl ester derivatives. *Journal of Chromatography A* 862: 199-208.

Woo W., La Gasse J., Zhou Z., Patel R., Palmer J., Campus H., and Haopian W. (2000). A novel high throughput method for accurate, rapid and economical measurement of multiple Type 1 diabetes antibodies. *Journal of Immunological methods* 244(1): 91-103.

Zhang N., Rogers K., Gajda K., and Rossi D. (2000a). Integrated sample collection and handling for drug discovery biocatalysis. *Journal of Pharmacology and Biomedical Science Analysis* 23: 551-560.

Zhang N., Hoffman K., Li W., and Rossi D. (2000b). Semi automated 96-well liquid-liquid extraction for quantification of drugs in biological fluids. *Journal of Pharmaceutical and Biomedical Analysis* 22: 131-138.

Zimmermann M. (2000). Liquid handling: a systems approach. *International Biotechnology* 18(5): 35-43.

Zweigenbaum J., Heinig K., Steinborner S., Wachs T., and Henion J. (1999). High throughput bioanalytical LC/MS determination of benzodiazepines in human urine: 1000 samples per 12 hours. *Analytical Biochemistry* 71: 2294-2300.